NUREG/CR-6948, Vol. 2

Integrated Ground-Water Monitoring Strategy for NRC-Licensed Facilities and Sites: Case Study Applications

Advanced Environmental Solutions, LLC

U.S. Nuclear Regulatory Commission
Office of Nuclear Regulatory Research
Washington, DC 20555-0001

AVAILABILITY OF REFERENCE MATERIALS IN NRC PUBLICATIONS

NRC Reference Material

As of November 1999, you may electronically access NUREG-series publications and other NRC records at NRC's Public Electronic Reading Room at http://www.nrc.gov/reading-rm.html. Publicly released records include, to name a few, NUREG-series publications; *Federal Register* notices; applicant, licensee, and vendor documents and correspondence; NRC correspondence and internal memoranda; bulletins and information notices; inspection and investigative reports; licensee event reports; and Commission papers and their attachments.

NRC publications in the NUREG series, NRC regulations, and *Title 10, Energy*, in the Code of *Federal Regulations* may also be purchased from one of these two sources.

1. The Superintendent of Documents
   U.S. Government Printing Office
   Mail Stop SSOP
   Washington, DC 20402–0001
   Internet: bookstore.gpo.gov
   Telephone: 202-512-1800
   Fax: 202-512-2250
2. The National Technical Information Service
   Springfield, VA 22161–0002
   www.ntis.gov
   1–800–553–6847 or, locally, 703–605–6000

A single copy of each NRC draft report for comment is available free, to the extent of supply, upon written request as follows:

Address: U.S. Nuclear Regulatory Commission
Office of Administration
Mail, Distribution and Messenger Team
Washington, DC 20555-0001
E-mail: DISTRIBUTION@nrc.gov
Facsimile: 301–415–2289

Some publications in the NUREG series that are posted at NRC's Web site address http://www.nrc.gov/reading-rm/doc-collections/nuregs are updated periodically and may differ from the last printed version. Although references to material found on a Web site bear the date the material was accessed, the material available on the date cited may subsequently be removed from the site.

Non-NRC Reference Material

Documents available from public and special technical libraries include all open literature items, such as books, journal articles, and transactions, *Federal Register* notices, Federal and State legislation, and congressional reports. Such documents as theses, dissertations, foreign reports and translations, and non-NRC conference proceedings may be purchased from their sponsoring organization.

Copies of industry codes and standards used in a substantive manner in the NRC regulatory process are maintained at—

The NRC Technical Library
Two White Flint North
11545 Rockville Pike
Rockville, MD 20852–2738

These standards are available in the library for reference use by the public. Codes and standards are usually copyrighted and may be purchased from the originating organization or, if they are American National Standards, from—

American National Standards Institute
11 West 42nd Street
New York, NY 10036–8002
www.ansi.org
212–642–4900

Legally binding regulatory requirements are stated only in laws; NRC regulations; licenses, including technical specifications; or orders, not in NUREG-series publications. The views expressed in contractor-prepared publications in this series are not necessarily those of the NRC.

The NUREG series comprises (1) technical and administrative reports and books prepared by the staff (NUREG–XXXX) or agency contractors (NUREG/CR–XXXX), (2) proceedings of conferences (NUREG/CP–XXXX), (3) reports resulting from international agreements (NUREG/IA–XXXX), (4) brochures (NUREG/BR–XXXX), and (5) compilations of legal decisions and orders of the Commission and Atomic and Safety Licensing Boards and of Directors' decisions under Section 2.206 of NRC's regulations (NUREG–0750).

NUREG/CR-6948, Vol. 2

Integrated Ground-Water Monitoring Strategy for NRC-Licensed Facilities and Sites: Case Study Applications

Manuscript Completed: August 2007
Date Published: November 2007

Prepared by
V. Price, T. Temples, R. Hodges, Z. Dai, D. Watkins, J. Imrich

Advanced Environmental Solutions, LLC
407 West Main Street
Lexington, SC 29072

T.J. Nicholson, NRC Project Manager

Prepared for
Division of Fuel, Engineering and Radiological Research
Office of Nuclear Regulatory Research
U.S. Nuclear Regulatory Commission
Washington, DC 20555-0001
NRC Job Code Y6020

ABSTRACT

This document discusses results of applying the Integrated Ground-Water Monitoring Strategy (the Strategy) to actual waste sites using existing field characterization and monitoring data. The Strategy is a systematic approach to dealing with complex sites. Application of such a systematic approach will reduce uncertainty associated with site analysis, and therefore uncertainty associated with management decisions about a site. The Strategy can be used to guide the development of a ground-water monitoring program or to review an existing one. The sites selected for study fall within a wide range of geologic and climatic settings, waste compositions, and site design characteristics and represent realistic cases that might be encountered by the NRC. No one case study illustrates a comprehensive application of the Strategy using all available site data. Rather, within each case study we focus on certain aspects of the Strategy, to illustrate concepts that can be applied generically to all sites. The test sites selected include:

- Charleston, South Carolina, Naval Weapons Station,
- Brookhaven National Laboratory on Long Island, New York,
- The USGS Amargosa Desert Research Site in Nevada,
- Rocky Flats in Colorado,
- C-Area at the Savannah River Site in South Carolina, and
- The Hanford 300 Area.

A Data Analysis section provides examples of detailed data analysis of monitoring data.

Paperwork Reduction Act Statement

This NUREG does not contain information collection requirements and, therefore, is not subject to the requirements of the Paperwork Reduction Act of 1995 (44 U.S.C. 3501 et seq.).

Public Protection Notification

The NRC may not conduct or sponsor, and a person is not required to respond to, a request for information or an information collection requirement unless the requesting document displays a currently valid OMB control number.

FOREWORD

This research report was prepared by Advanced Environmental Solutions, LLC (AES), under a commercial research contract (NRC-04-03-061) with the U.S. Nuclear Regulatory Commission (NRC). As such, this two-volume report presents a logical framework for assessing what, when, where, and how to monitor with regard to subsurface ground-water flow and transport, in order to ensure that the environs of a licensed nuclear site or facility behave within the expected limits, as prescribed by the performance assessment (PA).

Volume 1 provides the logic, strategic approach, and examples of how to integrate ground-water monitoring with modeling. Specifically, the integrated ground-water monitoring strategy is implemented in an iterative manner, beginning with analysis of any existing site and facility characterization and monitoring data and the relevant conceptual site model (CSM), hydrogeologic model, and/or risk assessment or PA model. The iterative nature of this strategy provides a graded approach for use in developing or evaluating a ground-water monitoring program. In so doing, the analyst derives an initial assessment of what, when, where, and how to monitor to evaluate system performance. The monitoring is then integrated with modeling through the identification, measurement, and analysis of performance indicators (PIs). These PIs include hydrogeologic conditions and process attributes; chemical conditions and constituents; and other features, events, or processes (FEPs) that may significantly influence contaminant flow and transport. As such, PIs may be directly measurable using a monitoring program, or may be derived from compilations and interpretations of geophysical or other indirect data. This integrated ground-water monitoring and modeling strategy offers the following benefits:

- Characterization allows the development of a CSM.
- The CSM allows modeling and/or numerical simulation.
- Modeling allows prediction of system behavior, while monitoring allows refinement of models.
- Refinement supports confidence in the performance assessment, as well as the need for (and selection of) remediation approaches in the event of a contaminant release.

Volume 2 presents practical examples of the applications of this strategy, which provide practical means of testing, evaluating, and improving both the ground-water monitoring program and its related model. Although the strategy and its applications were originally planned for decommissioning sites, they are also very useful for assessing ground-water monitoring programs, remediating ground water, and identifying and selecting approaches to preclude offsite migration of abnormal radionuclide releases at nuclear facilities.

This approach is consistent with the NRC's strategic performance goal of making the agency's activities and decisions more effective, efficient, realistic, and timely by characterizing and monitoring radionuclide transport in ground water. Toward that end, this report demonstrates, using examples relevant to nuclear facility performance, that ground-water monitoring and modeling can be integrated within a systems approach. This information will assist NRC licensing staff and regional inspectors, Agreement State regulators, and licensees in their decision-making by promoting a greater understanding of ground-water monitoring concepts that relate to PA models. Nonetheless, this report is not a substitute for NRC regulations, and compliance is not required. Consequently, the approaches and methods described in this report are provided for information only, and publication of this report does not necessarily constitute NRC approval or agreement with the information contained herein. Similarly, use of product or trade names in this report is intended for identification purposes only, and does not constitute endorsement by either the NRC or AES.

Christiana Lui, Director
Division of Risk Analysis
Office of Nuclear Regulatory Research

EXECUTIVE SUMMARY

This document discusses results of applying the Integrated Ground-Water Monitoring Strategy (the Strategy) to actual sites using existing field characterization and monitoring data. The sites selected for study fall within a wide range of geologic and climatic settings, inventory compositions, and site design characteristics and represent realistic cases that might be encountered by the NRC.

Within each case study we focus on certain aspects of the Strategy, to illustrate concepts that can be applied generically to all sites.

The six test sites selected include:

Chapter 2. Charleston, SC Naval Weapons Station. This study illustrates the value of detailed geological study aided by shallow seismic reflection data to develop a conceptual site model (CSM). The resulting model explained monitoring observations and allowed simulation of plume movement that matched observed concentrations. Wells could be recommended for deletion, and an additional sentinel well for model confirmation was recommended.

Chapter 3. Brookhaven National Laboratory on Long Island, New York. At this site 3-D visualization (e.g., Figures 3-11 and 3-12 on page 3-20) allowed better communication of plume movement.

Chapter 4. The USGS Amargosa Desert Research Site in Nevada. A revised CSM integrating all available site data, including resistivity soundings, allowed re-interpretation of observed tritium vapor movements. With the revised CSM, a simple spreadsheet model was used and provided a good match to observed tritium distribution.

Chapter 5. Rocky Flats in Colorado. This site provides an opportunity to observe episodic pulses of contaminant apparently being released from a vadose zone source in response to water table changes. Data from one well are used to address the issue of defining long-term trends (the Mann-Kendall test) and when it is appropriate to stop sampling a well. The data are also discussed in Chapter 8.

Chapter 6. C-Area at the Savannah River Site in South Carolina. This site has both tritium and chlorinated solvent plumes. An adjacent location that was characterized as a potential landfill site provides data that may not be consistent with the CSM used to model the C-Area ground water. Because of the site's isolation, there are no risk consequences of the possible CSM error.

Chapter 7. The Hanford 300 Area. A revision to the CSM is suggested that includes river water dynamics as part of the hydrogeologic model.

In addition a section on Data Analysis appears as Chapter 8 of this document. This chapter is not intended to be a review of statistics, but to give some examples of data analysis. A FORTRAN program to calculate well to well correlations and Mann-Kendall parameters is included.

CONTENTS

ABSTRACT iii
FOREWORD v
EXECUTIVE SUMMARY vi
CONTENTS vii
FIGURES xi
TABLES xvi
ACRONYMS AND ABBREVIATIONS xvii
1 Introduction 1-1
1.1 Charleston Naval Weapons Station 1-4
1.2 Brookhaven National Laboratory 1-4
1.3 USGS Amargosa Desert Research Site 1-5
1.4 Rocky Flats 1-5
1.5 Savannah River C-Area 1-5
1.6 Hanford Site 300 Area 1-6
1.7 Data Analysis 1-6
2 Charleston Naval Weapons Station 2-1
2.1 Introduction 2-1
2.2 Compilation and Analysis of Available Data 2-2
2.2.1 Regional Geology 2-2
2.2.2 Site Hydrogeology 2-3
2.3 Conceptual Site Modeling 2-6
2.3.1 First Approach: Analytical Model: 2-6
2.3.2 Second Approach: Numerical Model / Simple Geology: 2-7
2.3.3 Third Approach: Numerical Model / Complex Geology 2-8
2.4 Designing a Performance Confirmation Monitoring Network 2-10
2.5 Strategy Application Conclusions 2-14
2.6 Charleston References 2-16
Appendix 2-A 2-17
3 Brookhaven National Laboratory 3-1
3.1 Introduction 3-1
3.2 Compilation of Available Data 3-2
3.2.1 Site Background 3-2
3.2.2 Geologic Information 3-4
3.2.3 Hydrogeologic Information 3-4
3.2.4 Hydrologic Data 3-5
3.2.5 Tritium Plume Ground-Water Monitoring Data 3-12
3.3 Ground-Water Modeling and Visualization 3-19
3.3.1 Plume visualization 3-19
3.3.2 Flow and transport modeling 3-21
3.3.3 Active Monitoring 3-21
3.3.4 Performance Indicators 3-23
3.4 Monitoring Strategy Application Conclusions 3-24

3.5 Brookhaven References 3-24
4 Amargosa Desert Research Site 4-1
4.1 Introduction 4-1
4.2 Compilation of Available Data 4-1
4.2.1 Geologic Setting 4-2
4.2.2 Regional Geologic Information 4-4
4.2.3 Site-specific Geologic and Analytical Data 4-4
4.3 Application of the Strategy 4-13
4.3.1 Chemical Constituents in Ground Water or Soil Gas 4-13
4.3.2 Chemical Constituents in Other Fluids 4-13
4.3.3 Chemical Constituents in Plants and Animals 4-14
4.3.4 Geophysical Modeling and Evaluation 4-15
4.3.5 Hydrologic Data 4-18
4.3.6 Vadose Zone Data 4-21
4.3.7 Meteorological Data 4-25
4.3.8 Transport Modeling 4-26
4.4 Monitoring Strategy Application Conclusions 4-30
4.5 Amargosa References 4-31
Appendix 4-A 4-33
Appendix 4-B 4-47
5 Rocky Flats Facility 5-1
5.1 Introduction 5-1
5.2 Compilation of Available Data 5-3
5.3 Geologic Setting 5-3
5.3.1 Hydrologic Data 5-4
5.4 Application of the Strategy 5-6
5.4.1 Case Study 1: Conceptual Site Model Assessment 5-6
5.4.2 Case 1: Existing Site Monitoring Data 5-7
5.4.3 Case 1: Application of the Strategy 5-7
5.4.4 Case 2: VOC Plume Analysis 5-12
5.4.5 Case 2: Application of the Strategy 5-12
5.4.6 Performance Indicators and FEPs 5-14
5.5 Monitoring Strategy Application Conclusions 5-15
5.6 Rocky Flats References 5-16
6 Savannah River Site, C Area 6-1
6.1 Introduction 6-1
6.2 Compilation of Available Data 6-3
6.3 C-Area Background 6-3
6.3.1 Geology and Hydrogeology 6-4
6.3.2 Site Characterization and Monitoring 6-5
6.3.3 Contaminant Distribution 6-6
6.4 Synthesis of a Conceptual Site Model and Flow and Transport Simulations 6-8
6.5 Data Visualization 6-11
6.6 Alternative Conceptual Models 6-12
6.7 Performance Indicators and FEPs 6-14
6.8 Monitoring Strategy Application Conclusions 6-15

6.8.1 Possible Future Actions 6-16
6.9 References 6-17
7 Hanford 300 Area 7-1
7.1 Introduction 7-1
7.2 Compilation of Available Data 7-2
7.2.1 Geologic Setting 7-2
7.2.2 Regional Geologic Information 7-2
7.2.3 Site-specific Geologic Information 7-4
7.2.4 Site-specific Hydrogeologic Information 7-5
7.2.5 Vadose Zone Data 7-8
7.2.6 Hydrologic Data 7-9
7.2.7 Seasonal Variability in Water-Table Conditions 7-10
7.2.8 300 Area Uranium Plume 7-12
7.2.9 Monitoring Considerations 7-14
7.3 Application of Ground Water Monitoring Performance Strategy 7-15
7.3.1 Performance Indicators and FEPs 7-19
7.4 Monitoring Strategy Application Conclusions 7-20
7.5 Hanford References 7-21
8 Analysis of Characterization and Monitoring Data 8-1
8.1 Introduction 8-1
8.1.1 Data Types – Characterization versus Monitoring 8-1
8.1.2 Data Evaluation versus Statistical Analysis 8-2
8.2 Univariate data 8-3
8.2.1 Basic Statistical Analysis 8-4
8.2.2 Identification of Outlier Points 8-4
8.2.3 Quality Control Charts: the T-Test 8-5
8.2.4 Applying the Mann-Kendall Test 8-7
8.3 Rainfall Data – Sources of Uncertainty for Infiltration 8-11
8.3.1 Consider All Water Infiltration Sources 8-12
8.3.2 Ensure Rain Station Data Match Facility-Specific Gauging 8-12
8.4 Correlations between different wells 8-15
8.5 Water Level Measurements 8-18
8.6 Unmixing of Multimodal Data 8-19
8.7 Multivariate Analysis Methods: Cluster and Factor Analysis 8-23
8.7.1 Case Study: Multivariate Data Analysis at Mill Tailing Site 8-23
8.8 Analysis of Mapped (Spatial) Data 8-28
8.8.1 Outliers in Mapped Data 8-29
8.8.2 Uncertainty in Mapped Data 8-29
8.8.3 Incongruity between Mapped Variables 8-31
8.9 Quality Assurance 8-34
8.9.1 Quality Assurance Case Studies 8-35
8.10 References 8-39
Appendix 8-A 8-42
Appendix 8-B Fortran 90 code for well-well correlations and for the Mann-Kendall test 8-45
GLOSSARY G-1

FIGURES

Figure 1-1. Integrated Ground Water Monitoring Strategy framework 1-2
Figure 2-1. Map showing the location of SWMU 12 at the Charleston Naval Weapons Station (Danielsen, 2003)..... 2-1
Figure 2-2. This cross section is an example of the complex geology that can result from a changing coastal environment. (Figure from Ferm in Saxena, 1976, Fig. 2) 2-2
Figure 2-3. Map of SWMU 12 showing locations of wells and nearby marshes (Danielsen, 2003). 2-3
Figure 2-4. Seismic reflection profiles. The green line is interpreted as the base of the major channel or the older channel, the red line indicates the base of younger channel that has incised into the older channel..... 2-4
Figure 2-5. Elevation of the base of the channel contoured from seismic data and well picks. The orange shows the lower elevations, the green shows the higher elevations, and the grey lines represent the seismic profile locations. 2-5
Figure 2-6. Graph of data from the slug test, with hydraulic conductivity (ft/d) on the vertical axis and the cumulative percentage of samples having that value or less plotted on the horizontal axis. 2-6
Figure 2-7. Cross Section of the assumed geology for the analytical solution CSM. 2-7
Figure 2-8. Cross Section of the "Layer Cake Geology" used for our second approach. 2-8
Figure 2-9. The PCE plume from Model II is presented at left, and the computed PCE concentrations at monitoring well MW-03 are much lower than the observed values (right). 2-8
Figure 2-10. The cross-section shows the Major channel and Younger channel, as well as the other hydrofacies in the site. 2-9
Figure 2-11. The simulated PCE plume from Model III is presented at left; computed PCE concentrations at monitoring well MW-03 more closely match observed values (right). 2-9
Figure 2-12. The predicted PCE plume in five years. Circled wells are suggested to be removed from the monitoring program to save money, while a new point is suggested to be added at the yellow dot to test the CSM and simulation results. . 2-11
Figure 2-13. Change in water table over time. Note how MW-08 is the only well that doesn't match the others. 2-12
Figure 2-14. Contour Map of water table using data from July 2004 (feet above MSL) . 2-13
Figure 2-15. Contour map of water table using data from July 2004, without well MW-08 (feet above MSL) 2-13
Figure 2-16. Activities and results of the Strategy application at Charleston Naval Weapons Station 2-15
Figure 3-1. Schematic of tritium/VOC plume pump and treat system (DOE, 2000) 3-2
Figure 3-2. Location of the Brookhaven National Laboratory (Scorca et al., 1999)..... 3-3
Figure 3-3. Hydrostratigraphy of the Brookhaven National Laboratory (BNL, 2004) . 3-4
Figure 3-4. Precipitation and water-table altitude at Brookhaven National Laboratory, Suffolk County, N.Y.,1970-97. A. Annual precipitation at Upton. B. Typical water levels in wells (Scorca et al., 1999) 3-9

Figure 3-5. Water-table altitude in 300-mi^2 study area surrounding Brookhaven National Laboratory, Suffolk County, N.Y., August 1995 (Scorca et al., 1999) 3-10
Figure 3-6. Schematic of plume configuration below the HFBR (Looney and Paquette, 2000). Used by permission of Battelle Press 3-13
Figure 3-7. Simplified calculation of plume thickness immediately downgradient of a vadose zone source (Looney and Paquette, 2000). Used by permission of Battelle Press. 3-14
Figure 3-8. Cross section of tritium plume emanating from the HFBR (Looney and Paquette, 2000). Used by permission of Battelle Press. 3-16
Figure 3-9. December 2005 water table map of BNL with extraction wells (BNL, 2005) 3-17
Figure 3-10. Location of tritium plume emanating from the High Flux Beam Reactor (DOE, 2000)..... 3-18
Figure 3-11. Oblique view looking northeast of tritium plume with concentrations emanating from the HFBR. 3-20
Figure 3-12. Oblique view looking northwest of tritium plume with concentrations emanating from the HFBR. 3-20
Figure 3-13. Computer simulation of tritium plume emanating from the HFBR after twenty years, no pumping 3-21
Figure 3-14. Computer simulation of tritium plume emanating from the HFBR after twenty years, pumping monitoring well. 3-22
Figure 4-1. Location of ADRS (Stonestrom et al., 2003)..... 4-2
Figure 4-2. Cross section of a typical horst and graben sequence (CG, 1992)..... 4-3
Figure 4-3. Oblique view of a typical alluvial fan in Death Valley..... 4-3
Figure 4-4. Location of ADRS and soil gas sampling boreholes UZB-2 and UZB-3 (Stonestrom et al., no date) 4-4
Figure 4-5. Geologic distribution of clay lenses and marsh deposits in ADRS Wells 301, 302, and 303 (Fischer, 1992) 4-5
Figure 4-6. ADRS water table contours (measured in meters MSL) and well locations (Walvoord et al., 2005) 4-6
Figure 4-7. Map of tritium concentrations in ground water below ADRS (Data from Prudic, 1997)..... 4-7
Figure 4-8. Map showing numbered survey locations of Schlumberger soundings (modified from Bisdorf, 2002)..... 4-8
Figure 4-9. Cross section of interpreted resistivity and basin fault (Bisdorf, 2002). (Triangles along the top axis correspond to sounding locations as mapped in Figure 4-8. Subvertical solid black line represents basin fault as defined by Bisdorf 2002.) 4-9
Figure 4-10. Map showing contours of interpreted resistivity at a depth of 97 m overlying topographic contours (Bisdorf, 2002)..... 4-10
Figure 4-11. A vertical cross section made by direct current electrical resistivity (DC-resistivity) imaging near the ADRS (Stonestrom et al., no date)..... 4-11
Figure 4-12. Monitoring shaft and instrument borehole showing locations of TCPs and respective geologic information (Fischer, 1992). Thermocouple psychrometers installed in the monitoring shaft are designated with L (left), M (middle), and R (right), followed by a number from 1 to 11 that indicates level in shaft.

Thermocouple psychrometers installed in the instrument borehole are designated OD1 through OD13. Depth of each thermocouple psychrometer, in meters below land surface, is given in parentheses. (Fischer, 1992). 4-11
Figure 4-13. Monitoring shaft geologic and geophysical information (Fisher, 1992).. 4-13
Figure 4-14. Plant sample locations and contours of plant-water tritium concentrations (Andraski et al., 2005) 4-14
Figure 4-15. A comparison of plant water tritium with soil water tritium (Stonestrom et al., no date)..... 4-15
Figure 4-16. Simplified geologic cross section of the ADRS looking northwest..... 4-15
Figure 4-17. Three-dimensional resistivity block model of the ADRS looking northwest (Well UZB-2 can be seen in the southwestern portion of the figure) (created with data from Bisdorf, 2002)..... 4-17
Figure 4-18. Location of the Southern Structural offset as defined by resistivity data in relation to the burial trenches (adapted from Stonestrom et al., no date) 4-18
Figure 4-19. Map of tritium concentrations in ground water below ADRS in relation to the Southern Structural Offset (data from Prudic, 1997)..... 4-20
Figure 4-20. Plan view of tritium soil gas concentrations in the 1.5m below ground surface interval (data from Striegl et al., 1997) 4-22
Figure 4-21. Soil vapor concentrations of tritium in UZB-2 4-23
Figure 4-22. Tritium soil gas concentrations from UZB-3 (modified from Stonestrom et al., no date)..... 4-24
Figure 4-23. Carbon dioxide and carbon-14 soil gas concentrations from UZB-2 and UZB-3 (Stonestrom et al., no date)..... 4-24
Figure 4-24. Data from southeast corner of ADRS (Prudic, 1996) 4-25
Figure 4-25. Conceptual Model for the movement of tritium proposed by Striegl et al., 1996..... 4-26
Figure 4-26. Comparison of actual data to modeled tritium concentrations in UZB-2 in pCi/L (UZB-2 tritium data from Striegl et al., 1997) 4-28
Figure 4-27. Alternative conceptual model for the distribution of tritium in vadose zone based on Southern Structural offset and UZB-2 tritium concentrations (tritium data from Striegl et al., 1997)..... 4-29
Figure 5-1. Location of the Rocky Flats Facility in Colorado (DOE, 2005)..... 5-2
Figure 5-2 Photograph of the Rocky Flats Facility (looking east) Photo is in "Linking Legacies", DOE publication EM-0319 (DOE 1997) Appendix B, page 190. 5-3
Figure 5-3. Map of Rocky Flats Facility drainage basins (from: http://lanl.gov/source/orgs/nmt/nmtdo/AQarchive/06springsummer/page5.shtml) 5-5
Figure 5-4. Ground-water monitoring well locations and depiction of VOC and nitrate plumes for the Rocky Flats Facility (CDPHE, (No Date))..... 5-6
Figure 5-5. Conceptual cross-section for the Rocky Flats Facility (Modified from K-H, 2004) 5-7
Figure 5-6. Diagram of multiyear variability in ground-water contaminant concentrations due to water table changes (K-H, 2004) 5-8
Figure 5-7. Conceptual cross section showing affects of water table changes on contaminant movement (modified from K-H, 2004)..... 5-8
Figure 5-8. Potential changes in ground-water movement due to closure..... 5-10
Figure 5-9. Predicted water level changes after closure (K-H, 2004) 5-11

Figure 5-10. Generalized depiction of the Rocky Flats Facility TCE plume 5-12
Figure 5-11. Conceptual model of complex flow of contaminants 5-14
Figure 6-1. Savannah River Site location map. Courtesy of Bill Jones, SRNL. 6-1
Figure 6-2. Photograph of the A Area Burning/Rubble Pit during operation..... 6-2
Figure 6-3. Map of C Area with facilities and wells (WSRC, 1998)..... 6-3
Figure 6-4. Simplified hydrogeologic cross section near C Area (Kegley et al., 1994). Courtesy of W.P. Kegley. 6-5
Figure 6-5. Topographic map of C-Area facility boundary with TCE plume and detected TCE concentrations..... 6-6
Figure 6-6. C Area tritium CPT data 6-7
Figure 6-7. C Area TCE CPT data..... 6-8
Figure 6-8. C Area hydrologic Conceptual Site Model 6-9
Figure 6-9. C Area simulated transport model for Layer 3 from the CBRP..... 6-10
Figure 6-10. C Area simulated transport model for Layer 7 from the CBRP..... 6-10
Figure 6-11. Cross section of C Area hydrogeologic conceptual model. The Gordon confining unit (green clay) is shown as a green band above the Gordon aquifer. Fourmile Branch is correctly called Four Mile Creek elsewhere in this document... 6-11
Figure 6-12. Looking from beneath the Gordon confining unit to the NE towards the plume (All dim points are above the Gordon confining unit)..... 6-12
Figure 6-13. Structural contour map of the top of the Gordon confining unit (WSRC, 1992) 6-13
Figure 6-14. Maps of ground water flow directions within the Gordon aquifer..... 6-14
Figure 7-1. Hanford Site map including the 300 Area (DOE, 1999)..... 7-2
Figure 7-2. Hanford Site regional geologic setting (Vermeul et al., 2003) 7-3
Figure 7-3. Structural geologic features of the Hanford Site within the Pasco Basin (Vermeul et al., 2003) 7-4
Figure 7-4. Major geological units at the Hanford Site (DOE, 1999) 7-5
Figure 7-5. Index map to cross sections shown in Figures 6, 7, and 8 (Peterson, 2005) 7-6
Figure 7-6. West to east cross section along flow path from 300 Area process trenches to the Columbia River (Peterson, 2005)..... 7-7
Figure 7-7. North to south cross section along shoreline wells (Peterson, 2005)..... 7-7
Figure 7-8. West to east cross section through central portion of 300 Area (Peterson, 2005) 7-7
Figure 7-9. Conceptual model of fluid flow beneath single shell tanks at Hanford Site showing fingering, funnel flow, and flow associated with clastic dikes or poorly sealed borehole annular space (Faybishenko, 2000)..... 7-9
Figure 7-10. 300 Area water-table elevation, March 1992 (averaged hourly) (Peterson, 2005) 7-10
Figure 7-11. 300 Area water-table elevation, May 1992 (averaged hourly) (Peterson, 2005) 7-10
Figure 7-12. 300 Area water-table elevation, June 1992 (averaged hourly) (Peterson, 2005) 7-11
Figure 7-13. 300 Area water-table elevation, September 1992 (averaged hourly) (Peterson, 2005) 7-11

Figure 7-14. 300 Area water-table elevation, December 1992 (averaged hourly) (Peterson, 2005) 7-11
Figure 7-15. 300 Area ground water monitoring locations (Peterson, 2005) 7-14
Figure 7-16. Hydrogeologic conceptual model of contaminant movement below the Hanford 300 Area (DOE, 2002) 7-15
Figure 7-17. Transient storage mechanisms (Runkel, 1998) 7-16
Figure 7-18. Alternative conceptual model of Hanford 300 Area showing potential infiltration and downstream flushing of formation 7-17
Figure 7-19. Extent of river water intrusion as estimated from nitrate concentrations in 2002(Yabusaki et al, 2004) 7-18
Figure 7-20. 300 Area Ground-Water Uranium Concentrations, August 1997 7-19
Figure 8-1. Example control chart 8-6
Figure 8-2. Mann-Kendall Example 8-8
Figure 8-3. Published figure indicating declining PCE concentrations in ug/L (DOE, 2006) 8-9
Figure 8-4. Linear regression fit to PCE data from MS-EXCEL 8-10
Figure 8-5. Parsing time series data into three groups. 8-11
Figure 8-6. SRS rain gauging station and well locations. Rain stations are located under respective station identifier A, C, F, H, and S. Well locations are denoted by black dots. Adapted from Jones, 1990. 8-13
Figure 8-7. Rain data for Stations F and H, which are only two miles apart, show that particularly in summer, rainfall patterns are highly variable, even over short distances. 8-13
Figure 8-8. Rain Gauges C and S are about 7 miles apart and show significant variation in observed rainfall. 8-14
Figure 8-9. Correlation of rainfall as a function of distance in July and January. 8-15
Figure 8-10. Rejection of outliers 8-16
Figure 8-11 Periodic and continuous water level measurements compared for SRS well P-13D. Courtesy Bill Jones, SRNL. 8-18
Figure 8-12. Unmixing bimodal data 8-20
Figure 8-13. Probability plot 8-22
Figure 8-14. Tri-modal distribution 8-22
Figure 8-15. Cross section showing concept of merged water bodies. Our study examines whether this water is separated into two isolated chambers. 8-24
Figure 8-16. Dendrogram (partial) of the clusters for the water analyses presented in Appendix 8-A. The left-most column is the well name and the right column indicates the observation number 8-26
Figure 8-17. Map of chloride plume (blue) superimposed on a vector potentiometric data (arrows), and contoured hydraulic conductivity data (red). 8-31
Figure 8-18. Typical alluvial fan 8-32
Figure 8-19. Diagram of alluvial fans in Wyoming 8-33
Figure 8-20. Schematic of monitoring well with steps in installation. 8-36
Figure 8-21. pH with time for well ASB8B 8-37
Figure 8-22. pH with time for well ABP3 8-38
Figure 8-23 Field and laboratory measurements compared. 8-39

TABLES

Table 1-1 Classification of Performance Indicators 1-3
Table 2-1. Slug test data compared to the number of hammer blows needed to penetrate 1 ft, averaged over the length of the screen zone. 2-5
Table 2-2. Estimated flow and transport parameters for Model III. 2-10
Table 2-3. Water elevations (ft above MSL) in wells..... 2-12
Table 3-1. Generalized description of geologic and hydrogeologic units underlying Brookhaven National Laboratory and vicinity, Suffolk County, N.Y. (Scorca et al., 1999) 3-6
Table 3-2. Hydraulic conductivity of Upper Glacial aquifer at Brookhaven National Laboratory, Suffolk County, N.Y., as indicated by aquifer tests (Scorca et al., 1999) 3-7
Table 4-1. Summary of model for estimation of tritium movement in the vadose zone between the Southern Structural Offset and UZB-2 4-27
Table 4-2. Tritium model dispersivity values assigned to various materials..... 4-29
Table 4-3. Comparison of results from the tritium model to actual concentrations in UZB-2 (UZB-2 data from Striegl et al., 1997) 4-30
Table 6-1. Hydrologic layer parameters (adapted from Flach et al. (1999) and Geotrans (2001))..... 6-9
Table 8-1 . Statistical analysis of water head observations from Savannah River Site . 8-17
Table 8-2. The identified distributions of three sources and the estimated parameters 8-21
Table 8-3. Correlations between monitoring data variables 8-28
Table 8-4. Hydraulic conductivity data 8-34

ACRONYMS AND ABBREVIATIONS

°C	degrees celcius
µg/L	micrograms per liter
ADRS	Amargosa Desert Research Site
AEA	Atomic Energy Act
AES	Advanced Environmental Solutions, LLC
AEC	Atomic Energy Commission
AOCs	Areas of Concern
ASTM	American Society for Testing and Materials
bgs	below ground surface
BNL	Brookhaven National Laboratory
BRP	burning and ruble pit
CERCLA	Comprehensive Environmental Response Compensation and Liability Act
CFC	chlorofluorocarbon
cfs	cubic feet per second
Ci	Curie
cm	centimeters
cm/day	centimeters per day
CO_2	carbon dioxide
COC	contaminant of concern
cpt	cone penetrometer test
CRBG	Columbia River Basalt Group
CSM	conceptual site model
CV	coefficient of variation
DC-resistivity	direct current resistivity
DCE	dichloroethylene
DNAPL	dense nonaqueous phase liquid
DoD	Department of Defense
DOE	United States Department of Energy
DQO	data quality objective
EDB	ethylene dibromide
EM	electromagnetic
EM	expectation-maximization
EPA	Environmental Protection Agency
ft	feet
ft/d	feet per day
ft/ft	feet per foot
FEPs	features, events, or processes
GC	green clay
GIS	geographic information system
gpm	gallons per minute
GPR	ground-penetrating radar
HFBR	High Flux Beam Reactor
INEEL	Idaho National Engineering and Environmental Laboratory
Kd	distribution coefficient
LANL	Los Alamos National Laboratory
LBNL	Lawrence Berkeley National Laboratory
LLNL	Lawrence Livermore National Laboratory
LLW	low-level waste
LNAPL	light non-aqueous phase liquid
m	meter
MCL	maximum contaminant level
m/d	meters per day

m/m	meters per meter
mg/g	milligrams per gram
MDL	method detection limit
mi	miles
mi^2	square miles
MLE	maximum likelihood estimation
MNA	monitored natural attenuation
ND	no date
NE	northeast
NRC	Nuclear Regulatory Commission
NURE	National Uranium Resource Evaluation
ORNL	Oak Ridge National Laboratory
OU	Operable Unit
PA	Performance Assessment
PAH	polycyclic aromatic hydrocarbon
pCi/L	picocuries per liter
PCB	polychlorinated biphenyl
PCE	tetrachloroethylene
PCP	pentachlorophenol
PNNL	Pacific Northwest National Laboratory
ppb	parts per billion
PVC	polyvinyl chloride
QA	quality assurance
RCRA	Resource Conservation & Recovery Act
RSB	reactor seepage basin
SCDHS	Suffolk County Department of Health Services
SNL	Sandia National Laboratories
SP	spontaneous potential
SPSS	Statistical Package for the Social Sciences
SRS	Savannah River Site
SRTC	Savannah River Technology Center
SSE	south/southeast
SVE	soil vapor extraction
SWMU	Solid Waste Management Unit
TCA	l,l,l-trichloroethane
TCE	trichloroethylene
TCLP	toxicity characteristics leaching procedure
TCPs	thermocouple psychrometers
TOC	total organic carbon
U(VI)	hexavalent uranium
UMTRA	uranium mill tailings remedial action
USGS	United States Geological Survey
VOC	volatile organic compound

1 Introduction

This document discusses results of applying the Integrated Ground-Water Monitoring Strategy (the Strategy) to actual waste sites using existing field characterization and monitoring data. The sites selected for study fall within a wide range of geologic and climatic settings, waste compositions, and site design characteristics and represent realistic cases that might be encountered by the NRC.

We gratefully acknowledge the U.S. Navy, the U.S. Geological Survey, and the U.S. Department of Energy for data used in this report.

A Test Plan submitted to NRC in July, 2005, set forth a plan that was applied to produce this report. No one case study illustrates a comprehensive application of the Strategy using all available site data. Rather, within each case study we focus on certain aspects of the Strategy, to illustrate concepts that can be applied generically to all sites.

The six test sites selected include:

Chapter 2. Charleston, SC Naval Weapons Station,

Chapter 3. Brookhaven National Laboratory on Long Island, New York,

Chapter 4. The USGS Amargosa Desert Research Site in Nevada,

Chapter 5. Rocky Flats in Colorado,

Chapter 6. C-Area at the Savannah River Site in South Carolina, and

Chapter 7. The Hanford 300 Area.

In addition a section on Data Analysis appears as Chapter 8 of this document. This chapter is not intended to be a review of statistics, but to give some examples of data analysis. The Strategy is a systematic approach to dealing with complex sites. Application of such a systematic approach will reduce uncertainty associated with site analysis, and therefore uncertainty associated with management decisions about a site. The Strategy can be used to guide the development of a ground-water monitoring program or to review an existing one. The high level logic, as expressed in Figure 1-1, is simple.

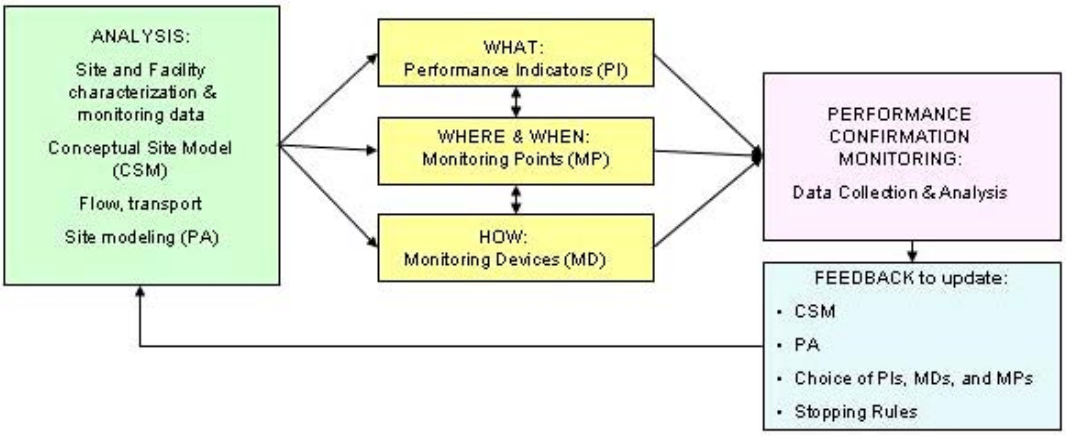

Figure 1-1. Integrated Ground Water Monitoring Strategy framework .

One begins by gathering, compiling, and analyzing all available data about the site and its geological and hydrological context. A Conceptual Site Model (CSM) based on geology and hydrogeology is constructed from the data. Engineered features such as trenches and back-filled areas may be important in the CSM. Numerical simulations based on this model may be made to estimate ground water flow directions and rates of contaminant transport.

For any site, there will be performance criteria to be met. Using the CSM, which incorporates hydrogeologic and geochemical information and knowledge of inventory, measurable or observable indicators of site performance can be selected. In this Strategy, these are called Performance Indicators (PIs). Locations and frequency for measuring indicators can also be selected. The indicators may be risk-related potential contaminants, or they may be physical measurements like water levels. The objective is to measure something that helps to indicate whether the overall site/facility/ground-water system is actually functioning as modeled.

The purpose of monitoring in the context of this guide is confirmation of a performance assessment model. Once we have confidence that the site is understood, we can place monitoring points as sentinels to give early detection of off-normal behavior, and to assure compliance with ground-water protection standards. But it is worth repeating that understanding system behavior, not regulatory compliance is the goal of this work.

Site and system Performance Indicators are measurable or observable features that provide insight into reliability of the Conceptual Site Model (CSM). During analysis of data from each site, performance indicators are identified and examined. A table of potential Performance Indicators (PIs) is shown below. Actual PIs will be site-specific.

Table 1-1 Classification of Performance Indicators

Class 1 - Chemical

A. Regulated and Direct Drivers of Risk - U, Cs-134, Pu, Sr-90 these are Primary Performance Indicators (PIs)

B. Surrogates and Indicators that a process is occurring –
   1. gross Alpha for Uranium
   2. Cl or NO3 from same source as risk drivers
   3. degradation products - Am241 for Pu, organic breakdown products for MNA

C. Process control chemical indicators needed to model transport
   - pH, alkalinity, conductivity, major cations, major anions, redox indicators...

Class 2 - Physical

- examples include water content, pressure distributions
- physical properties of rocks
- physical properties of subsurface fluids

Class 3 - Modeled or Derived from Data Analysis

A. Distribution of uncertainty

   This would be determined by examining the distribution of characterization data available to develop a site conceptual model and flow model. Areas of sparse or questionable data would have high uncertainty.

B. Lack of Congruity - Tests of site conceptual and flow / transport models -
   - Do actual plume maps match predicted plumes?
   - Does site geology match regional geology?
   - Does site geology match geology reported from adjacent areas?

C. Outliers

   Spatial - for example:
   - bulls eyes around data points on contoured maps
   - areas of high characterization uncertainty

   Statistical (no spatial component) -
   - univariate includes control chart anomaly,
   - multivariate would include single-sample cluster

Short discussions of each site follow and highlight the unique site features, Performance Indicators or lessons learned. More detailed discussions are in subsequent chapters and include data that were available for the analysis.

1.1 Charleston Naval Weapons Station

At this site, a leaking solvent storage tank produced a plume of contaminated ground water. Initial site investigations were conditioned by proximity to a tidal creek, assumed to be the likely surface discharge place for ground water, and by a well with a low water level. Monitoring wells placed between the tank and the creek were free of contamination. Examination of water levels with time revealed that a well initially thought to be down-gradient should have been considered up-gradient. A seismic reflection survey and other geologic data were combined to produce a better Conceptual Site Model (CSM). This model included sandy channels interpreted from the seismic survey. The improved model led to practical suggestions regarding placement of monitoring wells for the purpose of Performance Confirmation Monitoring. Specifically, these results suggest that several wells can be abandoned, and that one additional well should be placed to test whether the plume is advancing.

This case highlighted the importance of continued validation of the conceptual model using site data. In this case three iterations of conceptual and transport modeling were necessary to produce a model with sufficient geologic complexity to reproduce observed results. This iterative process was key to identifying Performance Indicators for the site and for guiding recommended monitoring strategies.

A lesson learned is that periodic water level measurements might not give a true picture of the water table if wells respond differently to rainfall events or surface runoff.

1.2 Brookhaven National Laboratory

At Brookhaven National Laboratory (BNL), tritium leaked from a fuel storage pool into the ground water. Early attempts to understand the leak with horizontal wells beneath the reactor were confounded by the fact that tritium from this slow leak rode the top of the water table laterally until leaving the building footprint. Outside the area covered by the building, infiltrating precipitation moved the plume downward.

The shape of the plume has been delineated with wells and direct-push sampling. The plume shape is very narrow, prompting us to suspect geologic control, such as a sub-glacial channel, now buried, and to explore various modeling scenarios. Modeling suggests the plume shape may simply be a function of high hydraulic conductivity (without the need for a more complex geologic model), and that the plume migration is likely influenced by remediation pumping of extraction wells in the vicinity of the plume.

Because of a high density of sampling points, visualization of the plume is especially effective for communication of its extent. The cover illustration is of the BNL tritium plume.

Risk from the tritium is considered very low, and the main issue, rather than health, is public perception. Data visualization is a direct and readily understood way to share information with the all shareholders.

1.3 USGS Amargosa Desert Research Site

The U.S. Geological Survey (USGS) Amargosa Desert Research Site (ADRS) is at the location of the Nation's first licensed radioactive waste disposal site near Beatty, Nevada. USGS has maintained a research program here since 1975 with the objective of understanding dry climate hydrology. USGS has installed wells and collected data on migration of tritium and other contaminants including carbon-14 and mercury in the vadose zone. USGS has also conducted geophysical (e.g., resistivity) surveys and has modeled migration of tritium and mercury.

USGS reports that modeling results do not match the observed distribution of tritium. We evaluated all available site data to produce an alternative CSM which includes a fault as a preferential pathway for migration of tritium below the waste site. Rough spreadsheet modeling suggests the addition of the fault allows an improved match to the observed tritium concentrations.

The discussion points out the value of using all available data in constructing conceptual models, and the critical monitoring needed to test a proposed conceptual model.

Performance indicators that suggested issues with the conceptual site model included strong bending of water-table contours and the distribution of tritium at the water table.

1.4 Rocky Flats

Established in 1951, the primary mission of the Rocky Flats facility (RF) was to produce weapons components. Decades of these manufacturing operations led to several areas of contamination at this site. This report focuses on application of the Strategy at two areas of chlorinated organic solvent contamination.

In the first area of contamination, analysis of characterization data helped us identify a correlation in water table levels with observed episodic spikes in contaminant concentrations. This finding in turn led to an alternative conceptual model which can aid in determining how long some of the monitoring wells should remain in service.

In the second area of contamination, application of the Strategy revealed that careful plume mapping, including recognition of degradation products as key Performance Indicators, improves source definition. Some RF data are also used in the Data Analysis Chapter.

1.5 Savannah River C-Area

At the Savannah River Site (SRS), we find both tritium and chlorinated solvents issuing from a few sources near the reactor building. Because the facility is on a ground-water divide, contaminants from sources that are close together move in different directions. This site is very well characterized through monitoring wells and direct-push sampling.

Visualization of the ground-water sampling data is useful. Modeling suggests that solvents from this facility could have penetrated a regional confining unit and moved to the north beneath a local surface-water divide. Some sampling was done in the direction of plume movement, but modeling suggests the plume may not have reached the down-

gradient area at the time of sampling. This illustrates the importance of flow simulation to timing of sampling.

Additional data discovered during application of the Strategy suggest that the CSM used by all modelers, including ourselves, maybe too simplistic and that a confining unit could be breached by faulting. It appears that the current data distribution does not permit an adequate test of this hypothesis. The level of risk does not justify further characterization, but it is likely that the CSM is flawed.

Application of the Strategy helped guide recommendations made with regard to further monitoring activities.

1.6 Hanford Site 300 Area

DOE's Hanford Site 300 Area is located immediately adjacent to the Columbia River. River discharge is roughly 50,000 cfs adjacent to the Site, and river elevation (stage) is controlled by dams. Recent work reported by researchers at the Pacific Northwest National Laboratory is used as a backdrop to a discussion of some modeling and monitoring issues including the impact of river stage changes on movement of a uranium plume.

One possible addition to the current CSM is the inertia of river water impinging on the cutbank adjacent to the 300 Area. Indicators (PIs) of this model modification include the distribution of nitrate and uranium plumes adjacent to the river as well as average water table elevations.

1.7 Data Analysis

Chapter 8 briefly discusses approaches to data analysis techniques, and highlights some common pitfalls and issues which can confuse interpretation of monitoring data. Data analysis may lead to results that challenge an existing conceptual site model and the understanding of how site facilities, geology, and ground water interact and behave. Data analysis and data mining are essentially synonymous. This is not a chapter on statistical testing.

Data examples are drawn largely from the DOE Savannah River Site (SRS), the Rocky Flats Site, and from a uranium mining and milling site in the northwestern United States.

Quarterly water levels in wells cannot be simply and reliably related to rainfall data. There is some suggestion that data loggers may provide water level data that can be related to rainfall.

Rainfall data from weather stations across the SRS are compared. Results suggest that ground-water studies including infiltration estimated from rainfall must use very local rainfall data.

Analysis of 20 years of water level data highlights some QA issues with field measurements and with well construction. Data are used to illustrate some statistical methods to identify trends or to group data based on general chemistry as well as contaminants. Anomalous water levels occur at widely separated wells on the same

sampling date, suggesting opportunities for data QA. A FORTRAN program for well-to-well correlation and the Mann-Kendall test is listed.

Also discussed are simple tests of trends in data that may obscure data structure and require examination of the hydrogeologic conceptual model.

A proposed alternative conceptual model at the northwestern U.S. site is that the water table and a lower water bearing zone presented by the site custodian were actually one underground water body because of breach of a proposed confining unit by faulting. Data analysis indicates that a few contaminated wells stand out, but that most wells yield water that can be grouped into two chemically distinct groups or clusters. This supports the site custodian's original conceptual site model that a confining layer has some integrity across the site.

2 Charleston Naval Weapons Station

2.1 Introduction

The Charleston Naval Weapons Station is located just north of Charleston, South Carolina on about 17,000 acres of land. Solid Waste Management Unit 12 (SWMU 12) is located in the southeastern portion of the base, near the Cooper River (Figure 2-1). This site housed a wood treatment facility that operated from the early 1970s to 1981 (Danielsen, 2003).

The site is relatively flat with a total relief ranging from 3.0 to 8.5 feet above mean sea level. Four structures were located at the site. The area outside of the fence line consists of forest, wetlands, and marshes.

Past operations at the site included use of the hazardous wood preservative pentachlorophenol (PCP). In 1998, a breached 500-gallon underground storage tank was found during a RCRA Facility Investigation, and elevated levels of chlorinated organic solvents were confirmed in site ground water (Danielsen, 2003).

Figure 2-1. Map showing the location of SWMU 12 at the Charleston Naval Weapons Station (Danielsen, 2003).

In 2001, a seismic survey performed at the site revealed the presence of shallow high permeability channels in the subsurface. Conceptual site models which included these channels were developed for computer simulations of flow and transport as part of this strategy application. Visualization of contaminant transport over time using these simulations enabled AES to design a Performance Confirmation Monitoring plan that included abandonment of several existing monitoring wells, as well as the placement of one additional sentinel well.

2.2 Compilation and Analysis of Available Data

2.2.1 Regional Geology

The geology of the Charleston Naval Weapons Station is made up of sediments deposited through near-shore coastal processes. Sands grade into clays and back into sands, presenting a complex pattern of layers, as ancient tidal channels meandered through the ancient salt marsh, with intervening beach ridges and sand dunes (Weems and Lemon, 1993). Figure 2-2 is an example of a cross section through a complex coastal environment.

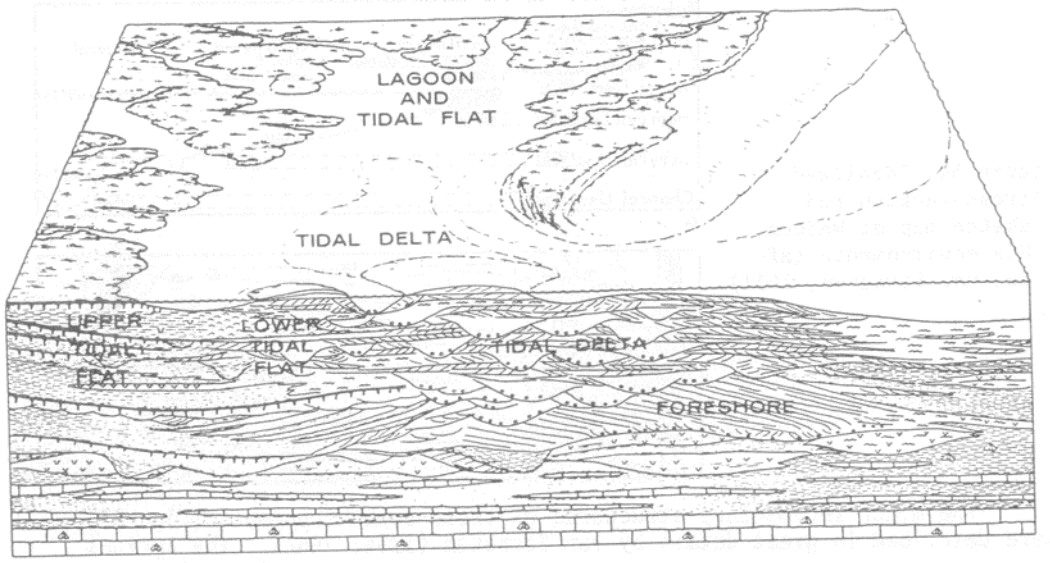

Figure 2-2. This cross section is an example of the complex geology that can result from a changing coastal environment. (Figure from Ferm in Saxena, 1976, Fig. 2)

The surface unit in the area is the Wando Formation. The Wando Formation lithology is variable and includes both fluvial and estuarine facies. Typically these include coarse-grained, poorly sorted, cross-bedded sands and clayey, fine- to medium-grained quartz sands, sandy to clayey silts, and sandy to silty clays (Gohn et al., 2000).

At a depth of about 40 ft the Ashley Formation is present. This unit is referred to in characterization reports as the Cooper Marl. The Ashley Formation consists of a relatively homogeneous section of calcareous, phosphatic, microfossiliferous, silty and sandy clays deposited in a fluvial and estuarine environment.

2.2.2 Site Hydrogeology

The total area of the contaminant release site, referred to as Solid Waste Management Unit 12 (SWMU 12), is approximately 3 acres. SWMU 12 is relatively flat with a total relief ranging from 3.0 to 8.5 feet above mean sea level. The water table is very shallow, ranging from 2 to 3 feet below ground surface. Danielsen (2003) interprets the ground-water flow to be primarily toward the east with a minor northerly component, except in wet periods, where it flows toward the northern marsh with a slight easterly component (Figure 2-3).

Figure 2-3. Map of SWMU 12 showing locations of wells and nearby marshes (Danielsen, 2003).

In down-gradient parts of the plume, a shallow clay layer does not allow the contaminants to encounter water until a depth of about 8 to 10 ft below ground surface. The contaminated aquifer consists of fine sand beneath clay. The average horizontal

hydraulic conductivity of the aquifer is approximately 1.2 ft/day (DOD, 2005). The potentiometric surface is relatively flat lying, with an average hydraulic gradient of 0.0015 to 0.0017 ft/ft. Recharge most likely occurs primarily through infiltration in areas where the surficial clay is breached or absent (DOD, 2005).

Seismic evidence suggests that parts of the sand aquifer may be ancient buried channels (Figure 2-4 and Figure 2-5). This hypothesis is supported by hydraulic conductivity estimates from slug test data (Table 2-1). When the hydraulic conductivity is graphed verses the cumulative percentage of samples having that value or less (Figure 2-6), we can see two distinct sample populations, these populations correspond to where the slope of the line changes. We interpret the higher conductivity values to belong to wells screened in the channels.

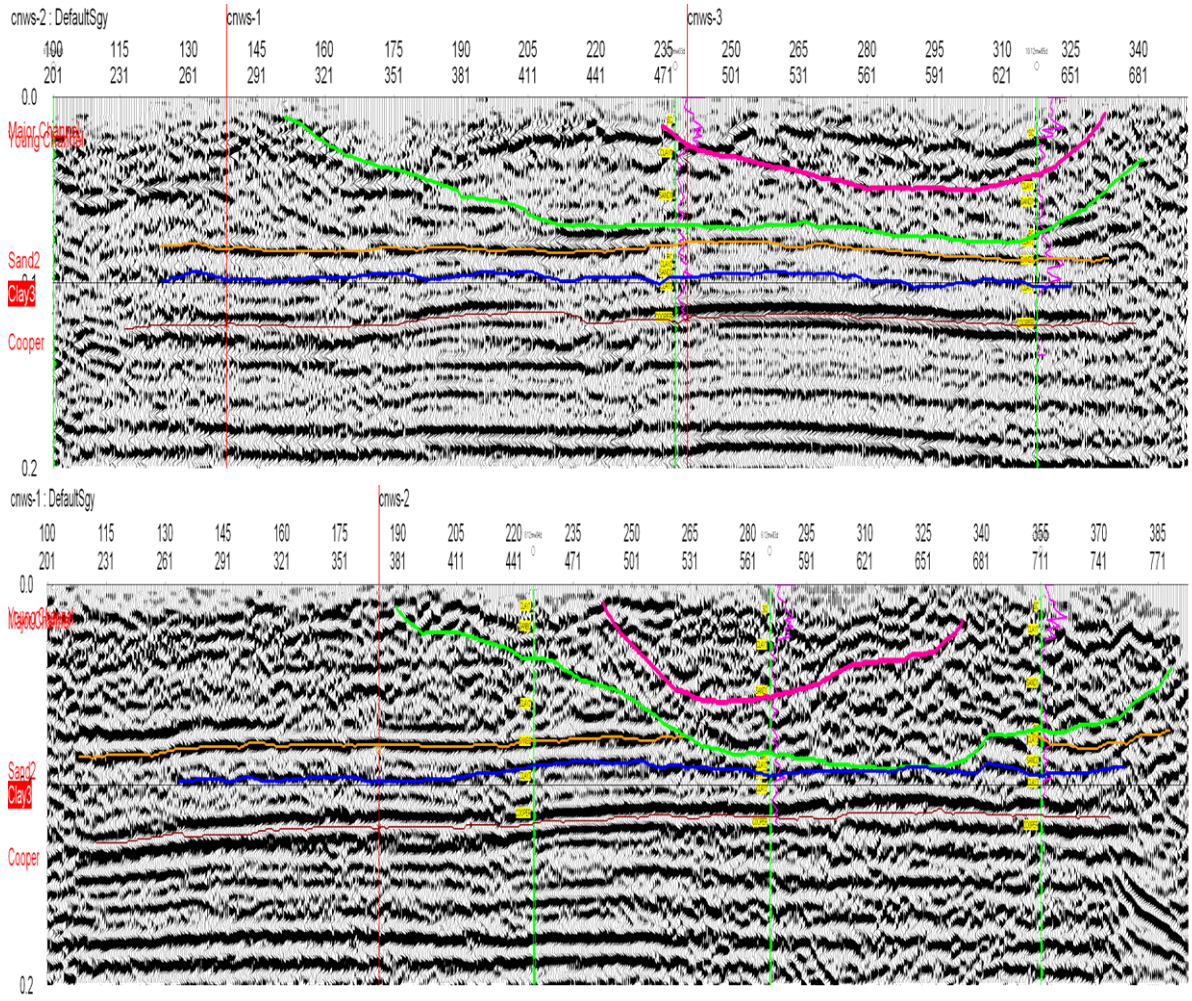

Figure 2-4. Seismic reflection profiles. The green line is interpreted as the base of the major channel or the older channel, the red line indicates the base of younger channel that has incised into the older channel.

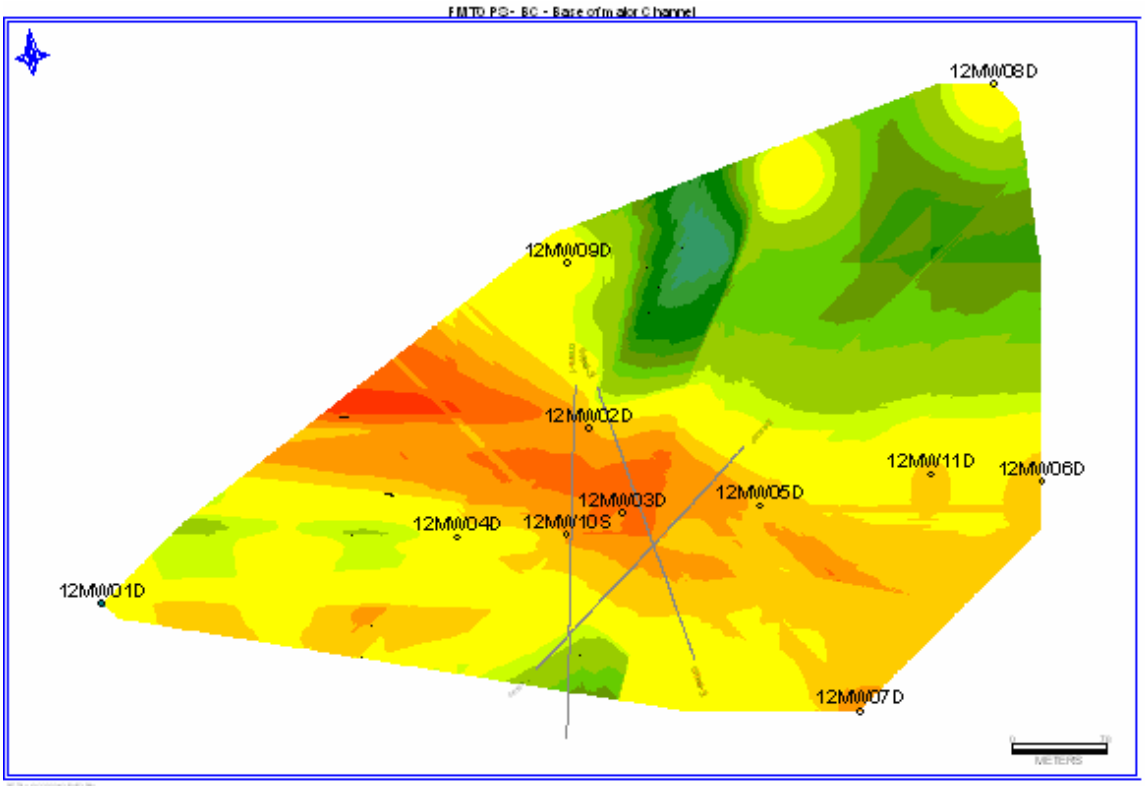

Figure 2-5. Elevation of the base of the channel contoured from seismic data and well picks. The orange shows the lower elevations, the green shows the higher elevations, and the grey lines represent the seismic profile locations.

Table 2-1. Slug test data compared to the number of hammer blows needed to penetrate 1 ft, averaged over the length of the screen zone.

Well	Screen Zone Depth (ft)	Average Blow Counts	Slug test results (ft/d)
12mw01D	29-39	3.43	2.86
12mw01S	4-14	3.95	3.69
12mw02D	21-31	2.38	2.98
12mw02S	4-14	5.14	1.06
12mw03D	20-30	2.29	3.19
12mw03S	4-14	6.10	4.19
12mw04D	22-32	3.19	1.47
12mw04S	4-14	4.00	7.22
12mw05D	38.5-48.5	0.69	0.432
12mw05S	4-14	4.46	3.7
12mw06D	32-42	1.48	0.36
12mw06S	4-14	5.46	0.0873
12mw07D	35-45	1.52	0.19
12mw07S	4-14	2.29	0.93
12mw08D	29-39	0.29	0.073
12mw08S	4-14	5.96	0.17
12mw09D	26-36	1.48	5.3
12mw09S	4-14	4.96	3.2

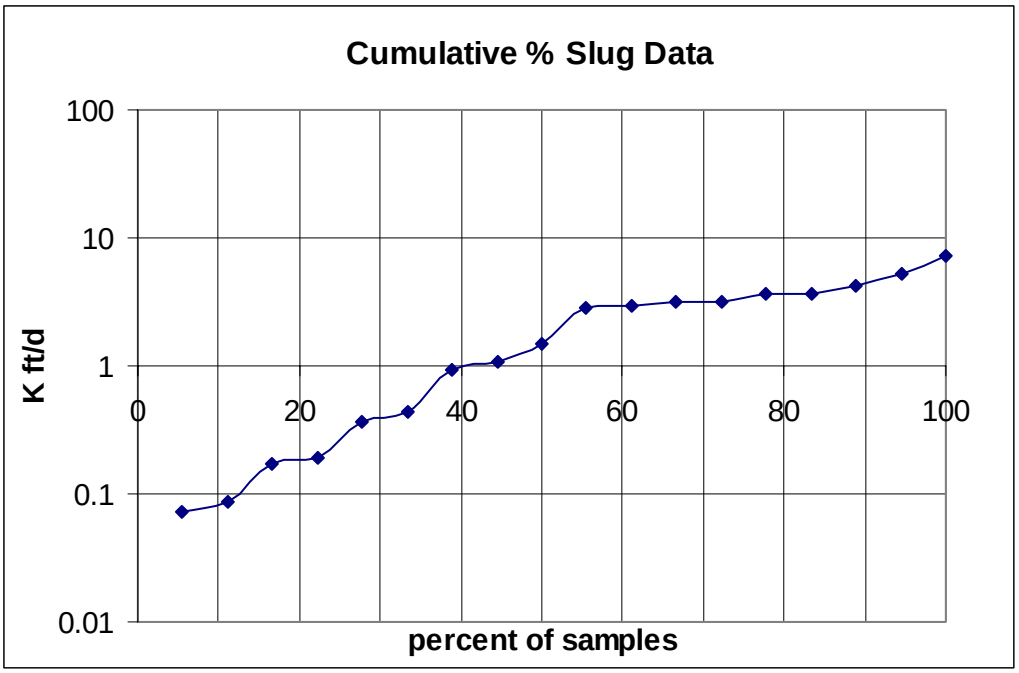

Figure 2-6. Graph of data from the slug test, with hydraulic conductivity (ft/d) on the vertical axis and the cumulative percentage of samples having that value or less plotted on the horizontal axis.

2.3 Conceptual Site Modeling

Prior to modeling, the data must be collected and formatted to allow for sequential modeling using a graded approach. Our approach began with a simple Conceptual Site Model that honored existing data. The CSMs were gradually increased in complexity until the model output adequately represented the flow regime for the site as judged by comparison of predicted contaminant levels with monitoring results. In total, three conceptual models were developed. Each of these models is discussed in detail below.

2.3.1 First Approach: Analytical Model:

The first approach assumed a one-layer homogeneous aquifer structure with semi-infinite boundary conditions (Figure 2-7). An analytical solution of the reactive solute transport can be obtained with BIOCHLOR (Aziz et al., 2000). The results completely failed to match the plume data. Multiple iterations using different parameters failed to achieve results that matched the field conditions at the site.

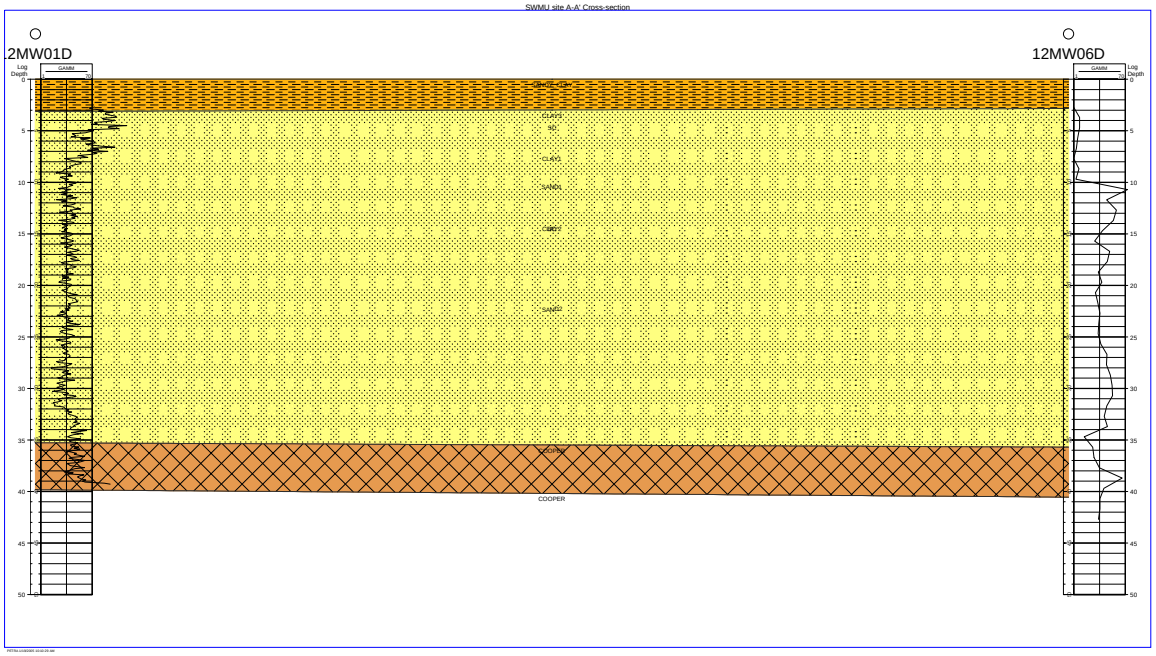

Figure 2-7. Cross Section of the assumed geology for the analytical solution CSM.

2.3.2 Second Approach: Numerical Model / Simple Geology:

The second approach used only borehole descriptions and geophysical log data to develop the CSM. This model incorporated a layer-cake multi-aquifer system (Figure 2-8). Petra was used to perform the correlations that were exported into GMS for modeling. In GMS MODFLOW and RT3D were used to simulate the migration of the chlorinated solvents.

The results from Model II yielded a better fit than the first approach but did not adequately define the plume (Figure 2-9).

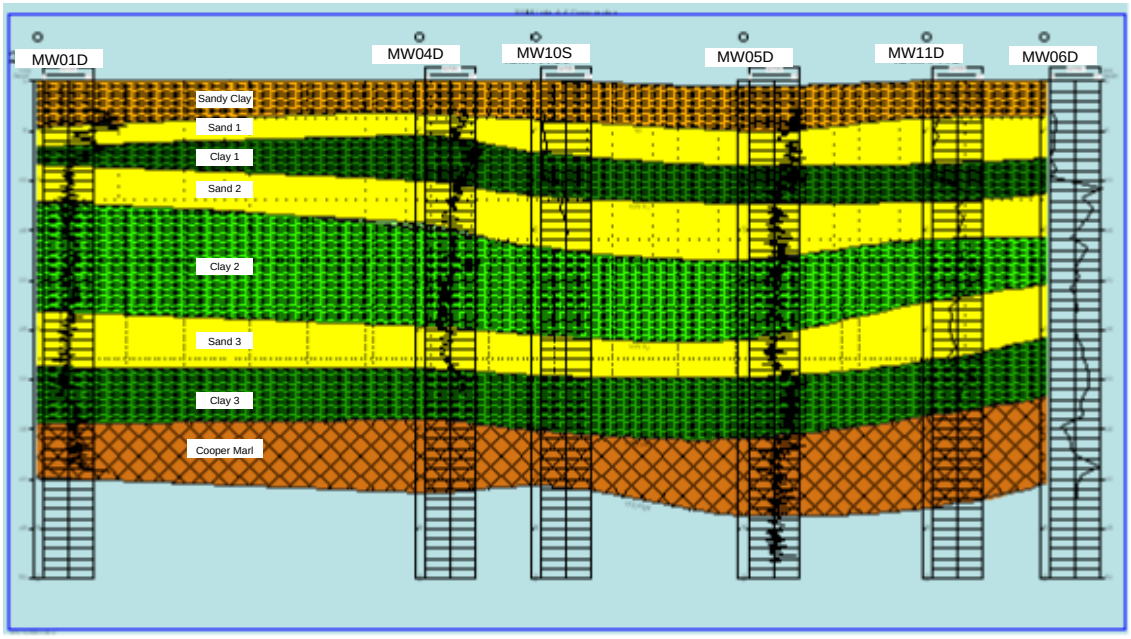

Figure 2-8. Cross Section of the "Layer Cake Geology" used for our second approach.

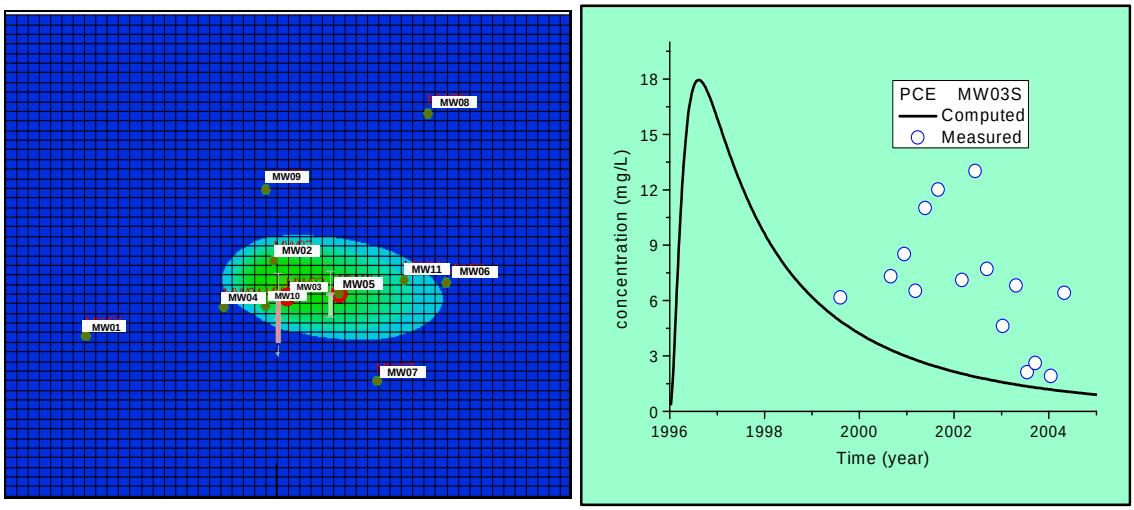

Figure 2-9. The PCE plume from Model II is presented at left, and the computed PCE concentrations at monitoring well MW-03 are much lower than the observed values (right).

2.3.3 Third Approach: Numerical Model / Complex Geology

The third approach entailed development of a site model that incorporated both the geologic and seismic data in an attempt to more accurately represent the subsurface geology. These data were input into Petra and PetraSeis (Figure 2-10). Table 2-2 contains the input parameters for Model III. Based on the seismic data two ancient stream channels were mapped through the middle of the PCE source. The channels control the local ground-water flow direction and provide a preferential chemical transport pathway. This new interpretation of the conceptual site model was used to run simulations again in GMS.

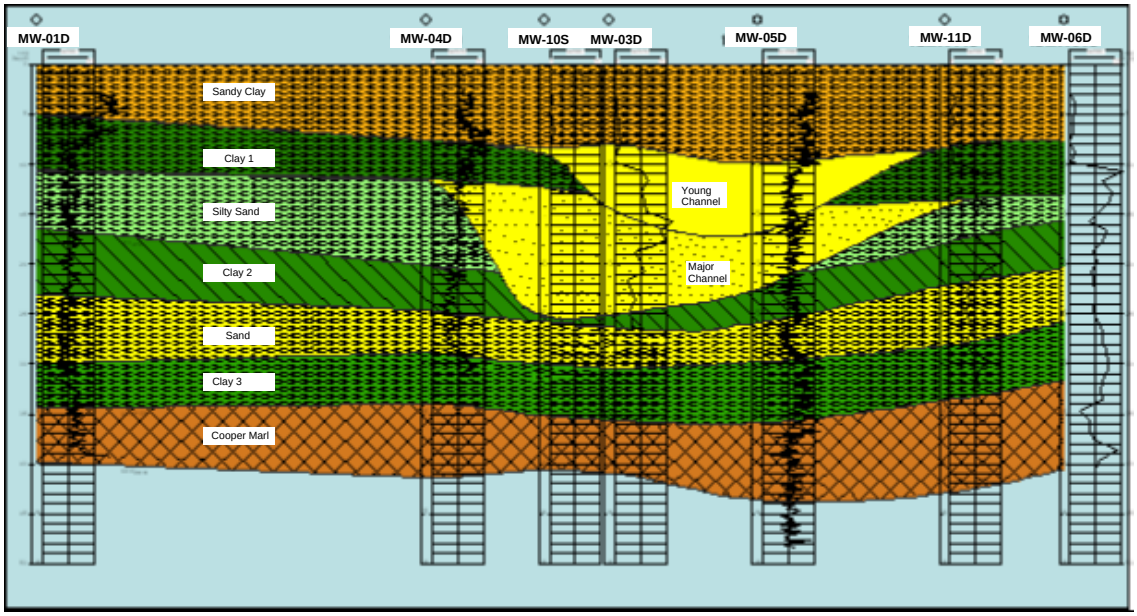

Figure 2-10. The cross-section shows the Major channel and Younger channel, as well as the other hydrofacies in the site.

By using a relatively high Horizontal K, and a low Kd for both of the channels (Table 2-2), model output from the third simulation closely matched observed PCE concentrations and accurately predicted the direction and extent of the plume (Figure 2-11).

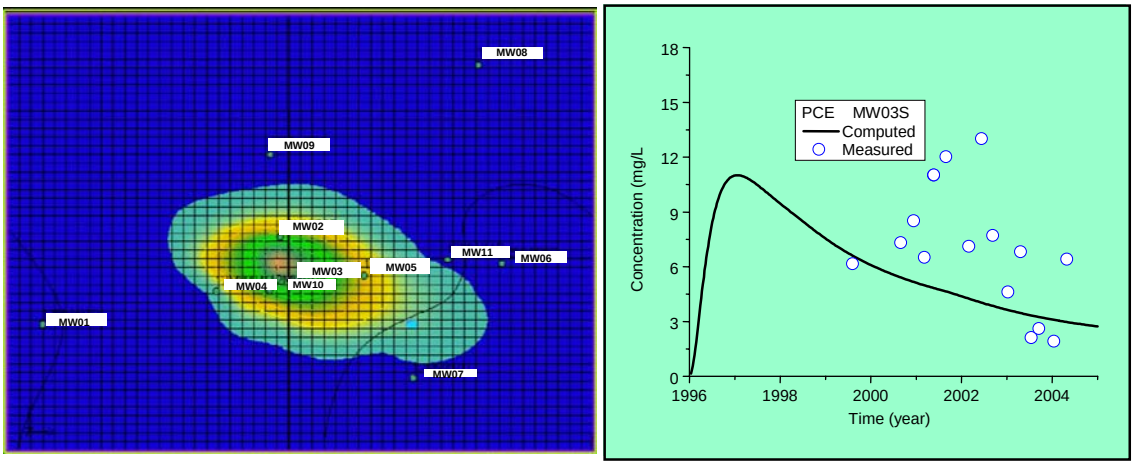

Figure 2-11. The simulated PCE plume from Model III is presented at left; computed PCE concentrations at monitoring well MW-03 more closely match observed values (right).

Table 2-2. Estimated flow and transport parameters for Model III.

Stratigraphic units	Horizontal K (ft/d)	Vertical K (ft/d)	Long dispersivity	PCE K_d (mL/g)	TCE K_d (mL/g)
Sandy clay	0.085	0.05	65	1.15	0.96
Young channel	48	1.2	112	0.43	0.28
Clay 1	0.06	0.01	83	1.36	0.84
Major channel	41	1	98	0.48	0.35
Silty sand	0.2	0.1	75	1.18	0.91
Clay 2	0.05	0.009	50	1.28	0.82
Sand	8	2	50	0.99	0.60
Clay 3	0.005	0.001	50	1.28	0.60
Cooper marl	0.2	0.05	50	1.15	0.96

2.4 Designing a Performance Confirmation Monitoring Network

After validation of the CSM with actual site data, AES used this model to determine an appropriate monitoring scheme for the contaminant plume. Specifically, the current monitoring program included four wells located outside the predicted 5-year footprint of the PCE plume (see circled wells in Figure 2-12). Removal of these 4 wells from future monitoring is recommended. The monitoring scheme also lacked any monitoring in the vicinity of the predicted plume head. A new monitoring point was recommended to be added at the yellow dot in Figure 2-12.

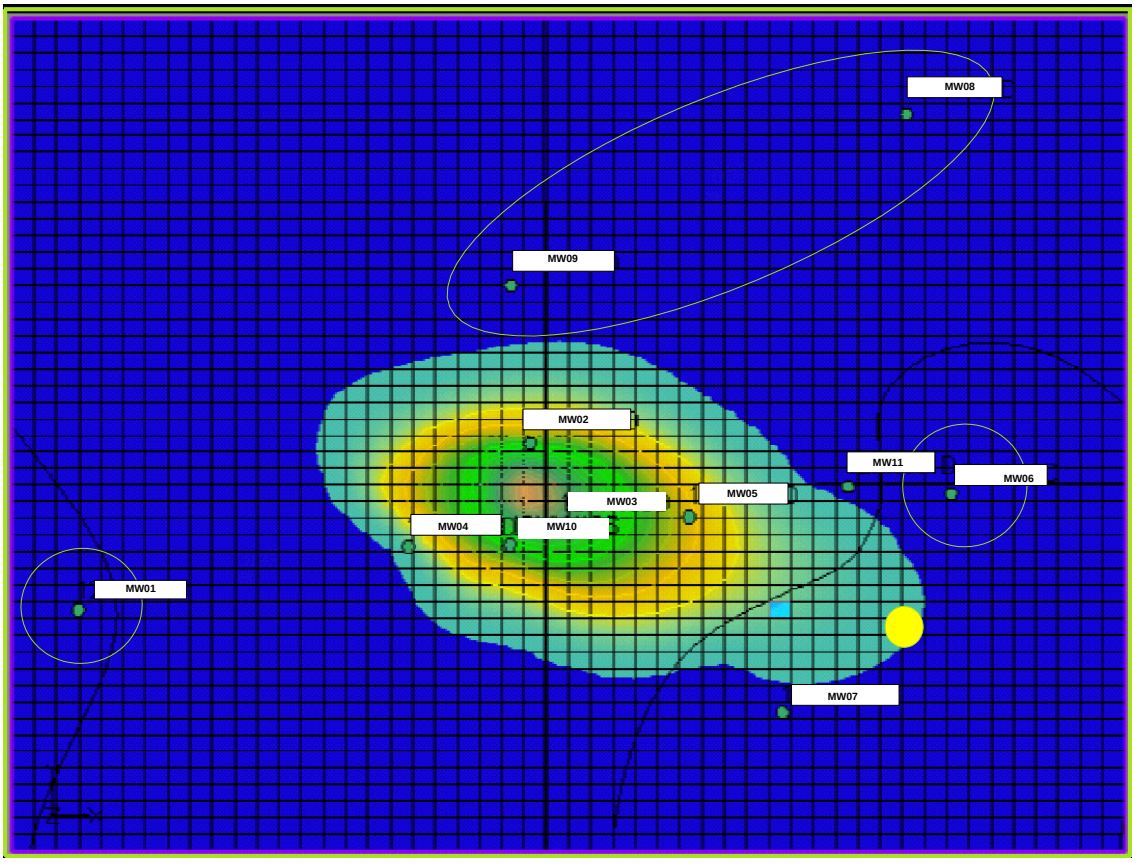

Figure 2-12. The predicted PCE plume in five years. Circled wells are suggested to be removed from the monitoring program to save money, while a new point is suggested to be added at the yellow dot to test the CSM and simulation results.

2.4.1.1 Alternate Conceptual Site Model

Further review of water level data (Table 2-3), revealed that MW-08 was an outlier because the water levels did not follow the same patterns as the other wells (Figure 2-13). Because of the nearly flat water table, the water level differences in MW-08 can seriously alter contour maps of the water table (Figure 2-14 and Figure 2-15).

This well should be investigated to determine the cause of the observed water level discrepancies. If the discrepancies are caused by poor well construction or poor data quality, then the water levels in this well should be ignored. If, however, the data proves reliable, this well could indicate the need to further revise the CSM. In particular, close attention should be paid to how the ground-water flow changes with respect to climatic conditions.

Table 2-3. Water elevations (ft above MSL) in wells.

Well Name	Apr-98	Jun-98	Aug-99	Jul-04	May-05
12MW01S	5.34	3.32	3.39		
12MW02S	5.26	3.16	3.29		2
12MW03S	5.27	3.16	3.3	2.74	2.07
12MW04S	5.35	3.23	3.4	2.72	2.14
12MW05S			3.19	2.52	1.79
12MW06S			2.65	2.47	1.71
12MW07S			3.14	2.53	1.82
12MW08S			3.61	3.81	1.25
12MW09S			3.28	2.67	1.88

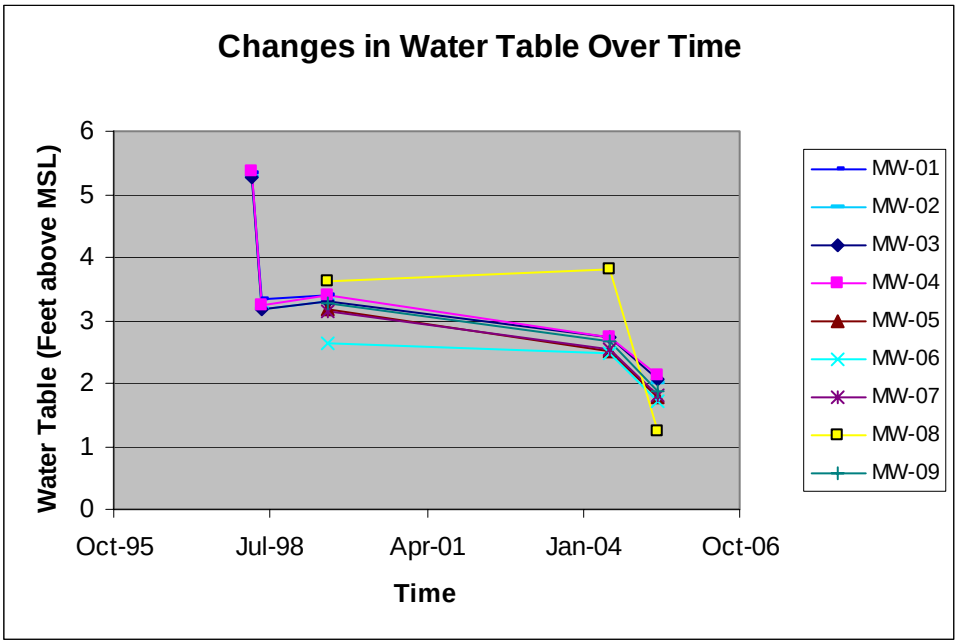

Figure 2-13. Change in water table over time. Note how MW-08 is the only well that doesn't match the others.

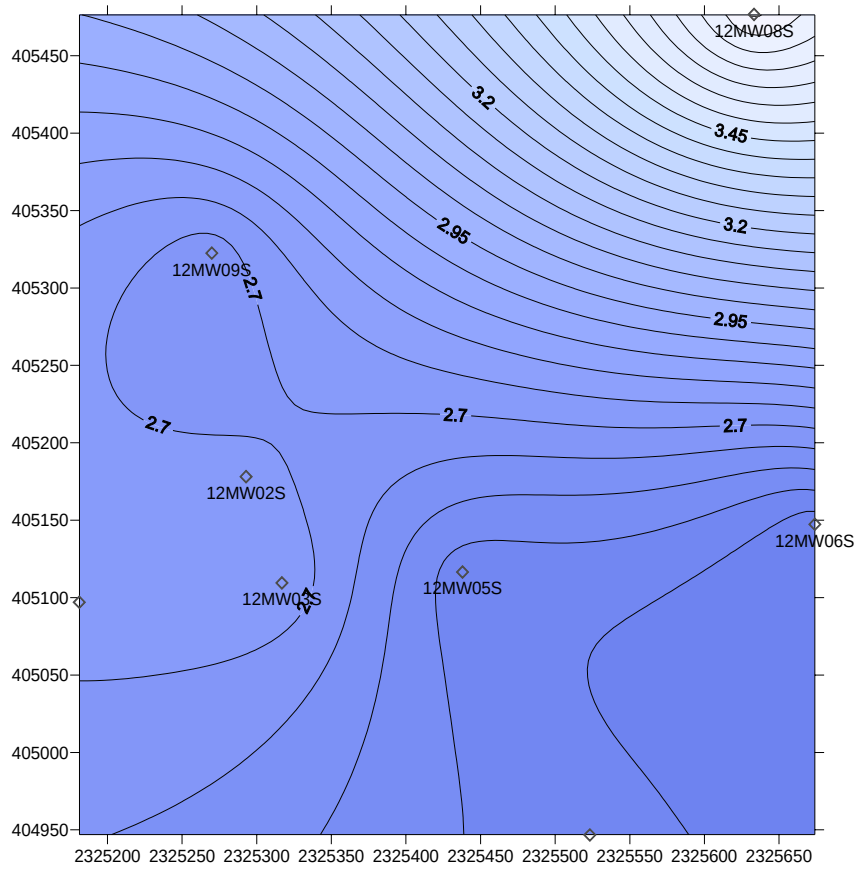

Figure 2-14. Contour Map of water table using data from July 2004 (feet above MSL)

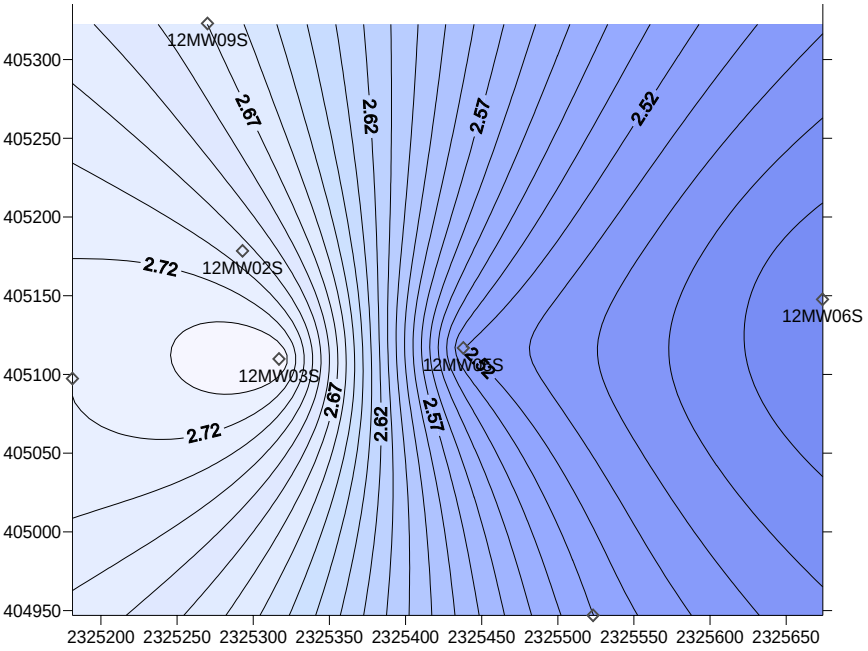

Figure 2-15. Contour map of water table using data from July 2004, without well MW-08 (feet above MSL)

2.5 Strategy Application Conclusions

This study demonstrates the importance of adequate conceptual site modeling as a tool to assess monitoring network performance. In this case, the conceptual site model simulation helped improve understanding of the extent of contamination and guided suggestions which may increase efficiency of the existing monitoring scheme and, significantly reduce monitoring costs. Specifically in this case, four monitoring wells were removed from the network, and one was added in order to better observe the plume frontier.

Outcome from this case suggests that the bias and uncertainty introduced from inadequate conceptual models can exceed those introduced from an inadequate choice of model parameter values. In particular, adequate mapping of the subsurface geology through incorporation of log and seismic survey data with geophysical software was important in developing an accurate conceptual site model.

Time trend analysis of water levels from monitoring wells results in very good correlation, with the exception of MW-08. The discrepancies between MW-08 and the other monitoring wells result in significant variations in the modeled water table surface. Because MW-08 has been identified as an outlier, these discrepancies should be evaluated.

Figure 2-16 presents a visual illustration of the activities and outcomes resulting from application of the Strategy at the Charleston Naval Weapons Station below.

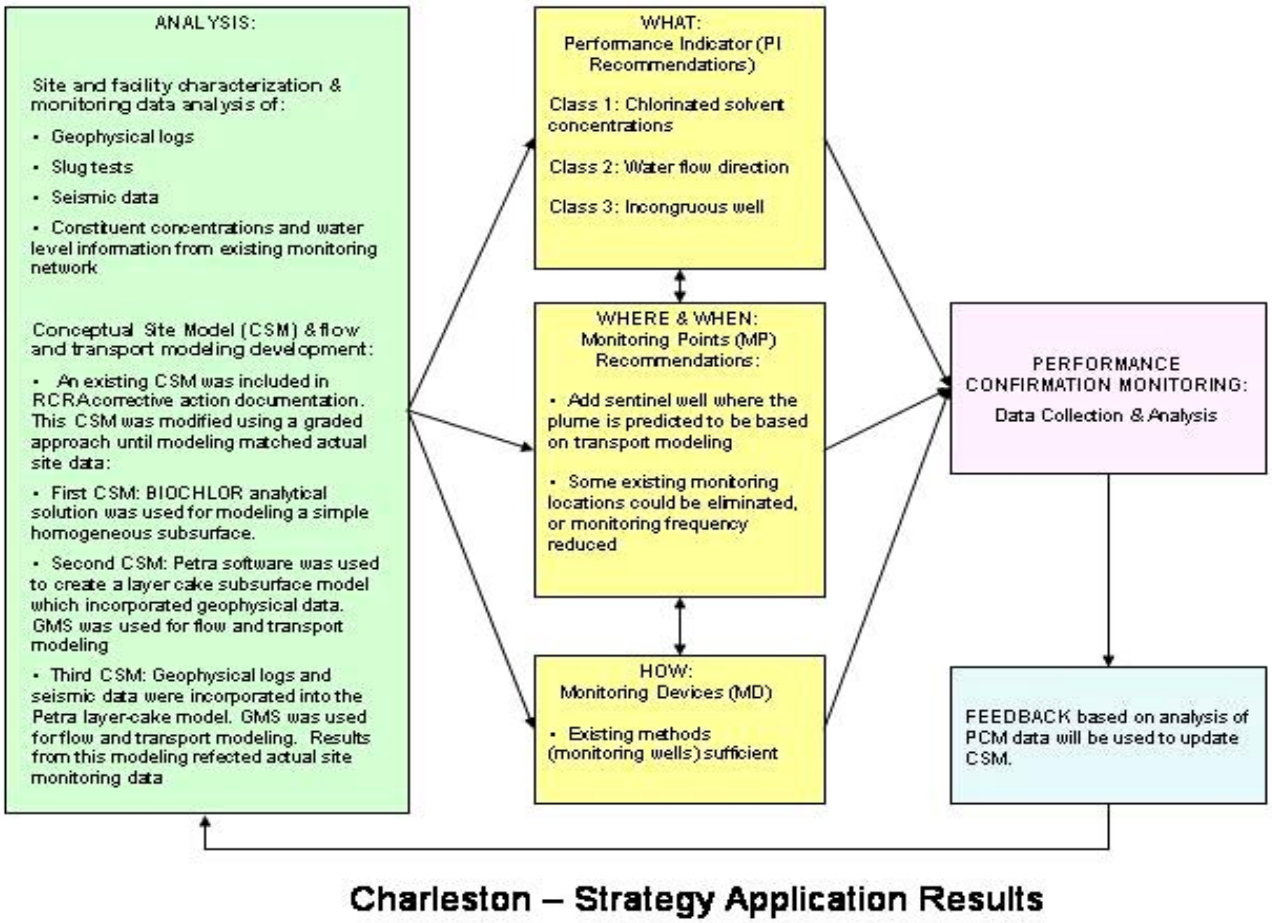

Figure 2-16. Activities and results of the Strategy application at Charleston Naval Weapons Station

2.6 Charleston References

Aziz, C.E., et al. EPA /600/R-00/008. "BIOCHLOR Version 1.0, User's Manual." 2000.

Department of Defense. *Site Information for RDT&E Opportunities, Strategic Environmental Research and Development Program.* November 2005.

Ferm, J.C.. *Depositional Model in Coal Exploration and Development, Sedimentary Environments and Hydrocarbons,* R.S. Saxena, ed. AAPG/NOGS Short Course, New Orleans Geological Society. pp. 60–78. 1976.

Gohn, G.S., et al. "Preliminary Stratigraphic Database for the Subsurface Tertiary and Uppermost Cretaceous Sediments of Dorchester County, South Carolina." U.S. Geological Survey Open-File Report 00-049-A. 2000.

Danielsen, M.W. *The Use and Implementation of Innovative Technologies for Investigating Selected Sites at the Naval Weapons Station, Charleston, South Carolina.* Master Thesis for University of South Carolina. 2003.

Weems, R.E., and E.M., Jr. Lemon. *Geologic Map of the Cainhoy, Charleston, Fort Moultrie, and North Charleston quadrangles, S.C., with text (1:24,000).* U.S. Geological Survey Map I-1935. 1993.

Appendix 2-A.

Summary of Selected Volatile Organic Compounds in Ground Water

SWMU 12 Naval Weapons Station, Charleston

Location ID	Sample Date	PCE ug/L	TCE ug/L	cis-1,2-DCE ug/L	Vinyl Chloride ug/L	1,1,1-TCA ug/L	1,1-DCE ug/L	1,1-DCA ug/L	1,2-DCA ug/L
12MW02D	8/30/00	< 5	< 5	< 5	< 2	< 5	< 5	< 5	< 5
12MW02D	11/29/00	< 0.21	< 0.17	< 0.17	< 0.15	< 0.18	0.22	< 0.18	< 0.21
12MW02D	2/27/01	< 0.13	< 0.14	< 0.24	< 0.17	< 0.22	< 0.16	< 0.23	< 0.2
12MW02D	5/15/01	< 0.38	1.5	< 0.31	< 0.19	< 0.27	< 0.26	< 0.29	< 0.35
12MW02D	8/29/01	< 0.13	< 0.14	< 0.24	< 0.17	< 0.22	0.32	< 0.23	< 0.2
12MW02D	12/3/01	< 0.13	< 0.14	< 0.24	< 0.17	< 0.22	< 0.16	< 0.23	< 0.2
12MW02D	2/28/02	< 0.13	< 0.14	< 0.24	< 0.17	< 0.22	< 0.16	< 0.23	< 0.2
12MW02D	6/10/02	< 0.1	< 0.13	< 0.28	< 0.18	< 0.17	< 0.13	< 0.64	< 0.15
12MW02D	9/9/02	2.1	1.2	0.25	< 0.2	0.52	1.2	0.39	< 0.18
12MW02D	1/8/03	0.2	0.36	< 0.28	< 0.18	< 0.17	0.35	< 0.64	< 0.15
12MW02D	4/15/03	< 0.17	< 0.12	< 0.22	< 0.1	< 0.16	< 0.17	< 0.11	< 0.14
12MW02D	7/16/03	< 0.31	< 0.25	< 0.4	< 0.11	< 0.27	< 0.41	< 0.3	< 0.34
12MW02D	8/16/04	< 0.31	< 0.25	< 0.4	< 0.11	< 0.27	< 0.41	< 0.3	< 0.34
12MW02S	8/30/00	0	0	0	0	0	200	12	0
12MW02S	11/29/00	< 0.21	0.24	0.75	< 0.15	< 0.18	110	5.7	< 0.21
12MW02S	2/27/01	< 1.3	< 1.4	< 2.4	< 1.7	< 2.2	160	8.6	< 2
12MW02S	5/15/01	< 3.8	6.4	< 3.1	< 1.9	< 2.7	81	5.4	< 3.5
12MW02S	8/29/01	< 0.21	4.8	< 0.56	< 0.35	< 0.33	23	2.1	< 0.3
12MW02S	12/3/01	< 0.25	0.47	0.66	< 0.35	< 0.44	69	5.5	< 0.39
12MW02S	2/28/02	< 0.63	< 0.68	< 1.2	< 0.87	< 1.1	46	2.8	< 0.98
12MW02S	6/10/02	< 0.52	< 0.64	< 1.4	< 0.88	< 0.84	84	6.7	< 0.76
12MW02S	9/9/02	< 0.82	< 0.83	< 1	< 0.99	< 1.3	58	5.4	< 0.88
12MW02S	1/8/03	< 0.52	2.3	1.6	< 0.88	< 0.84	130	15	< 0.76
12MW02S	4/15/03	< 2.2	< 1.5	2.9	< 1.3	< 2.1	250	27	< 1.8
12MW02S	7/15/03	< 3.1	< 2.5	< 4	< 1.1	< 2.7	100	14	< 3.4
12MW02S	9/17/03	< 1.7	2.1	< 2.2	2.8	< 1.6	150	26	< 1.4
12MW02S	1/14/04	< 2.2	< 1.5	< 2.7	< 1.3	< 2.1	140	29	< 1.8
12MW02S	4/28/04	< 2.6	11	11	3.4	< 2.4	530	200	< 2.7
12MW02S	8/16/04	< 0.31	< 0.25	< 0.4	< 0.11	< 0.27	1.9	< 0.3	< 0.34
12MW03D	8/30/00	0	6	18	0	0	0	0	0
12MW03D	11/30/00	< 0.41	5.8	24	< 0.31	< 0.36	0.99	< 0.35	< 0.42
12MW03D	2/27/01	< 0.13	1.4	6.8	< 0.17	< 0.22	0.54	< 0.23	< 0.2
12MW03D	5/15/01	6	15	15	0.88	9.8	7.5	1.6	< 0.35
12MW03D	8/29/01	< 0.1	12	19	0.73	< 0.17	2.7	< 0.64	< 0.15
12MW03D	12/4/01	< 0.1	33	44	1.3	< 0.17	6.3	< 0.64	< 0.15
12MW03D	3/1/02	< 0.13	3.3	13	0.2	< 0.22	1.2	< 0.23	< 0.2
12MW03D	6/11/02	< 0.1	19	21	< 0.18	< 0.17	3.2	< 0.64	< 0.15
12MW03D	9/10/02	0.7	4.6	14	0.3	0.57	2.1	0.45	< 0.18
12MW03D	1/9/03	< 0.1	2	11	0.73	< 0.17	1.2	< 0.64	< 0.15
12MW03D	4/15/03	< 0.31	3.2	11	0.65	< 0.27	1.9	1.8	< 0.34
12MW03D	7/15/03	< 0.17	3.3	13	0.82	< 0.16	1.9	1.5	< 0.14
12MW03D	8/16/04	< 0.31	4	16	1.8	< 0.27	4.3	4.7	< 0.34
12MW03S	8/30/00	7300	9,500	7,600	1,600	16,000	4,500	4,000	2,300
12MW03S	11/30/00	8500	9000	7000	160	31000	11000	5100	< 170
12MW03S	2/27/01	6500	5200	12000	230	3700	3100	2100	< 200
12MW03S	5/15/01	11000	7900	8900	< 940	76000	29000	20000	< 1700

12MW03S	8/29/01	12000	16000	12000	< 880	73000	34000	23000	< 760
12MW03S	12/5/01	16000	12000	14000	< 880	92000	46000	35000	< 760
12MW03S	3/1/02	7100	5600	13000	600	5300	5400	4500	< 200
12MW03S	6/11/02	13000	5900	13000	1100	32000	20000	16000	260
12MW03S	9/10/02	7700	4700	13000	430	5200	6100	5300	< 190
12MW03S	1/9/03	4600	4300	7300	370	4000	5100	3300	45
12MW03S	4/21/03	6800	3600	9900	640	15000	12000	8800	150
12MW03S	7/17/03	2100	1900	3100	140	580	1200	960	< 85
12MW03S	9/16/03	2600	1400	2800	120	1700	2300	1200	< 50
12MW03S	1/14/04	1900	3000	3300	150	940	1700	1000	< 17
12MW03S	4/27/04	6400	5300	5700	380	8100	10000	5100	65
12MW03S	8/18/04	1200	1400	1700	96	370	1000	590	< 27
12MW04D	8/28/00	< 5	< 5	< 5	< 2	< 5	< 5	< 5	< 5
12MW04D	11/28/00	< 0.21	< 0.17	< 0.17	< 0.15	< 0.18	< 0.17	< 0.18	< 0.21
12MW04D	2/26/01	< 0.13	< 0.14	< 0.24	< 0.17	< 0.22	< 0.16	< 0.23	< 0.2
12MW04D	5/14/01	< 0.38	< 0.34	< 0.31	< 0.19	< 0.27	< 0.26	< 0.29	< 0.35
12MW04D	8/27/01	< 0.38	< 0.34	< 0.31	< 0.19	< 0.27	< 0.26	< 0.29	< 0.35
12MW04D	12/3/01	< 0.1	< 0.13	< 0.28	< 0.18	< 0.17	< 0.13	< 0.64	< 0.15
12MW04D	2/28/02	< 0.13	< 0.14	< 0.24	< 0.17	< 0.22	< 0.16	< 0.23	< 0.2
12MW04D	6/11/02	< 0.1	< 0.13	< 0.28	< 0.18	< 0.17	< 0.13	< 0.64	< 0.15
12MW04D	9/9/02	< 0.16	< 0.17	< 0.2	< 0.2	< 0.26	< 0.33	< 0.24	< 0.18
12MW04D	1/7/03	< 0.1	< 0.13	< 0.28	< 0.18	< 0.17	< 0.13	< 0.64	< 0.15
12MW04D	4/15/03	< 0.31	0.28	< 0.4	< 0.11	< 0.27	< 0.41	< 0.3	< 0.34
12MW04D	7/14/03	< 0.17	< 0.12	< 0.22	< 0.1	< 0.16	< 0.17	< 0.11	< 0.14
12MW04D	8/18/04	< 0.2	< 0.2	< 0.15	< 0.15	< 0.19	< 0.18	< 0.2	< 0.22
12MW04S	8/28/00	< 5	< 5	< 5	< 2	< 5	< 5	< 5	< 5
12MW04S	11/28/00	< 0.21	< 0.17	< 0.17	< 0.15	< 0.18	< 0.17	< 0.18	< 0.21
12MW04S	2/26/01	< 0.13	< 0.14	< 0.24	< 0.17	< 0.22	< 0.16	< 0.23	< 0.2
12MW04S	5/14/01	< 0.38	< 0.34	< 0.31	< 0.19	< 0.27	< 0.26	< 0.29	< 0.35
12MW04S	8/27/01	< 0.38	< 0.34	< 0.31	< 0.19	< 0.27	< 0.26	< 0.29	< 0.35
12MW04S	12/3/01	< 0.1	< 0.13	< 0.28	< 0.18	< 0.17	< 0.13	< 0.64	< 0.15
12MW04S	2/28/02	< 0.13	< 0.14	< 0.24	< 0.17	< 0.22	< 0.16	< 0.23	< 0.2
12MW04S	6/11/02	< 0.1	< 0.13	< 0.28	< 0.18	< 0.17	< 0.13	< 0.64	< 0.15
12MW04S	9/9/02	< 0.16	< 0.17	< 0.2	< 0.2	< 0.26	< 0.33	< 0.24	< 0.18
12MW04S	1/7/03	< 0.1	< 0.13	< 0.28	< 0.18	< 0.17	< 0.13	< 0.64	< 0.15
12MW04S	4/15/03	< 0.31	< 0.25	< 0.4	< 0.11	< 0.27	< 0.41	< 0.3	< 0.34
12MW04S	7/14/03	< 0.17	< 0.12	< 0.22	< 0.1	< 0.16	< 0.17	< 0.11	< 0.14
12MW04S	9/16/03	< 0.17	< 0.12	< 0.22	< 0.1	< 0.16	< 0.17	< 0.11	< 0.14
12MW04S	1/12/04	< 0.31	< 0.25	< 0.4	< 0.11	< 0.27	< 0.41	< 0.3	< 0.34
12MW04S	4/26/04	< 0.31	< 0.25	< 0.4	< 0.11	< 0.27	< 0.41	< 0.3	< 0.34
12MW04S	8/18/04	< 0.31	< 0.25	< 0.4	< 0.11	< 0.27	< 0.41	< 0.3	< 0.34
12MW05D	8/30/00	< 5	9.6	6.2	< 2	< 5	< 5	< 5	< 5
12MW05D	11/30/00	3.1	5.3	2.5	< 0.15	1.4	2.6	< 0.18	< 0.21
12MW05D	2/28/01	< 0.13	1.8	1.4	< 0.17	< 0.22	0.68	< 0.23	< 0.2
12MW05D	5/15/01	< 0.38	1.8	2.1	< 0.19	< 0.27	0.83	< 0.29	< 0.35
12MW05D	8/28/01	< 0.1	0.55	3.5	< 0.18	< 0.17	0.97	< 0.64	< 0.15
12MW05D	12/4/01	< 0.13	1	0.75	< 0.17	< 0.22	0.3	< 0.23	< 0.2
12MW05D	3/1/02	< 0.13	0.74	0.76	< 0.17	< 0.22	0.37	< 0.23	< 0.2
12MW05D	6/11/02	< 0.1	0.89	0.97	< 0.18	< 0.17	0.39	< 0.64	< 0.15
12MW05D	9/10/02	< 0.16	0.56	0.54	< 0.2	< 0.26	< 0.33	< 0.24	< 0.18

12MW05D	1/8/03	< 0.1	0.64	0.39	< 0.18	< 0.17	0.34	< 0.64	< 0.15
12MW05D	4/15/03	< 0.31	0.47	< 0.4	< 0.11	< 0.27	< 0.41	< 0.3	< 0.34
12MW05I	8/30/00	< 5	< 5	< 5	< 2	< 5	< 5	< 5	< 5
12MW05I	11/30/00	12	20	23	0.43	23	12	3.3	< 0.42
12MW05I	2/28/01	0.46	0.73	1.1	< 0.17	0.33	0.46	< 0.23	< 0.2
12MW05I	5/16/01	0.86	0.71	0.31	< 0.19	1.4	0.6	< 0.29	< 0.35
12MW05I	8/29/01	0.7	0.73	< 0.31	< 0.19	0.48	0.59	< 0.29	< 0.35
12MW05I	12/4/01	< 0.13	1	< 0.24	< 0.17	< 0.22	0.25	< 0.23	< 0.2
12MW05I	3/1/02	< 0.13	1.5	< 0.24	< 0.17	< 0.22	0.4	< 0.23	< 0.2
12MW05I	6/11/02	< 0.1	1	< 0.28	< 0.18	< 0.17	0.35	< 0.64	< 0.15
12MW05I	9/10/02	0.17	0.63	< 0.2	< 0.2	< 0.26	< 0.33	< 0.24	< 0.18
12MW05I	1/8/03	< 0.1	0.61	< 0.28	< 0.18	< 0.17	< 0.13	< 0.64	< 0.15
12MW05I	4/15/03	< 0.31	0.3	< 0.4	< 0.11	< 0.27	< 0.41	< 0.3	< 0.34
12MW05I	7/14/03	< 0.17	0.37	< 0.22	< 0.1	< 0.16	< 0.17	< 0.11	< 0.14
12MW05I	8/18/04	< 0.31	< 0.25	< 0.4	< 0.11	< 0.27	< 0.41	< 0.3	< 0.34
12MW05S	8/30/00	580	27,000	1,500	33	640	10,000	66	13
12MW05S	11/30/00	400	22000	890	< 31	440	8500	< 35	< 42
12MW05S	2/28/01	270	12000	580	< 170	360	7100	< 230	< 200
12MW05S	5/16/01	500	16000	690	< 190	590	8900	< 290	< 350
12MW05S	8/29/01	3100	23000	1400	< 190	2600	16000	310	< 350
12MW05S	12/4/01	740	25000	1100	< 350	< 330	13000	< 1300	< 300
12MW05S	3/1/02	360	18000	800	< 350	< 440	9300	< 460	< 390
12MW05S	6/11/02	< 210	23000	1600	< 350	790	13000	< 1300	< 300
12MW05S	9/10/02	600	20000	1600	< 350	< 330	12000	< 1300	< 300
12MW05S	1/8/03	460	20000	1200	< 350	< 330	11000	< 1300	< 300
12MW05S	4/22/03	< 61	21000	1200	< 21	< 53	9400	< 60	< 68
12MW05S	7/17/03	740	20000	1200	< 210	< 330	10000	< 210	< 280
12MW05S	9/16/03	660	16000	1200	< 350	< 460	8900	< 430	< 400
12MW05S	1/14/04	620	18000	1200	< 21	230	8600	< 60	< 68
12MW05S	4/27/04	880	21000	1300	58	210	7800	36	< 34
12MW05S	8/18/04	910	22000	1400	120	290	9600	68	< 43
12MW06D	8/29/00	< 5	< 5	< 5	< 2	< 5	< 5	< 5	< 5
12MW06D	11/29/00	< 0.21	< 0.17	< 0.17	< 0.15	< 0.18	< 0.17	< 0.18	< 0.21
12MW06D	2/27/01	< 0.13	< 0.14	< 0.24	< 0.17	< 0.22	< 0.16	< 0.23	< 0.2
12MW06D	5/14/01	< 0.13	< 0.14	< 0.24	< 0.17	< 0.22	< 0.16	< 0.23	< 0.2
12MW06D	8/28/01	< 0.1	< 0.13	< 0.28	< 0.18	< 0.17	< 0.13	< 0.64	< 0.15
12MW06S	8/29/00	< 5	< 5	< 5	< 2	< 5	< 5	< 5	< 5
12MW06S	11/29/00	< 0.21	< 0.17	< 0.17	< 0.15	0.42	< 0.17	< 0.18	< 0.21
12MW06S	2/27/01	< 0.13	< 0.14	< 0.24	< 0.17	0.29	< 0.16	< 0.23	< 0.2
12MW06S	5/14/01	< 0.13	< 0.14	< 0.24	< 0.17	< 0.22	< 0.16	< 0.23	< 0.2
12MW06S	8/28/01	< 0.38	< 0.34	< 0.31	< 0.19	< 0.27	< 0.26	< 0.29	< 0.35
12MW06S	12/4/01	< 0.13	0.15	< 0.24	< 0.17	< 0.22	< 0.16	< 0.23	< 0.2
12MW06S	3/1/02	< 0.13	< 0.14	< 0.24	< 0.17	< 0.22	< 0.16	< 0.23	< 0.2
12MW06S	6/11/02	< 0.1	< 0.13	< 0.28	< 0.18	< 0.17	< 0.13	< 0.64	< 0.15
12MW06S	9/9/02	< 0.16	< 0.17	< 0.2	< 0.2	< 0.26	< 0.33	< 0.24	< 0.18
12MW06S	1/7/03	< 0.16	< 0.17	< 0.2	< 0.2	< 0.26	< 0.33	< 0.24	< 0.18
12MW06S	4/15/03	< 0.31	< 0.25	< 0.4	< 0.11	< 0.27	< 0.41	< 0.3	< 0.34
12MW07D	8/28/00	< 5	< 5	< 5	< 2	< 5	< 5	< 5	< 5
12MW07D	11/29/00	< 0.21	< 0.17	< 0.17	< 0.15	< 0.18	< 0.17	< 0.18	< 0.21
12MW07D	2/26/01	< 0.13	< 0.14	< 0.24	< 0.17	< 0.22	< 0.16	< 0.23	< 0.2

12MW07D	5/14/01	< 0.13	< 0.14	< 0.24	< 0.17	< 0.22	< 0.16	< 0.23	< 0.2
12MW07D	8/29/01	1	0.44	< 0.31	< 0.19	0.7	0.78	< 0.29	< 0.35
12MW07S	8/28/00	< 5	< 5	< 5	< 2	< 5	< 5	< 5	< 5
12MW07S	11/28/00	< 0.21	< 0.17	< 0.17	< 0.15	< 0.18	< 0.17	< 0.18	< 0.21
12MW07S	2/26/01	< 0.13	< 0.14	< 0.24	< 0.17	< 0.22	< 0.16	< 0.23	< 0.2
12MW07S	5/14/01	< 0.13	< 0.14	< 0.24	< 0.17	< 0.22	< 0.16	< 0.23	< 0.2
12MW07S	8/29/01	0.77	0.38	< 0.31	< 0.19	0.55	0.67	< 0.29	< 0.35
12MW08D	8/29/00	< 5	< 5	< 5	< 2	< 5	< 5	< 5	< 5
12MW08D	11/28/00	< 0.21	< 0.17	< 0.17	< 0.15	< 0.18	< 0.17	< 0.18	< 0.21
12MW08D	2/26/01	< 0.13	< 0.14	< 0.24	< 0.17	< 0.22	< 0.16	< 0.23	< 0.2
12MW08D	5/14/01	< 0.38	< 0.34	< 0.31	< 0.19	< 0.27	< 0.26	< 0.29	< 0.35
12MW08D	8/27/01	< 0.38	< 0.34	< 0.31	< 0.19	< 0.27	< 0.26	< 0.29	< 0.35
12MW08S	8/28/00	< 5	< 5	< 5	< 2	< 5	< 5	< 5	< 5
12MW08S	11/28/00	< 0.21	< 0.17	< 0.17	< 0.15	< 0.18	< 0.17	< 0.18	< 0.21
12MW08S	2/26/01	< 0.13	< 0.14	< 0.24	< 0.17	< 0.22	< 0.16	< 0.23	< 0.2
12MW08S	5/14/01	< 0.38	< 0.34	< 0.31	< 0.19	< 0.27	< 0.26	< 0.29	< 0.35
12MW08S	8/27/01	< 0.38	< 0.34	< 0.31	< 0.19	< 0.27	< 0.26	< 0.29	< 0.35
12MW09D	8/29/00	< 5	< 5	< 5	< 2	< 5	0	0	< 5
12MW09D	11/29/00	< 0.21	< 0.17	< 0.17	< 0.15	< 0.18	0.18	0.24	< 0.21
12MW09D	2/27/01	< 0.13	< 0.14	< 0.24	< 0.17	< 0.22	0.34	0.34	< 0.2
12MW09D	5/15/01	< 0.38	< 0.34	< 0.31	< 0.19	< 0.27	0.3	0.31	< 0.35
12MW09D	8/29/01	< 0.13	< 0.14	< 0.24	< 0.17	< 0.22	0.52	0.33	< 0.2
12MW09D	12/3/01	< 0.1	< 0.13	< 0.28	< 0.18	< 0.17	< 0.13	< 0.64	< 0.15
12MW09D	2/28/02	< 0.13	< 0.14	< 0.24	< 0.17	< 0.22	0.19	< 0.23	< 0.2
12MW09D	6/10/02	< 0.1	< 0.13	< 0.28	< 0.18	< 0.17	< 0.13	< 0.64	< 0.15
12MW09D	9/10/02	< 0.16	< 0.17	< 0.2	< 0.2	< 0.26	< 0.33	< 0.24	< 0.18
12MW09D	1/7/03	< 0.1	< 0.13	< 0.28	< 0.18	< 0.17	< 0.13	< 0.64	< 0.15
12MW09D	4/15/03	< 0.17	< 0.12	< 0.22	< 0.1	< 0.16	< 0.17	0.14	< 0.14
12MW09D	7/16/03	< 0.31	< 0.25	< 0.4	< 0.11	< 0.27	< 0.41	< 0.3	< 0.34
12MW09D	8/16/04	< 0.2	< 0.2	< 0.15	< 0.15	< 0.19	< 0.18	< 0.2	< 0.22
12MW09S	8/29/00	< 5	< 5	< 5	< 2	< 5	120	120	< 5
12MW09S	11/29/00	< 0.21	0.94	0.3	0.49	1	98	97	< 0.21
12MW09S	2/27/01	< 0.13	0.89	0.32	0.24	0.79	86	86	< 0.2
12MW09S	5/15/01	< 3	< 2.7	< 2.4	< 1.5	< 2.2	60	73	< 2.8
12MW09S	8/29/01	< 1	1.3	< 1.9	< 1.4	< 1.7	83	76	< 1.6
12MW09S	12/3/01	< 0.82	< 1	< 2.2	< 1.4	< 1.3	69	73	< 1.2
12MW09S	2/28/02	< 1	< 1.1	< 1.9	< 1.4	< 1.7	52	51	< 1.6
12MW09S	6/10/02	< 0.82	< 1	< 2.2	< 1.4	< 1.3	110	100	< 1.2
12MW09S	9/10/02	< 0.66	1.3	< 0.81	< 0.79	< 1	31	35	< 0.7
12MW09S	1/7/03	< 0.41	< 0.51	< 1.1	< 0.7	< 0.67	18	20	< 0.6
12MW09S	4/16/03	< 0.34	0.47	< 0.44	< 0.21	< 0.33	23	22	< 0.28
12MW09S	7/15/03	< 0.61	0.71	< 0.8	0.39	< 0.53	32	30	< 0.68
12MW09S	9/17/03	< 0.34	0.61	< 0.44	< 0.21	< 0.33	28	28	< 0.28
12MW09S	1/13/04	< 0.43	< 0.31	< 0.55	< 0.26	< 0.41	24	23	< 0.35
12MW09S	4/28/04	< 0.51	< 0.5	< 0.36	< 0.39	< 0.47	26	23	< 0.54
12MW09S	8/16/04	< 0.61	< 0.49	< 0.8	< 0.21	< 0.53	25	20	< 0.68
12MW10S	11/30/00	3300	1900	9300	660	19000	2400	7000	< 420
12MW10S	2/28/01	3100	1100	5500	480	38000	5100	15000	< 390
12MW10S	5/16/01	3500	1800	6400	1600	17000	5600	5000	< 440
12MW10S	8/29/01	4200	3500	9200	1800	19000	7000	6600	< 190

12MW10S	12/5/01	4400	2600	12000	2200	16000	12000	6100	< 300
12MW10S	3/1/02	3400	1600	7300	1400	16000	9300	5400	< 390
12MW10S	6/11/02	2400	1200	6800	1600	6800	4900	2800	< 140
12MW10S	9/10/02	3400	1300	7000	1400	11000	4800	4400	< 120
12MW10S	1/8/03	2400	950	3900	900	17000	5700	7700	79
12MW10S	4/23/03	1800	710	2300	470	5600	4800	2400	< 170
12MW10S	7/16/03	3400	1100	3000	610	9300	9700	4200	< 270
12MW10S	9/16/03	1600	550	2100	480	3600	4400	1800	< 140
12MW10S	1/14/04	1600	580	1900	460	2700	4300	1600	< 27
12MW10S	4/27/04	2200	840	2100	460	4200	5400	2400	37
12MW10S	8/18/04	2100	730		630	3100	3900	2100	27
12MW11D	8/29/00	< 5	< 5	< 5	< 2	< 5	< 5	< 5	< 5
12MW11D	11/29/00	< 0.21	< 0.17	< 0.17	< 0.15	< 0.18	< 0.17	< 0.18	< 0.21
12MW11D	2/27/01	2.3	0.98	0.75	< 0.17	< 0.22	0.41	< 0.23	< 0.2
12MW11D	5/15/01	< 0.38	< 0.34	< 0.31	< 0.19	< 0.27	< 0.26	< 0.29	< 0.35
12MW11D	8/28/01	< 0.13	0.47	< 0.24	< 0.17	< 0.22	0.24	< 0.23	< 0.2
12MW11D	12/4/01	< 0.13	< 0.14	< 0.24	< 0.17	< 0.22	< 0.16	< 0.23	< 0.2
12MW11D	3/1/02	< 0.13	< 0.14	< 0.24	< 0.17	< 0.22	< 0.16	< 0.23	< 0.2
12MW11D	6/10/02	< 0.1	< 0.13	< 0.28	< 0.18	< 0.17	< 0.13	< 0.64	< 0.15
12MW11D	9/9/02	< 0.16	< 0.17	< 0.2	< 0.2	< 0.26	< 0.33	< 0.24	< 0.18
12MW11D	1/8/03	< 0.1	< 0.13	< 0.28	< 0.18	< 0.17	< 0.13	< 0.64	< 0.15
12MW11D	4/15/03	< 0.17	< 0.12	< 0.22	< 0.1	< 0.16	< 0.17	< 0.11	< 0.14
12MW11D	7/16/03	< 0.31	< 0.25	< 0.4	< 0.11	< 0.27	< 0.41	< 0.3	< 0.34
12MW11S	8/29/00	< 5	7.6	< 5	< 2	< 5	130	20	< 5
12MW11S	11/29/00	< 0.21	3.8	0.37	< 0.15	0.34	65	6.1	< 0.21
12MW11S	2/27/01	15	16	8.9	< 0.7	< 0.87	70	9.3	< 0.78
12MW11S	5/15/01	< 1.5	2.6	< 1.2	< 0.75	< 1.1	41	5.5	< 1.4
12MW11S	8/28/01	< 0.5	38	1.3	< 0.7	1.1	80	7	< 0.78
12MW11S	1/8/03	< 0.1	1.4	0.58	< 0.18	< 0.17	71	12	0.23
12MW12D	8/28/01	< 0.13	2.3	< 0.24	< 0.17	< 0.22	0.34	< 0.23	< 0.2
12MW12S	8/28/01	15	2900	29	0.44	10	420	5.8	0.95
12MW12S	12/4/01	65	2400	38	< 7	< 8.7	680	< 9.2	< 7.8
12MW12S	3/1/02	< 31	1800	< 61	< 44	< 55	280	< 58	< 49
12MW12S	6/10/02	110	2400	< 70	< 44	< 42	880	< 160	< 38
12MW12S	9/9/02	94	2200	< 51	< 49	< 64	400	< 59	< 44
12MW12S	1/8/03	< 13	1400	< 35	< 22	< 21	190	< 80	< 19
12MW12S	4/22/03	< 6.9	430	9.2	< 4.1	< 6.6	140	4.7	< 5.6
12MW12S	7/16/03	< 7.7	250	< 10	< 2.7	< 6.6	99	< 7.5	< 8.5
12MW12S	9/15/03	< 7.7	180	< 10	< 2.7	< 6.6	68	< 7.5	< 8.5
12MW12S	1/13/04	2.6	120	4	< 0.21	1.2	48	2.7	< 0.28
12MW12S	4/27/04	2.6	84	4.1	< 0.31	0.94	44	3	< 0.43
12MW12S	8/17/04	2.7	93	4.2	0.24	1.2	58	3.1	0.29

3 Brookhaven National Laboratory

3.1 Introduction

The Brookhaven National Laboratory (BNL) site was chosen to test the applicability of the Strategy to a glacial till environment in the Northeastern United States. In this case study we focus on applying certain concepts in the Strategy to an area of tritium contamination at the BNL site.

As outlined in the Strategy, our application began with a compilation and analysis of existing characterization and monitoring data and synthesis of an alternative conceptual site model. Information in Section 3.2 is background information including location, geology and hydrology of the site. Discussion of the tritium contamination begins in Section 3.2.5 and is summarized below.

Tritium Plume and Remediation

In early 1997, monitoring data revealed a plume of tritium contaminated ground water from the High Flux Beam Reactor (HFBR) at the BNL site. Tritium, radioactive hydrogen that forms water, was leaking from the spent fuel pool within the HFBR.

In May 1997, a system to pump the leading edge of the tritium plume was started as an interim action to prevent any further movement of the tritium and to ensure that the contamination remains entirely on-site. The contaminated water is being recharged on-site at levels below the Federal and State standards farther from the site boundary. The spent fuel has all been shipped off-site and the water was drained from the fuel pool, eliminating further leaks. The reactor is currently shut down, and the United States Department of Energy (DOE) has decided not to restart the reactor (DOE, 2006).

Currently, to remediate the tritium in the ground water at the BNL, a series of extraction and re-injection wells provide a recirculation system (Figure 3-1). Because the half-life of tritium is 12.5 years, this recirculation system allows time for the tritium to decay before exiting the BNL boundary. The schematic in Figure 3-1 also mentions a VOC plume in the HBFR vicinity. While this plume is not the focus of this Case Study, it is worthwhile to note that understanding of the flow and transport behavior of this plume may provide useful information about the potential pathway of the tritium plume

Key Conclusions

This case study illustrates the following key points:

Conceptual Site Models and flow and transport simulations are powerful visualization techniques for communicating the impact of Performance Indicators. In this Chapter, we show examples of models developed using, Excel, MODFLOW, and GMS (Section 3.3).

Conceptual Site Models and flow and transport simulations can be useful in evaluating the effectiveness of various pumping alternatives, and thus, can aid in development of an efficient and cost effective monitoring and/or remediation program (Section 3.3.2).

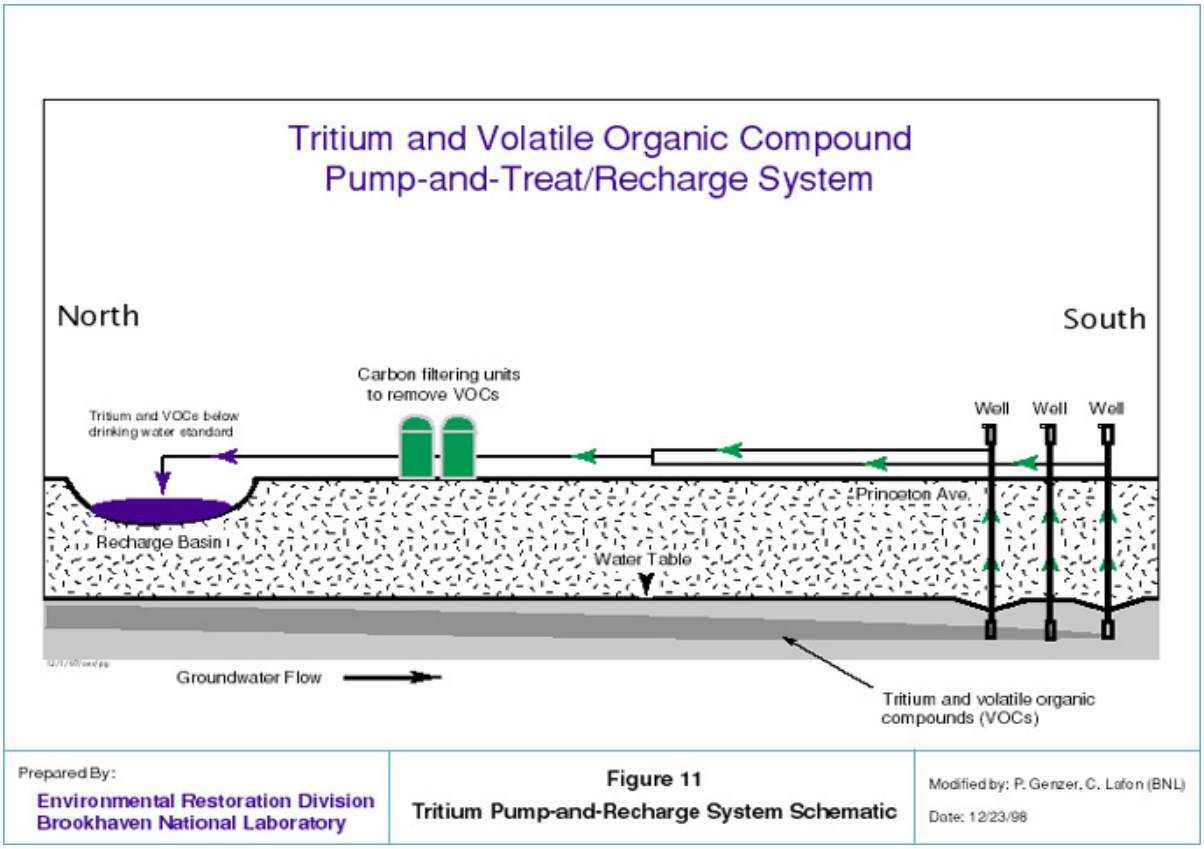

Figure 3-1. Schematic of tritium/VOC plume pump and treat system (DOE, 2000)

3.2 Compilation of Available Data

This section provides a summary of the readily available data compiled to prepare this evaluation with the majority of the information collected from BNL online reports.

3.2.1 Site Background

Brookhaven National Laboratory, located on Long Island in New York, is a multi-program DOE National Laboratory (Figure 3-2). Established in 1947, BNL has been operated by contractors, first to the Atomic Energy Commission (AEC), and now to the United States Department of Energy (DOE) - the site owners. Since March 1998, BNL has been operated and managed by Brookhaven Science Associates. BNL conducts basic and applied research in high energy nuclear and solid state physics, fundamental material and structure properties and the interaction of matter, nuclear medicine, biomedical and environmental sciences, and selected energy technologies. To conduct this research BNL has designed, built, and run installations for scientific research, such as particle accelerators and nuclear reactors. Most of its main facilities are in an area of approximately 900 acres near the center of the site (DOE, 2006).

There are a number of areas at BNL where ground-water contamination is known or suspected. Over 30 Areas of Concern (AOCs) have been identified. On-site soil is contaminated with volatile organic compounds (VOCs), heavy metals, polycyclic aromatic hydrocarbons (PAHs), and radioactive materials including cesium-137,

strontium-90 and tritium. On-site and off-site ground water is contaminated with VOCs, radionuclides, and the pesticide/fumigant ethylene dibromide (EDB). On-site contaminated drinking water wells have been closed or treatment systems have been added. VOCs in off-site ground water exceed Federal and State drinking water standards, so the DOE has connected neighboring properties to public water as a protective measure until the final cleanup is complete. Radionuclides in off-site ground water do not exceed Federal or State standards (DOE, 2006).

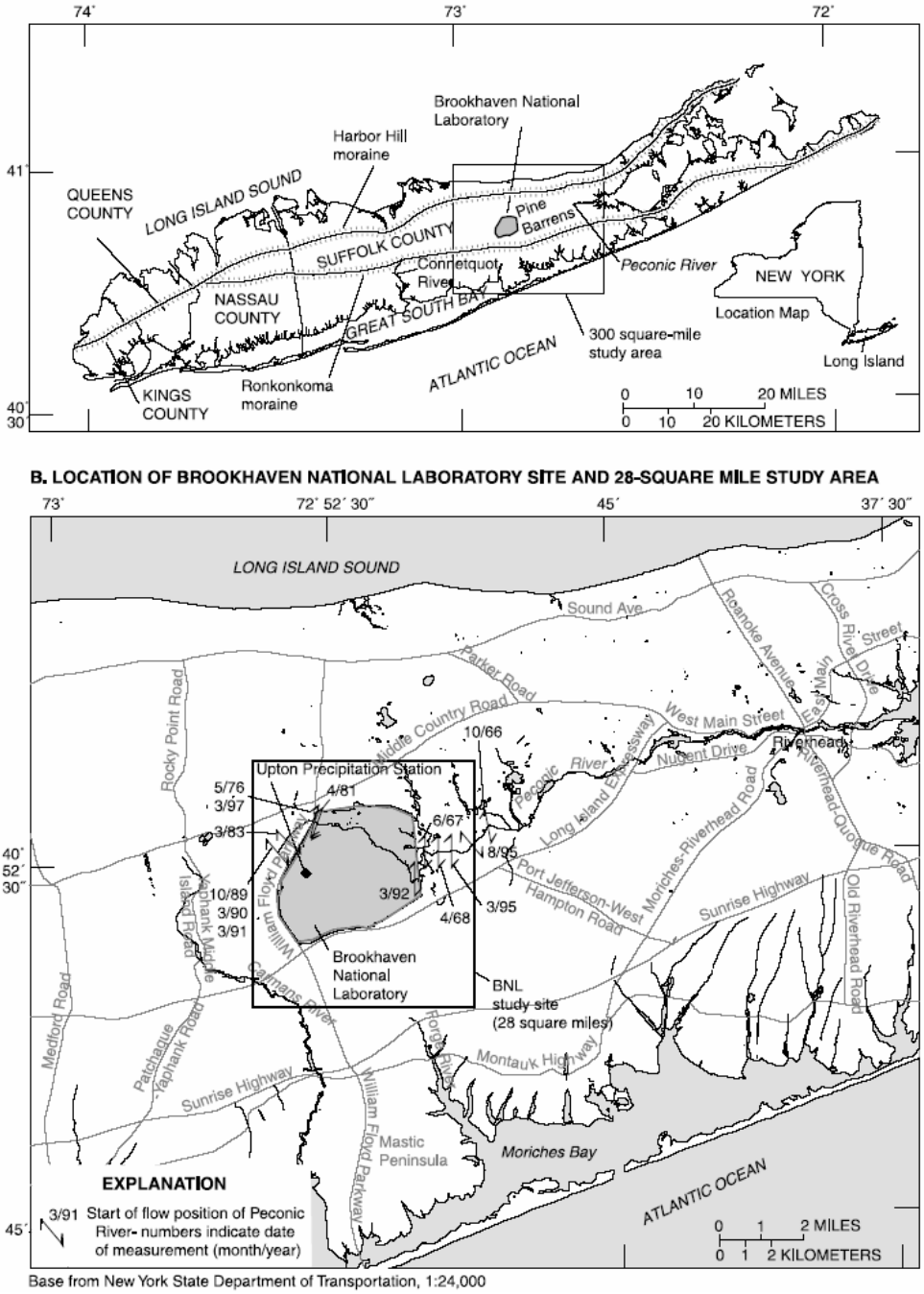

Figure 3-2. Location of the Brookhaven National Laboratory (Scorca et al., 1999)

3.2.2 Geologic Information

Brookhaven National Lab is located on Pleistocene glacial deposits of the Northeastern United States. The stratigraphy in the region of the BNL consists of approximately 1,300 feet of unconsolidated deposits overlying pre-Cambrian bedrock (Figure 3-3). Among these unconsolidated deposits, the Ground-Water Monitoring Programs at BNL currently focus on ground-water quality within upper Pleistocene glacial deposits, and the upper portions of the Matawan Group-Magothy Formation.

The Pleistocene deposits are about 100 to 200 feet thick and are divided into two primary hydrogeologic units: undifferentiated sand and gravel outwash and moraine deposits; and finer-grained, more poorly sorted fine to medium white to greenish sand with interstitial clay.

The most obvious Pleistocene glacial features are the large erratics (glacier transported boulders) and scattered deposits of glacial till (a mix of fine silt, sand, gravel, and large boulders). The flowing ice of the southward advancing ice sheet sculpted the landscape by not only eroding and transporting vast quantities of rock and sediment, but also by blocking and altering the course of rivers, filling valleys with sediment, and depositing large quantities of till in the terminal moraines along its leading edge. These hills are apparent throughout Long Island (BNL, 2004).

3.2.3 Hydrogeologic Information

Table 3-1 presents a generalized comparison of the geologic and hydrogeologic units below BNL. Descriptions of the units in the table are limited to the unconsolidated Pleistocene and Cretaceous material overlying the Paleozoic bedrock. Hydrostratigraphic relationships are shown in cross-section in Figure 3-3.

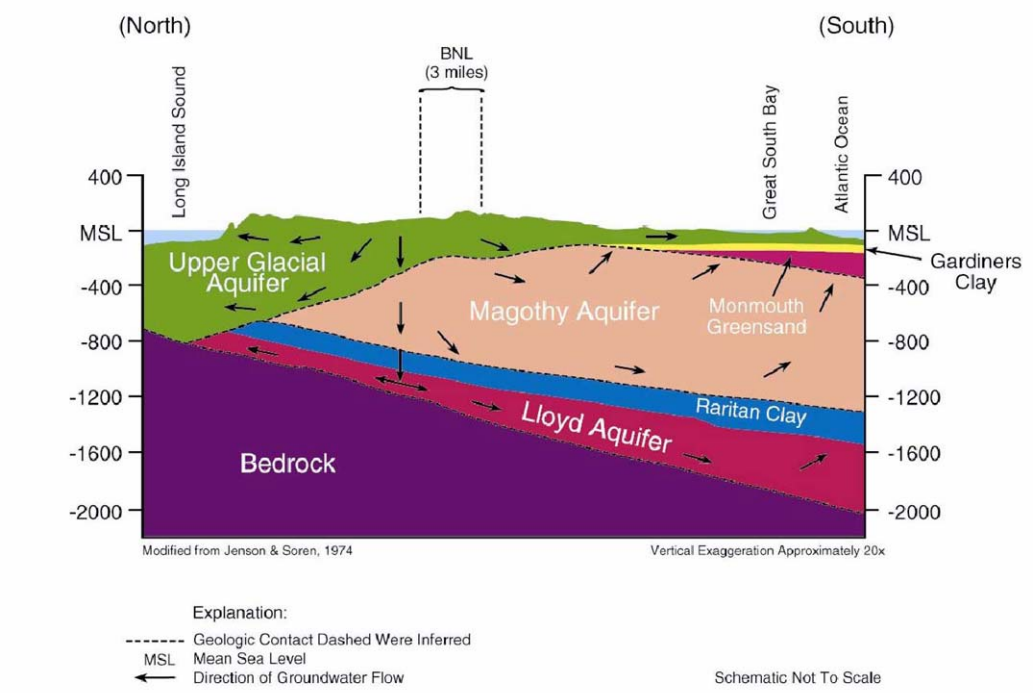

Figure 3-3. Hydrostratigraphy of the Brookhaven National Laboratory (BNL, 2004)

3.2.4 Hydrologic Data

The saturated part of the upper Pleistocene deposit forms the Upper Glacial Aquifer, which contains the water table throughout most of Long Island. This unit consists mostly of moderately to well-sorted sand and fine gravel and is highly permeable in most places. The Upper Glacial aquifer underlies the entire 300-square mile (mi^2) study area and is the source of base flow to streams.

The average island-wide horizontal hydraulic conductivity value for the Upper Glacial aquifer is about 270 ft/d (Smolensky et al., 1989), but aquifer tests conducted at BNL by Warren et al. (1968) indicated the value at the site to be one-third lower—about 175 ft/d (based on an aquifer thickness of 145 ft), and the specific yield (effective porosity) to be 0.24. Subsequent tests at BNL have measured similar hydraulic conductivities (Holzmacher et al., 1985). Total porosity of the Upper Glacial aquifer is estimated to be 0.33 (Warren et al., 1968). A summary of aquifer properties obtained from onsite pumping tests is presented in Table 3-2 (Scorca et al., 1999).

Data from aquifer tests and infiltration tests conducted at BNL (Warren et al., 1968) indicate that the anisotropy (ratio of vertical to horizontal hydraulic conductivity) of the Upper Glacial aquifer is between 1:4 and 1:18. The average value for the Upper Glacial aquifer throughout Long Island has been estimated to be 1:10 (Smolensky et al., 1989).

The hydraulic properties of the basal Upton unit cannot be defined with certainty from the current well network, but the high clay and silt content of the Upton unit, especially in the northwestern part of the BNL site, indicate that these deposits are probably less permeable than the overlying glacial outwash sand and gravel.

The Gardiners Clay, where present, confines water and affects ground-water flow, but its limited extent indicates that the effects are only local. Studies by Warren et al. (1968) indicate that the hydraulic conductivity of the Gardiners Clay is about 0.040 ft/d, but the hydraulic conductivity of sandy zones within the unit is higher.

Table 3-1. Generalized description of geologic and hydrogeologic units underlying Brookhaven National Laboratory and vicinity, Suffolk County, N.Y. (Scorca et al., 1999)

Series	Geologic Unit	Hydrogeologic Unit	Description and Water-bearing Characteristics
PLIESTOCENE	Upper Pleistocene deposits	Upper glacial aquifer	Mainly brown and gray sand and gravel deposits of moderately high horizontal hydraulic conductivity (270 ft/d average for Long Island; about 180 ft/d measured at Brookhaven National Laboratory); may also include deposits of clayey till and lacustrine clay of low hydraulic conductivity. A major aquifer.
	Upton unit	Upper glacial aquifer	Mainly greenish, with shades of yellow-green, greenish-gray, olive-brown, and gray, poorly to well sorted sand, with some silt and clay. Upper surface in some borings is marked by a clay or silty layer, generally less than 10 ft thick, that produces a noticeable response on a gamma-ray log. Horizontal hydraulic conductivity is estimated to be similar to or slightly less than that of the shallow part of the upper glacial aquifer.
	Gardiners Clay	Gardiners Clay	Green and gray clay, silt, clayey and silty sand, and some interbedded clayey and silty gravel. Unit has low vertical hydraulic conductivity (0.001 ft/d) and tends to confine water in underlying aquifer.
	Sand below Gardiners Clay	Upper glacial aquifer	Mainly light brown, olive-brown, and grayish-brown, poorly to well sorted sand. Hydrologically, unit could also be considered part of Magothy aquifer because of confinement by Gardiners Clay.
CRETACEOUS	Monmouth Group	Monmouth greensand	Interbedded marine deposits of green, dark-greenish gray, greenish-black, dark gray, and black clay, silt, and sand, containing much glauconite. Unit has low hydraulic conductivity (0.001 ft/d) and tends to confine water in underlying aquifer.
	Matawan Group and Magothy Formation, undifferentiated	Magothy aquifer	Gray, white, and brownish-gray, poorly to well sorted, fine to coarse sand of moderate horizontal hydraulic conductivity (50 ft/d). Contains much interstitial clay and silt, and lenses of clay of low hydraulic conductivity. Generally contains sand and gravel beds of low to high conductivity in basal 100 to 200 ft. A major aquifer.
	grayish-brown clay		Dark grayish-brown to yellow-brown, solid to silty clay, in some layers laminated with beds of very fine sand up to 1 in. thick. Unit is encountered in upper part of Magothy Formation. Has low hydraulic conductivity and tends to confine water.
	Unnamed clay member of the Raritan Formation	Raritan confining unit	Gray, black, and multicolored clay and some silt and fine sand. Unit has low vertical hydraulic conductivity (0.001 ft/d) and confines water in underlying aquifer.
	Lloyd Sand Member of the Raritan Formation	Lloyd aquifer	White and gray fine-to-coarse sand and gravel of moderate horizontal hydraulic conductivity (40 ft/d) and some clayey beds of low hydraulic conductivity.
PALEOZOIC AND PRECAMBRIAN	Bedrock	Undifferentiated crystalline bedrock	Mainly metamorphic rocks of low hydraulic conductivity; considered to be the base of the ground-water flow system.

Table 3-2. Hydraulic conductivity of Upper Glacial aquifer at Brookhaven National Laboratory, Suffolk County, N.Y., as indicated by aquifer tests (Scorca et al., 1999)

Source of data	Hydraulic conductivity (in feet per day)
Warren et al. (1968)	180
Holzmacher et al.(1985)	180
Camp Dresser and McKee (1995)	200
Grosser (1997)	60-160
Geraghty & Miller (1997)	150

The Monmouth Group, which lies along the southern shore of Long Island, forms the hydrogeologic unit known as the Monmouth greensand. Monmouth greensand and the Gardiners Clay underlie the Upper Glacial aquifer and confine water in the Magothy aquifer. The Upper Glacial aquifer directly overlies the Magothy aquifer in areas where both of these units are absent.

Deltaic sediments of the Matawan Group- Magothy Formation make up the Magothy aquifer. The hydraulic conductivity of this unit is estimated to average 50ft/d (Smolensky et al., 1989) but varies widely as a result of local differences in lithology, thickness, and lateral extent. This hydraulic variation can affect local ground-water flow patterns and contaminant transport. Warren et al. (1968) conducted an aquifer test in a coarse sand zone of the Magothy aquifer and obtained a hydraulic conductivity value of 57ft/d.

Much of the Magothy aquifer consists of silty sand with clayey layers. The upper Magothy sediment at BNL is mostly a silty sand with clayey layers but includes layers of well-sorted sand as well as locally extensive clay layers, such as the grayish-brown clay unit. Although the grayish-brown clay unit has a sandy texture in some intervals, it is fairly solid in general and forms a major local confining unit (Scorca et al., 1999).

Hydrologic Cycle

The hydrologic cycle on Long Island was summarized by Scorca (1997) and discussed at length by Franke and McClymonds (1972), who evaluated the relations among major hydrologic factors, including precipitation, evapotranspiration, direct runoff, ground-water recharge, ground-water movement, and pumpage, to develop an island-wide water budget. The hydrologic cycle can be thought of as beginning with precipitation, which has averaged 48.29 in/yr at Upton station since 1949. Upon reaching the ground,

precipitation flows as direct runoff into streams, infiltrates into the highly permeable unsaturated zone, or evaporates. Part of the water that infiltrates the soil evaporates or is transpired by plants; the rest infiltrates downward to the water table (Scorca et al., 1999).

Ground-Water Recharge and Discharge

The water table recharge rate varies from year to year as a function of precipitation. It also fluctuates seasonally because plants capture and transpire most of the water that enters the unsaturated zone during the growing season (May through October) (Figure 3-4). Thus, in most years, virtually all recharge occurs during the non-growing season (November through April) (Warren et al., 1968). The water table rises in response to recharge and typically undergoes a net rise in years when precipitation is notably higher than in the preceding year. This rise, in turn, results in increased ground-water discharge to streams, bays, and the ocean. Under long-term conditions in undeveloped areas of Long Island, about 50 percent of precipitation is lost through evapotranspiration and direct runoff to streams. The other 50 percent infiltrates the soils and recharges the ground-water system (Aronson and Seaburn, 1974; Franke and McClymonds, 1972).

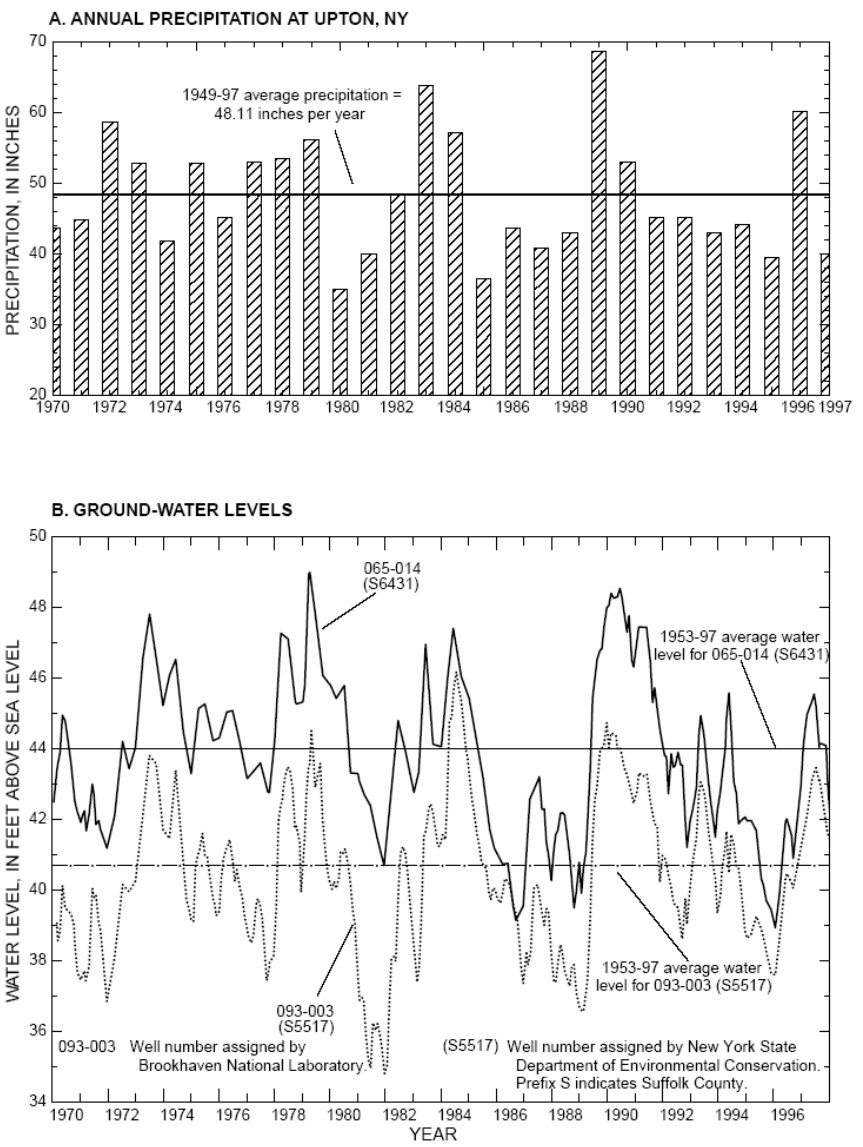

Figure 3-4. Precipitation and water-table altitude at Brookhaven National Laboratory, Suffolk County, N.Y.,1970-97. A. Annual precipitation at Upton. B. Typical water levels in wells (Scorca et al., 1999)

Regional Ground-Water Flow

The Long Island ground-water system consists of two major components—the regional (deep) flow system and the shallow flow system associated with streams. Ground water enters the regional flow system of Long Island in the area bordering the main ground-water divide, where it moves downward through the Upper Glacial aquifer into the underlying aquifers and eventually moves seaward. Water that enters the regional flow system south of the main divide flows southward, and water that infiltrates north of the divide flows northward. All precipitation that infiltrates upgradient of each stream's shallow-flow system becomes part of the regional flow system, and precipitation that infiltrates within the ground-water contributing area of a stream becomes part of that stream's shallow-flow system (Prince et al., 1988).

Ground-Water Divide

The position of a ground-water divide depends on the water-table configuration. The main ground-water divide on Long Island is aligned generally east-west and lies about 0.5 mi north of BNL's northern boundary (Figure 3-5). Ground water north of the divide flows northward and ultimately discharges to Long Island Sound; ground water south of the divide flows southward and discharges to south-shore streams, the Peconic River, Great South Bay, Peconic Bay, and the Atlantic Ocean. Ground water near the divide has a large downward vertical-flow component and recharges the deep aquifers of the ground-water system.

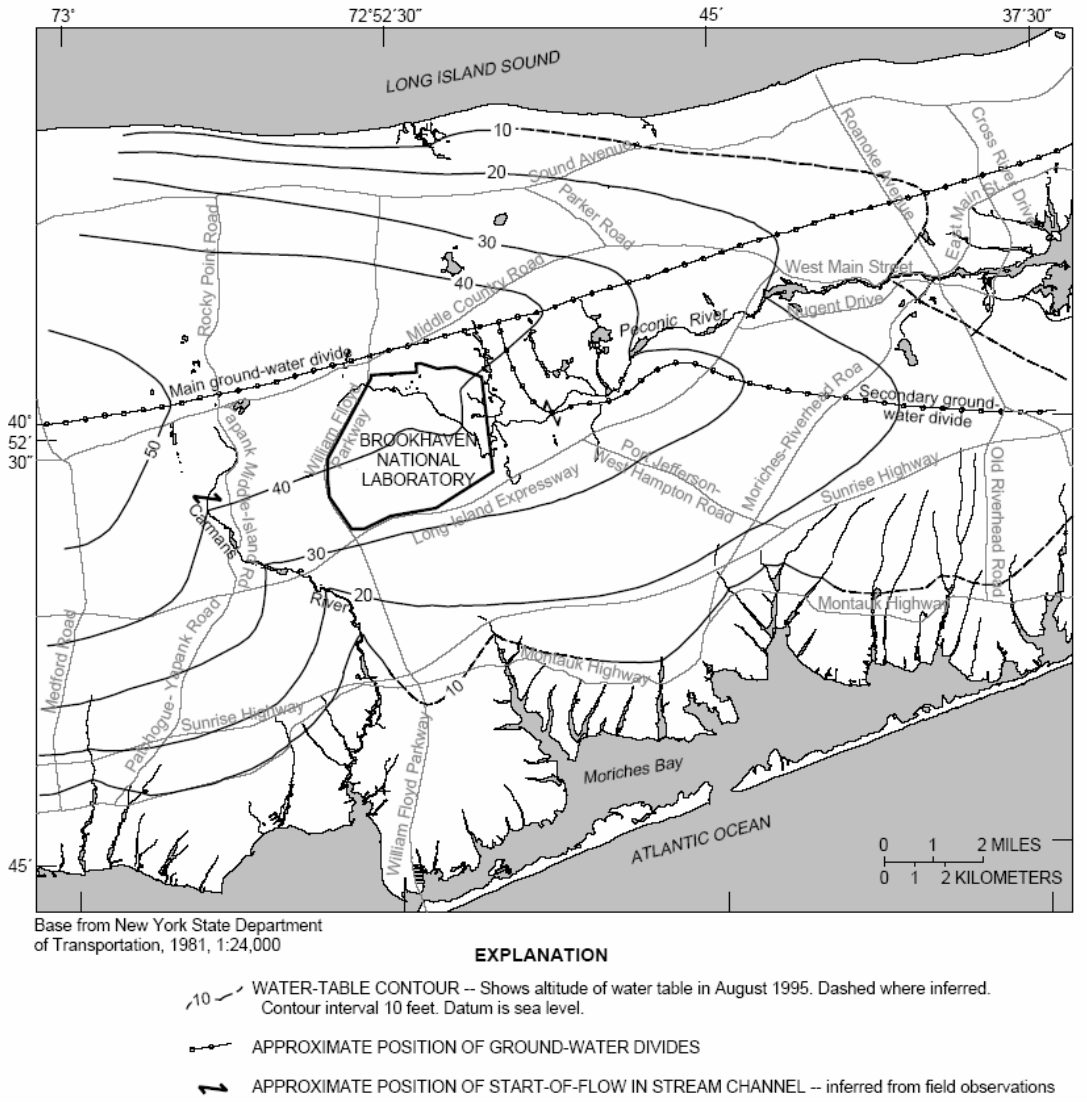

Figure 3-5. Water-table altitude in 300-mi^2 study area surrounding Brookhaven National Laboratory, Suffolk County, N.Y., August 1995 (Scorca et al., 1999)

Local Ground-Water Flow Patterns near Brookhaven National Laboratory

Ground-water flow and contaminant movement through the aquifer system below the BNL site are affected by several factors. First, pumping of ground water for supply at the site lowers ground-water levels and affects hydraulic gradients in the local ground-water system. Second, discharge from BNL's sewage-treatment plant to the Peconic River can affect the position of the start of flow and the discharge of Peconic River. Recharge basins and pumping of onsite ground-water-remediation systems also affect ground-water levels locally. The stream channel of the Peconic River extends onto the site, but the start of flow can be either east or west of the site under extreme hydrologic conditions. The amount of flow in Peconic River and base-flow discharge to the stream affect the position of the secondary (southeastward trending) ground-water divide. The hydraulic properties of several hydrogeologic units, including the Upper Glacial aquifer, Magothy aquifer, grayish-brown clay, Gardiners Clay and localized near-surface clay units along the Peconic River drainage system also affect ground-water flow (see Table 3-1 for a description of these units).

Water-table elevations at the site in March 1997 declined not only near supply wells, but near remediation (extraction) wells along the southern boundary of the site. At the same time, treated water from these systems was discharged to recharge basins and produced localized ground-water mounds near the basins (Scorca et al., 1999).

Flow Gradients in Brookhaven National Laboratory Area

The horizontal hydraulic gradient at BNL is typically 0.001 feet per foot (ft/ft), but in recharge areas and pumping areas, it can steepen to 0.0024 ft/ft or greater (Scorca et al., 1999). The natural ground-water flow velocity in most parts of the site is estimated to be about 0.75 ft/d, but flow velocities in recharge areas can be as high as 1.45 ft/d, and those in areas near BNL supply wells have been estimated to have velocities as great as 28 ft/d (Scorca et al., 1999).

Water-level measurements at paired water-table wells and deep wells screened in the Upper Glacial aquifer along the northern boundary of the site (near the regional ground-water divide) indicate significant deep-flow recharge areas, with downward vertical hydraulic gradients of as much as 0.007 ft/ft. Head differences at paired wells in the central and southern areas of the site become negligible, indicating that ground-water flow within the Upper Glacial aquifer is predominantly horizontal in these areas. Vertical gradients between the deep part of the Upper Glacial aquifer and the shallow part of the Magothy aquifer were about 0.018 ft/ft throughout the BNL site.

The BNL site is located within a Suffolk County Department of Health Services - designated deep-flow recharge area for the Magothy and Lloyd aquifers (Koppleman, 1978). Comparison of water level measurements from Upper Glacial aquifer and Magothy aquifer wells indicate significant downward flow across the BNL site (BNL, 1998, Paquette, 1998).

Ground-water flow in the vicinity of the HFBR varies due to BNL pumping and recharge operations in the area. In general, ground-water flow is toward the south or southeast. Evaluation of ground-water flow and quality data indicate that the downgradient portion of the tritium plume (south of Brookhaven Avenue) has shifted to the east since 1997 in

response to changing flows to various recharge basins, and the reduced pumping of BNL supply wells (BNL, 2004).

Ground water in the Upper Glacial aquifer beneath BNL generally exists under unconfined conditions (BNL, 2000). The Upper Glacial aquifer supplies both private and public water on Long island and is the exclusive source of drinking water and process water at BNL. The Laboratory currently operates six potable water supply wells that can be pumped at rates of 1,200 gallons per minute (gpm), and five process supply wells that can be pumped at rates between 50 and 1,200 gpm. During maximum water usage at BNL, up to 6 million gallons per day are pumped from the Upper Glacial aquifer. Most of this water returns to the aquifer by way of recharge basins or discharge of effluent to the Peconic River.

A main east-west trending regional ground-water divide lies approximately 0.5 miles north of BNL (Figure 3-5). A second ground-water divide, which transects portions of the BNL site during periods of high water table position (i.e., during periods of inflow from the aquifer to the stream bed), defines the southern boundary of the area contributing ground water to the Peconic River watershed (Scorca et al., 1996, Scorca et al., 1997). Natural drainage systems influence shallow ground-water flow directions across the BNL site: flow runs eastward along the Peconic River, southeastward toward the Forge River, and southward toward the Carmans River. Additionally, pumping and recharge induces considerable stress on the aquifer system in the central area of the site. Due to variable supply well pumping schedules and rates, considerable variations in ground-water flow directions and velocities occur. Pumping at the Suffolk County Water Authority well field located on the west side of the William Floyd Parkway also influences ground-water flow directions in the southwest corner of the site (Paquette, 1998).

Aquifer pumping tests conducted at BNL indicate that the horizontal hydraulic conductivity of the Upper Glacial aquifer is approximately 1,300 gpd/ft^2 (or 175 ft/d) based upon an aquifer thickness of 145 feet and a specific yield (effective porosity) of 0.24 (Warren et al., 1968; H2M/Roux Associates, 1985; CDM, 1995; Grosser, 1997). Total porosity value for the Upper Glacial aquifer is estimated to be 0.33 (Warren et al., 1968). Data from aquifer pumping tests and infiltration tests conducted at BNL by the United States Geological Survey (USGS) indicate that the vertical to horizontal anisotropy within the Upper Glacial aquifer is between 1:4 to 1:18 (Warren et al., 1968). The average vertical to horizontal anisotropy within the Upper Glacial aquifer on Long Island has been estimated to be 1:10 (Smolensky et al., 1989). The hydraulic properties of the basal Unidentified Unit cannot be determined with any degree of certainty using the current well network. Since the Unidentified Unit contains significant clay and silt, it is expected that these deposits are less permeable than the overlying glacial outwash and morainal sand and gravel (Paquette, 1998).

3.2.5 Tritium Plume Ground-Water Monitoring Data

Ground-water monitoring has been ongoing at BNL since the beginning of operation of the facility. The current HFBR monitoring well network consists of 159 wells, sampled quarterly (BNL, 2004). In 1996, a tritium leak was discovered from the spent storage canal of the High Flux Beam Reactor (HFBR) Facility. Initial concentrations of tritium

in proximal down-gradient monitoring wells were in the range of 600,000 picocuries per liter (pCi/L) (maximum contaminant level [MCL] for drinking water is 20,000 pCi/L).

After determining the tritium source was from the fuel canal associated with the HFBR, two 125 meter-long horizontal wells were installed upgradient and downgradient of the canal and between 0.6 to 1.6 meters below the water table, respectively (Figure 3-6). Both wells were constructed with six separated screen zones running parallel to and within five meters of the canal footprint. The stated goal of the wells was to rapidly and absolutely confirm that the canal was the source of the tritium contamination by showing that the upgradient well was clean and the downgradient well was contaminated. Unfortunately, the lateral spread of moisture and tritium in the vadose zone resulted in tritium concentrations that were similar in the two wells. Also, the concentrations measured in the horizontal wells during their first sampling were <5,000 pCi/L, significantly lower than the 140 million pCi/L concentration of the canal water and approximately 600,000 pCi/L concentrations detected in nearby downgradient monitoring wells. At the time, the project was viewed by some as a failure because it did not provide rapid and absolute confirmation. In fact, the project resulted in the successful and high-quality installation of two horizontal wells that would have provided useful confirmatory information when sampled over a period of several years. Importantly, vadose zone processes influenced the data in a manner consistent with theory (Looney and Paquette, 2000).

The vadose zone at the BNL is relatively thin (approximately 15 m). The flow path of water and tritium in the vadose zone immediately below the HFBR reactor building is shown schematically in Figure 3-6.

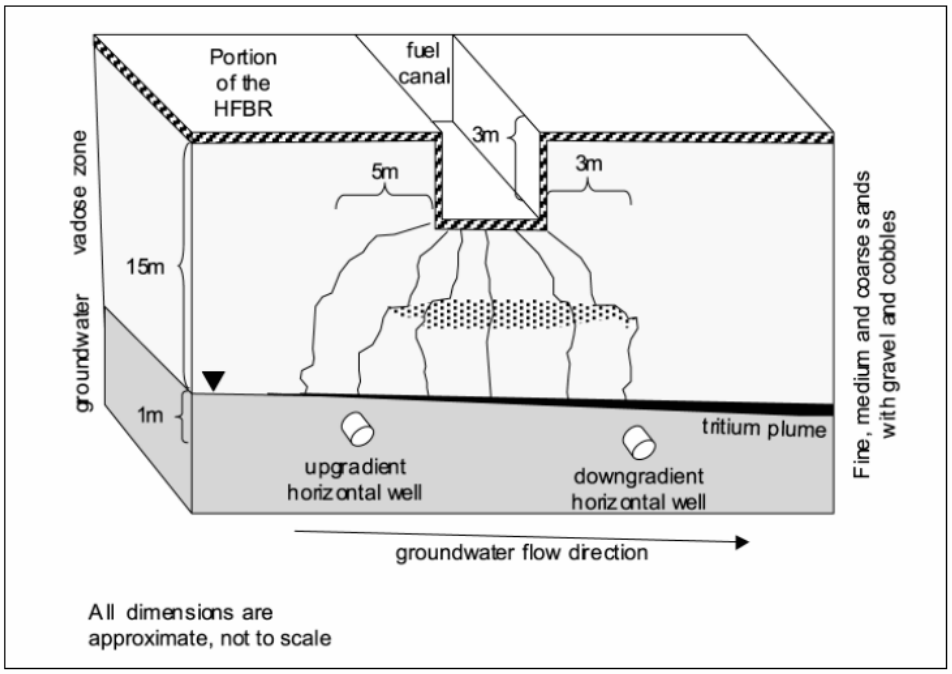

Figure 3-6. Schematic of plume configuration below the HFBR (Looney and Paquette, 2000). Used by permission of Battelle Press

In this situation, the vadose zone is dry because it is capped by the large building. The small leak from the fuel storage canal spreads out laterally and makes its way slowly to the water table. The lateral spread in the vadose zone is enhanced as the water tends to accumulate in and move through fine grained zones (silt and sand) and around coarse grained (gravel) zones (that is, water does not fill the holes in the sponge under these conditions). These vadose zone behaviors caused problems in interpreting data from two horizontal wells (discussed in the following section) that were installed in the water table to confirm the source of contamination

The overall geometry of the contaminant plume beneath the reactor is a direct result of the slow leak rate and the lateral spread in the vadose zone. As the contaminated vadose zone moisture slowly enters the relatively fast moving aquifer (~0.3 meters per day [m/d]), the plume forms a thin plume at the top of the water table. The thickness of this contaminated layer can be estimated from a simple analysis of the relative flow rates and areas (Figure 3-7)

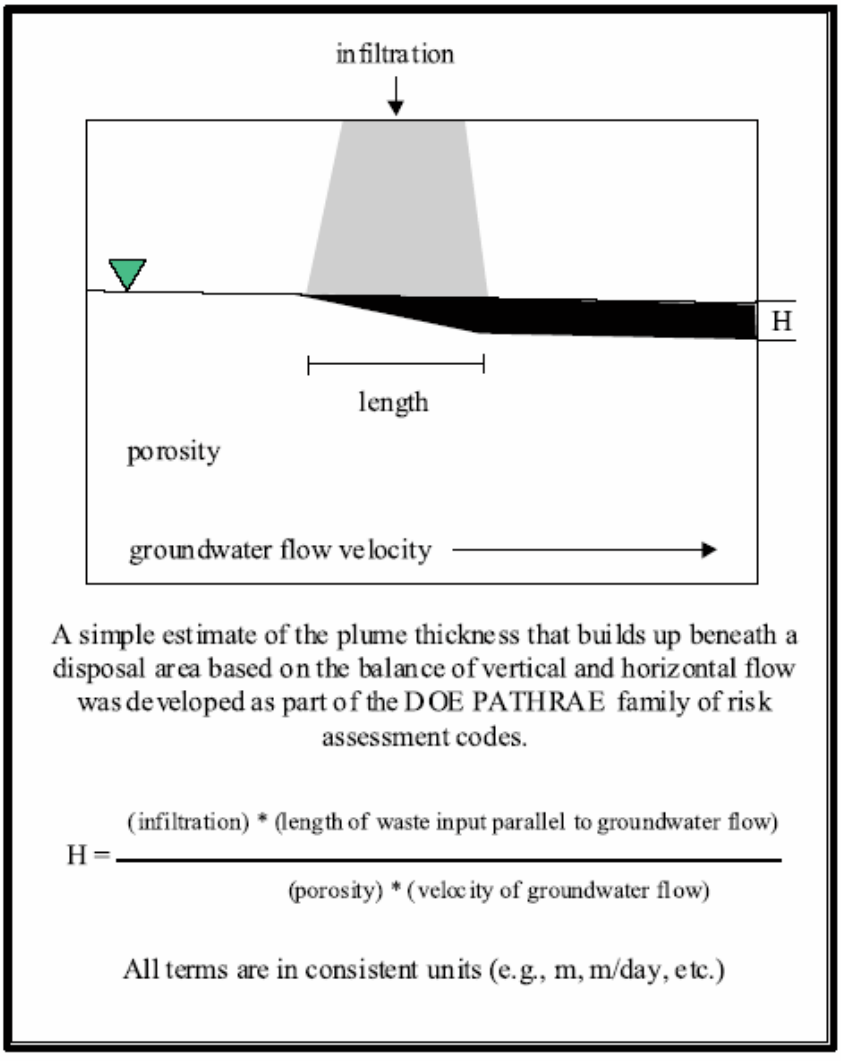

Figure 3-7. Simplified calculation of plume thickness immediately downgradient of a vadose zone source (Looney and Paquette, 2000). Used by permission of Battelle Press.

Based on leak rate data, measured lateral migration in the vadose zone, and typical hydrogeological values for this site, the tritium plume immediately beneath the reactor is expected to be very thin (<0.2 m). Even if this layer is smeared by seasonal water level fluctuations and other complexities, a simple evaluation of vadose zone delivery versus ground-water flow provides a clear understanding of why the initial sampling of the horizontal wells yielded low concentrations. Despite the wells being installed within a few feet of the water table, each of these wells were collecting water beneath the main body of the plume throughout most of the year. Thus, data from these wells were not providing an accurate picture of the plume location. Only when the wells were sampled during a seasonal drop in the ground water level was the plume location -- beneath HFBR primarily within a thin discrete zone at the water table surface – confirmed. Tritium concentrations of >650,000 pCi/L were detected in the upgradient well when the ground water level was within 0.3 meters of the well's screened zone. However, during the same period, low tritium concentrations continued to be low in the downgradient horizontal well (<2,000 pCi/L) because the sample was taken approximately 1 meter below the water table. Because water levels have remained greater than 0.6 meters above the downgradient well since its installation, the originally expected high levels of tritium have not been observed (Looney and Paquette 2000). By 1998, the highest concentrations of tritium in ground water downgradient of the HFBR exceeded 5,000,000 pCi/L.

When the plume exits the footprint of the HFBR, infiltration places clean water above the plume. Vertical migration of the plume accelerates, and the plume is expected to exhibit a classic downward trajectory (

Figure 3-8). Once again, actual monitoring data proved to be of high quality, and the large-scale measured Brookhaven plume behavior matches the expected pattern. This highly discrete vertical plume behavior resulted in additional complexity in the data interpretation from monitoring wells—highly variable measurements for samples collected at different times. Figure 3-6 documents the principal source of this variability for an example water table well located immediately down gradient of the source (Looney and Paquette, 2000).

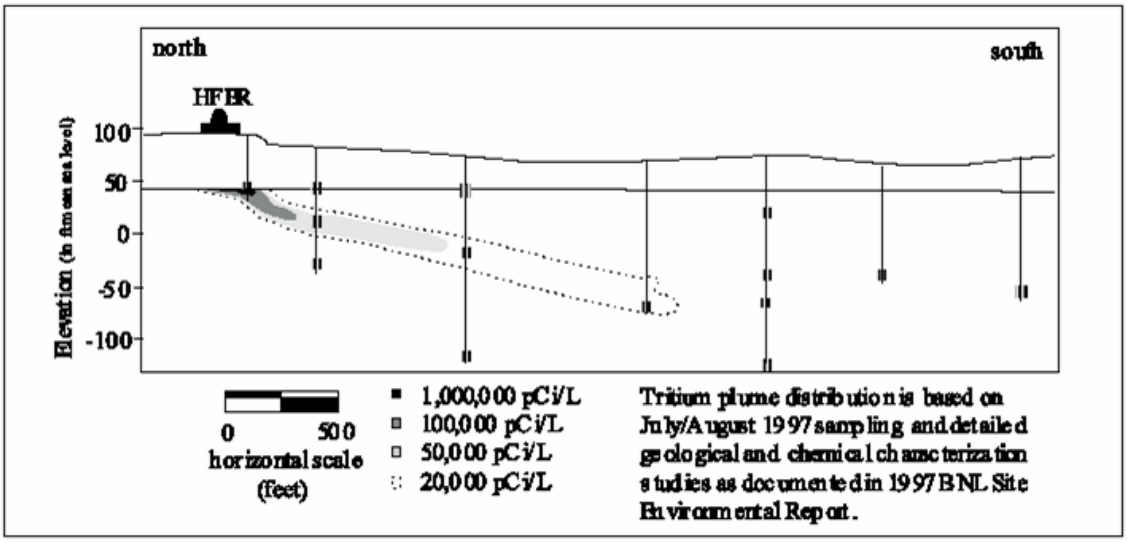

Figure 3-8. Cross section of tritium plume emanating from the HFBR (Looney and Paquette, 2000). Used by permission of Battelle Press.

Based on simple geometry for the case of a thin plume (<0.3 m thick), the tritium measurement in a water table well is simply the plume concentration adjusted by the ratio of the plume thickness to the wetted screen thickness (

Figure 3-8). As site operations and seasonal events impact ground-water levels, tritium levels in vertical monitoring wells will vary widely. While most pronounced for water table wells, the issue of plume/well geometry impacting concentration data is general and should be evaluated for all sites (Looney and Paquette, 2000).

As shown in Figure 3-9, ground-water flow below BNL is to the south-southeast and swings to the south-southwest upon exiting the site. However, the shape of the tritium plume bulges from the westin 1998 (Figure 3-10). This is not in agreement with the regional flow data in the water table and is likely influenced by remediation pumping on extraction wells EW-13 and EW-14, (Figure 3-9). After the plume passes EW-13 and -14, it swings back to the southeast most likely due to a combination of conditions including:

- the presence of other extraction wells in line and down gradient of the plume, including EW-15 (Figure 3-9),
- the direction of regional flow, and
- a circular topographic low located where the split in the plume occurs represents a relative increase in contribution to the water table that may result in localized mounding, and may act as a diversion to the movement of water.

Contaminant capture zones below the HFBR are large because of the high permeability of the water table aquifer and are obvious when comparing the water table contour maps with the contaminant plume maps.

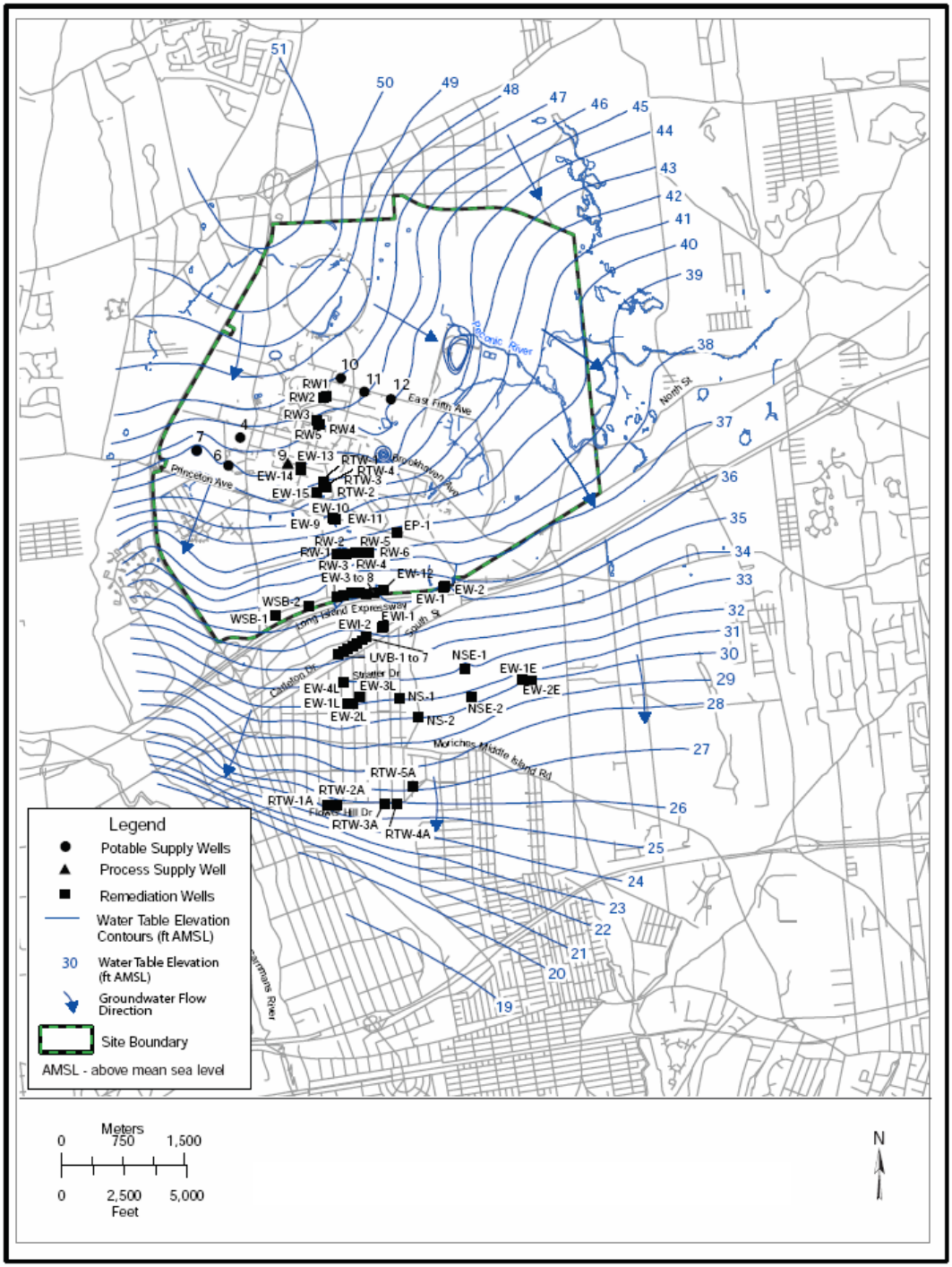

Figure 3-9. December 2005 water table map of BNL with extraction wells (BNL, 2005)

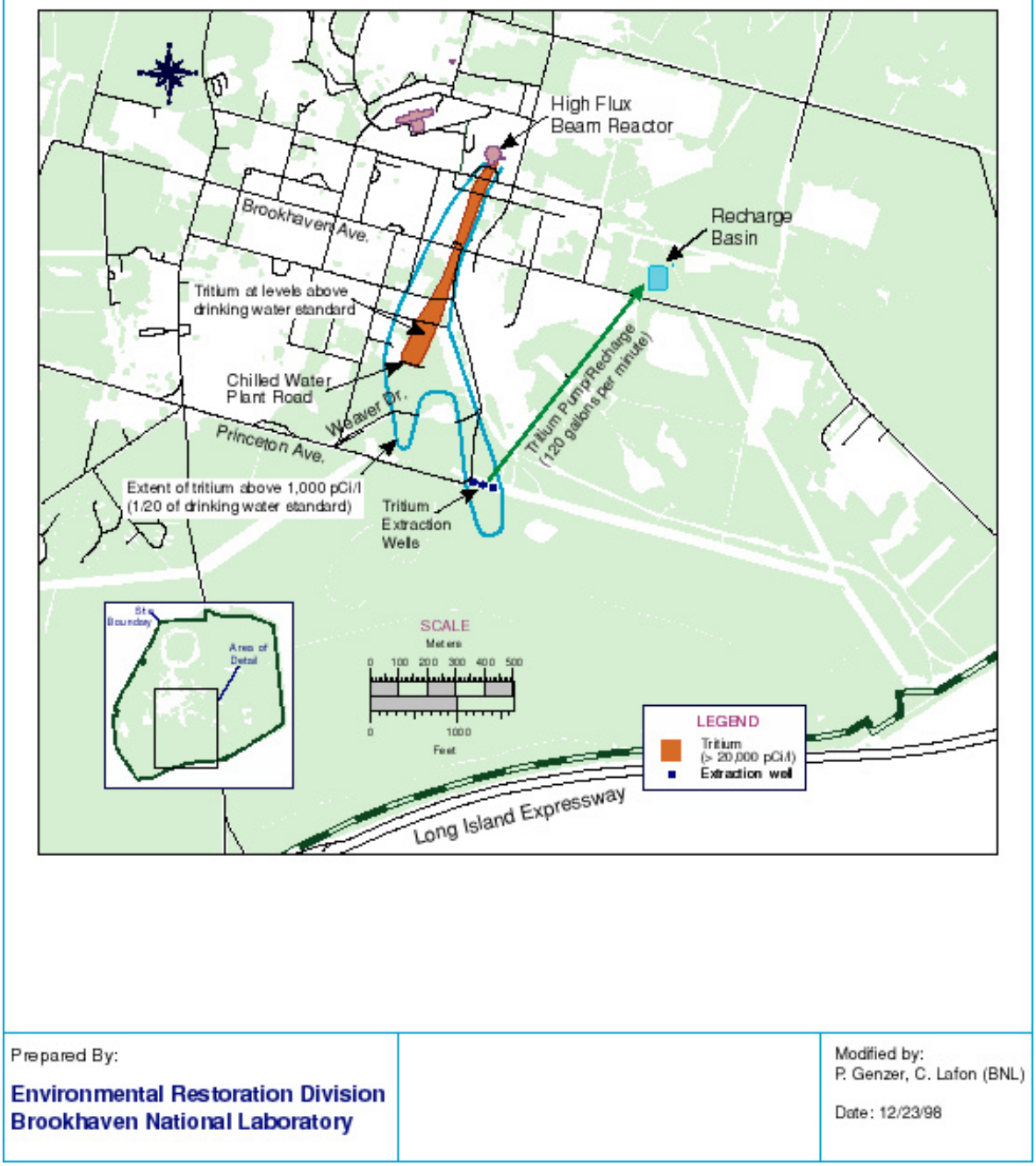

Figure 3-10. Location of tritium plume emanating from the High Flux Beam Reactor (DOE, 2000)

3.3 Ground-Water Modeling and Visualization

Through examination of existing site characterization and monitoring data, it became clear that nearby process and remediation well pumping significantly influenced migration of the tritium plume. Recognizing this fact, we realized that it was necessary to include these influencers in our conceptual site model. Based on earlier research on vadose zone transport at BNL (largely done by Looney and Falta), we also recognized the importance in developing flow and transport models that accurately accounted for this transport. In this Section 3.3, we describe the CSM and flow and transport models we developed to evaluate contaminant migration.

3.3.1 Plume visualization

For the three-dimensional data presentation, ground-water analytical data, along with survey information for the temporary monitoring wells, were loaded into a three dimensional data presentation software database (Arcview with 3D Analyst). From this information, a three-dimensional model of the actual tritium plume was created that allows a 360 degree horizontal and vertical perspective of the model. In addition, levels can be placed in the model corresponding to various surfaces such as ground images, water table surfaces, and geologic layers. By evaluating these complex data in three dimensions, a more complete picture of the temporal distribution of contamination can be visualized. As demonstrated below, this conceptual model assisted understanding of the observed data from the existing monitoring wells and guided our analysis regarding how and where future contaminant monitoring or remediation should occur.

Figure 3-11 and Figure 3-12 present two perspectives of temporary monitoring well data extracted from the BNL tritium database. The ability of 3D Analyst to present complex analytical data in an easily manipulated format makes the program ideal for presentations to anyone especially people who do not have a scientific or engineering background. Data used to prepare Figures 11 and 12 were current in April, 2006.

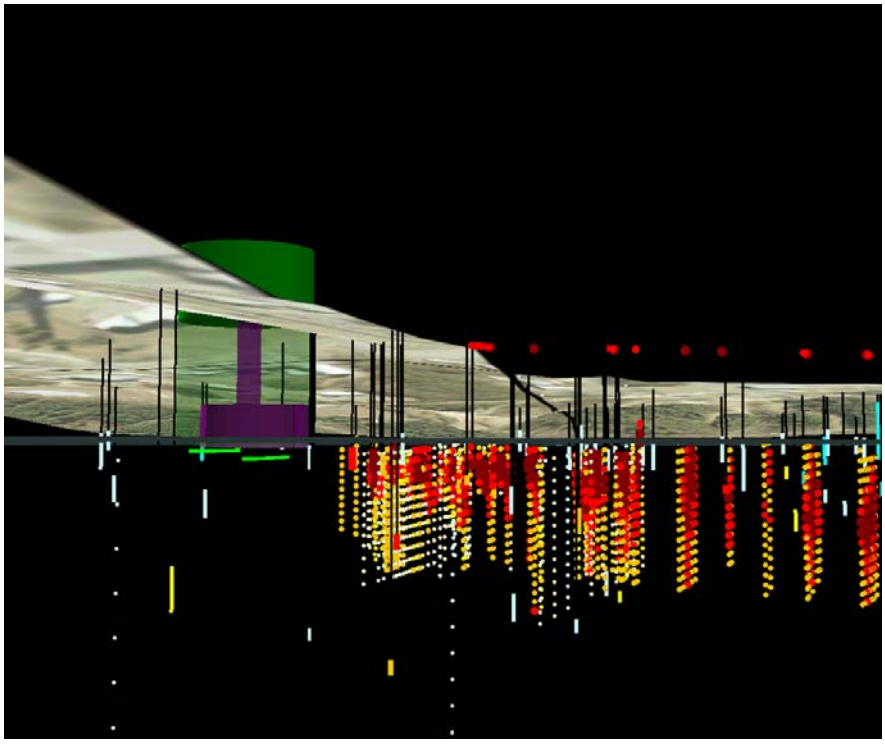

Figure 3-11. Oblique view looking northeast of tritium plume with concentrations emanating from the HFBR.

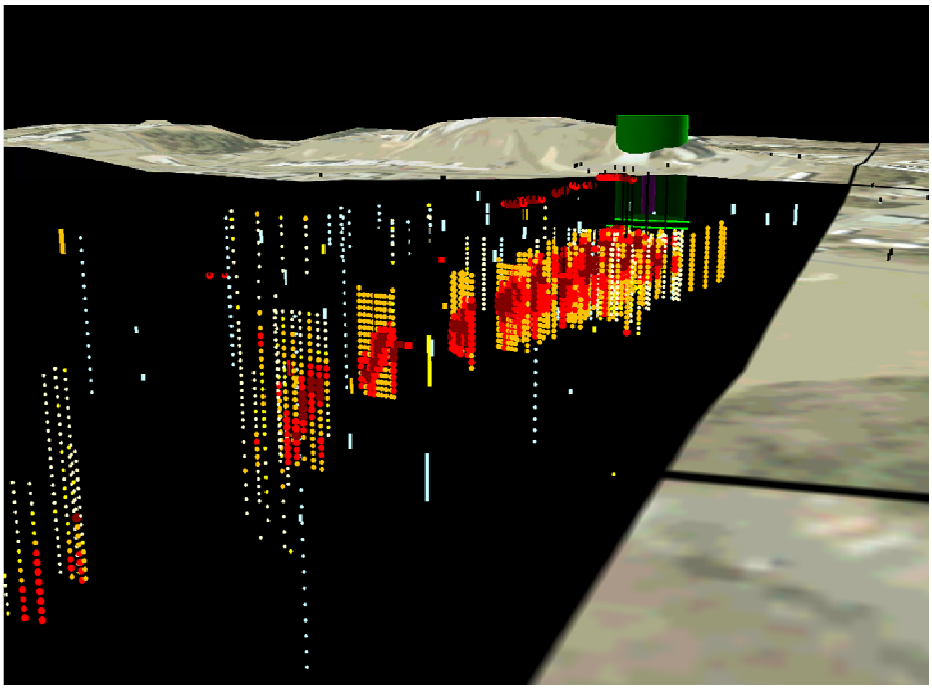

Figure 3-12. Oblique view looking northwest of tritium plume with concentrations emanating from the HFBR.

3.3.2 Flow and transport modeling

The second part of this exercise was to evaluate the effects of aquifer pumping on plume configuration by an active system that continuously pumps water from one or more monitor wells near the facility. Ground-water flow and transport simulation was performed utilizing a combination of techniques including excel spreadsheets, MODFLOW and GMS. Figure 3-13 and Figure 3-14 present the results of the ground-water modeling using GMS for visualization. The model assumed a homogeneous matrix with a hydraulic conductivity of 200 ft/day and a porosity of 0.3. Each square on the grid is 100 by 100 feet.

Modeling predicts, after 20 years with no pumping or remediation, the contaminant plume should be moving south by southeast, following the slope of the water table. Figure 3-13 presents the slope of the observed water table with the modeled tritium plume in color and the actual tritium plume uncolored. The actual plume did not follow the slope of the water table surface, but was pulled to the west by site extraction wells.

3.3.3 Active Monitoring

As has been observed from historical monitoring data, the tritium plume is relatively narrow, making it difficult to sample the plume through passive ground-water monitoring. For a similar facility and situation, an active extraction well monitoring program increases the size of the capture zone and the likelihood of detection.

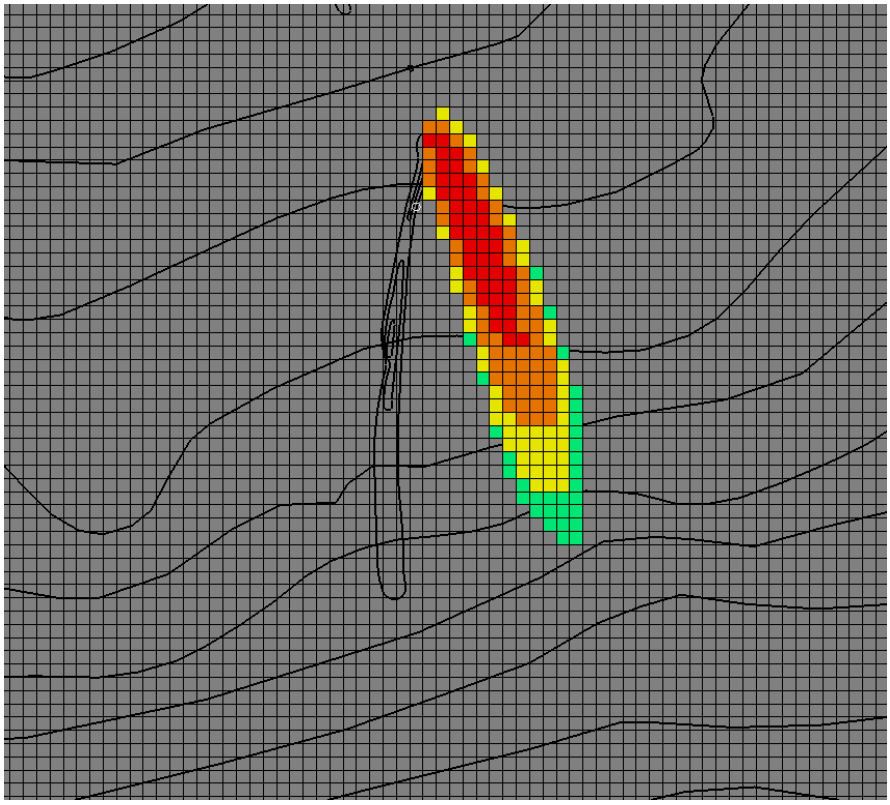

Figure 3-13. Computer simulation of tritium plume emanating from the HFBR after twenty years, no pumping

Because an active extraction well creates a large capture zone both vertically and horizontally, there is a greater opportunity for early detection. In the case of the HFBR, the tritium plume was confined to the upper 0.3 m of the water table and as stated above, the horizontal wells place below the HFBR failed to detect the tritium plume until the water level dropped enough to allow the wells to capture water from the top of the water table. By placing an active pumping monitor well just down gradient of the facility, a larger cone of influence can be evaluated, resulting in earlier detection.

The principal contaminants of concern at nuclear facilities are radionuclides, which can be detected at low concentrations, minimizing the concern of dilution due to pumping. Early detection of mobile contaminants through pumping could mitigate contamination, prevent offsite migration, minimize efforts associated with remediation of a larger, multi-contaminant plume, as well as serve as a Performance Indicator to validate and revise the conceptual model. Figure 3-14 provides the results of the modeling program shown in Figure 3-13 utilizing the same parameters, only with the addition of an active pumping well adjacent to the HFBR, pumping at a continuous rate of 100 gallons per minute. In this scenario, the plume has been pulled to the west by the pumping. A passive monitoring well at this location would not have detected this tritium plume; however, the active well easily captured the plume.

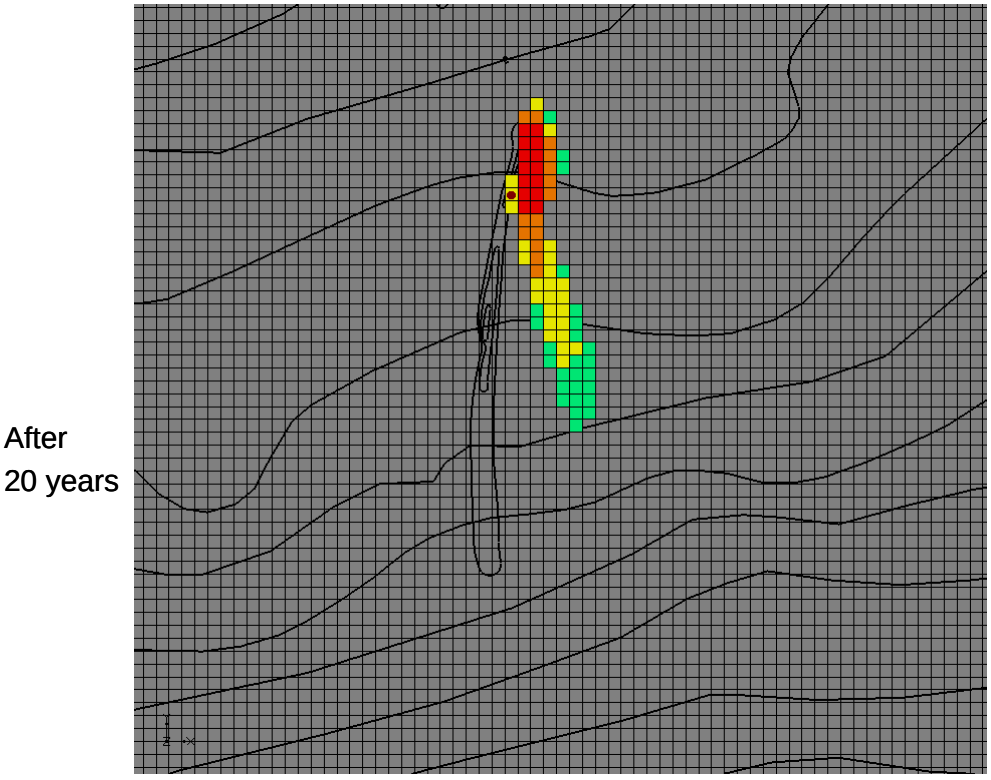

Figure 3-14. Computer simulation of tritium plume emanating from the HFBR after twenty years, pumping monitoring well.

3.3.4 Performance Indicators

Ground-water monitoring does not only entail analyzing for constituents of concern, but also various Performance Indicators that could trigger monitoring and/or remedial actions. These indicators can be used to validate or refine the conceptual site model. Performance Indicators and features, events, or processes (FEPs) which influence HFBR plume flow and transport include, but are not limited to:

tritium concentrations in the ground water – Tritium needs to be evaluated to not only determine if concentrations have exceeded monitoring limits (e.g., drinking water limits, etc..), but also to trigger low-flow pumping of extraction wells for removal and re-injection up gradient.

ground-water level distributions – The tritium plume emanating from below the HFBR is very narrow and the direction of movement of the plume is susceptible to slight changes in water table orientation due to varying meteorological conditions or changes in infiltration related to surface changes. Thus, in this environment, it is essential to account for ground-water level distributions when modeling and monitoring performance.

nearby remediation well pumping – Brookhaven is a rather small site in geographic extent. Any pumping on the site regardless of whether it is for remediation or process water can impact how plumes behave and interact. Ongoing remediation of other plumes in the vicinity may impact movement and capture rate of the HFBR tritium plume. Inception or termination of ground-water extraction for other plumes can significantly affect the orientation of the water table surface regionally. An adjacent pumping system could result in the migration of the HFBR tritium plume out of the path of current monitoring.

process water extraction- Production wells that are used to extract water for industrial processes can alter the direction, speed and concentrations of plumes. Water levels in monitoring wells should be carefully evaluated to determine if the cycling of process wells have an influence on contaminant plumes.

tritium as a tracer for other ground-water contamination – Because of its high mobility, tritium acts a tracer for the movement of future, less mobile contaminants. Because strontium-90 has been identified in the vicinity of the HFBR tritium plume, the tritium plume movement data can be applied to future strontium-90 monitoring and remediation efforts. Careful examination of older plumes (TCE plume) in the vicinity of the tritium plume can give insight to how the tritium plume and any subsequent plume might behave in the future.

tritium as a tracer for early warning – Tritium is very mobile within the vadose zone and is usually detected on the leading edge of contaminant plumes making the presence in soil vapors an excellent candidate for early warning of potential releases.

While the VOC plume mentioned in Figure 3-1 is not discussed in this Chapter, it may be worthwhile to note that flow and transport behavior of this plume may provide useful information about the potential pathway of the tritium plume.

3.4 Monitoring Strategy Application Conclusions

This case study illustrates how 3-D modeling can be a powerful tool for evaluating the shape, progress, and future paths of contaminant plumes. Because examination of existing site characterization and monitoring data led us to believe that the flow path of the tritium plume emanating from HBFR facility was being influenced by nearby process water and remediation well pumping, we realized the importance of incorporating these nearby wells into our CSM. In addition, based on earlier work done by Looney and Paquette, we realized that it was necessary to develop flow and transport simulations that could accurately model the observed tritium transport through the vadose zone.

The flow and transport simulations, which were developed using Excel, MODFLOW, and GMS, are effective tools for evaluating the effectiveness of various pumping alternatives, and thus, can aid in development of an efficient and cost effective monitoring and/or remediation program.

An optimally designed and operated monitoring network will increase the likelihood of early detection of plume migration. These flow and transport simulations can not only help place monitoring wells, but they can also help establish optimal pump rates. In this case, for example actively pumping monitoring wells may help create a larger cone of influence, resulting in less chance of a narrow plume being missed. By increasing the cone of influence, less monitoring wells may be required. By detecting these plumes earlier, remediation efforts can be put in place sooner, minimizing the chance for the plume to spread offsite or to other aquifers.

Detailed contour maps of changing water table surfaces may also be helpful to evaluate the effects of seasonal changes to the water table as well as the effects of extraction/injection activities at remediation start up, during operation, or after termination of activities. The narrow nature of these plumes makes understanding changes vital.

3.5 Brookhaven References

Aronson, D.A., and G.E Seaburn. "Appraisal of the operating efficiency of recharge basins on Long Island, N.Y., in 1969." U.S. Geological Survey Water- Supply Paper 2001-D, 22 p. 1974.

Brookhaven National Labortary (BNL). "1997 Environmental Restoration Division Sitewide." Groundwater Monitoring Report. June 1998.

BNL. *Source Water Assessment for Drinking Water Supply Wells*. Brookhaven National Laboratory, December 2000.

BNL. "2003 BNL Groundwater Status Report." Environmental and Waste Management Services Division/Environmental Restoration. June 2004.

BNL. 2005 Site Environmental Report, Brookhaven National Laboratory, p. 7-5.2005.

CDM Federal Programs Corporation. "Technical Memorandum, Pre-Design Aquifer Test, October 10-20, 1995." Brookhaven National Laboratory. December 1995.

Department of Energy (DOE). Brookhaven National Laboratory, EPA Region 2, Operable Unit III, Record of Decision, Environmental Restoration Division, April 14, 2000.

DOE. Brookhaven National Laboratory, EPA Region 2, NPL Listing History, www.epa.gov/region02/superfund/npl/0202841c.pdf, August 17, 2006.

Franke, O.L., and N.E. McClymonds. "Summary of the Hydrologic Situation on Long Island, New York, as a Guide to Water-Management Alternatives." U.S. Geological Survey Professional Paper 627-F, 59 p. 1972.

Grosser, P.W. (Consulting Engineer and Hydrogeologist, P.C.). Operable Unit III Pump Test Report.1997.

Holzmacher, McLendon and Murrel, P.C. (H2M), and Roux Associates, Inc. *Waste Management Area, Aquifer Evaluation and program Design for Restoration. Volumes I and II.* 1985.

Koppelman, L.E. (Ed.). *The Long Island Comprehensive Water Treatment Management Plan (Long Island 208 Study).* Nassau-Suffolk Regional Planning Board. Hauppague, New York. Volumes I and II. July 1978.

Looney, B.B., and D.E. Paquette. *Tritium Source Characterization at the High Flux Beam Reactor Brookhaven National Laboratory*. Compiled in Vadose Zone Science and Technology Solutions. Vol. 1, p. 50-59.2000.

Paquette, D.E. *Brookhaven National Laboratory AGS Booster Applications Facility, Potential Impacts to Groundwater Quality*. September 1998.

Prince, K.R., O.L Franke, and T.E. Reilly. "Quantitative Assessment of the Shallow Ground-Water Flow System Associated with Connetquot Brook, Long Island, New York:" U.S. Geological Survey Water- Supply Paper 2309. 28 p. 1988.

Quadrel, M., and R. Lundgren. *Managing an Effective Vadose Zone Project.* Compiled in Vadose Zone Science and Technology Solutions. Vol. 1, p. 61-124.2000.

Scorca, M.P. "Urbanization and Recharge in the Vicinity of East Meadow Brook, Nassau County, New York, Part 1—Streamflow and Water-Table Altitude, 1939-90." U.S. Geological Survey Water-Resources Investigations Report 96-4187, 39 p. 1997.

Scorca, M.P., W.R Dorsch, and D.E Paquette. "Water-Table Altitude Near the Brookhaven National Laboratory, Suffolk County, New York, in March 1995." U.S. Geological Survey Fact Sheet FS-128-96. December 1996.

Scorca, M.P., W.R Dorsch, and D.E Paquette. "Water-Table Altitude Near the Brookhaven National Laboratory, Suffolk County, New York, in August 1995." U.S. Geological Survey Fact Sheet FS-233-96. April 1997.

Scorca, M.P., W.R. Dorsch, and D.E Paquette. "Stratigraphy and Hydrologic Conditions near the Brookhaven National Laboratory and Vicinity, Suffolk County, New York, 1994-1997." U.S. Geological Survey Water Resource Investigations Report 99-4086. 1999.

Smolensky, D.A., H.T Buxton, and P.K Shernoff. "Hydrogeologic Framework of Long Island, New York." U.S. Geological Survey, Hydrogeologic Investigations Atlas 709, 3 Sheets. 1989.

Warren, M.A., W. deLaguna, and N.J Lusczynski. "Hydrogeology of Brookhaven National Laboratory and Vicinity, Suffolk County, New York." U.S. Geological Survey Bulletin 1156-C, 127 p. 1968.

Woodward-Clyde Consultants. *Potable Well Stud.,* Brookhaven National Laboratory, Upton, Long Island, New York. 10 p. 1993.

4 Amargosa Desert Research Site

4.1 Introduction

The Amargosa Desert Research Site (ADRS), located in Nevada's Mojave Desert, was selected to test the applicability of the Advanced Environmental Solutions, LLC (AES) Strategy to an arid environment. This exercise is for demonstration only. This report is based on readily available information and does not constitute a comprehensive evaluation of all data for the site. Data used in this exercise were provided courtesy of the United States Geological Survey (USGS).

The Amargosa Desert Research Site was previously a commercially-operated low-level waste-burial facility on the Mojave Desert, about 40 km east of Death Valley, near Beatty, Nevada. Beginning in 1962, low-level waste was disposed in unlined trenches. By 1970, hazardous waste was also placed in unlined trenches. Starting in 1988, the hazardous material was placed in lined trenches. Low-level disposal was ceased in 1992.

In 1976, the USGS began studies of water movement at the Beatty Low-Level Waste Disposal Facility. In 1997, after unexpectedly high levels of tritium were discovered in shallow soil gas samples, the site was included in the USGS's Toxic Substances Hydrology Program and became known as the Amargosa Desert Research Site.

The primary issue of concern at the ADRS is the migration of radionuclides and VOCs from the waste buried in the facility trenches. Tritium, when present in the ground water or the vadose zone, is an excellent indicator for the movement of contaminants.

Evaluation of all available data for the ADRS has resulted in several questions, the most significant of which is: Why is tritium present across the vadose zone and in the ground water below the ADRS? Research has indicated that overall soil moisture in the vadose zone adjacent to the ADRS exhibits an upward movement (Andraski et al., 2005). However, the presence of elevated tritium across the vadose zone, to a depth of over 100 meters below ground surface (bgs), would indicate that there is a mechanism for the downward migration of contamination.

Soil vapor modeling by Striegl et al., 1996 failed to produce a mechanism for the vertical component of movement of tritium within the vadose zone below the ADRS. Striegl et al., 1996 also proposed that the only mechanism for the vertical migration of tritium was in liquid form along complex hydrogeologic layers, but were unable to find specific geologic data to support this hypothesis.

Because of the necessity for a fast pathway for the downward movement of soil gases containing tritium and after a comprehensive review of all available data for the site, an alternate conceptual model for movement of tritium through the vadose zone and into the underlying water table below the ADRS is proposed in the following sections.

4.2 Compilation of Available Data

This section provides a summary of the readily available data compiled to prepare this evaluation. The majority of the data used in this evaluation has been provided by or is available on line from the USGS.

4.2.1 Geologic Setting

The ADRS is located in the Basin and Range Province of southern Nevada (Figure 4-1). This area of the Mojave Desert southwestern United States is considered one of the driest in the United States (Andraski et al., 2005).

The Basin and Range Province of Nevada is characterized by a series of north-south-trending extensional sedimentary basins represented by patchwork mountain ranges or "horsts", commonly 10 miles wide and rarely longer than 80 miles long, bounded by faults and adjacent downthrown valleys or "grabens". The bounding faults have been active during the last 20 million years and represent an extensional geologic regime. The normal bounding fault planes usually dip approximately 60 degrees and extend deep into the crust, creating vertical displacement of as much as 10,000 feet. Figure 4-2 presents a generalized cross section of a horst and graben sequence (CG 1992).

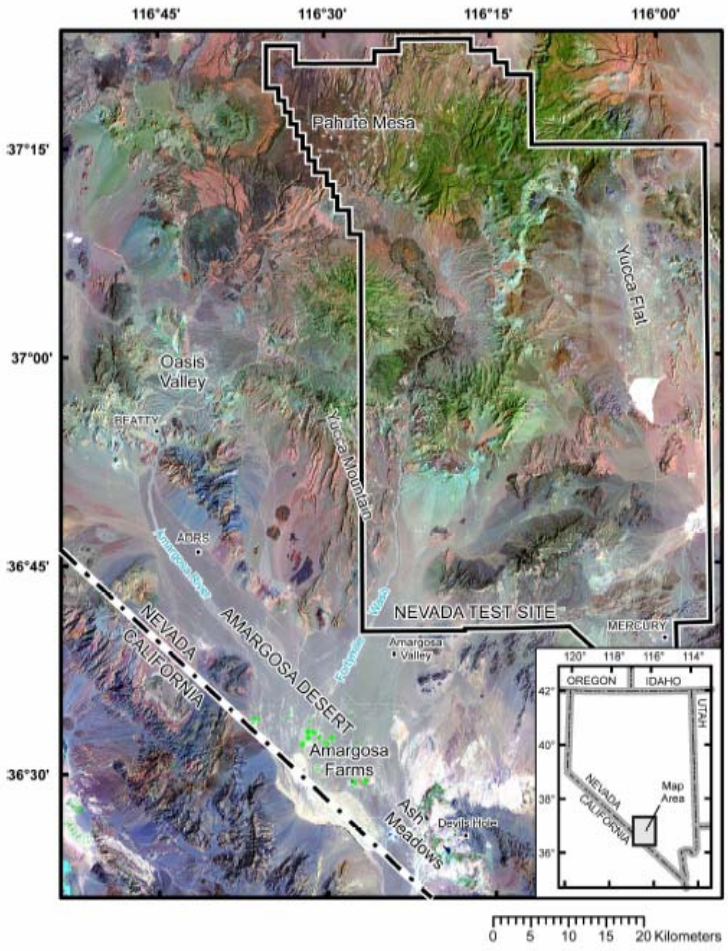

Figure 4-1. Location of ADRS (Stonestrom et al., 2003)

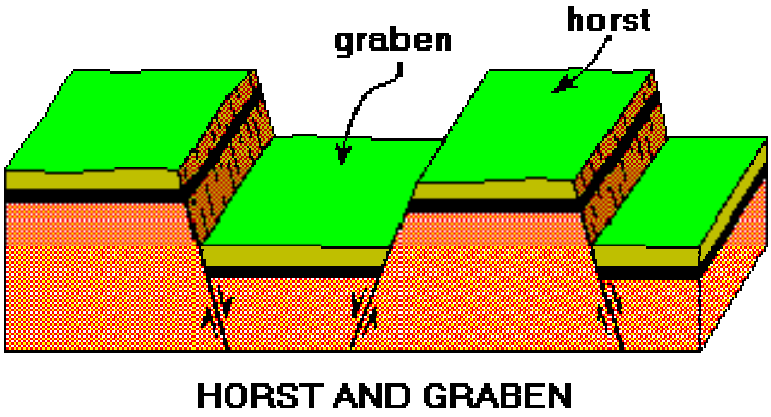

Figure 4-2. Cross section of a typical horst and graben sequence (CG, 1992)

Weathering and erosion began soon after formation of the horsts. The movement of the sediments into the adjacent basins created alluvial fans on top of basin sediments. Figure 4-3 provides an oblique view of a typical alluvial fan. These fans form when upland streams with steep gradients leave rugged terrain and enter a valley. Alluvial fans contain sequences of poorly sorted material. In addition, they contain series of active and abandoned interlacing channels.

The interlacing of these channels results in complex patterns of alternating high and low permeability, which significantly affects ground-water movement. However, because the fans were deposited with a generally radial pattern, the permeability of the sediments should also generally follow the same trends.

Figure 4-3. Oblique view of a typical alluvial fan in Death Valley

4.2.2 Regional Geologic Information

The Amargosa Desert Research Site is located in a 13 km wide northwest-trending graben of the Basin and Range Province of southern Nevada (Figure 4-4). The regional geology underlying the ADRS appears to consist of shallow river gravels overlying unconsolidated alluvial fan, fluvial, and marsh deposits, and ultimately Paleozoic bedrock (Fischer, 1992). Since the ADRS is located adjacent to the northeast flank of the graben, the promulgation of the alluvial fan is from the northeast to the southwest across the site. The graben is bounded by mountain ranges composed of lower Paleozoic carbonate and clastic sediments, metasediments, and volcanics. The valley floor below the ADRS is presumably composed of similar material.

In addition to the alluvial fan deposition at the ADRS, the Amargosa River has subsequently overprinted a floodplain of coarse river gravels near ground surface, covered by a thin (1 m thick) layer of finer grained sediments.

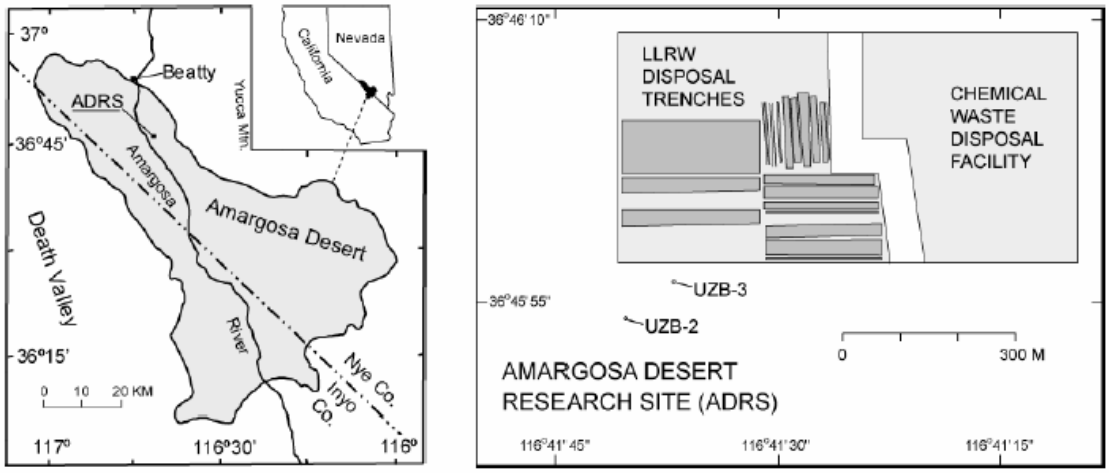

Figure 4-4. Location of ADRS and soil gas sampling boreholes UZB-2 and UZB-3 (Stonestrom et al., no date)

4.2.3 Site-specific Geologic and Analytical Data

Available data sources for this analysis included:

- Geophysical borehole log data (neutron-moisture, natural gamma, and gamma-gamma)
- Monitoring well data from existing wells
- Schlumberger soundings
- Soil gas data
- Thermocouple psychrometer / water potential data
- Soil moisture data
- A summary of each of these data sets, and relevant conclusions is below:

Geophysical borehole log data analysis (neutron-moisture, natural gamma, and gamma-gamma):

While core logs are not available for these wells, Geophysical borehole logging suggests the presence of isolated clay lenses (Figure 4-5) (Fischer, 1992). For example, thin clay lenses were detected at 10, 20, and 25 m bgs in Well 303, but were not seen in the other wells. Also, a clay lens was observed in the log of Well 302 at a depth of 37 m, but was not observed in the other wells. Low moisture content at various intervals may indicate coarse, more permeable gravel; however, some of these low moisture intervals also have elevated gamma readings.

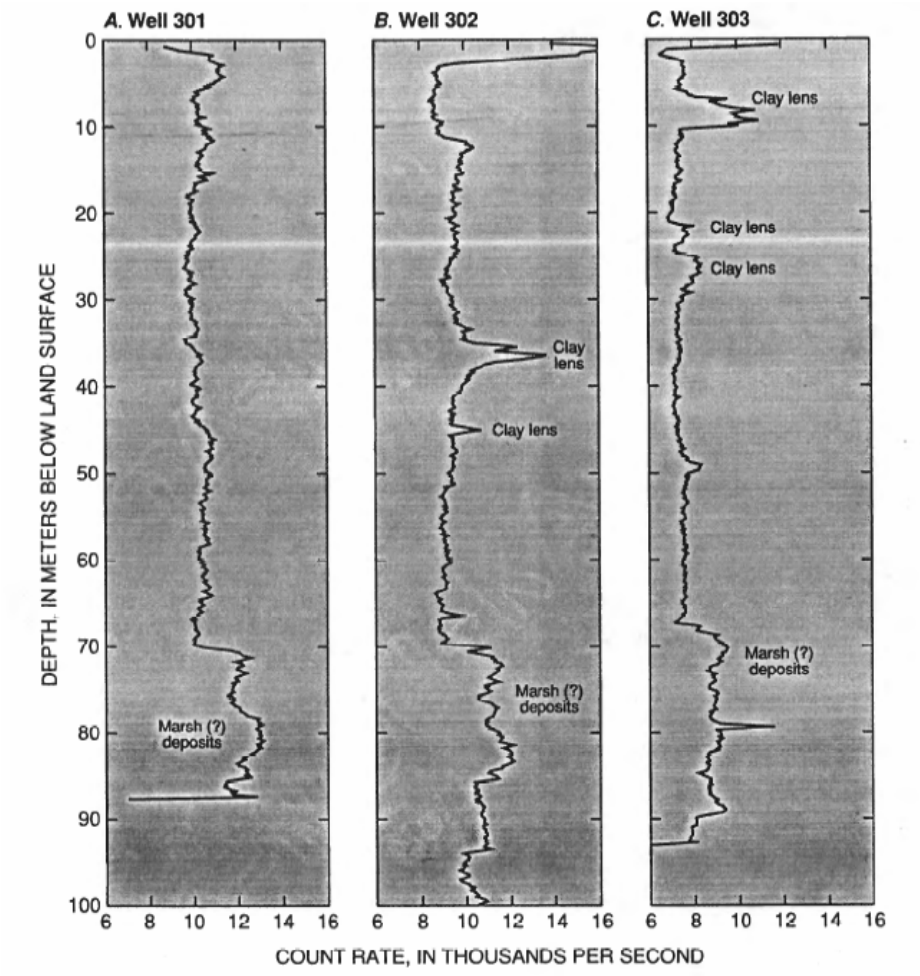

Figure 4-5. Geologic distribution of clay lenses and marsh deposits in ADRS Wells 301, 302, and 303 (Fischer, 1992)

The most consistent subsurface layer appears to be a 20 m thick clay marsh deposit at a depth of 70 to 90 m bgs and is present in all three boreholes (Fischer, 1992). Based on the top of the clay horizon, Fisher determines the unit dips to the south-southeast at a rate of approximately 0.07 meters per meter (m/m).

Figure 4-6 presents contours of the water table surface which show a south-southwest dip in the water table toward the southwestern portion of the facility. Depth to bedrock below the ADRS is approximately 170 m and depth to ground water is approximately 100 meters bgs. This Figure also shows the location of 14 monitoring wells within the ADRS burial site and several others in the surrounding vicinity (shown as circles in the Figure); however, data for these wells were unavailable.

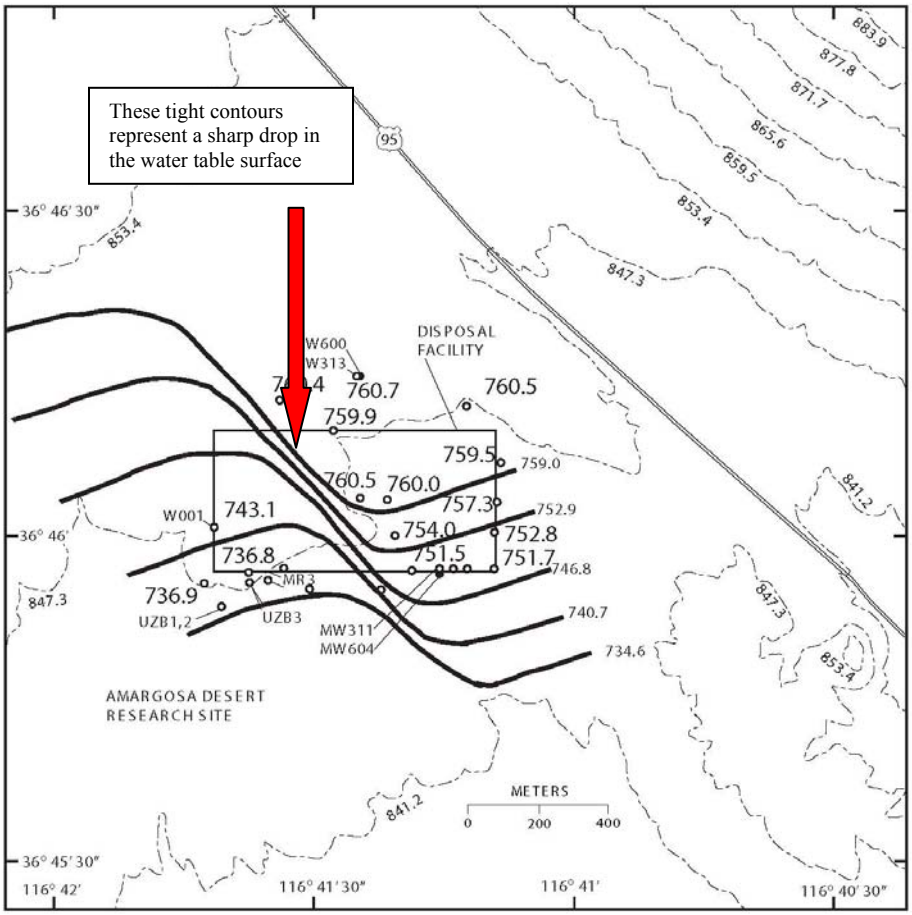

MR3 734.3
UZB3 736.8
MW302 736.9
MW311 751.6
MW317 751.0
Site Well 760.5

MR1 near Amargosa River 3,200 m west of northwest corner; Water table 757.82 m.

Well MW319 76.2 meters north; 181.92 m east of northwest corner
Elevation of water table is 760.4 m; May 6, 2004

Well MW318 71.4 meters north; 705.46 m east of northwest corner
Elevation of water table is 760.5 m; May 6, 2004.

Well MW325 449.53 meters south; 28.91 m west of northwest corner
Elevation of water table is 736.9 m; May 6, 2004

Well MW326 447,22 meters south; 266.39 m east of northwest corner
Elevation of water table is 737.7 m; May 6, 2004

Well MW327 446.5 meters south; 472.33 m east of northwest corner
Elevation of water table is 741.6 m; May 6, 2004

Figure 4-6. ADRS water table contours (measured in meters MSL) and well locations (Walvoord et al., 2005)

Monitoring well data analysis

Tritium is present in the water table over 100 meters below the ADRS, albeit in concentrations well below drinking water standards. Figure 4-7 provides a map of tritium concentrations in water table monitoring wells (monitoring well data is summarized in Appendix 4-A). The elevated tritium concentrations in ground water at location MR-3 in relation to the other facility monitoring wells brings into question the source of this tritium and the potential need for a revised CSM of contaminant movement in the vadose zone.

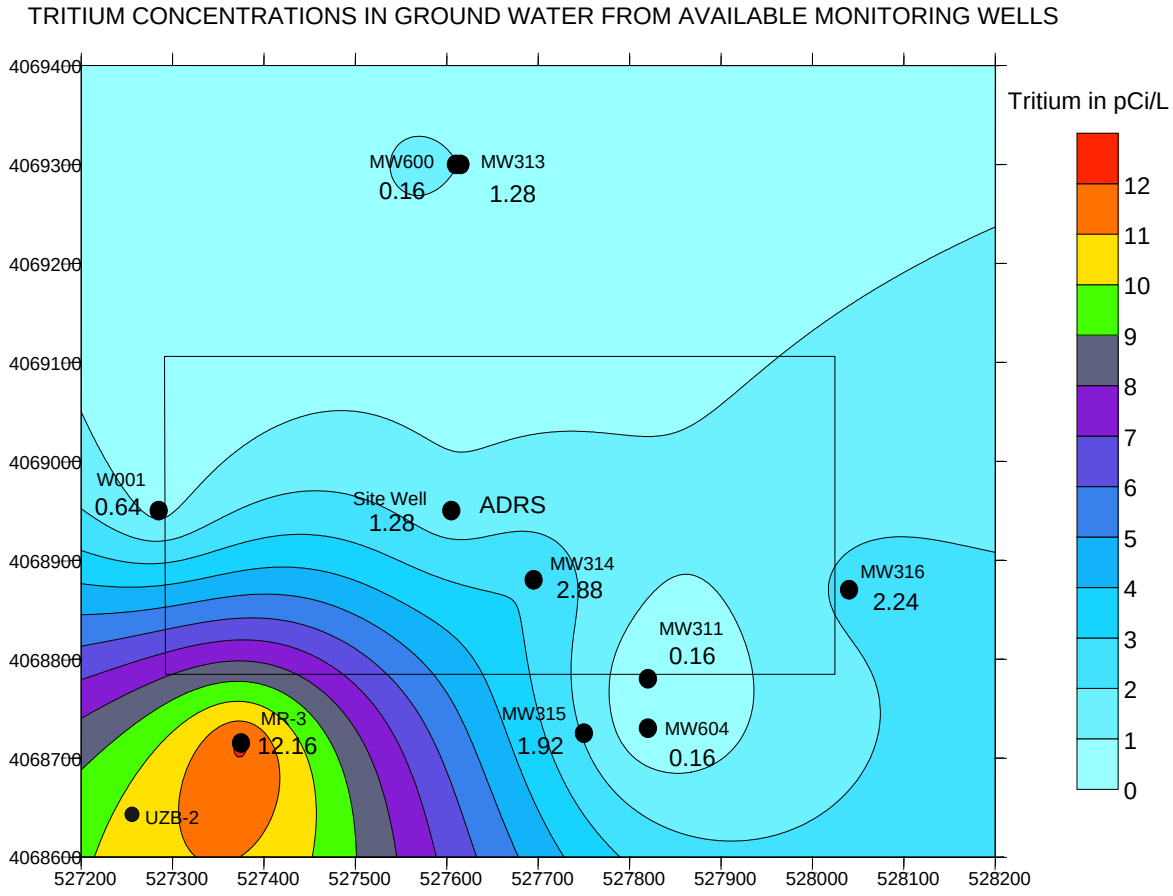

Figure 4-7. Map of tritium concentrations in ground water below ADRS (Data from Prudic, 1997)

Based on the regional geologic setting of the ADRS in a graben, with the nearest horst fault boundary to the northeast, the alluvial fan pattern for the geology below the site should dip to the west-southwest with some degree of radial dispersion present. Vertical variability in the fine to medium grain portion of the layering creates a significant anisotropic effect for movement of constituents within the vadose zone that should be accounted for in a monitoring program. In addition, the coarse gravel layer present at approximately 1.5 m bgs appears to act as a conduit for the lateral transport of contaminants.

Schlumberger sounding data analysis

A resistivity survey of Schlumberger soundings conducted in 2002 (Bisdorf, 2002) over the ADRS area indicates the presence of a significant northwest to southeast striking basin fault approximately 500 feet northeast of the site. The sounding results suggest that the fault line dips steeply to the southwest beneath the subsurface. This fault orientation is most likely related to the regional horst and graben faulting (Figure 4-8 depicts numbered Schlumberger sounding survey locations with faults; Figure 4-9 shows the suggested location and fault orientations).

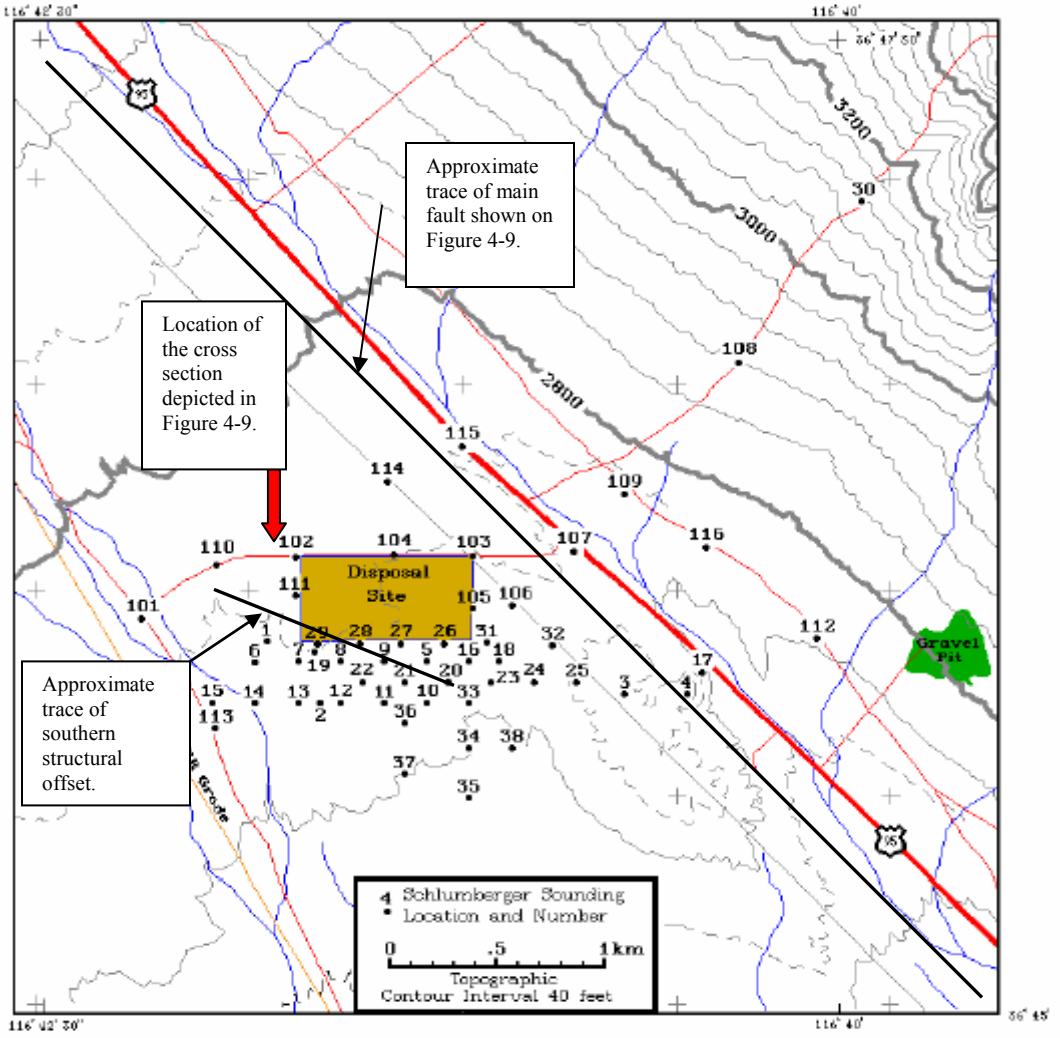

Figure 4-8. Map showing numbered survey locations of Schlumberger soundings (modified from Bisdorf, 2002)

The trace of US Highway 95 on Figure 4-8 appears to follow the toe of the alluvial fan as it emerges from below the alluvial river gravel. The trace of the basin fault, as defined by the results of the Schlumberger Soundings, also roughly parallels the trace of US Highway 95. The thin blue lines on the map represent intermittent stream drainages. The trace of the cross section presented in Figure 4-9 runs between sounding locations 110 and 116. An additional fault was later identified during the application of this Strategy

and is referenced in this report as the "southern structural offset". This offset was identified through the application of three-dimensional visualization of the resistivity data and is discussed further in Section 4.3.4 below.

Figure 4-9 presents a cross section of the Bisdorf resistivity soundings indicating the location and orientation of the fault between sounding locations 103 and 107. As shown in Figure 4-9, Bisdorf infers the location of the basin fault by the presence of the steep resistivity gradient between sounding locations 103 and 107.

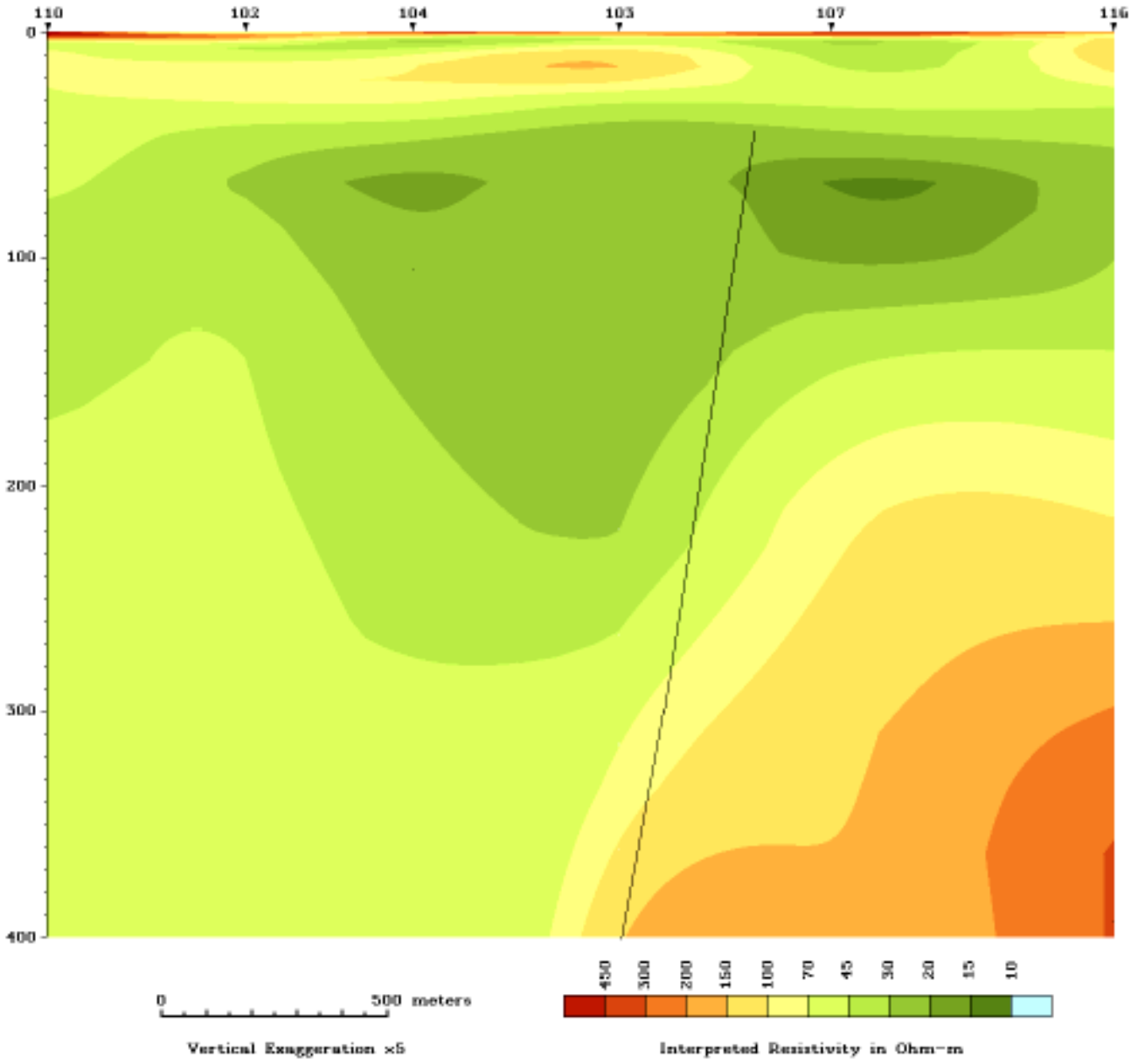

Figure 4-9. Cross section of interpreted resistivity and basin fault (Bisdorf, 2002). (Triangles along the top axis correspond to sounding locations as mapped in Figure 4-8. Subvertical solid black line represents basin fault as defined by Bisdorf 2002.)

Figure 4-10 is a contour map of the resistivity survey at approximately 97 m bgs and shows the displacement of sediments down on the southwest side of the northwest-trending structure.

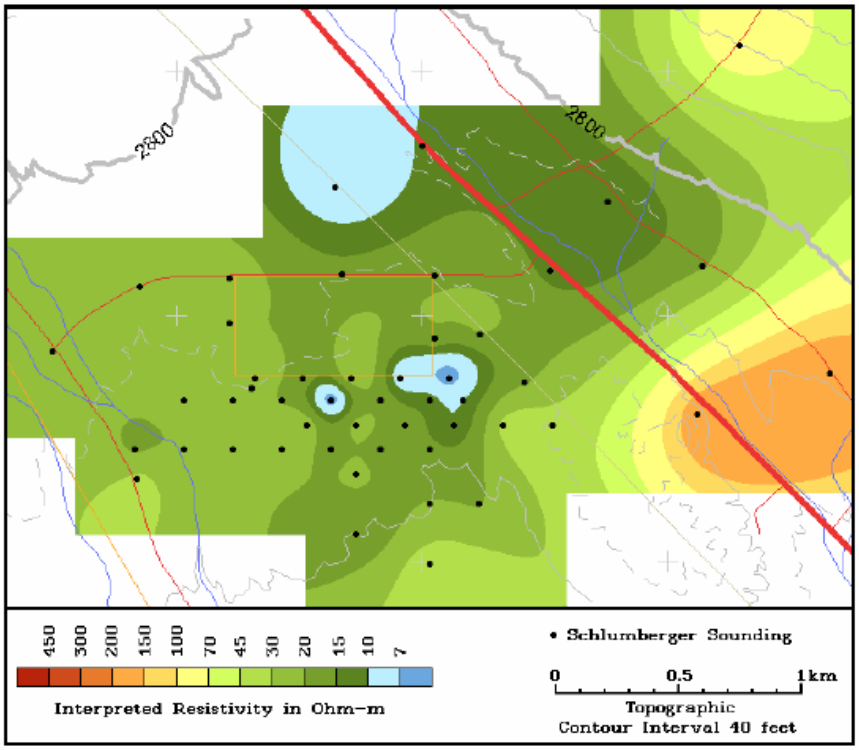

Figure 4-10. Map showing contours of interpreted resistivity at a depth of 97 m overlying topographic contours (Bisdorf, 2002)

Surficial soil gas data analysis

Surficial soil gas data and terrestrial sampling seem to indicate that, at least in the near surface, contaminant migration is along gravel layers to the south and west from the burial trenches, following topography and away from this fault.

Direct current electrical resistivity (DC-resistivity) imaging

A vertical cross section (Figure 4-11) made by Stonestrom using direct current electrical resistivity (DC-resistivity) imaging near UZB-2 and UZB-3 (vadose zone soil gas sampling wells) shows intermittent gravel layers that thicken to the southwest toward the center of the basin, providing preferential pathways for contaminant migration (Stonestrom et al., no date).

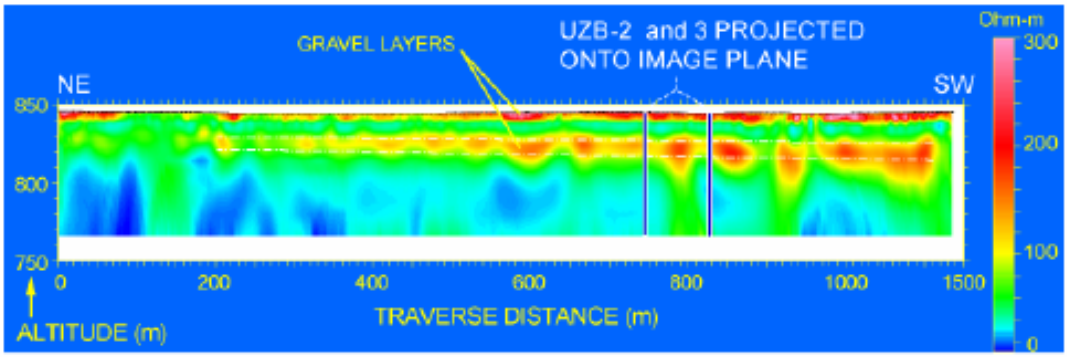

Figure 4-11. A vertical cross section made by direct current electrical resistivity (DC-resistivity) imaging near the ADRS (Stonestrom et al., no date)

Moisture Data

The vadose zone below the ADRS is between 85 m and 115 m thick. A monitoring shaft was installed in the vadose zone southwest of the waste facility to a depth of 13.7 m bgs. Within this shaft were installed a series of thermocouple psychrometers (TCPs) as shown in Figure 4-12. These TCPs were installed horizontally out of the shaft into the surrounding vadose zone sediments and were used for measuring water potentials.

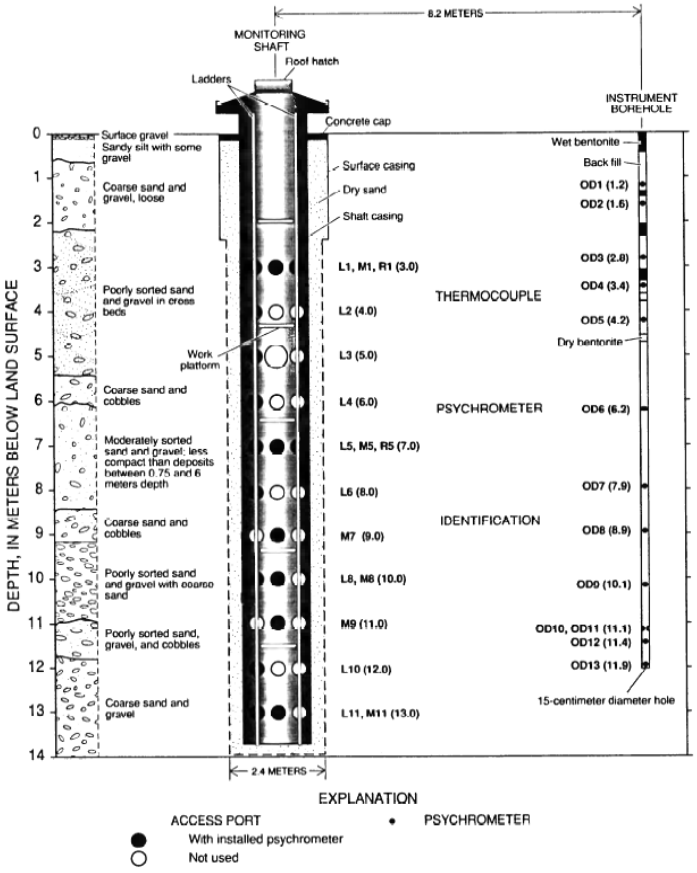

Figure 4-12. Monitoring shaft and instrument borehole showing locations of TCPs and respective geologic information (Fischer, 1992). Thermocouple psychrometers installed in the monitoring shaft

are designated with L (left), M (middle), and R (right), followed by a number from 1 to 11 that indicates level in shaft. Thermocouple psychrometers installed in the instrument borehole are designated OD1 through OD13. Depth of each thermocouple psychrometer, in meters below land surface, is given in parentheses. (Fischer, 1992).

Moisture content of soils was estimated using a neutron probe. Figure 4-13 provides a relative comparison between the varying lithology at the monitoring shaft location and the variable moisture content of the different gravel horizons.

In the gravel layers at 1.5 and 9 m bgs, moisture contents were less than 3%, below 1.5 m bgs, moisture content was in the 4 to 8% range. Temporally invariant water contents below 0.75-1 m bgs indicate that the textural discontinuity between the two uppermost soil layers (loamy sand over gravelly coarse sand) provides a natural capillary break that impedes downward percolation of moisture (Andraski, 1995).

Hydraulic conductivities

Hydraulic conductivities were estimated using air permeability tests. Saturated hydraulic conductivities of the sediments ranged from 1 to 48 centimeters per day (cm/day), which are not unreasonable for poorly sorted sediments with at least 10 percent fines and silt. For unsaturated sediments, hydraulic conductivities were estimated at between $3x10^{-4}$ to $9x10^{-20}$ cm/day. Porosity ranges from 25 to 43 percent and bulk density ranges from 1.4 to 1.8 g/cm^{-3} (Fischer, 1992).

In the sediments directly below the gravel layer at 1.5 m bgs, a significant increase occurs in the chloride content from <5 milligrams per gram (mg/g) to 160 mg/g by 3 m and remains above 100 mg/g to 7 m, then falls off steadily until it returns to <5mg/g at 11 m bgs. These elevated chloride readings basically are bracketed in the zone between the two major gravel layers that occur at 1.5 and 9 m bgs.

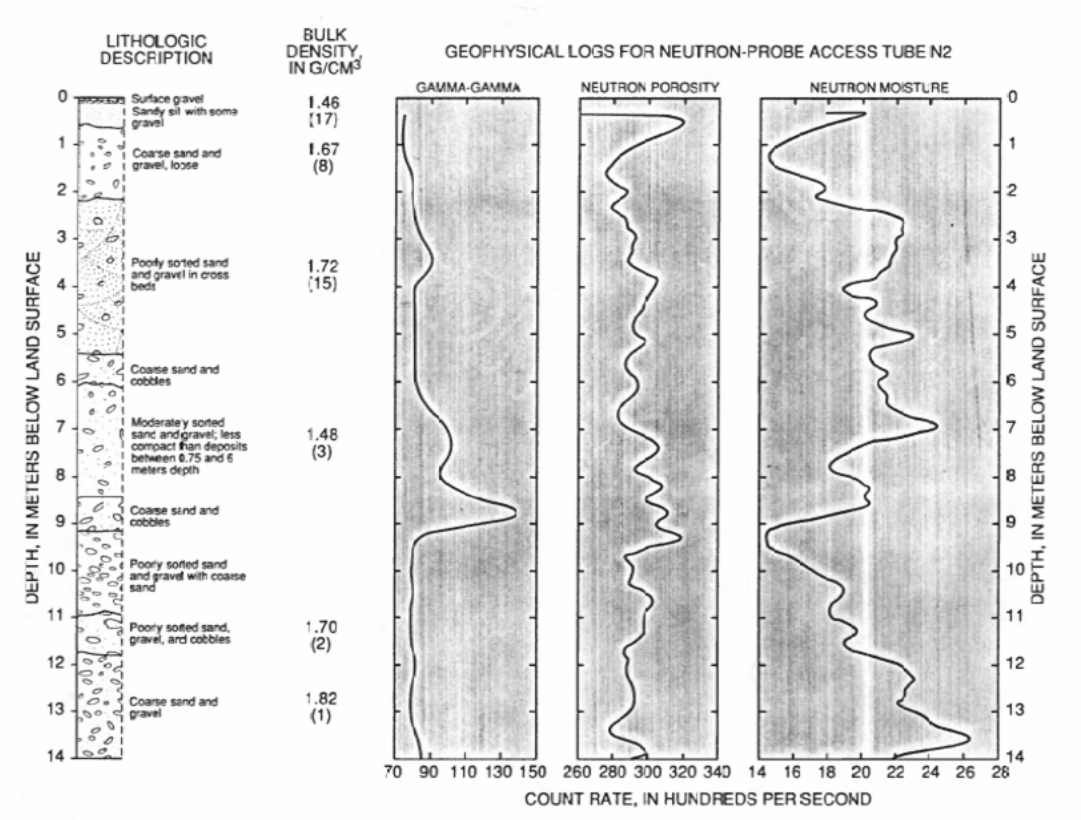

Figure 4-13. Monitoring shaft geologic and geophysical information (Fisher, 1992)

4.3 Application of the Strategy

Although on a regional basis, movement within the vadose zone below the ADRS is upward, contamination is moving downward along preferential pathways and has already reached the water table over 109 meters below ground surface. Past modeling efforts have failed to provide a conceptual site model that reproduces the observed vadose zone and ground water contamination. To evaluate the potential for hydrogeologic fast pathways below the ADRS and to prepare a revised conceptual site model, a more thorough examination of the available geologic and geophysical data was performed.

4.3.1 Chemical Constituents in Ground Water or Soil Gas

Based on available data, tritium is by far the most pervasive and anomalous constituent in either ground water or soil gas. Tritium partitions well between water and gas phases and is usually the most mobile constituent detected at sites with radiological contamination. The path of the tritium plume can be used to infer the potential path of other constituents in either ground water or soil gas.

4.3.2 Chemical Constituents in Other Fluids

This is an arid environment, but many constituents can migrate without the use of water, such as: mercury, iodine, radon, argon, krypton, and other waste components such as organic liquids. It is critical to determine the nature of the material contained within the burial trenches to know what constituents need potential evaluation. Based on available

information, constituents contained in the waste at the ADRS include, but are not limited to various isotopes of radionuclides including tritium and various hazardous compounds including carbon-14; three chlorofluorocarbon (CFC) compounds, eight chlorinated solvent compounds, and toluene although data for constituents other than tritium were not available for this exercise.

4.3.3 Chemical Constituents in Plants and Animals

Plants have been used in geochemical exploration for many years. Andraski et al., (2005) have demonstrated that sampling of creosote bushes in the vicinity of the waste site confirms the presence of tritium in the shallow gravels (1.5 m bgs). Figure 4-14 shows the distribution of sampling points for the creosote bush sampling. The contours indicate the concentration of tritium in plant water in BqL^{-1}. The tritium plume as defined by the creosote bush sampling shows two potential sources of contamination emanating from the waste facility, one on the west side and one on the south side.

Figure 4-15 shows a comparison (in tritium units) of plant water tritium with soil water tritium that correlates extremely well. Based on these results, it becomes apparent that analysis of plant material in this type of environment can act as a performance indicator for tracking movement of contamination within the underlying formation.

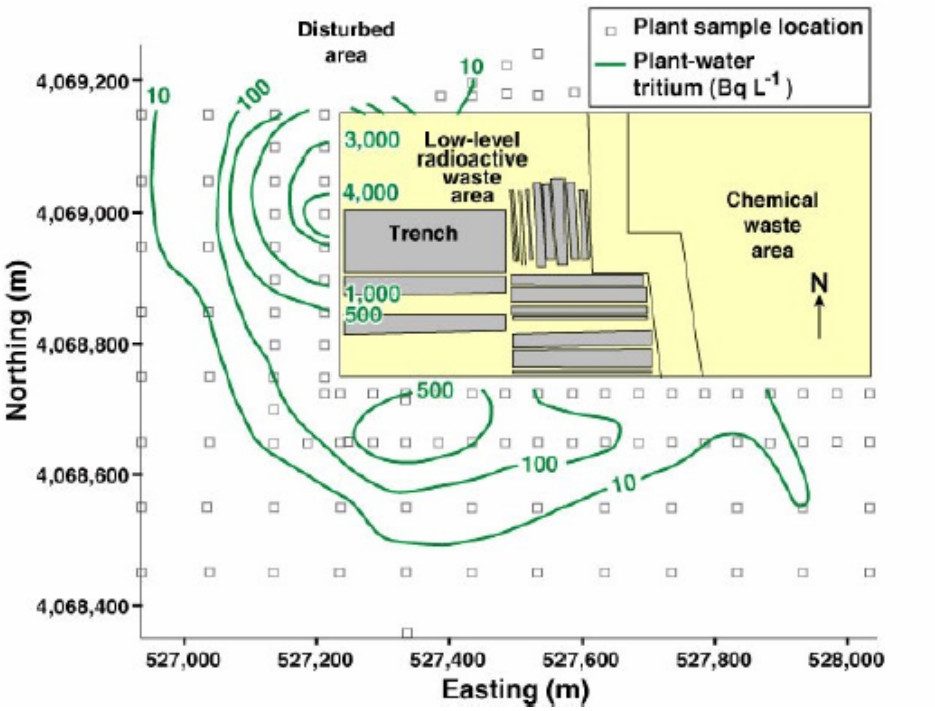

Figure 4-14. Plant sample locations and contours of plant-water tritium concentrations (Andraski et al., 2005)

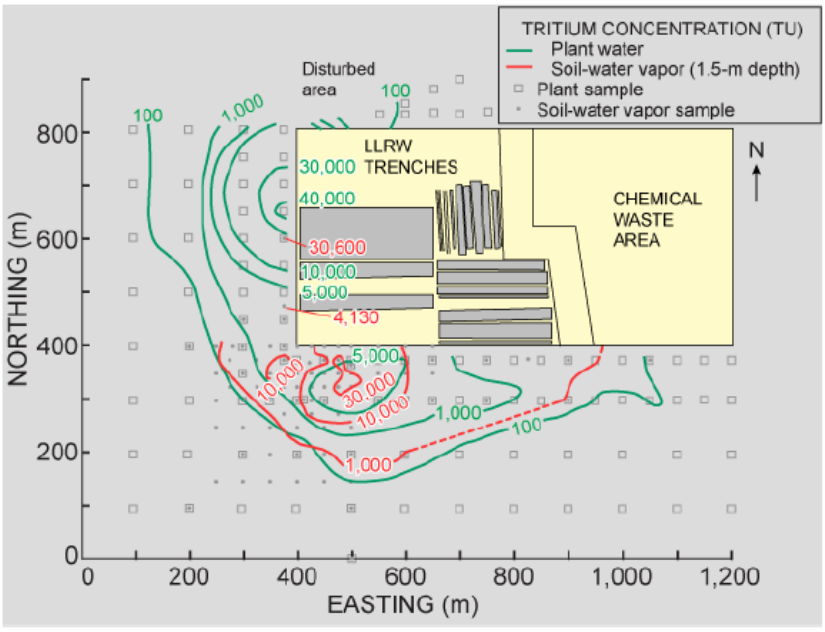

Figure 4-15. A comparison of plant water tritium with soil water tritium (Stonestrom et al., no date)

4.3.4 Geophysical Modeling and Evaluation

After assembling and reviewing the available data for the ADRS, it became apparent that there was a previously undefined mechanism for the downward migration of tritium across the vadose zone to the water table.

Based on the limited geologic data available for the ADRS, the following simplified geologic CSM for the ADRS was proposed (Figure 4-16).

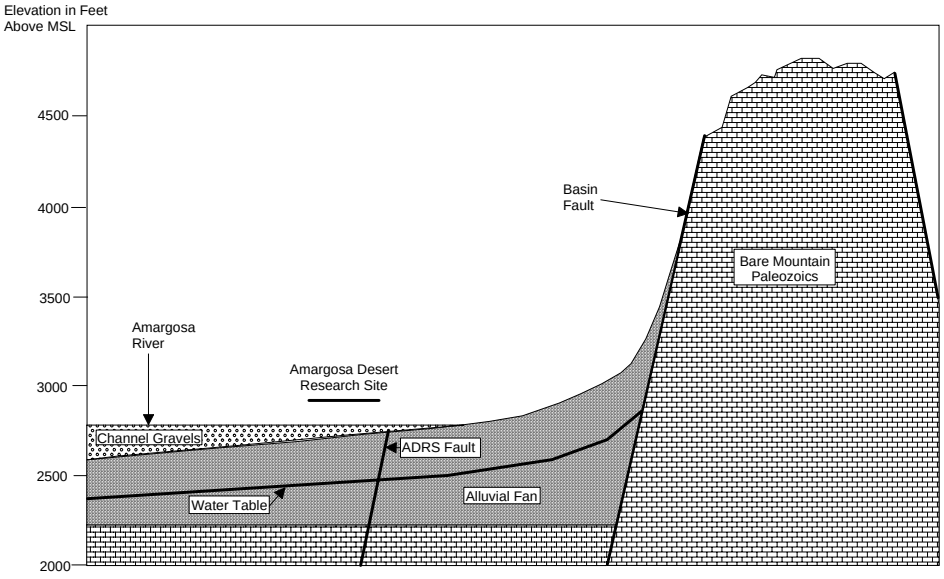

Figure 4-16. Simplified geologic cross section of the ADRS looking northwest

As there is limited geologic information available for the ADRS, the Strategy application process turned to available geophysical data. After evaluating the available geophysical information it appears that the most useful geophysical technique applied in relation to observed patterns of contaminant transport at the ADRS is direct-current electrical-resistivity (DC-resistivity) imaging, a surface-based technique employing automated, inverse-Schlumberger-array soundings (Bisdorf, 2002).

Bisdorf (2002) presents a significant database of Schlumberger resistivity soundings across the ADRS. Figure 4-8 and Figure 4-9 show the resistivity data from Bisdorf 2002 in cross section and plan view, respectively. These two figures are the only two representations of the resistivity data provided in Bisdorf 2002; however, the appendix to Bisdorf 2002 presented all of the collected data.

Based on the resistivity data provided in the appendix of Bisdorf (2002), AES prepared an electronic database of the sounding information (Appendix 4-A). Sounding locations were estimated from Figure 4-8 of Bisdorf (2002). Elevations of sounding points were extracted from regional topographic maps. AES loaded all data into a geologic modeling package (HydroGeo Analyst 2.0) and a three-dimensional (3-D) block model of the site was created by kriging the data.

Three dimensional kriging of this resistivity data identified a subtle fault not previously recognized in the data (heretofore referenced as the "Southern Structural offset"). The Southern Structural offset cuts across the southwest corner of the ADRS. The Structure runs nearly east-west and dips steeply southwest beneath the ground with approximately 30 meters of vertical offset. The Southern Structural offset coincides with the location of the southern tritium plume emanating from low-level waste trenches of the ADRS.

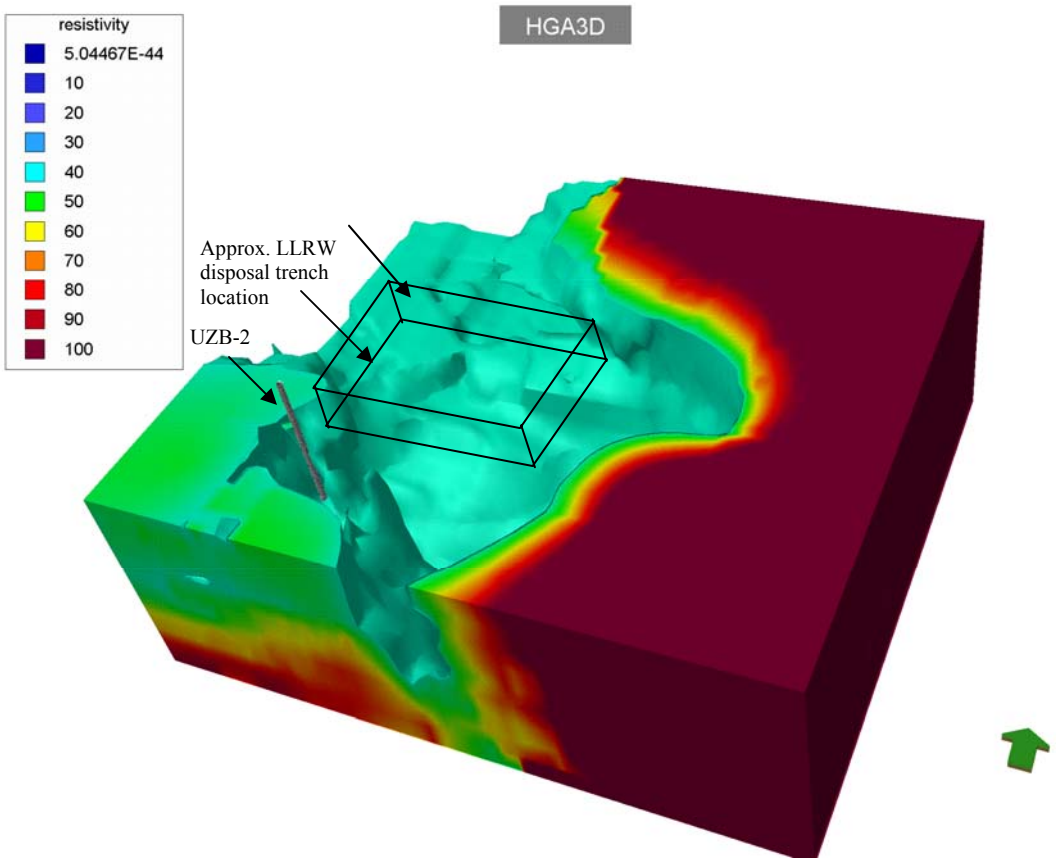

Figure 4-17. Three-dimensional resistivity block model of the ADRS looking northwest (Well UZB-2 can be seen in the southwestern portion of the figure) (created with data from Bisdorf, 2002)

Figure 4-17 presents the three-dimensional block model of the ADRS looking to the northwest. Well UZB-2 can be seen in the southwestern portion of the model. The upper 1.5 meters of undisturbed soil at the ADRS consists of highly resistive material. The upper 20 meters are not shown in order to remove high resistivity soils including the 1.5 meters near the surface. In addition, the block model has all lower resistivity values (values below 42 Ohm-m) removed for clarity. By comparing Figure 4-8 and Figure 4-9 with the 3-D model provided in Figure 4-17, the increase in the level of geologic detail becomes apparent.

The Southern Structural offset is located directly north of UZB-2. It cuts across the southwestern corner of the low-level trenches. To the northeast can be seen the major regional west-northwest-striking horst and graben structural offset originally defined in Bisdorf, 2002, represented by a sharp vertical gradient in the resistivity data. Localized lateral variations in gravel content within the alluvial fan are defined by the horizontal layering seen in the northern portion of the model.

Figure 4-18 shows the location of the Southern Structural offset in relation to the ADRS and UZB-2 both at ground surface and projected to 100 meters bgs (the intersection with the water table).

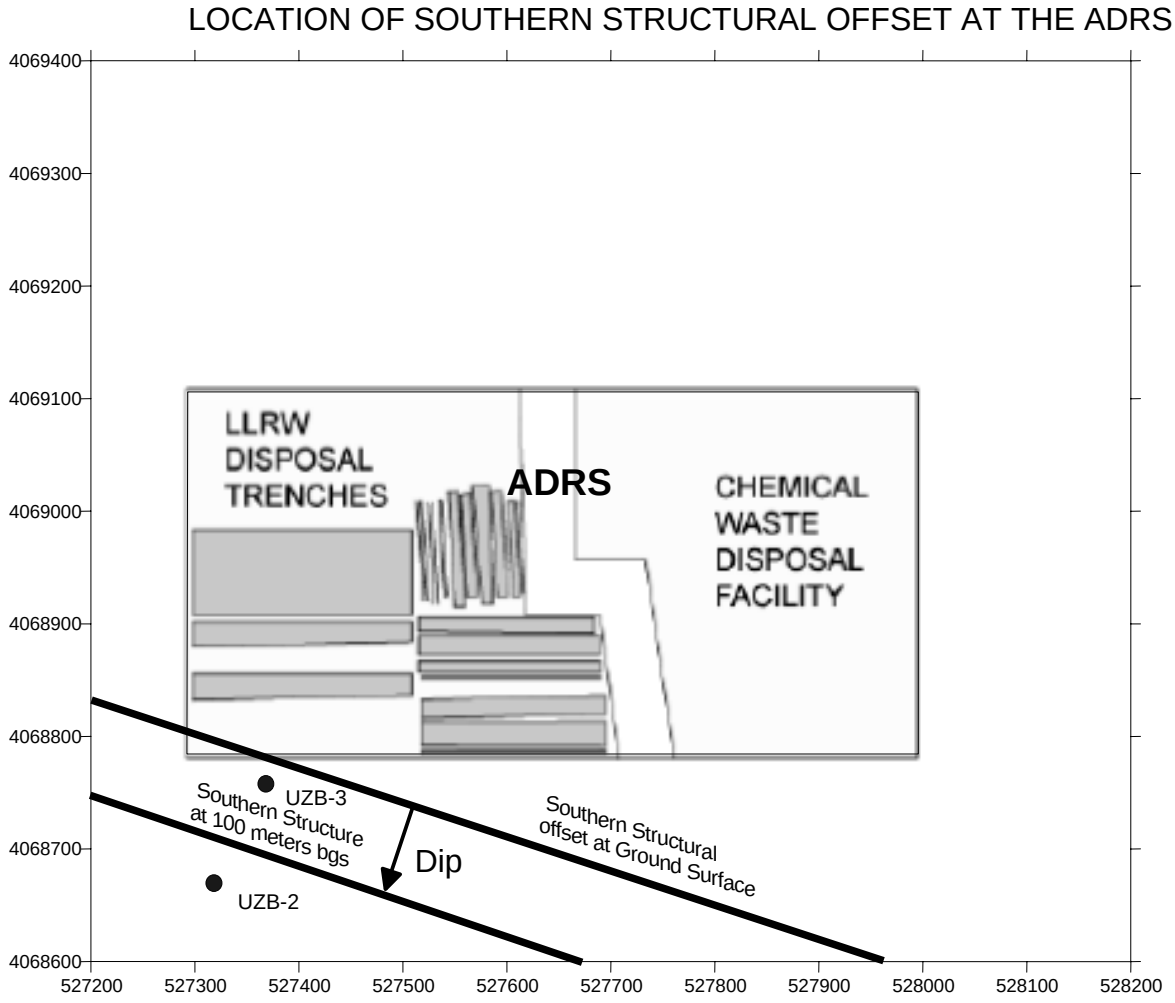

Figure 4-18. Location of the Southern Structural offset as defined by resistivity data in relation to the burial trenches (adapted from Stonestrom et al., no date)

4.3.5 Hydrologic Data

Water levels in the monitoring wells indicate that the water table surface is between 85 and 115 m bgs and dips at approximately 0.06 m/m (Figure 4-6). The contours of the water table appear to contain aspects of two flow directions; 1) flow toward the southwest (corresponding with the dip of the alluvial fan), and 2) flow toward the southeast (corresponding with the regional dip of the paleo river channel). However, the apparent curve in the water table to the southeast may not be related to the shallow river channel, which does not extend down into the water table, but instead may be due to structural features, such as the proposed Southern Structural Offset.

Figure 4-6 has an arrow showing a northwest kink in the water table contours that closely parallels the strike of the Southern Structural offset. If the regional dip of the water table

parallels the dip of the alluvial fan, then the water table should flow to the west-southwest with a sharp drop in water table expected northeast (upgradient) of the offset.

Figure 4-19 provides a copy of the same map of the tritium concentrations in water table monitoring wells presented in Figure 4-7 with the location of the Southern Structural offset added. The offset is depicted by two lines, one at ground surface and one 100 meters bgs at the intersection with the water table to show the tilt of the structure. As noted in the Strategy, initial evaluation of available data may ultimately point to a need to revise our CSM. In the case of the ADRS, the presence of a bulls-eye on the water table contour map in Figure 4-19 infers a potential fast path for tritium, as the water table surface is over 100 meters bgs.

As shown in Figure 4-19, monitoring well MR-3 cuts the Southern Structural offset but based on the projection of the dip of the structure, the well is screened slightly up dip of the intersection of the Southern Structural offset with the water table. There is slightly elevated tritium in the ground water adjacent to MR-3 (4 to 6 times higher) in contrast to the other available ground-water monitoring wells associated with the ADRS. These elevated concentrations of tritium in the ground water presumably are due to vertical contaminant migration and confirm the fast path movement of soil gas downward from the ADRS to the water table along the Southern Structural offset. Furthermore, because the half-life of tritium is 12.5 years, and the ground water in the vicinity of the ADRS is described as thousands of years old (Prudic, 1996), this suggests a continued contaminant influx into the area.

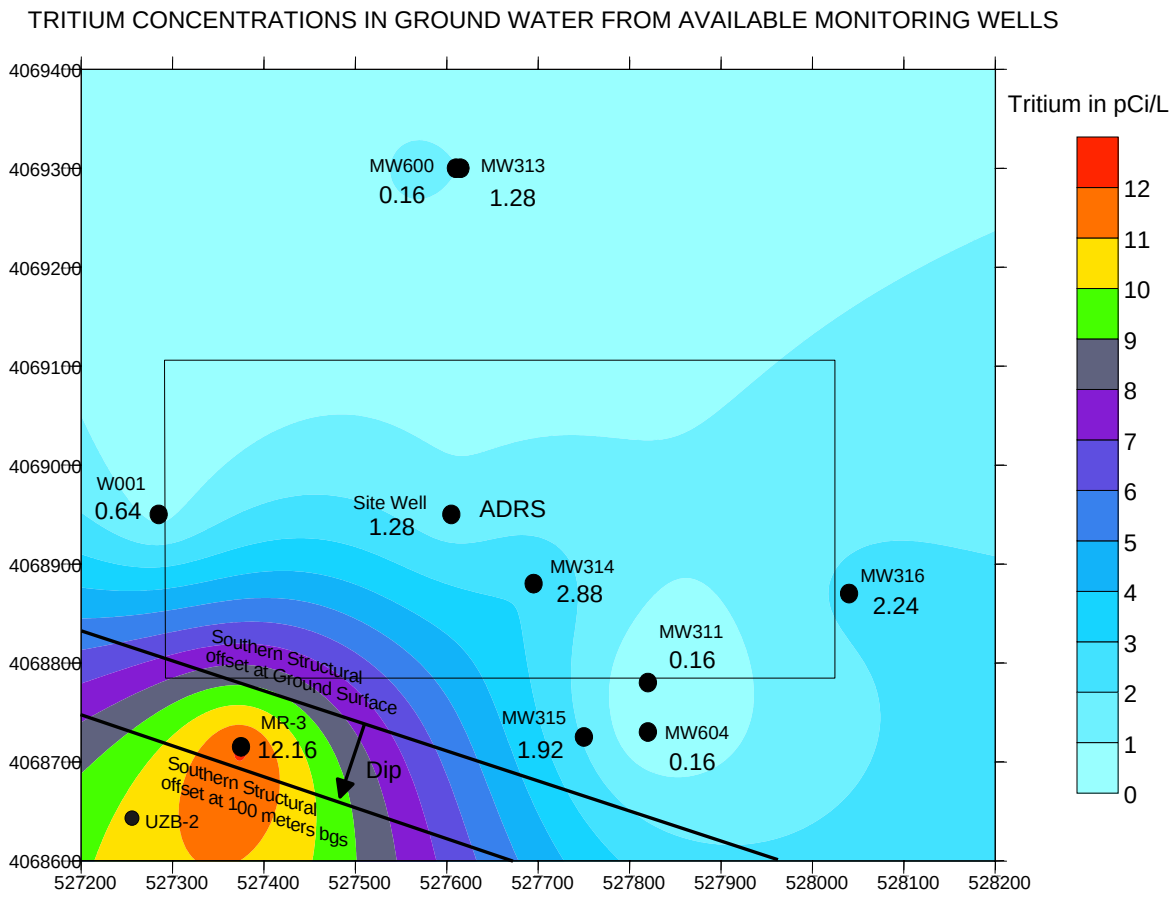

Figure 4-19. Map of tritium concentrations in ground water below ADRS in relation to the Southern Structural Offset (data from Prudic, 1997)

Geophysical logs of three monitoring wells (MW-301, 302, and 303), collected within the boundaries of the ADRS all indicate the presence of a significant continuous clay layer at approximately 70 meters bgs showing no vertical offset (Figure 4-5). However, all of these wells are northwest of the Southern Structural offset. The resistivity change across the offset indicates a change from a lower resistivity material (clays to silty clay gravels) to coarser, higher resistivity gravels. A significant drop in the water table across this feature is reflected in the water table values provided in Figure 4-6. Contouring in Figure 4-6 suggests an offset in stratigraphy across the center of the ADRS may be causing the drop in water table surface; however, the lateral continuity of the clays in monitoring wells 301 through 303 suggest that if a geologic feature is causing the significant drop in head, the feature is not located directly below the ADRS, but is more likely in the vicinity of the proposed Southern Structural offset. In addition, as the water table surface occurs within the lower clay horizon below the ADRS, there could be a local aspect of perching occurring in the water table surface where the lower clay is present. Further evaluation of geologic well logs from monitoring wells installed beyond the boundary of the ADRS would provide necessary information to evaluate the presence of the Southern Structural offset, the lateral continuity of the clays, and the nature of the overall site geologic setting.

Based on regional topography, it appears that the structural offset predates the final deposition of the uppermost gravel layers at the ADRS, as it is not reflected at ground surface. Evaluation of any additional geologic or geophysical logs below or adjacent to the ADRS, collected during the installation of monitoring wells, would assist in the evaluation of the distribution of geologic units at depth and any potential offsets in these units.

4.3.6 Vadose Zone Data

In arid environments, assessment of water flux must be considered as a performance indicator. Water flux potentials in the vadose zone indicate persistent upward driving forces for water (both liquid and vapor) (Andraski et al., 2005). In addition geothermal gradient suggests an upward driving force (Andraski et al., 2005); however, this does not explain how tritium has reached the water table over 100 m bgs. In addition, chloride mass balance suggests that percolation of precipitation has been limited to the upper 10 m bgs during the last 16,000 to 33,000 years. However, the presence of tritium in the deeper vadose zone (to the water table at 108.8 meters bgs) and ground water would tend to indicate that some other mechanism exists for moving contaminants downward. One option is the movement of water downward along fault planes, such as the Southern Structural offset.

Tritium in both the vadose zone and water table at many radioactively-contaminated sites has historically proven to be an excellent indicator of contaminant migration pathways because of its high mobility. Tritium concentrations in vadose zone sediments are highest in the vicinity of the waste unit and are highly concentrated within the gravel zone located at 1.5 m bgs. Figure 4-20 presents the results of a soil gas survey taken from the 1.5 m bgs interval over the shallow tritium plume in the southwest corner of the ADRS.

Tritium concentrations are in excess of 64,000 pCi/L in the gravel at 1.5 m bgs and immediately fall to within the 600 to 1,900 pCi/L range by 6 m bgs, then steadily increase to 1,920 to 3,840 pCi/L by 30 m bgs. Below 30 m, the tritium falls back to below 640 pCi/L (and generally below 16 pCi/L) to at least 100 m bgs. One exception, test hole UZB-2 (located on the downthrown side of the Southern Structural offset) maintains tritium concentrations down to 94 m bgs in excess of 5,648 pCi/L. Although the highest tritium contamination are confined to the upper 1.5 m bgs gravel layer, the presence of tritium down to the water table indicates that there is a mechanism for the downward migration of contaminants through the vadose zone. More characterization of the entire vadose zone is necessary to determine the mechanism for transport and the extent of the contaminant plume. The vertical movement of tritium downward appears to be related to the presence of the Southern Structural offset.

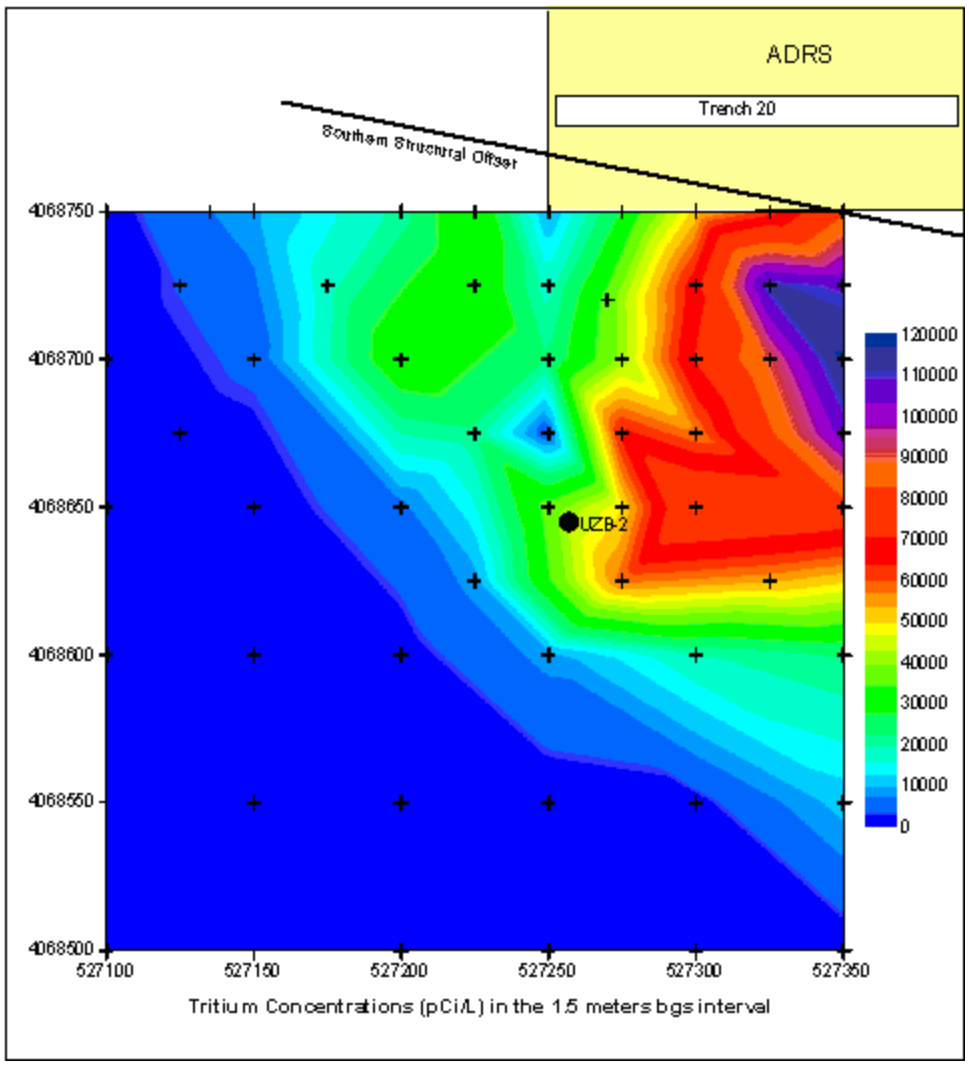

Figure 4-20. Plan view of tritium soil gas concentrations in the 1.5m below ground surface interval (data from Striegl et al., 1997)

Tritium concentrations shown in Figure 4-21 for UZB-2 are highest in the 1.5 meter bgs sampling interval (49,632 pCi/L); however, concentrations of tritium from just below the 1.5 meter interval (1,174 pCi/L) increase steadily down to the water table, with the maximum concentration occurring just above the water table surface at 108.8 meters bgs (5,648 pCi/L). This downward increasing trend in tritium appears to consist of two separate trends: a lower concentration tritium trend associated with finer grained/relatively higher soil moisture materials; and a higher concentration tritium trend associated with coarser grained/relatively lower moisture materials (Figure 4-21). Concentrations increase steadily downward as UZB-2 approaches the southwestern dipping Southern Structural offset. Tritium concentrations in all intervals sampled in UZB-2 have increased steadily at a rate of between 50 and 230 pCi/L per year, between the time the well was completed in 1993, and the latest available analytical data from 1996.

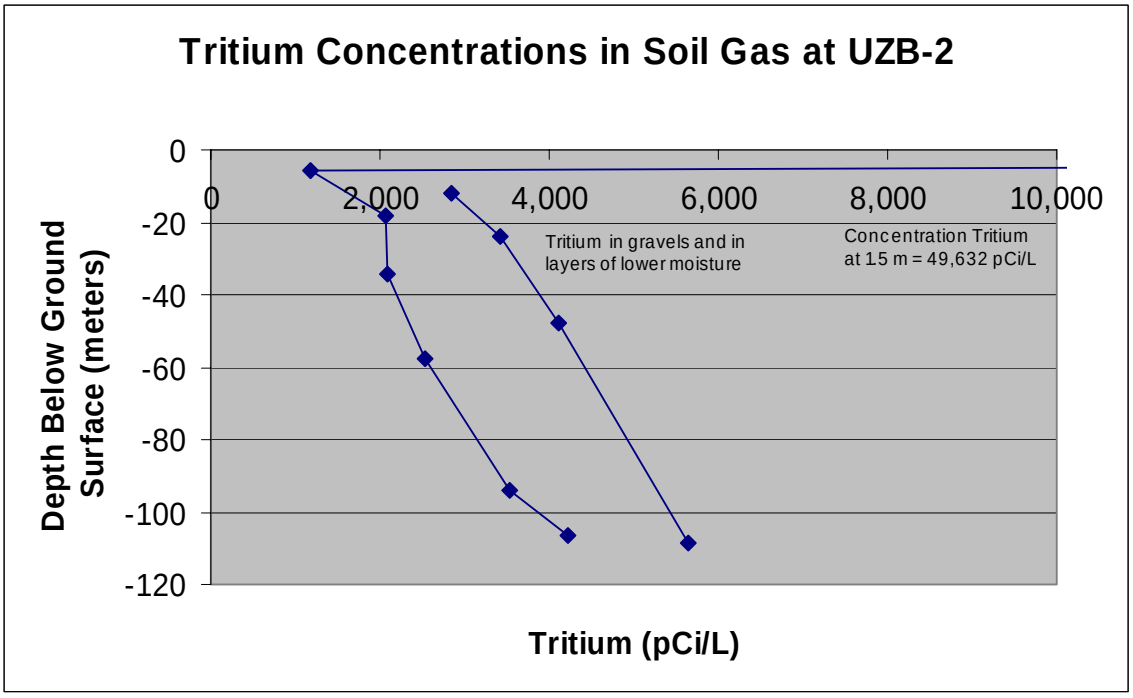

Figure 4-21. Soil vapor concentrations of tritium in UZB-2

In addition, UZB-3, which at the surface is located on the downthrown side of the Southern Structural offset (Figure 4-18), crosses the structure at approximately 25 to 30 meters below ground surface. The downward movement of contaminants, including tritium, and carbon-14, is presented in Figure 4-22 and Figure 4-23, respectively (Stonestrom et al., no date). Tritium concentrations in UZB-3 are from 2001. Note that tritium concentrations in UZB-3, below the high concentrations in the 1.5 m bgs interval, increase steadily downward to the point of intersection with the Southern Structural offset (around 30 meters bgs).

As the well passes the structure, the concentrations drop back off dramatically to near detection limits. The presence of carbon-14, in addition to the tritium, indicates that other constituents are moving downward along the Southern Structural offset. Based on available data for UZB-3, CFCs, VOCs, and toluene are present in UZB-3, but quantities and depths are not readily available. Because of lack of readily available data, it is impossible to determine the nature and extent of any other contaminants that may have leached from the trenches into the vadose zone.

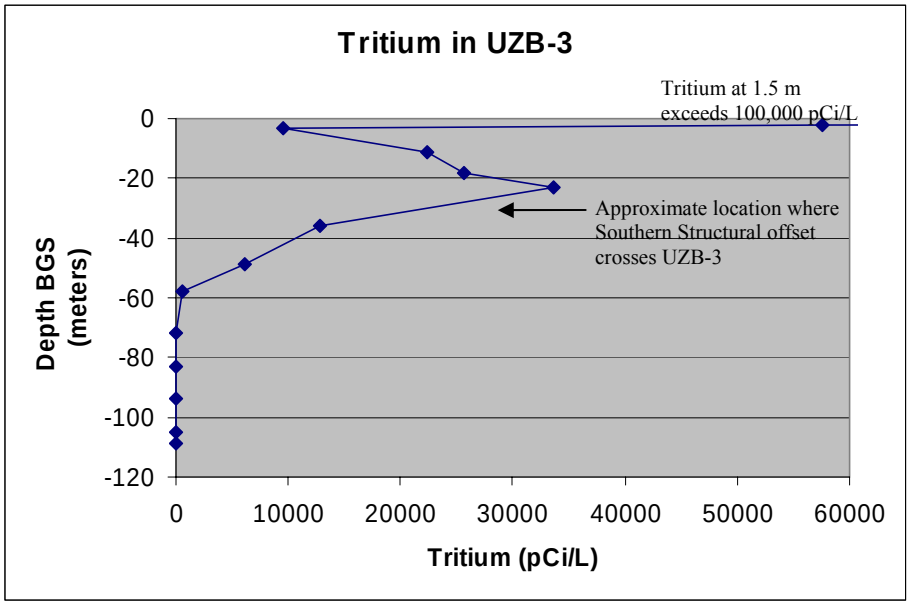

Figure 4-22. Tritium soil gas concentrations from UZB-3 (modified from Stonestrom et al., no date)

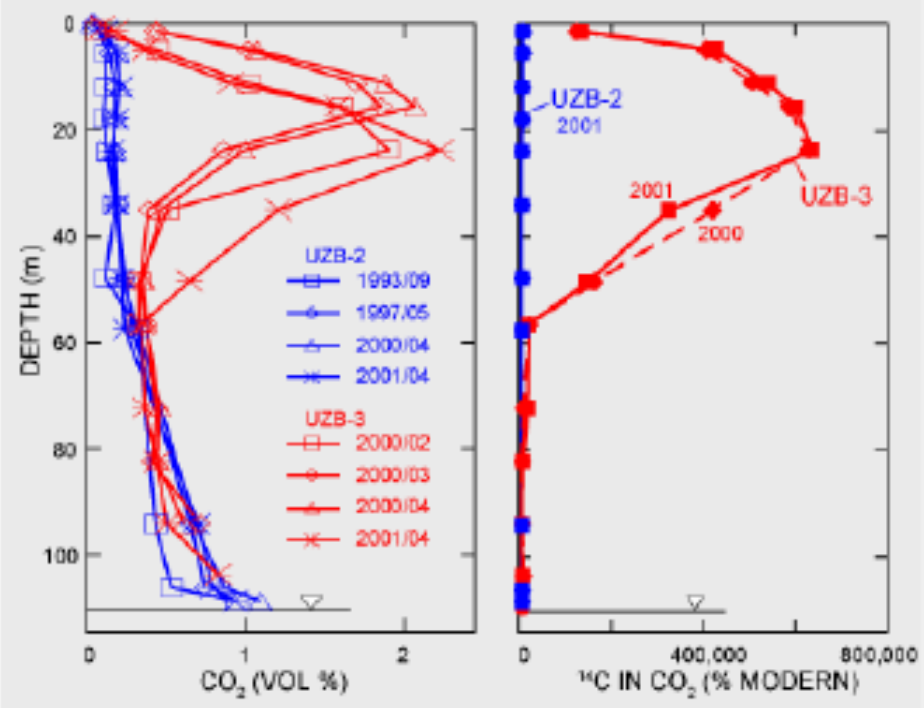

Figure 4-23. Carbon dioxide and carbon-14 soil gas concentrations from UZB-2 and UZB-3 (Stonestrom et al., no date)

4.3.7 Meteorological Data

USGS Annual Open File Reports for the ADRS provide a significant database of meteorological data. Based on the results of data from the ADRS and other similar facilities in arid environments, it becomes apparent that changes in barometric pressure at ground surface are also reflected at depth.

Figure 4-24 presents barometric pressure data for the southeast corner of the ADRS (The original source report only stated that the well was from the southeast corner of the ADRS, so the actual well used is unknown). This figure also shows a strong correlation of changes in surficial barometric pressure with changes at depth, down to 30 meters bgs. Below 30 meters, even at 89 meters bgs, minor responses to surficial barometric pressure changes are evident (Prudic, 1996). This data indicates that there is significant soil gas interaction between the surface and depth. The barometric pumping of the vadose zone could produce significant vertical migration of soil contaminants along preferential pathways. As it is unclear of the source well, a determination of the source of the data needs to be performed and additional barometric pressure data needs to be collected.

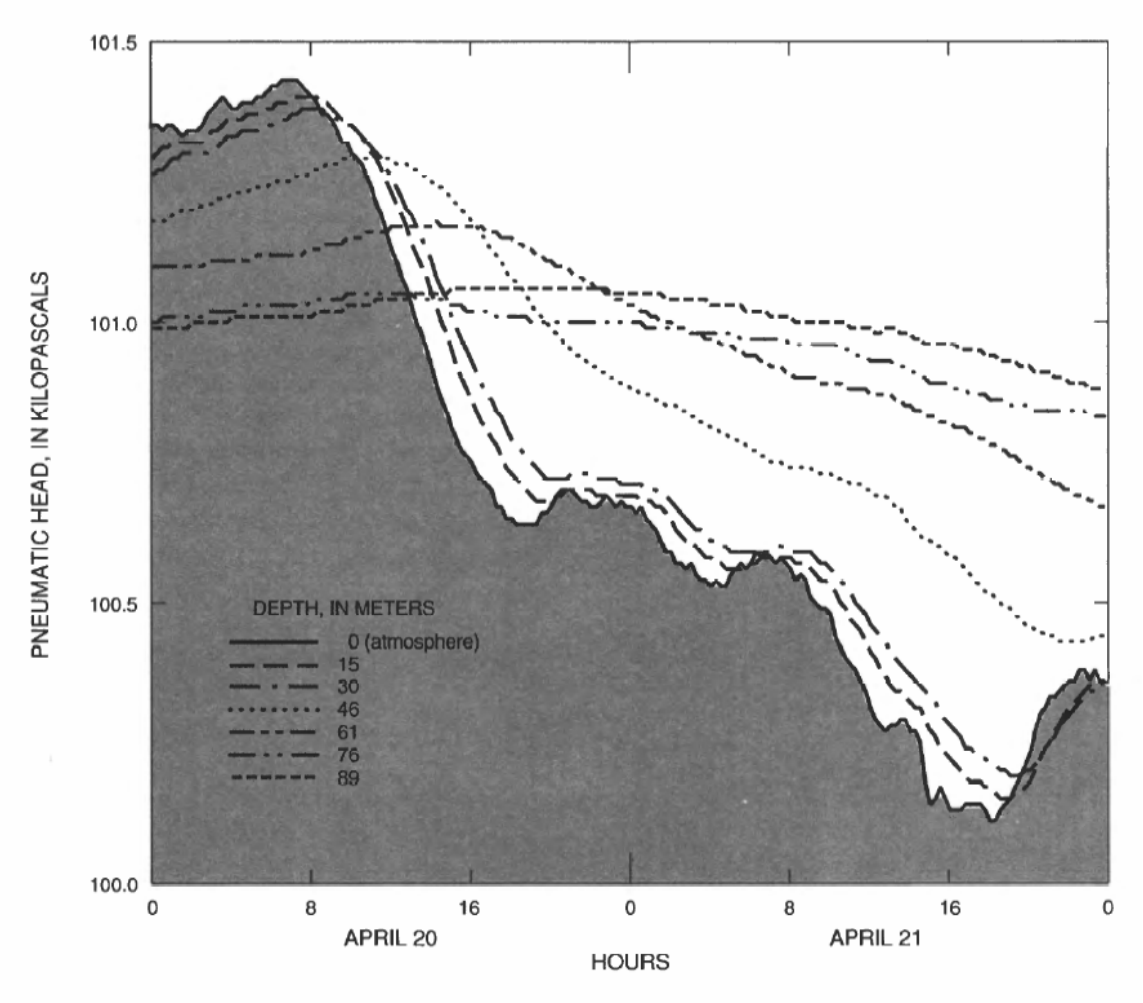

Figure 4-24. Data from southeast corner of ADRS (Prudic, 1996)

4.3.8 Transport Modeling

As noted in Striegl et al., 1996, the distribution of tritium cannot be explained simply by vapor transport, either by diffusive or advective mechanisms. Thus, liquid transport appears to have played a role in moving tritium to well UZB-2. Liquid transport may have been enhanced by precipitation and runoff into open trenches that resulted in the occasional accumulation of ponded water in the trenches and flow along preferential pathways in the underlying unsaturated zone (Striegl et al., 1996). As the conceptual model proposed by Striegl et al., 1996 failed to produce a mechanism for the vertical component of movement of tritium in soil gas within the vadose zone below the ADRS, an alternative conceptual model needed to be developed.

Striegl et al., 1996 then proposed an alternative conceptual model for tritium transport stating that liquid tritiated water may have moved laterally at shallow depth from one or more of the trenches to some point near UZB-2 and then percolated downward, resulting in the tritium activity distribution shown in Figure 4-25. Such lateral flow could occur along complex, preferential pathways formed in the presence of large-scale hydrogeologic heterogeneities during periods when liquid waste was being released directly into open trenches, and/or when the trenches received runoff from large precipitation events (Striegl et al., 1996).

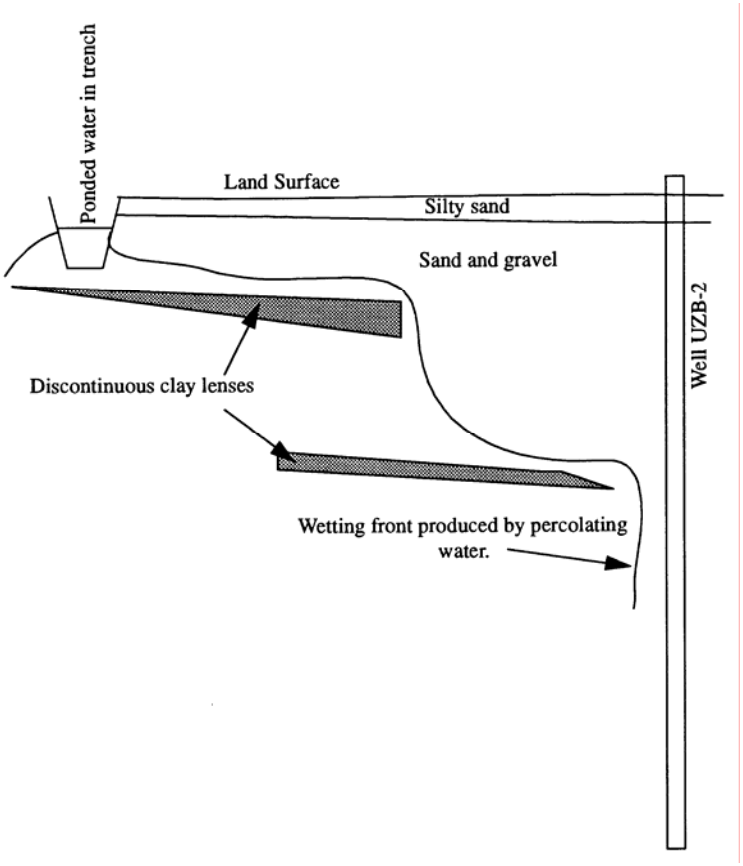

Figure 4-25. Conceptual Model for the movement of tritium proposed by Striegl et al., 1996

Based on this hypothesis, Striegl et al., 1996 proposed that water could collect in an open trench due to liquid waste disposal and/or collection of runoff from precipitation events. This ponded water could percolate rapidly through the clean sands and gravels down to a discontinuous sloping clay lens, where it could mound and move horizontally as saturated flow. Once the mounded water reached the edge of the clay lens, it could spill into the sand and gravel, and presumably move as unsaturated flow until it reached the next lens.

Based on the limited geologic and hydrogeologic data available, there are a significant number of parameters we can use to refine flow and transport simulations. We can define multiple hydrogeologic environments (river gravels, alluvial sediments, Paleozoic bedrock, etc.); make informed decisions on ground water and soil vapor flow; provide specific structural parameters for preferential vertical vadose zone flow pathways; apply variable horizontal flow variography based on geologic sediment type; and include various parameters for hydraulic conductivity and porosity.

Based on the assumption that the Southern Structural offset acts as a preferential pathway for the migration of soil gas, a spreadsheet matrix model of the dispersion of tritium through the vadose zone was prepared by AES. Table 4-1 presents a summary of the results of the model.

For simplicity, the model assumes that the Southern Structural offset is vertical and the calculated values for UZB-2 can be extracted from the matrix at the appropriate depth and distance from the fault. The model was prepared on a 1-foot by 1-foot grid. The first column of the model contains a formula assuming a dispersion constant for the Southern Structural offset. The subsequent columns utilize the value for the Southern Structural offset at the given depth and utilize the dispersion constant for the different geologic environments. The dispersion model utilizes a first order decay rate with the dispersion constant encompassing several parameters including the decay rate of the tritium, the permeability of the sediments, and the rate of movement of the soil gas through the sediments.

Table 4-1. Summary of model for estimation of tritium movement in the vadose zone between the Southern Structural Offset and UZB-2

		Distance from Fault (m)									
Depth (m)	**Fault (pCi/L)**	**20**	**40**	**60**	**80**	**100**	**120**	**140**	**160**	**180**	**200**
2	911775	675460	500393	370700	274621	203445	150715	111653	82714	61276	45395
6	48932	34620	24494	17330	12261	8675	6138	4342	3072	2174	1538
12	46863	35418	26768	20231	15290	11556	8734	6601	4989	3771	2850
18	44881	31754	22466	15895	11246	7957	5630	3983	2818	1994	1411
24	42984	32486	24553	18557	14025	10600	8011	6055	4576	3458	2614
34	39998	28299	20022	14166	10022	7091	5017	3550	2511	1777	1257
48	36163	27331	20656	15612	11799	8918	6740	5094	3850	2910	2199
58	33650	23808	16844	11918	8432	5966	4221	2986	2113	1495	1058
70	30865	21837	15450	10931	7734	5472	3871	2739	1938	1371	970
80	28721	20320	14377	10172	7197	5092	3602	2549	1803	1276	903
94	25967	18372	12998	9197	6507	4604	3257	2304	1630	1154	816
106	23818	16851	11922	8435	5968	4222	2987	2114	1495	1058	749
109	23309	17616	13314	10063	7605	5748	4344	3283	2481	1875	1417

Note: Tritium concentrations in pCi/L

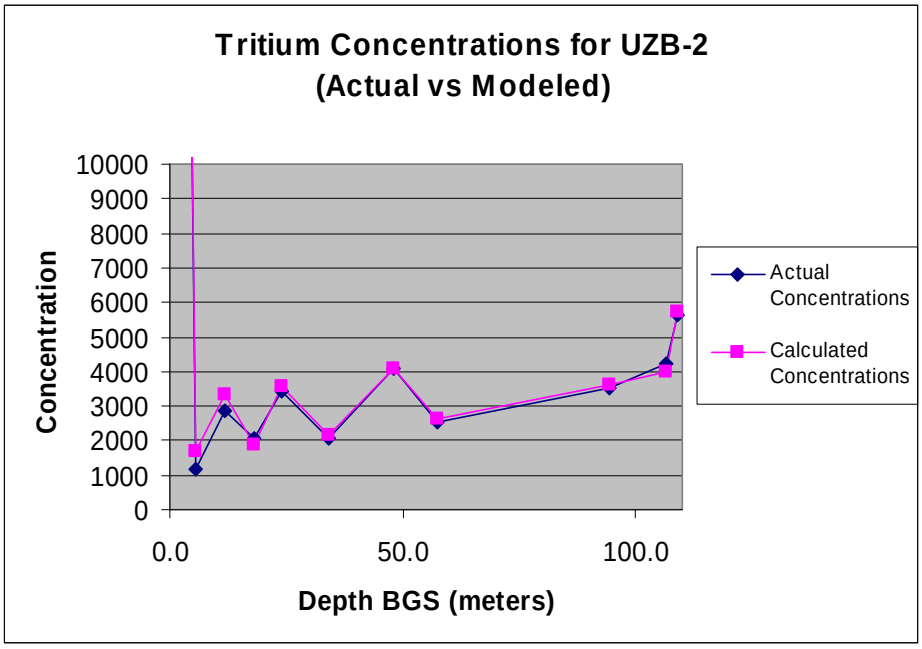

Figure 4-26. Comparison of actual data to modeled tritium concentrations in UZB-2 in pCi/L (UZB-2 tritium data from Striegl et al., 1997)

Separate dispersion values were assigned to the surficial gravel at 1.5 meters bgs, the coarser gravels, and the finer materials (Table 4-2). Table 4-3 summarizes the results of the model as compared to actual tritium concentrations in UZB-2. Figure 4-26 provides a comparison of the results of the model to the actual tritium concentrations in UZB-2 from Striegl et al. (1997), illustrating tightly correlated results between expected and observed tritium concentration levels. Figure 4-27 is a hypothetical cross section prepared using Surfer to contour the modeling result values summarized in Table 4-1 along with the tritium values collected from UZB-2. The gravel horizons presented in Figure 4-27 are interpreted from soil moisture data from Prudic (1994) and from relative tritium concentrations. Zones with higher moisture are interpreted to be more clay rich, lower moisture horizons are interpreted to be coarser gravels.

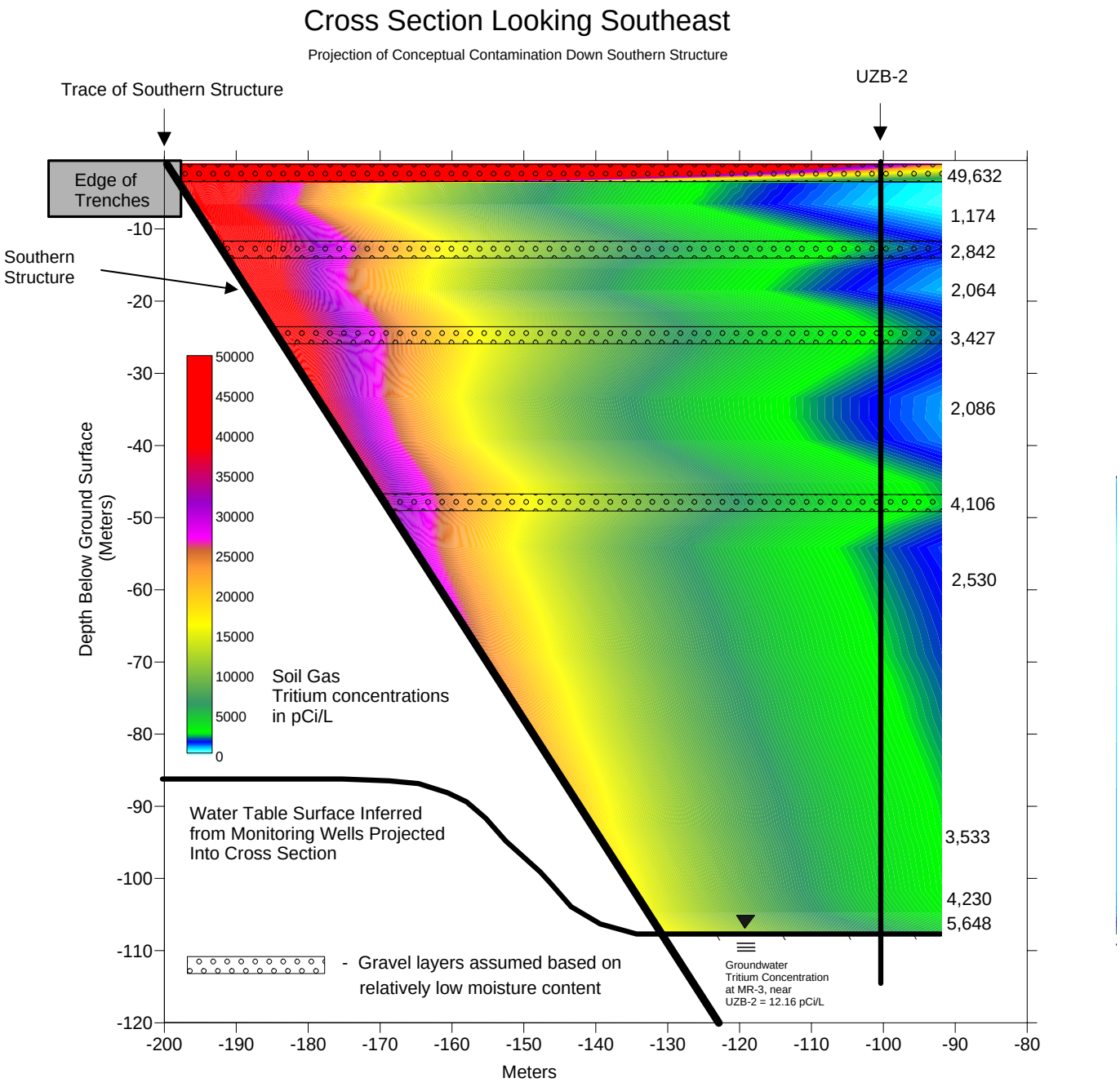

Figure 4-27. Alternative conceptual model for the distribution of tritium in vadose zone based on Southern Structural offset and UZB-2 tritium concentrations (tritium data from Striegl et al., 1997)

Table 4-2. Tritium model dispersivity values assigned to various materials

Material	Lambda
Fault	0.0072
Surface Gravel	0.0150
Coarser Dryer Gravel	0.0173
Finer Moist Gravel	0.0140

Table 4-3. Comparison of results from the tritium model to actual concentrations in UZB-2 (UZB-2 data from Striegl et al., 1997)

Depth (m)	UZB-2 Tritium	Model Estimate	Model Depth (m)	Percent Comp.
1.5	49632	49670	2	100%
5.5	1174	1706	6	69%
11.9	2842	3324	12	85%
18.0	2064	1893	18	109%
24.1	3427	3557	24	96%
34.1	2086	2149	34	97%
47.9	4106	4072	48	101%
57.6	2531	2646	58	96%
94.2	3533	3613	94	98%
106.4	4230	4009	106	106%
108.8	5648	5748	109	98%

Tritium concentrations in pCi/L

4.4 Monitoring Strategy Application Conclusions

Based on the results of initial evaluation of data for the Amargosa Desert Research Site, it was unclear how tritium was reaching ground water over 109 meters below ground surface in an arid environment.

A Schlumberger resistivity survey was conducted over the site as presented in Bisdorf (2002). Bisdorf identified a large scale structural feature northeast of the ADRS. As part of this Strategy application, three dimensional modeling of the resistivity data from Bisdorf (2002) using the capabilities of a geological modeling program (HydroGeo Analyst 2.0) resulted in the confirmation of the large fault identified by Bisdorf as well as the identification of a fault labeled the "Southern Structural offset" in the southwest corner of the ADRS. The Southern Structural offset appears to coincide with the location of the downward movement of tritium within the vadose zone to the water table. Modeling of the downward movement of contaminants could now be simulated once consideration was given to this additional structural feature as a fast path for the migration of contamination.

Projection of the Southern Structural offset with a steep southwest dip intersected UZB-3 at approximately 25 to 30 meters bgs. Analytical results of soil gas from this interval confirm the location of the feature. In addition, the steady increase in tritium detected down monitoring borehole UZB-2 indicates that the Southern Structural offset is approaching UZB-2 with depth. The Southern Structural offset intersects the water table slightly up dip of UZB-2. Ground water in the vicinity of monitoring well MR-3, screened in the water table slightly up dip of the intersection of the Southern Structural offset, contains elevated levels of tritium (4 to 6 times higher) in contrast to the other available ground-water monitoring wells associated with the ADRS. The presence of the elevated tritium in the water table also confirms the fast path movement of contaminants downward from the ADRS to the water table along the Southern Structural offset.

The presence of significant barometric pressure interaction between the surface and the subsurface within the vadose zone indicates that there is potential for significant soil gas movement. The barometric pumping of the vadose zone could produce significant vertical migration of soil contaminants along preferential pathways such as the Southern Structural offset.

Only by analyzing the total data package for the site were we able to create a model that allows both an upward component of flow and localized downward migration of contaminants along a fast pathway. In addition, through examination of all geophysical and geologic information available, structures were identified that influence the movement of water and soil gas. Based on this more complete picture, an improved conceptual site model was developed and from this assessment informed decisions can be made for future site monitoring and assessment.

4.5 Amargosa References

Andraski, B.J., D.E Prudic, and W.D Nichols. "Waste Burial in Arid Environments--Application of Information from a Field Laboratory in the Mojave Desert, Southern Nevada." U.S. Geological Survey Fact Sheet FS-179-95, 4 p. 1995.

Andraski, B.J., et al. *Plant-Based Plume-Scale Mapping of Tritium Contamination in Desert Soils.* Online Publication. August 16, 2005.

Bisdorf, R.J. "Schlumberger Soundings at the Amargosa Desert Research Site, Nevada." U.S. Geological Survey Open-File Report 02-140. 2002.

California Geology Magazine. *Detachment Faults, California's Extended Past; Mineralization Along Detachment Faults; California Has Its Faults; Faulted Wave-Cut Terrace Near Point Arena [Mendocino County]*. A Photo Essay. January/February 1992.

Fischer, J.M. "Sediment Properties and Water Movement Through Shallow Unsaturated Alluvium at an Arid Site for Disposal of Low-Level Radioactive Waste Near Beatty, Nye County, Nevada." U.S. Geological Survey Water-Resources Investigations Report 92-4032, 48 p.1992.

Johnson, M.J., C.J Mayers, and B.J Andraski. "Selected micrometeorological and soil-moisture data at Amargosa Desert Research Site in Nye County near Beatty, Nevada, 1998-2000." U.S. Geological Survey Open-File Report 02-348, available on the World Wide Web only. 2002.

Prudic, D.E. "Estimates of Percolation Rates and Ages of Water in Unsaturated Sediments at Two Mojave Desert Sites, California-Nevada." U.S. Geological Survey, Water Resources Investigation Report 91-4160. 1994.

Prudic, D.E. "Water-vapor movement through unsaturated alluvium in Amargosa Desert near Beatty, Nevada--Current understanding and continuing studies, in Stevens,

P.R., and Nicholson, T.J., eds., Joint U.S. Geological Survey, U.S. Nuclear Regulatory Commission Workshop on research related to low-level radioactive waste disposal, May 4-6, 1993." National Center, Reston, Virginia, Proceedings. U.S. Geological Survey Water-Resources Investigations Report 95-4015, p. 157-166. 1996.

Prudic, D.E., D.A Stonestrom, and R.G Striegl. "Tritium, deuterium, and oxygen-18 in water collected from unsaturated sediments near a low-level radioactive-waste burial site south of Beatty, Nevada." U.S. Geological Survey Water-Resources Investigations Report 97-4062, 23 p.1997.

Stonestrom, D.A., et al. "Estimates of deep percolation beneath native vegetation, irrigated fields, and the Amargosa River channel, Amargosa Desert, Nye County, Nevada`" U.S. Geological Survey Open-File Report 03-104, available on the world wide web. 2003.

Stonestrom, D.A., et al. *Monitoring Radionuclide Contamination in the Vadose Zone-Lessons Learned at the Amargosa Desert Research Site, Nye County, Nevada.* No Date.

Striegl, R.G., et al. "Factors affecting tritium and 14carbon distributions in the unsaturated zone near the low-level radioactive-waste burial site south of Beatty, Nevada." U.S. Geological Survey Open-File Report 96-110, 16 p. 1996.

Striegl, R.G., et al. "Tritium in unsaturated zone gases and air at the Amargosa Desert Research Site, and in spring and river water, near Beatty, Nevada, May 1997." U.S. Geological Survey Open-File Report 97-778, 13 p. 1997.

Walvoord, M. A., *CO2 dynamics in the Amargosa Desert: Fluxes and isotopic speciation in a deep unsaturated zone.* Water Resources Research, 41, W02006, doi:10.1029/2004WR003599. 2005.

Appendix 4-A

Appendix 4-A. Schlumberger Resistivity Data for the ADRS from Bisdorf, 2002

Station	Easting	Northing	Ground Elev. (m)	Calculated Resistivity Reading (Ohm-m)	Depth (m)	Sample Elev. (m)
ADRS 001	527081	4068750	846.5	300.55	0.47	846.03
ADRS 001	527081	4068750	846.5	373.28	0.69	845.81
ADRS 001	527081	4068750	846.5	514.87	1.01	845.49
ADRS 001	527081	4068750	846.5	617.03	1.48	845.02
ADRS 001	527081	4068750	846.5	467.72	2.17	844.33
ADRS 001	527081	4068750	846.5	184.39	3.19	843.31
ADRS 001	527081	4068750	846.5	50.72	4.68	841.82
ADRS 001	527081	4068750	846.5	36.88	6.88	839.62
ADRS 001	527081	4068750	846.5	61.97	10.09	836.41
ADRS 002	527331	4068450	844.2	517.15	0.59	843.61
ADRS 002	527331	4068450	844.2	730.4	0.87	843.33
ADRS 002	527331	4068450	844.2	896.3	1.28	842.92
ADRS 002	527331	4068450	844.2	832.2	1.87	842.33
ADRS 002	527331	4068450	844.2	524.13	2.75	841.45
ADRS 002	527331	4068450	844.2	203.44	4.04	840.16
ADRS 002	527331	4068450	844.2	58.43	5.93	838.27
ADRS 002	527331	4068450	844.2	36.49	8.7	835.5
ADRS 002	527331	4068450	844.2	60.98	12.77	831.43
ADRS 002	527331	4068450	844.2	91.39	18.74	825.46
ADRS 002	527331	4068450	844.2	93.76	27.5	816.7
ADRS 002	527331	4068450	844.2	69.75	40.37	803.83
ADRS 003	528755	4068491	847.5	245.39	0.55	846.95
ADRS 003	528755	4068491	847.5	179.54	0.81	846.69
ADRS 003	528755	4068491	847.5	142.8	1.19	846.31
ADRS 003	528755	4068491	847.5	116.74	1.74	845.76
ADRS 003	528755	4068491	847.5	101.03	2.55	844.95
ADRS 003	528755	4068491	847.5	74.23	3.75	843.75
ADRS 003	528755	4068491	847.5	47.5	5.5	842
ADRS 003	528755	4068491	847.5	43.35	8.074	839.426
ADRS 003	528755	4068491	847.5	46.72	11.85	835.65
ADRS 003	528755	4068491	847.5	40.64	17.39	830.11
ADRS 003	528755	4068491	847.5	29.85	25.53	821.97
ADRS 003	528755	4068491	847.5	27.5	37.47	810.03
ADRS 003	528755	4068491	847.5	39.27	55.01	792.49
ADRS 003	528755	4068491	847.5	63.25	80.74	766.76
ADRS 003	528755	4068491	847.5	80.41	118.51	728.99
ADRS 003	528755	4068491	847.5	75.13	173.94	673.56
ADRS 003	528755	4068491	847.5	64.74	255.31	592.19
ADRS 003	528755	4068491	847.5	71.71	374.75	472.75
ADRS 003	528755	4068491	847.5	108.44	550.06	297.44
ADRS 003	528755	4068491	847.5	186.24	807.37	40.13
ADRS 004	529050	4068495	842.5	3076.99	0.4	842.1
ADRS 004	529050	4068495	842.5	5680.3	0.59	841.91
ADRS 004	529050	4068495	842.5	6983.81	0.87	841.63
ADRS 004	529050	4068495	842.5	4788.29	1.27	841.23
ADRS 004	529050	4068495	842.5	1720.84	1.87	840.63
ADRS 004	529050	4068495	842.5	591.05	2.74	839.76
ADRS 004	529050	4068495	842.5	617.39	4.02	838.48
ADRS 004	529050	4068495	842.5	1152.72	5.9	836.6

ADRS 004	529050	4068495	842.5	1714.99	8.66	833.84
ADRS 004	529050	4068495	842.5	1797.17	12.72	829.78
ADRS 005	527831	4068650	845	1121.78	0.55	844.45
ADRS 005	527831	4068650	845	845.5	0.81	844.19
ADRS 005	527831	4068650	845	471.77	1.19	843.81
ADRS 005	527831	4068650	845	201.04	1.74	843.26
ADRS 005	527831	4068650	845	63.05	2.55	842.45
ADRS 005	527831	4068650	845	35.46	3.75	841.25
ADRS 005	527831	4068650	845	50.5	5.5	839.5
ADRS 005	527831	4068650	845	71.77	8.074	836.926
ADRS 005	527831	4068650	845	89.96	11.85	833.15
ADRS 005	527831	4068650	845	99.83	17.39	827.61
ADRS 005	527831	4068650	845	88.93	25.53	819.47
ADRS 005	527831	4068650	845	60.82	37.47	807.53
ADRS 005	527831	4068650	845	37.92	55.01	789.99
ADRS 005	527831	4068650	845	28.37	80.74	764.26
ADRS 006	527031	4068650	846.5	1129.27	0.55	845.95
ADRS 006	527031	4068650	846.5	1934.75	0.81	845.69
ADRS 006	527031	4068650	846.5	2302.09	1.19	845.31
ADRS 006	527031	4068650	846.5	1674.72	1.74	844.76
ADRS 006	527031	4068650	846.5	603.86	2.55	843.95
ADRS 006	527031	4068650	846.5	99.42	3.75	842.75
ADRS 006	527031	4068650	846.5	31.98	5.5	841
ADRS 006	527031	4068650	846.5	66.81	8.074	838.426
ADRS 006	527031	4068650	846.5	102.26	11.85	834.65
ADRS 006	527031	4068650	846.5	125.95	17.39	829.11
ADRS 006	527031	4068650	846.5	121.54	25.53	820.97
ADRS 006	527031	4068650	846.5	78.09	37.47	809.03
ADRS 006	527031	4068650	846.5	41.58	55.01	791.49
ADRS 006	527031	4068650	846.5	31.49	80.74	765.76
ADRS 007	527231	4068650	847.3	639.98	0.55	846.75
ADRS 007	527231	4068650	847.3	657.29	0.81	846.49
ADRS 007	527231	4068650	847.3	607.2	1.19	846.11
ADRS 007	527231	4068650	847.3	494.27	1.74	845.56
ADRS 007	527231	4068650	847.3	354.49	2.55	844.75
ADRS 007	527231	4068650	847.3	183.12	3.75	843.55
ADRS 007	527231	4068650	847.3	64.93	5.5	841.8
ADRS 007	527231	4068650	847.3	45.76	8.074	839.226
ADRS 007	527231	4068650	847.3	63.73	11.85	835.45
ADRS 007	527231	4068650	847.3	84.52	17.39	829.91
ADRS 007	527231	4068650	847.3	94.6	25.53	821.77
ADRS 007	527231	4068650	847.3	82.32	37.47	809.83
ADRS 007	527231	4068650	847.3	56.02	55.01	792.29
ADRS 007	527231	4068650	847.3	39.32	80.74	766.56
ADRS 008	527431	4068650	846.5	710.48	0.55	845.95
ADRS 008	527431	4068650	846.5	766.9	0.81	845.69
ADRS 008	527431	4068650	846.5	698	1.19	845.31
ADRS 008	527431	4068650	846.5	487.68	1.74	844.76
ADRS 008	527431	4068650	846.5	216.52	2.55	843.95
ADRS 008	527431	4068650	846.5	62.59	3.75	842.75
ADRS 008	527431	4068650	846.5	38.92	5.5	841
ADRS 008	527431	4068650	846.5	56.22	8.074	838.426
ADRS 008	527431	4068650	846.5	72.55	11.85	834.65
ADRS 008	527431	4068650	846.5	79.96	17.39	829.11
ADRS 008	527431	4068650	846.5	79.16	25.53	820.97
ADRS 008	527431	4068650	846.5	71.52	37.47	809.03
ADRS 008	527431	4068650	846.5	59.5	55.01	791.49
ADRS 008	527431	4068650	846.5	43.49	80.74	765.76
ADRS 009	527631	4068650	846.9	619.56	0.55	846.35
ADRS 009	527631	4068650	846.9	749.02	0.81	846.09
ADRS 009	527631	4068650	846.9	737.69	1.19	845.71

ADRS 009	527631	4068650	846.9	473.6	1.74	845.16
ADRS 009	527631	4068650	846.9	144.64	2.55	844.35
ADRS 009	527631	4068650	846.9	35.12	3.75	843.15
ADRS 009	527631	4068650	846.9	45.75	5.5	841.4
ADRS 009	527631	4068650	846.9	97.83	8.074	838.826
ADRS 009	527631	4068650	846.9	117.38	11.85	835.05
ADRS 009	527631	4068650	846.9	96.6	17.39	829.51
ADRS 009	527631	4068650	846.9	74.32	25.53	821.37
ADRS 009	527631	4068650	846.9	65.33	37.47	809.43
ADRS 009	527631	4068650	846.9	67.67	55.01	791.89
ADRS 009	527631	4068650	846.9	52.66	80.74	766.16
ADRS 010	527831	4068450	843.4	1015.95	0.55	842.85
ADRS 010	527831	4068450	843.4	1020.61	0.81	842.59
ADRS 010	527831	4068450	843.4	601.78	1.19	842.21
ADRS 010	527831	4068450	843.4	168.41	1.74	841.66
ADRS 010	527831	4068450	843.4	42.01	2.55	840.85
ADRS 010	527831	4068450	843.4	42.76	3.75	839.65
ADRS 010	527831	4068450	843.4	67.91	5.5	837.9
ADRS 010	527831	4068450	843.4	88.2	8.074	835.326
ADRS 010	527831	4068450	843.4	96.36	11.85	831.55
ADRS 010	527831	4068450	843.4	93.18	17.39	826.01
ADRS 010	527831	4068450	843.4	83.65	25.53	817.87
ADRS 010	527831	4068450	843.4	67.94	37.47	805.93
ADRS 010	527831	4068450	843.4	43.19	55.01	788.39
ADRS 010	527831	4068450	843.4	24.92	80.74	762.66
ADRS 011	527631	4068450	843.8	678.23	0.55	843.25
ADRS 011	527631	4068450	843.8	685.34	0.81	842.99
ADRS 011	527631	4068450	843.8	645.88	1.19	842.61
ADRS 011	527631	4068450	843.8	487.54	1.74	842.06
ADRS 011	527631	4068450	843.8	240.74	2.55	841.25
ADRS 011	527631	4068450	843.8	87.28	3.75	840.05
ADRS 011	527631	4068450	843.8	55.45	5.5	838.3
ADRS 011	527631	4068450	843.8	62.9	8.074	835.726
ADRS 011	527631	4068450	843.8	67.77	11.85	831.95
ADRS 011	527631	4068450	843.8	69.31	17.39	826.41
ADRS 011	527631	4068450	843.8	71.21	25.53	818.27
ADRS 011	527631	4068450	843.8	71.2	37.47	806.33
ADRS 011	527631	4068450	843.8	61.78	55.01	788.79
ADRS 011	527631	4068450	843.8	42.01	80.74	763.06
ADRS 012	527431	4068450	844.2	433.81	0.55	843.65
ADRS 012	527431	4068450	844.2	471.29	0.81	843.39
ADRS 012	527431	4068450	844.2	471.28	1.19	843.01
ADRS 012	527431	4068450	844.2	396.9	1.74	842.46
ADRS 012	527431	4068450	844.2	246.86	2.55	841.65
ADRS 012	527431	4068450	844.2	109.89	3.75	840.45
ADRS 012	527431	4068450	844.2	56.97	5.5	838.7
ADRS 012	527431	4068450	844.2	56.43	8.074	836.126
ADRS 012	527431	4068450	844.2	72.58	11.85	832.35
ADRS 012	527431	4068450	844.2	89	17.39	826.81
ADRS 012	527431	4068450	844.2	92.64	25.53	818.67
ADRS 012	527431	4068450	844.2	75.26	37.47	806.73
ADRS 012	527431	4068450	844.2	52.53	55.01	789.19
ADRS 012	527431	4068450	844.2	39.6	80.74	763.46
ADRS 013	527231	4068450	844.2	380.67	0.55	843.65
ADRS 013	527231	4068450	844.2	412.17	0.81	843.39
ADRS 013	527231	4068450	844.2	456.31	1.19	843.01
ADRS 013	527231	4068450	844.2	368.39	1.74	842.46
ADRS 013	527231	4068450	844.2	191.12	2.55	841.65
ADRS 013	527231	4068450	844.2	85.67	3.75	840.45
ADRS 013	527231	4068450	844.2	56.85	5.5	838.7
ADRS 013	527231	4068450	844.2	55.04	8.074	836.126

ADRS 013	527231	4068450	844.2	68.54	11.85	832.35
ADRS 013	527231	4068450	844.2	91.85	17.39	826.81
ADRS 013	527231	4068450	844.2	102.52	25.53	818.67
ADRS 013	527231	4068450	844.2	84.4	37.47	806.73
ADRS 013	527231	4068450	844.2	54.99	55.01	789.19
ADRS 013	527231	4068450	844.2	37.7	80.74	763.46
ADRS 014	527031	4068450	845.2	765.68	0.55	844.65
ADRS 014	527031	4068450	845.2	622.75	0.81	844.39
ADRS 014	527031	4068450	845.2	423.58	1.19	844.01
ADRS 014	527031	4068450	845.2	239.99	1.74	843.46
ADRS 014	527031	4068450	845.2	132.88	2.55	842.65
ADRS 014	527031	4068450	845.2	92.59	3.75	841.45
ADRS 014	527031	4068450	845.2	78.31	5.5	839.7
ADRS 014	527031	4068450	845.2	72.58	8.074	837.126
ADRS 014	527031	4068450	845.2	73.29	11.85	833.35
ADRS 014	527031	4068450	845.2	79.46	17.39	827.81
ADRS 014	527031	4068450	845.2	83.41	25.53	819.67
ADRS 014	527031	4068450	845.2	70.71	37.47	807.73
ADRS 014	527031	4068450	845.2	46.67	55.01	790.19
ADRS 014	527031	4068450	845.2	32.32	80.74	764.46
ADRS 015	526831	4068450	846.1	1730.67	0.55	845.55
ADRS 015	526831	4068450	846.1	1029.1	0.81	845.29
ADRS 015	526831	4068450	846.1	507.58	1.19	844.91
ADRS 015	526831	4068450	846.1	242.92	1.74	844.36
ADRS 015	526831	4068450	846.1	121.2	2.55	843.55
ADRS 015	526831	4068450	846.1	91.67	3.75	842.35
ADRS 015	526831	4068450	846.1	95.09	5.5	840.6
ADRS 015	526831	4068450	846.1	93.79	8.074	838.026
ADRS 015	526831	4068450	846.1	87.67	11.85	834.25
ADRS 015	526831	4068450	846.1	80.71	17.39	828.71
ADRS 015	526831	4068450	846.1	73.39	25.53	820.57
ADRS 015	526831	4068450	846.1	69.42	37.47	808.63
ADRS 015	526831	4068450	846.1	66.7	55.01	791.09
ADRS 015	526831	4068450	846.1	51.37	80.74	765.36
ADRS 016	528031	4068650	844.8	823.4	0.44	844.36
ADRS 016	528031	4068650	844.8	534.27	0.65	844.15
ADRS 016	528031	4068650	844.8	242.29	0.96	843.84
ADRS 016	528031	4068650	844.8	95.28	1.41	843.39
ADRS 016	528031	4068650	844.8	54.03	2.06	842.74
ADRS 016	528031	4068650	844.8	41.87	3.03	841.77
ADRS 016	528031	4068650	844.8	35	4.44	840.36
ADRS 016	528031	4068650	844.8	40.13	6.52	838.28
ADRS 016	528031	4068650	844.8	55.44	9.57	835.23
ADRS 016	528031	4068650	844.8	69.59	14.05	830.75
ADRS 016	528031	4068650	844.8	74.39	20.63	824.17
ADRS 016	528031	4068650	844.8	64.66	30.28	814.52
ADRS 016	528031	4068650	844.8	42.45	44.44	800.36
ADRS 016	528031	4068650	844.8	22.36	65.23	779.57
ADRS 016	528031	4068650	844.8	15.13	95.74	749.06
ADRS 016	528031	4068650	844.8	18.98	140.53	704.27
ADRS 016	528031	4068650	844.8	32.09	206.27	638.53
ADRS 016	528031	4068650	844.8	53.41	302.77	542.03
ADRS 017	529120	4068595	840.5	1052.67	0.59	839.91
ADRS 017	529120	4068595	840.5	576.82	0.87	839.63
ADRS 017	529120	4068595	840.5	349.45	1.28	839.22
ADRS 017	529120	4068595	840.5	237.41	1.87	838.63
ADRS 017	529120	4068595	840.5	202.82	2.75	837.75
ADRS 017	529120	4068595	840.5	217.88	4.04	836.46
ADRS 017	529120	4068595	840.5	207.57	5.93	834.57
ADRS 017	529120	4068595	840.5	158.57	8.7	831.8
ADRS 017	529120	4068595	840.5	132.73	12.77	827.73

ADRS 017	529120	4068595	840.5	155.58	18.74	821.76
ADRS 017	529120	4068595	840.5	216.59	27.5	813
ADRS 017	529120	4068595	840.5	281.55	40.37	800.13
ADRS 017	529120	4068595	840.5	315.72	59.25	781.25
ADRS 017	529120	4068595	840.5	303.47	86.97	753.53
ADRS 017	529120	4068595	840.5	250.52	127.66	712.84
ADRS 017	529120	4068595	840.5	194.4	187.37	653.13
ADRS 017	529120	4068595	840.5	175.19	275.03	565.47
ADRS 017	529120	4068595	840.5	189.49	403.69	436.81
ADRS 018	528168	4068650	846.5	391.05	0.55	845.95
ADRS 018	528168	4068650	846.5	369.58	0.81	845.69
ADRS 018	528168	4068650	846.5	234.21	1.19	845.31
ADRS 018	528168	4068650	846.5	89.01	1.74	844.76
ADRS 018	528168	4068650	846.5	31.15	2.55	843.95
ADRS 018	528168	4068650	846.5	25.72	3.75	842.75
ADRS 018	528168	4068650	846.5	34.28	5.5	841
ADRS 018	528168	4068650	846.5	44.53	8.074	838.426
ADRS 018	528168	4068650	846.5	51.31	11.85	834.65
ADRS 018	528168	4068650	846.5	53.69	17.39	829.11
ADRS 018	528168	4068650	846.5	54.07	25.53	820.97
ADRS 018	528168	4068650	846.5	49.57	37.47	809.03
ADRS 018	528168	4068650	846.5	34.77	55.01	791.49
ADRS 018	528168	4068650	846.5	20.09	80.74	765.76
ADRS 019	527306	4068700	847.3	772.14	0.64	846.66
ADRS 019	527306	4068700	847.3	828.66	0.94	846.36
ADRS 019	527306	4068700	847.3	802.56	1.38	845.92
ADRS 019	527306	4068700	847.3	643.98	2.02	845.28
ADRS 019	527306	4068700	847.3	371.31	2.96	844.34
ADRS 019	527306	4068700	847.3	135.86	4.35	842.95
ADRS 019	527306	4068700	847.3	51.43	6.38	840.92
ADRS 019	527306	4068700	847.3	46.96	9.37	837.93
ADRS 019	527306	4068700	847.3	61.19	13.75	833.55
ADRS 019	527306	4068700	847.3	72.53	20.18	827.12
ADRS 019	527306	4068700	847.3	73.71	29.63	817.67
ADRS 019	527306	4068700	847.3	67.44	43.49	803.81
ADRS 019	527306	4068700	847.3	58.09	63.83	783.47
ADRS 019	527306	4068700	847.3	44.13	93.69	753.61
ADRS 019	527306	4068700	847.3	28.83	137.51	709.79
ADRS 019	527306	4068700	847.3	19.33	201.84	645.46
ADRS 020	527931	4068550	843.5	809.31	0.55	842.95
ADRS 020	527931	4068550	843.5	687.48	0.81	842.69
ADRS 020	527931	4068550	843.5	370.81	1.19	842.31
ADRS 020	527931	4068550	843.5	116.71	1.74	841.76
ADRS 020	527931	4068550	843.5	43.3	2.55	840.95
ADRS 020	527931	4068550	843.5	40.78	3.75	839.75
ADRS 020	527931	4068550	843.5	50.25	5.5	838
ADRS 020	527931	4068550	843.5	32.6	8.074	835.426
ADRS 020	527931	4068550	843.5	74.97	11.85	831.65
ADRS 020	527931	4068550	843.5	81.39	17.39	826.11
ADRS 020	527931	4068550	843.5	75.32	25.53	817.97
ADRS 020	527931	4068550	843.5	58.16	37.47	806.03
ADRS 020	527931	4068550	843.5	40.89	55.01	788.49
ADRS 020	527931	4068550	843.5	29.69	80.74	762.76
ADRS 021	527731	4068550	843.9	964.98	0.55	843.35
ADRS 021	527731	4068550	843.9	929.65	0.81	843.09
ADRS 021	527731	4068550	843.9	790.15	1.19	842.71
ADRS 021	527731	4068550	843.9	633.56	1.74	842.16
ADRS 021	527731	4068550	843.9	389.16	2.55	841.35
ADRS 021	527731	4068550	843.9	130.76	3.75	840.15
ADRS 021	527731	4068550	843.9	44.4	5.5	838.4
ADRS 021	527731	4068550	843.9	45.61	8.074	835.826

ADRS 021	527731	4068550	843.9	64.46	11.85	832.05
ADRS 021	527731	4068550	843.9	79.5	17.39	826.51
ADRS 021	527731	4068550	843.9	80.28	25.53	818.37
ADRS 021	527731	4068550	843.9	65.64	37.47	806.43
ADRS 021	527731	4068550	843.9	47.84	55.01	788.89
ADRS 021	527731	4068550	843.9	37.22	80.74	763.16
ADRS 022	527531	4068550	844.3	900.89	0.55	843.75
ADRS 022	527531	4068550	844.3	1040.08	0.81	843.49
ADRS 022	527531	4068550	844.3	952.64	1.19	843.11
ADRS 022	527531	4068550	844.3	532.79	1.74	842.56
ADRS 022	527531	4068550	844.3	168.98	2.55	841.75
ADRS 022	527531	4068550	844.3	56.98	3.75	840.55
ADRS 022	527531	4068550	844.3	47.7	5.5	838.8
ADRS 022	527531	4068550	844.3	57.82	8.074	836.226
ADRS 022	527531	4068550	844.3	71.49	11.85	832.45
ADRS 022	527531	4068550	844.3	80.84	17.39	826.91
ADRS 022	527531	4068550	844.3	77.86	25.53	818.77
ADRS 022	527531	4068550	844.3	63.95	37.47	806.83
ADRS 022	527531	4068550	844.3	49.76	55.01	789.29
ADRS 022	527531	4068550	844.3	41.26	80.74	763.56
ADRS 023	528131	4068550	842.2	924.25	0.55	841.65
ADRS 023	528131	4068550	842.2	538.83	0.81	841.39
ADRS 023	528131	4068550	842.2	250.9	1.19	841.01
ADRS 023	528131	4068550	842.2	87.32	1.74	840.46
ADRS 023	528131	4068550	842.2	41.03	2.55	839.65
ADRS 023	528131	4068550	842.2	41.75	3.75	838.45
ADRS 023	528131	4068550	842.2	53.25	5.5	836.7
ADRS 023	528131	4068550	842.2	66.64	8.074	834.126
ADRS 023	528131	4068550	842.2	74.22	11.85	830.35
ADRS 023	528131	4068550	842.2	70.08	17.39	824.81
ADRS 023	528131	4068550	842.2	57.51	25.53	816.67
ADRS 023	528131	4068550	842.2	44.37	37.47	804.73
ADRS 023	528131	4068550	842.2	33.42	55.01	787.19
ADRS 023	528131	4068550	842.2	23.22	80.74	761.46
ADRS 024	528331	4068550	844.5	273.74	0.55	843.95
ADRS 024	528331	4068550	844.5	186.41	0.81	843.69
ADRS 024	528331	4068550	844.5	215.12	1.19	843.31
ADRS 024	528331	4068550	844.5	271.03	1.74	842.76
ADRS 024	528331	4068550	844.5	204.5	2.55	841.95
ADRS 024	528331	4068550	844.5	86.94	3.75	840.75
ADRS 024	528331	4068550	844.5	44.2	5.5	839
ADRS 024	528331	4068550	844.5	50.95	8.074	836.426
ADRS 024	528331	4068550	844.5	62.22	11.85	832.65
ADRS 024	528331	4068550	844.5	47.28	17.39	827.11
ADRS 024	528331	4068550	844.5	30.61	25.53	818.97
ADRS 024	528331	4068550	844.5	25.02	37.47	807.03
ADRS 024	528331	4068550	844.5	23.21	55.01	789.49
ADRS 024	528331	4068550	844.5	28.17	80.74	763.76
ADRS 025	528531	4068550	847.4	567.22	0.61	846.79
ADRS 025	528531	4068550	847.4	434.46	0.9	846.5
ADRS 025	528531	4068550	847.4	311.32	1.32	846.08
ADRS 025	528531	4068550	847.4	229.38	1.93	845.47
ADRS 025	528531	4068550	847.4	179.76	2.84	844.56
ADRS 025	528531	4068550	847.4	137.9	4.16	843.24
ADRS 025	528531	4068550	847.4	108.86	6.11	841.29
ADRS 025	528531	4068550	847.4	95.33	8.97	838.43
ADRS 025	528531	4068550	847.4	80.95	13.17	834.23
ADRS 025	528531	4068550	847.4	59.08	19.33	828.07
ADRS 025	528531	4068550	847.4	41.44	28.37	819.03
ADRS 025	528531	4068550	847.4	30.21	41.64	805.76
ADRS 025	528531	4068550	847.4	25.2	61.12	786.28

ADRS 025	528531	4068550	845	32.65	89.71	755.29
ADRS 026	527911	4068740	845	238.33	0.55	844.45
ADRS 026	527911	4068740	845	231.35	0.81	844.19
ADRS 026	527911	4068740	845	148.14	1.19	843.81
ADRS 026	527911	4068740	845	66.57	1.74	843.26
ADRS 026	527911	4068740	845	26.28	2.55	842.45
ADRS 026	527911	4068740	845	18.17	3.75	841.25
ADRS 026	527911	4068740	845	29.98	5.5	839.5
ADRS 026	527911	4068740	845	51.67	8.074	836.926
ADRS 026	527911	4068740	845	57.53	11.85	833.15
ADRS 026	527911	4068740	845	40.05	17.39	827.61
ADRS 026	527911	4068740	845	23.93	25.53	819.47
ADRS 026	527911	4068740	845	21.67	37.47	807.53
ADRS 026	527911	4068740	845	28.29	55.01	789.99
ADRS 026	527911	4068740	845	25.29	80.74	764.26
ADRS 027	527711	4068740	846.1	206.07	0.55	845.55
ADRS 027	527711	4068740	846.1	271.3	0.81	845.29
ADRS 027	527711	4068740	846.1	220.19	1.19	844.91
ADRS 027	527711	4068740	846.1	95.66	1.74	844.36
ADRS 027	527711	4068740	846.1	32.55	2.55	843.55
ADRS 027	527711	4068740	846.1	24.44	3.75	842.35
ADRS 027	527711	4068740	846.1	35.88	5.5	840.6
ADRS 027	527711	4068740	846.1	53.59	8.074	838.026
ADRS 027	527711	4068740	846.1	69.07	11.85	834.25
ADRS 027	527711	4068740	846.1	67.05	17.39	828.71
ADRS 027	527711	4068740	846.1	45.3	25.53	820.57
ADRS 027	527711	4068740	846.1	25.82	37.47	808.63
ADRS 027	527711	4068740	846.1	20.97	55.01	791.09
ADRS 027	527711	4068740	846.1	28.25	80.74	765.36
ADRS 028	527516	4068740	847.3	248.61	0.55	846.75
ADRS 028	527516	4068740	847.3	516.57	0.81	846.49
ADRS 028	527516	4068740	847.3	839.63	1.19	846.11
ADRS 028	527516	4068740	847.3	1002.71	1.74	845.56
ADRS 028	527516	4068740	847.3	753.23	2.55	844.75
ADRS 028	527516	4068740	847.3	290.52	3.75	843.55
ADRS 028	527516	4068740	847.3	60.38	5.5	841.8
ADRS 028	527516	4068740	847.3	23.6	8.074	839.226
ADRS 028	527516	4068740	847.3	57.29	11.85	835.45
ADRS 028	527516	4068740	847.3	73.03	17.39	829.91
ADRS 028	527516	4068740	847.3	45.78	25.53	821.77
ADRS 028	527516	4068740	847.3	32.91	37.47	809.83
ADRS 028	527516	4068740	847.3	32.67	55.01	792.29
ADRS 028	527516	4068740	847.3	31.92	80.74	766.56
ADRS 029	527321	4068740	847.3	725.68	0.55	846.75
ADRS 029	527321	4068740	847.3	799.65	0.81	846.49
ADRS 029	527321	4068740	847.3	946.52	1.19	846.11
ADRS 029	527321	4068740	847.3	977.51	1.74	845.56
ADRS 029	527321	4068740	847.3	668.64	2.55	844.75
ADRS 029	527321	4068740	847.3	274.54	3.75	843.55
ADRS 029	527321	4068740	847.3	96.49	5.5	841.8
ADRS 029	527321	4068740	847.3	66.81	8.074	839.226
ADRS 029	527321	4068740	847.3	89.67	11.85	835.45
ADRS 029	527321	4068740	847.3	111.46	17.39	829.91
ADRS 029	527321	4068740	847.3	94.08	25.53	821.77
ADRS 029	527321	4068740	847.3	57.02	37.47	809.83
ADRS 029	527321	4068740	847.3	35.91	55.01	792.29
ADRS 029	527321	4068740	847.3	32.83	80.74	766.56
ADRS 030	529866	4070887	950.67	2255.45	2.06	948.61
ADRS 030	529866	4070887	950.67	847.23	3.03	947.64
ADRS 030	529866	4070887	950.67	859.46	4.44	946.23
ADRS 030	529866	4070887	950.67	1278.99	6.52	944.15

ADRS 030	529866	4070887	950.67	1306.32	9.57	941.1
ADRS 030	529866	4070887	950.67	1130.57	14.05	936.62
ADRS 030	529866	4070887	950.67	1079.34	20.63	930.04
ADRS 030	529866	4070887	950.67	975.8	30.28	920.39
ADRS 030	529866	4070887	950.67	756.34	44.44	906.23
ADRS 030	529866	4070887	950.67	611.74	65.23	885.44
ADRS 030	529866	4070887	950.67	515.78	85.74	864.93
ADRS 030	529866	4070887	950.67	391.62	140.53	810.14
ADRS 030	529866	4070887	950.67	360.73	206.27	744.4
ADRS 030	529866	4070887	950.67	468.79	302.77	647.9
ADRS 031	528111	4068740	846.5	774.33	0.55	845.95
ADRS 031	528111	4068740	846.5	534.72	0.81	845.69
ADRS 031	528111	4068740	846.5	273.3	1.19	845.31
ADRS 031	528111	4068740	846.5	100.15	1.74	844.76
ADRS 031	528111	4068740	846.5	48.04	2.55	843.95
ADRS 031	528111	4068740	846.5	43.91	3.75	842.75
ADRS 031	528111	4068740	846.5	48.52	5.5	841
ADRS 031	528111	4068740	846.5	56.33	8.074	838.426
ADRS 031	528111	4068740	846.5	63.49	11.85	834.65
ADRS 031	528111	4068740	846.5	66.78	17.39	829.11
ADRS 031	528111	4068740	846.5	65.33	25.53	820.97
ADRS 031	528111	4068740	846.5	55.1	37.47	809.03
ADRS 031	528111	4068740	846.5	34.68	55.01	791.49
ADRS 031	528111	4068740	846.5	16.28	80.74	765.76
ADRS 032	528416	4068729	844.2	450.43	0.55	843.65
ADRS 032	528416	4068729	844.2	388.56	0.81	843.39
ADRS 032	528416	4068729	844.2	256.06	1.19	843.01
ADRS 032	528416	4068729	844.2	154.59	1.74	842.46
ADRS 032	528416	4068729	844.2	117.02	2.55	841.65
ADRS 032	528416	4068729	844.2	109.65	3.75	840.45
ADRS 032	528416	4068729	844.2	105.69	5.5	838.7
ADRS 032	528416	4068729	844.2	93.74	8.074	836.126
ADRS 032	528416	4068729	844.2	73.44	11.85	832.35
ADRS 032	528416	4068729	844.2	54.16	17.39	826.81
ADRS 032	528416	4068729	844.2	40.94	25.53	818.67
ADRS 032	528416	4068729	844.2	32.64	37.47	806.73
ADRS 032	528416	4068729	844.2	27.97	55.01	789.19
ADRS 032	528416	4068729	844.2	26.9	80.74	763.46
ADRS 033	528031	4068450	841.2	719.65	0.55	840.65
ADRS 033	528031	4068450	841.2	590.04	0.81	840.39
ADRS 033	528031	4068450	841.2	431.46	1.19	840.01
ADRS 033	528031	4068450	841.2	186.55	1.74	839.46
ADRS 033	528031	4068450	841.2	44.59	2.55	838.65
ADRS 033	528031	4068450	841.2	28.7	3.75	837.45
ADRS 033	528031	4068450	841.2	47.18	5.5	835.7
ADRS 033	528031	4068450	841.2	70.98	8.074	833.126
ADRS 033	528031	4068450	841.2	85.77	11.85	829.35
ADRS 033	528031	4068450	841.2	82.12	17.39	823.81
ADRS 033	528031	4068450	841.2	66.15	25.53	815.67
ADRS 033	528031	4068450	841.2	49.55	37.47	803.73
ADRS 033	528031	4068450	841.2	37.44	55.01	786.19
ADRS 033	528031	4068450	841.2	28.41	80.74	760.46
ADRS 034	528031	4068230	841.2	671.98	0.55	840.65
ADRS 034	528031	4068230	841.2	555.22	0.81	840.39
ADRS 034	528031	4068230	841.2	189.23	1.19	840.01
ADRS 034	528031	4068230	841.2	68.81	1.74	839.46
ADRS 034	528031	4068230	841.2	24.7	2.55	838.65
ADRS 034	528031	4068230	841.2	26.28	3.75	837.45
ADRS 034	528031	4068230	841.2	45.68	5.5	835.7
ADRS 034	528031	4068230	841.2	73.58	8.074	833.126
ADRS 034	528031	4068230	841.2	66.18	11.85	829.35

ADRS 034	528031	4068230	841.2	87.68	17.39	823.81
ADRS 034	528031	4068230	841.2	77.76	25.53	815.67
ADRS 034	528031	4068230	841.2	41.69	37.47	803.73
ADRS 034	528031	4068230	841.2	45.8	55.01	786.19
ADRS 034	528031	4068230	841.2	30.53	80.74	760.46
ADRS 035	528031	4067987	840.1	641.84	0.55	839.55
ADRS 035	528031	4067987	840.1	526.42	0.81	839.29
ADRS 035	528031	4067987	840.1	368.19	1.19	838.91
ADRS 035	528031	4067987	840.1	190.09	1.74	838.36
ADRS 035	528031	4067987	840.1	67.65	2.55	837.55
ADRS 035	528031	4067987	840.1	34.24	3.75	836.35
ADRS 035	528031	4067987	840.1	35.13	5.5	834.6
ADRS 035	528031	4067987	840.1	48.56	8.074	832.026
ADRS 035	528031	4067987	840.1	69.03	11.85	828.25
ADRS 035	528031	4067987	840.1	85.37	17.39	822.71
ADRS 035	528031	4067987	840.1	83.28	25.53	814.57
ADRS 035	528031	4067987	840.1	58.86	37.47	802.63
ADRS 035	528031	4067987	840.1	36.33	55.01	785.09
ADRS 035	528031	4067987	840.1	35.06	80.74	759.36
ADRS 036	527731	4068350	842.4	899.93	0.55	841.85
ADRS 036	527731	4068350	842.4	856.46	0.81	841.59
ADRS 036	527731	4068350	842.4	587.29	1.19	841.21
ADRS 036	527731	4068350	842.4	262.51	1.74	840.66
ADRS 036	527731	4068350	842.4	94.63	2.55	839.85
ADRS 036	527731	4068350	842.4	54.25	3.75	838.65
ADRS 036	527731	4068350	842.4	57.55	5.5	836.9
ADRS 036	527731	4068350	842.4	69.83	8.07	834.33
ADRS 036	527731	4068350	842.4	79.41	11.85	830.55
ADRS 036	527731	4068350	842.4	88.31	17.39	825.01
ADRS 036	527731	4068350	842.4	92.66	25.53	816.87
ADRS 036	527731	4068350	842.4	77.82	37.47	804.93
ADRS 036	527731	4068350	842.4	50.5	55.01	787.39
ADRS 036	527731	4068350	842.4	34.42	80.74	761.66
ADRS 037	527731	4068106	841.2	399.66	0.55	840.65
ADRS 037	527731	4068106	841.2	516.77	0.81	840.39
ADRS 037	527731	4068106	841.2	538.59	1.19	840.01
ADRS 037	527731	4068106	841.2	404.4	1.74	839.46
ADRS 037	527731	4068106	841.2	186.08	2.55	838.65
ADRS 037	527731	4068106	841.2	56.24	3.75	837.45
ADRS 037	527731	4068106	841.2	32.02	5.5	835.7
ADRS 037	527731	4068106	841.2	44.82	8.07	833.13
ADRS 037	527731	4068106	841.2	62.89	11.85	829.35
ADRS 037	527731	4068106	841.2	75.72	17.39	823.81
ADRS 037	527731	4068106	841.2	81.03	25.53	815.67
ADRS 037	527731	4068106	841.2	80.92	37.47	803.73
ADRS 037	527731	4068106	841.2	71.86	55.01	786.19
ADRS 037	527731	4068106	841.2	47.18	80.74	760.46
ADRS 038	528231	4068230	841.2	581.84	0.55	840.65
ADRS 038	528231	4068230	841.2	379.32	0.81	840.39
ADRS 038	528231	4068230	841.2	236.06	1.19	840.01
ADRS 038	528231	4068230	841.2	118.76	1.74	839.46
ADRS 038	528231	4068230	841.2	48.78	2.55	838.65
ADRS 038	528231	4068230	841.2	36.7	3.75	837.45
ADRS 038	528231	4068230	841.2	44.73	5.5	835.7
ADRS 038	528231	4068230	841.2	54.37	8.07	833.13
ADRS 038	528231	4068230	841.2	59.75	11.85	829.35
ADRS 038	528231	4068230	841.2	59.12	17.39	823.81
ADRS 038	528231	4068230	841.2	53.6	25.53	815.67
ADRS 038	528231	4068230	841.2	42.89	37.47	803.73
ADRS 038	528231	4068230	841.2	30.49	55.01	786.19
ADRS 038	528231	4068230	841.2	25.17	80.74	760.46

ADRS 101	526499	4068853	849.3	855.23	0.55	848.75
ADRS 101	526499	4068853	849.3	1003.53	0.81	848.49
ADRS 101	526499	4068853	849.3	1094.85	1.19	848.11
ADRS 101	526499	4068853	849.3	801.78	1.74	847.56
ADRS 101	526499	4068853	849.3	284.04	2.55	846.75
ADRS 101	526499	4068853	849.3	56.56	3.75	845.55
ADRS 101	526499	4068853	849.3	31.15	5.5	843.8
ADRS 101	526499	4068853	849.3	49.42	8.074	841.226
ADRS 101	526499	4068853	849.3	76.29	11.85	837.45
ADRS 101	526499	4068853	849.3	97.51	17.39	831.91
ADRS 101	526499	4068853	849.3	93.61	25.53	823.77
ADRS 101	526499	4068853	849.3	69.03	37.47	811.83
ADRS 101	526499	4068853	849.3	48.29	55.01	794.29
ADRS 101	526499	4068853	849.3	41.64	80.74	768.56
ADRS 101	526499	4068853	849.3	42.76	118.51	730.79
ADRS 101	526499	4068853	849.3	43.65	173.94	675.36
ADRS 101	526499	4068853	849.3	42.7	255.31	593.99
ADRS 101	526499	4068853	849.3	41.32	374.75	474.55
ADRS 101	526499	4068853	849.3	45.9	550.06	299.24
ADRS 101	526499	4068853	849.3	69.77	807.37	41.93
ADRS 102	527219	4069154	849.3	72.64	0.55	848.75
ADRS 102	527219	4069154	849.3	113.33	0.81	848.49
ADRS 102	527219	4069154	849.3	168.22	1.19	848.11
ADRS 102	527219	4069154	849.3	211.66	1.74	847.56
ADRS 102	527219	4069154	849.3	203.83	2.55	846.75
ADRS 102	527219	4069154	849.3	140.04	3.75	845.55
ADRS 102	527219	4069154	849.3	72.98	5.5	843.8
ADRS 102	527219	4069154	849.3	42.97	8.074	841.226
ADRS 102	527219	4069154	849.3	48.23	11.85	837.45
ADRS 102	527219	4069154	849.3	77.3	17.39	831.91
ADRS 102	527219	4069154	849.3	93.98	25.53	823.77
ADRS 102	527219	4069154	849.3	70.64	37.47	811.83
ADRS 102	527219	4069154	849.3	38.43	55.01	794.29
ADRS 102	527219	4069154	849.3	28.09	80.74	768.56
ADRS 102	527219	4069154	849.3	36.33	118.51	730.79
ADRS 102	527219	4069154	849.3	44.91	173.94	675.36
ADRS 102	527219	4069154	849.3	46.41	255.31	593.99
ADRS 102	527219	4069154	849.3	55.04	374.75	474.55
ADRS 102	527219	4069154	849.3	81.27	550.06	299.24
ADRS 102	527219	4069154	849.3	120.39	807.37	41.93
ADRS 103	528050	4069162	847.2	158.34	0.59	846.61
ADRS 103	528050	4069162	847.2	180.04	0.87	846.33
ADRS 103	528050	4069162	847.2	186.8	1.28	845.92
ADRS 103	528050	4069162	847.2	122.75	1.87	845.33
ADRS 103	528050	4069162	847.2	57.75	2.75	844.45
ADRS 103	528050	4069162	847.2	43.91	4.04	843.16
ADRS 103	528050	4069162	847.2	59.73	5.93	841.27
ADRS 103	528050	4069162	847.2	93.42	8.7	838.5
ADRS 103	528050	4069162	847.2	137.66	12.77	834.43
ADRS 103	528050	4069162	847.2	149.61	18.74	828.46
ADRS 103	528050	4069162	847.2	96.77	27.5	819.7
ADRS 103	528050	4069162	847.2	39.55	40.37	806.83
ADRS 103	528050	4069162	847.2	21.47	59.25	787.95
ADRS 103	528050	4069162	847.2	26.71	86.97	760.23
ADRS 103	528050	4069162	847.2	27.32	127.66	719.54
ADRS 103	528050	4069162	847.2	21.91	187.37	659.83
ADRS 103	528050	4069162	847.2	31.02	275.03	572.17
ADRS 103	528050	4069162	847.2	80.35	403.69	443.51
ADRS 104	527676	4069165	847.3	288.29	0.55	846.75
ADRS 104	527676	4069165	847.3	256.7	0.81	846.49
ADRS 104	527676	4069165	847.3	172.34	1.19	846.11

ADRS 104	527676	4069165	847.3	110.93	1.74	845.56
ADRS 104	527676	4069165	847.3	70.69	2.55	844.75
ADRS 104	527676	4069165	847.3	37.33	3.75	843.55
ADRS 104	527676	4069165	847.3	28.66	5.5	841.8
ADRS 104	527676	4069165	847.3	41.45	8.074	839.226
ADRS 104	527676	4069165	847.3	68.67	11.85	835.45
ADRS 104	527676	4069165	847.3	98.05	17.39	829.91
ADRS 104	527676	4069165	847.3	103.56	25.53	821.77
ADRS 104	527676	4069165	847.3	71.13	37.47	809.83
ADRS 104	527676	4069165	847.3	33.12	55.01	792.29
ADRS 104	527676	4069165	847.3	17.94	80.74	766.56
ADRS 105	528050	4068908	845.7	983.55	0.55	845.15
ADRS 105	528050	4068908	845.7	1033.81	0.81	844.89
ADRS 105	528050	4068908	845.7	652.68	1.19	844.51
ADRS 105	528050	4068908	845.7	187.22	1.74	843.96
ADRS 105	528050	4068908	845.7	34.36	2.55	843.15
ADRS 105	528050	4068908	845.7	30.05	3.75	841.95
ADRS 105	528050	4068908	845.7	69.86	5.5	840.2
ADRS 105	528050	4068908	845.7	120.02	8.074	837.626
ADRS 105	528050	4068908	845.7	126.94	11.85	833.85
ADRS 105	528050	4068908	845.7	83.92	17.39	828.31
ADRS 105	528050	4068908	845.7	41.83	25.53	820.17
ADRS 105	528050	4068908	845.7	24.3	37.47	808.23
ADRS 105	528050	4068908	845.7	20.66	55.01	790.69
ADRS 105	528050	4068908	845.7	21.43	80.74	764.96
ADRS 106	528235	4068922	845.7	605.34	0.55	845.15
ADRS 106	528235	4068922	845.7	381.86	0.81	844.89
ADRS 106	528235	4068922	845.7	222.86	1.19	844.51
ADRS 106	528235	4068922	845.7	145.32	1.74	843.96
ADRS 106	528235	4068922	845.7	117.84	2.55	843.15
ADRS 106	528235	4068922	845.7	113.23	3.75	841.95
ADRS 106	528235	4068922	845.7	119.23	5.5	840.2
ADRS 106	528235	4068922	845.7	122.5	8.074	837.626
ADRS 106	528235	4068922	845.7	105.14	11.85	833.85
ADRS 106	528235	4068922	845.7	77.51	17.39	828.31
ADRS 106	528235	4068922	845.7	59.3	25.53	820.17
ADRS 106	528235	4068922	845.7	45.07	37.47	808.23
ADRS 106	528235	4068922	845.7	24.81	55.01	790.69
ADRS 106	528235	4068922	845.7	17.49	80.74	764.96
ADRS 107	528520	4069180	845.2	320.06	0.55	844.65
ADRS 107	528520	4069180	845.2	355.46	0.81	844.39
ADRS 107	528520	4069180	845.2	354.82	1.19	844.01
ADRS 107	528520	4069180	845.2	270.42	1.74	843.46
ADRS 107	528520	4069180	845.2	136.74	2.55	842.65
ADRS 107	528520	4069180	845.2	52.38	3.75	841.45
ADRS 107	528520	4069180	845.2	29.17	5.5	839.7
ADRS 107	528520	4069180	845.2	32.35	8.074	837.126
ADRS 107	528520	4069180	845.2	39	11.85	833.35
ADRS 107	528520	4069180	845.2	43.99	17.39	827.81
ADRS 107	528520	4069180	845.2	51.9	25.53	819.67
ADRS 107	528520	4069180	845.2	49.77	37.47	807.73
ADRS 107	528520	4069180	845.2	28.23	55.01	790.19
ADRS 107	528520	4069180	845.2	14.69	80.74	764.46
ADRS 107	528520	4069180	845.2	18.21	118.51	726.69
ADRS 107	528520	4069180	845.2	41.17	173.94	671.26
ADRS 107	528520	4069180	845.2	86.63	255.31	589.89
ADRS 107	528520	4069180	845.2	138.13	374.75	470.45
ADRS 107	528520	4069180	845.2	172.69	550.06	295.14
ADRS 107	528520	4069180	845.2	200.55	807.37	37.83
ADRS 108	529293	4070102	877.8	1268.75	1.87	875.93
ADRS 108	529293	4070102	877.8	346.23	2.75	875.05

ADRS 108	529293	4070102	877.8	158.47	4.04	873.76
ADRS 108	529293	4070102	877.8	267.72	5.93	871.87
ADRS 108	529293	4070102	877.8	550.29	8.7	869.1
ADRS 108	529293	4070102	877.8	848.45	12.77	865.03
ADRS 108	529293	4070102	877.8	1064.11	18.74	859.06
ADRS 108	529293	4070102	877.8	1043.64	27.5	850.3
ADRS 108	529293	4070102	877.8	714.81	40.37	837.43
ADRS 108	529293	4070102	877.8	337.71	59.25	818.55
ADRS 108	529293	4070102	877.8	157.32	86.97	790.83
ADRS 108	529293	4070102	877.8	146.76	127.66	750.14
ADRS 108	529293	4070102	877.8	143.82	187.37	690.43
ADRS 108	529293	4070102	877.8	82.77	275.03	602.77
ADRS 108	529293	4070102	877.8	97.39	403.69	474.11
ADRS 109	528755	4069464	847.29	119.59	2.06	845.23
ADRS 109	528755	4069464	847.29	31.18	3.03	844.26
ADRS 109	528755	4069464	847.29	34.35	4.44	842.85
ADRS 109	528755	4069464	847.29	71.71	6.52	840.77
ADRS 109	528755	4069464	847.29	114.42	9.57	837.72
ADRS 109	528755	4069464	847.29	136.8	14.05	833.24
ADRS 109	528755	4069464	847.29	126.84	20.63	826.66
ADRS 109	528755	4069464	847.29	92.17	30.28	817.01
ADRS 109	528755	4069464	847.29	53.12	44.44	802.85
ADRS 109	528755	4069464	847.29	23.64	65.23	782.06
ADRS 109	528755	4069464	847.29	12.82	95.74	751.55
ADRS 109	528755	4069464	847.29	19.98	140.53	706.76
ADRS 109	528755	4069464	847.29	55.21	206.27	641.02
ADRS 109	528755	4069464	847.29	177.33	302.77	544.52
ADRS 110	526850	4069115	849.3	854.58	0.55	848.75
ADRS 110	526850	4069115	849.3	752.73	0.81	848.49
ADRS 110	526850	4069115	849.3	720.28	1.19	848.11
ADRS 110	526850	4069115	849.3	675.46	1.74	847.56
ADRS 110	526850	4069115	849.3	420.71	2.55	846.75
ADRS 110	526850	4069115	849.3	140.34	3.75	845.55
ADRS 110	526850	4069115	849.3	57.19	5.5	843.8
ADRS 110	526850	4069115	849.3	63.24	8.074	841.226
ADRS 110	526850	4069115	849.3	77.96	11.85	837.45
ADRS 110	526850	4069115	849.3	78.54	17.39	831.91
ADRS 110	526850	4069115	849.3	72.04	25.53	823.77
ADRS 110	526850	4069115	849.3	66.94	37.47	811.83
ADRS 110	526850	4069115	849.3	61.83	55.01	794.29
ADRS 110	526850	4069115	849.3	49.6	80.74	768.56
ADRS 111	527219	4068967	847.5	1513.99	0.61	846.89
ADRS 111	527219	4068967	847.5	425.78	0.9	846.6
ADRS 111	527219	4068967	847.5	275.63	1.32	846.18
ADRS 111	527219	4068967	847.5	435.2	1.93	845.57
ADRS 111	527219	4068967	847.5	438.13	2.84	844.66
ADRS 111	527219	4068967	847.5	174.03	4.16	843.34
ADRS 111	527219	4068967	847.5	48.76	6.11	841.39
ADRS 111	527219	4068967	847.5	39.82	8.97	838.53
ADRS 111	527219	4068967	847.5	64.48	13.17	834.33
ADRS 111	527219	4068967	847.5	74.94	19.33	828.17
ADRS 111	527219	4068967	847.5	51.61	28.37	819.13
ADRS 111	527219	4068967	847.5	30.6	41.64	805.86
ADRS 111	527219	4068967	847.5	34.65	61.12	786.38
ADRS 111	527219	4068967	847.5	47.63	89.71	757.79
ADRS 112	529660	4068760	847.28	311.93	0.61	846.67
ADRS 112	529660	4068760	847.28	359.02	0.89	846.39
ADRS 112	529660	4068760	847.28	291.16	1.3	845.98
ADRS 112	529660	4068760	847.28	162.74	1.91	845.37
ADRS 112	529660	4068760	847.28	102.12	2.81	844.47
ADRS 112	529660	4068760	847.28	117.29	4.13	843.15

ADRS 112	529660	4068760	847.28	172.42	6.06	841.22
ADRS 112	529660	4068760	847.28	207.88	8.89	838.39
ADRS 112	529660	4068760	847.28	194.84	13.05	834.23
ADRS 112	529660	4068760	847.28	148.24	19.15	828.13
ADRS 112	529660	4068760	847.28	100.74	28.11	819.17
ADRS 112	529660	4068760	847.28	87.17	41.25	806.03
ADRS 112	529660	4068760	847.28	126.47	60.55	786.73
ADRS 112	529660	4068760	847.28	217.17	88.88	758.4
ADRS 112	529660	4068760	847.28	295.51	130.46	716.82
ADRS 112	529660	4068760	847.28	286.74	191.49	655.79
ADRS 112	529660	4068760	847.28	212.06	281.06	566.22
ADRS 112	529660	4068760	847.28	162.05	412.54	434.74
ADRS 112	529660	4068760	847.28	181.96	605.53	241.75
ADRS 113	526840	4068330	845.2	552.1	0.55	844.65
ADRS 113	526840	4068330	845.2	518.17	0.81	844.39
ADRS 113	526840	4068330	845.2	514.35	1.19	844.01
ADRS 113	526840	4068330	845.2	501.75	1.74	843.46
ADRS 113	526840	4068330	845.2	400	2.55	842.65
ADRS 113	526840	4068330	845.2	232.36	3.75	841.45
ADRS 113	526840	4068330	845.2	109.37	5.5	839.7
ADRS 113	526840	4068330	845.2	64.9	8.074	837.126
ADRS 113	526840	4068330	845.2	72.27	11.85	833.35
ADRS 113	526840	4068330	845.2	101.57	17.39	827.81
ADRS 113	526840	4068330	845.2	107.94	25.53	819.67
ADRS 113	526840	4068330	845.2	76.67	37.47	807.73
ADRS 113	526840	4068330	845.2	49.5	55.01	790.19
ADRS 113	526840	4068330	845.2	44.86	80.74	764.46
ADRS 113	526840	4068330	845.2	48.43	118.51	726.69
ADRS 113	526840	4068330	845.2	43.24	173.94	671.26
ADRS 113	526840	4068330	845.2	34.83	255.31	589.89
ADRS 113	526840	4068330	845.2	31.56	374.75	470.45
ADRS 113	526840	4068330	845.2	36.15	550.06	295.14
ADRS 113	526840	4068330	845.2	57.33	807.37	37.83
ADRS 114	527649	4069521	849.8	685.06	0.44	849.36
ADRS 114	527649	4069521	849.8	679.46	0.65	849.15
ADRS 114	527649	4069521	849.8	645.62	0.96	848.84
ADRS 114	527649	4069521	849.8	437.54	1.41	848.39
ADRS 114	527649	4069521	849.8	169.78	2.06	847.74
ADRS 114	527649	4069521	849.8	58.91	3.03	846.77
ADRS 114	527649	4069521	849.8	47.9	4.44	845.36
ADRS 114	527649	4069521	849.8	65.44	6.52	843.28
ADRS 114	527649	4069521	849.8	87.81	9.57	840.23
ADRS 114	527649	4069521	849.8	102.76	14.05	835.75
ADRS 114	527649	4069521	849.8	106.46	20.63	829.17
ADRS 114	527649	4069521	849.8	100.25	30.28	819.52
ADRS 114	527649	4069521	849.8	75.85	44.44	805.36
ADRS 114	527649	4069521	849.8	35	65.23	784.57
ADRS 114	527649	4069521	849.8	12.07	95.74	754.06
ADRS 114	527649	4069521	849.8	9.46	140.53	709.27
ADRS 114	527649	4069521	849.8	16.19	206.27	643.53
ADRS 114	527649	4069521	849.8	36.31	302.77	547.03
ADRS 115	528000	4069690	847.6	554.22	0.66	846.94
ADRS 115	528000	4069690	847.6	552.13	0.97	846.63
ADRS 115	528000	4069690	847.6	523.24	1.42	846.18
ADRS 115	528000	4069690	847.6	421.63	2.08	845.52
ADRS 115	528000	4069690	847.6	241.46	3.06	844.54
ADRS 115	528000	4069690	847.6	89.91	4.49	843.11
ADRS 115	528000	4069690	847.6	40.64	6.58	841.02
ADRS 115	528000	4069690	847.6	43.25	9.66	837.94
ADRS 115	528000	4069690	847.6	54.54	14.18	833.42
ADRS 115	528000	4069690	847.6	58.38	20.82	826.78

ADRS 115	528000	4069690	847.6	55.66	30.56	817.04
ADRS 115	528000	4069690	847.6	51.18	44.85	802.75
ADRS 115	528000	4069690	847.6	42.23	65.84	781.76
ADRS 115	528000	4069690	847.6	24.22	96.64	750.96
ADRS 115	528000	4069690	847.6	10.46	141.84	705.76
ADRS 115	528000	4069690	847.6	9.98	208.19	639.41
ADRS 115	528000	4069690	847.6	25.71	305.59	542.01
ADRS 115	528000	4069690	847.6	91.02	448.54	399.06
ADRS 116	529143	4069201	847.28	155.37	0.44	846.84
ADRS 116	529143	4069201	847.28	155.76	0.65	846.63
ADRS 116	529143	4069201	847.28	112.64	0.96	846.32
ADRS 116	529143	4069201	847.28	82.27	1.41	845.87
ADRS 116	529143	4069201	847.28	84.69	2.06	845.22
ADRS 116	529143	4069201	847.28	98.96	3.03	844.25
ADRS 116	529143	4069201	847.28	114.52	4.44	842.84
ADRS 116	529143	4069201	847.28	134.11	6.52	840.76
ADRS 116	529143	4069201	847.28	143.48	9.57	837.71
ADRS 116	529143	4069201	847.28	132.12	14.05	833.23
ADRS 116	529143	4069201	847.28	105.49	20.63	826.65
ADRS 116	529143	4069201	847.28	67.61	30.28	817
ADRS 116	529143	4069201	847.28	39.28	44.44	802.84
ADRS 116	529143	4069201	847.28	28.82	65.23	782.05
ADRS 116	529143	4069201	847.28	25.53	95.74	751.54
ADRS 116	529143	4069201	847.28	32.72	140.53	706.75
ADRS 116	529143	4069201	847.28	62.52	206.27	641.01
ADRS 116	529143	4069201	847.28	137.52	302.77	544.51

Appendix 4-B

Appendix 4-B. Available Monitoring Well Information

UTM X	UTM Y	Elev. (ft)	Elev. (m)	Screened Interval (Top BGS)	Screened Interval Bottom BGS)	Depth to Water BGS	Water Surface Altitude in Meters	Well Bottom Altitude in Meters	Water Surface Altitude in Meters (May '04)	Tritium in units	Tritium in pCi/L
527375	4068715	2776.892	846.5	111	123	112.2	734.3	723.4	734.3	3.8	12.16
527550	4069125	2782.141	848.1				759.9	744.3			
527425	4068780	2776.236	846.3				dry	737.9	736.9		
527875	4068790	2771.644	844.9				N/A	N/A			
528025	4068980	2775.908	846.2				N/A	N/A			
528030	4069050	2778.205	846.9				N/A	N/A			
527910	4068950	2775.908	846.2				N/A	N/A			
528070	4068950	2772.3	845.1				752.5	746.5			
528040	4068780	2769.347	844.2				751.5	745.4			
528075	4069080	2778.205	846.9				759.9	755			
527820	4068780	2771.972	845	91	98	93	752	745.9	751.6	0.05	0.16
527680	4068980	2776.564	846.4				760.2	755.3			
527610	4069300	2785.422	849.1	86	92	87.8	761.3	755.2		0.4	1.28
527695	4068880	2776.564	846.4	90	96	92.4	754	748.5		0.9	2.88
527750	4068725	2772.628	845.2	92	98	93.3	751.9	745.8		0.6	1.92
528040	4068870	2775.908	846.2	85	91	89	757.2	753.1		0.7	2.24
527925	4068780	2770.66	844.6				751.3	745.3	751		
527605	4068950	2774.596	845.8	91	173	85.3	N/A	N/A	760.5	0.4	1.28
527615	4069300	2785.422	849.1	141	144	93.3	N/A	N/A		0.05	0.16
527820	4068730	2774.924	845.9	126	130	99.4	N/A	N/A		0.05	0.16
527285	4068950	2781.485	847.9	104	112	105.2				0.2	0.64
527336	4068713	2776.892	846.5	N/A	N/A	109.7			736.8		

5 Rocky Flats Facility

5.1 Introduction

The Rocky Flats Facility was selected to test the applicability of the AES Advanced Environmental Solutions, LLC (AES) Strategy to a semi-arid environment in the Midwestern United States. This exercise is for demonstration only. This report is based on readily available information and does not constitute a comprehensive evaluation of all data for the site.

The Rocky Flats Facility, a former nuclear weapons facility, is located west of Denver, Colorado in an area of complex terrain (Figure 5-1) (DOE, 2005). A primary mission of the Rocky Flats facility was to machine plutonium "buttons" into weapons components. Figure 5-2 presents an aerial view of the Rocky Flats Facility looking east in 1983, prior to decommissioning.

In this exercise, the AES Strategy is applied in two separate case studies at Rocky Flats, both of which focus on ground water contaminated by chlorinated organic solvents. In each instance, application of the Strategy yields improved understanding about the natural system at the site.

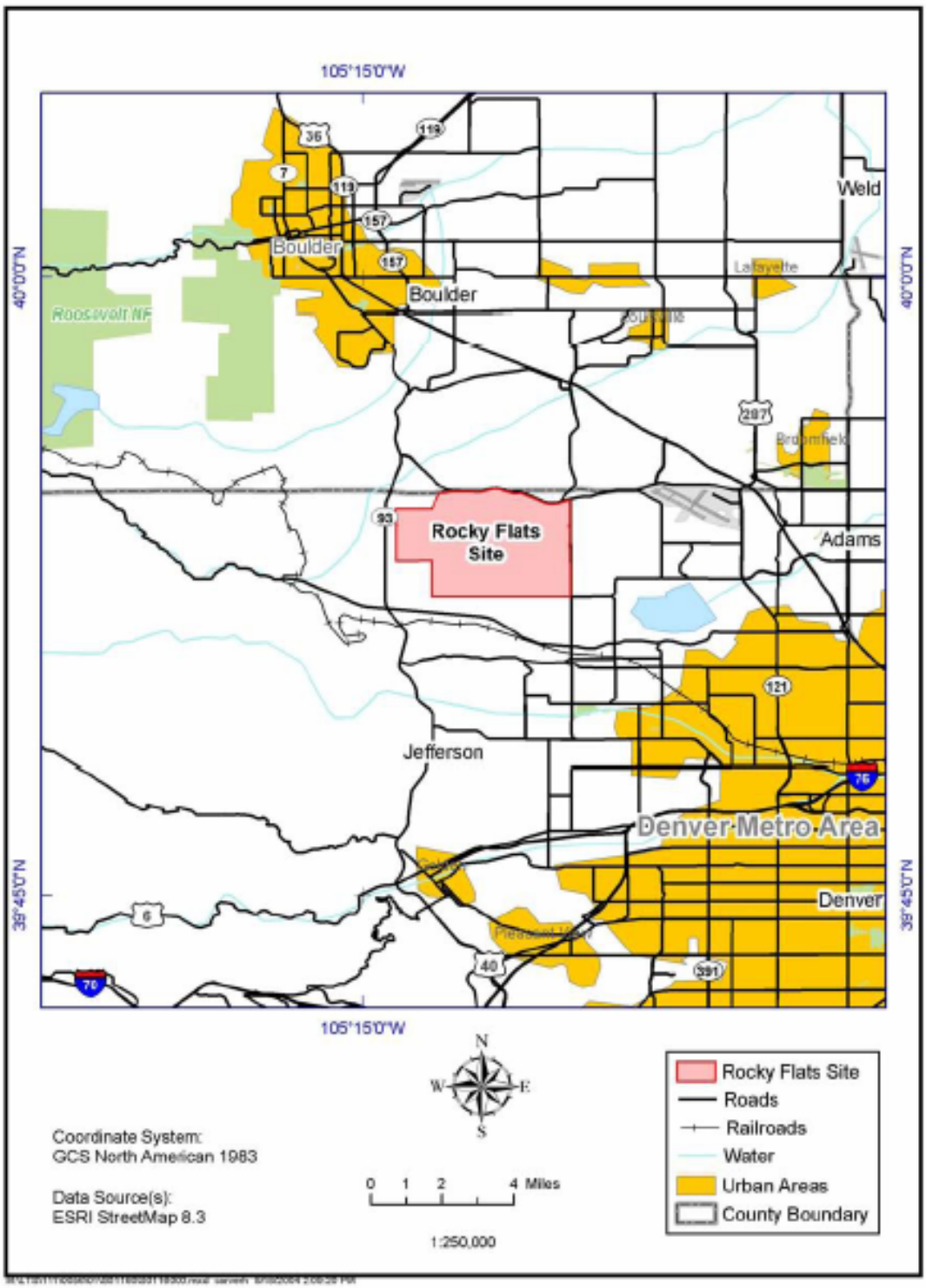

Figure 5-1. Location of the Rocky Flats Facility in Colorado (DOE, 2005)

Rocky Flats was established in 1951 to manufacture plutonium, enriched and depleted uranium, and steel nuclear weapons components. After a similar facility at Hanford shut down in 1965, Rocky Flats became the only source of plutonium "pits" for the U.S. nuclear weapons arsenal. *Rocky Flats Plant, Colorado. July 17, 1983.*

Figure 5-2. Photograph of the Rocky Flats Facility (looking east) Photo is in "Linking Legacies", DOE publication EM-0319 (DOE 1997) Appendix B, page 190.

5.2 Compilation of Available Data

This section provides a summary of the readily available data compiled for evaluation of both VOC case studies.

5.3 Geologic Setting

The Rocky Flats Facility sits approximately 6,000 feet above mean sea level on the western margin of the Colorado Piedmont section of the Great Plains Physiographic Province. The Colorado Piedmont is an old erosional surface along the eastern margin of the Rocky Mountains underlain by gently dipping sedimentary rocks (Paleozoic to Cenozoic in age) which are abruptly upturned at the Front Range (just west of the Rocky Flats Facility) to form hogback ridges parallel to the mountain front. The Piedmont surface is broadly rolling and slopes gently to the east with topographic relief of only several hundred feet. This relief is due both to resistant bedrock units that locally rise above the landscape and to the presence of incised stream valleys (DOE, 1990).

5.3.1 Hydrologic Data

Hydrogeology at the Rocky Flats Facility is characterized by three distinct units, the upper alluvial aquifer, lower aquitard, and the Laramie-Fox Hills aquifer.

The upper alluvial aquifer is largely unconsolidated materials that can be as much as 100 feet thick in the western portions of the site. The upper aquifer is generally recharged from precipitation or surface water bodies. Ground water in the unconsolidated alluvial aquifer is generally close to the land surface, with an average depth of 11 feet below ground surface. Several springs emerge in areas where the contact of the upper aquifer and the lower aquitard is exposed at the surface. While most of these springs occur within the Rock Creek drainage, Antelope Springs in the Woman Creek drainage has the largest discharge at Rocky Flats (Figure 5-3). Antelope Springs discharges continuously over several acres. The upper alluvial aquifer has a permeability of approximately 0.5 meters per day.

The lower aquitard comprises deeper claystone and siltstone of the Laramie and Arapahoe Formations. These formations combined are up to 800 feet thick below Rocky Flats. Recharge of the lower aquitard occurs from downward flow through the upper aquifer, or directly through precipitation in areas where the bedrock is exposed.

Beneath the aquitard lies the regional Laramie-Fox Hills aquifer. It is composed of the lower sandstone unit of the Laramie Formation and the Fox Hills Sandstone, and is confined by the overlying aquitard. Ground water levels in the bedrock aquifers are generally greater than 100 feet. Several portions of the upper alluvial aquifer east and northeast of the Industrial Area are known or suspected of being contaminated with radionuclides, volatile organic compounds, and metals. The aquitard is less contaminated than the upper alluvial aquifer. No contaminant plumes have been identified in the aquitard (ERO Resources, 2003).

Liquid contaminants spilled on the ground and certain substances that dissolve in water can easily move down through the soil and contaminate the shallow ground water. Data from on-site monitoring wells at Rocky Flats show areas of ground water contaminated with elevated radioactivity, nitrates, and volatile organic compounds at different locations (CDPHE, (No Date)). Figure 5-4 shows the location of monitoring wells and the extent of nitrate plumes and VOC plumes at or above maximum contaminant levels.

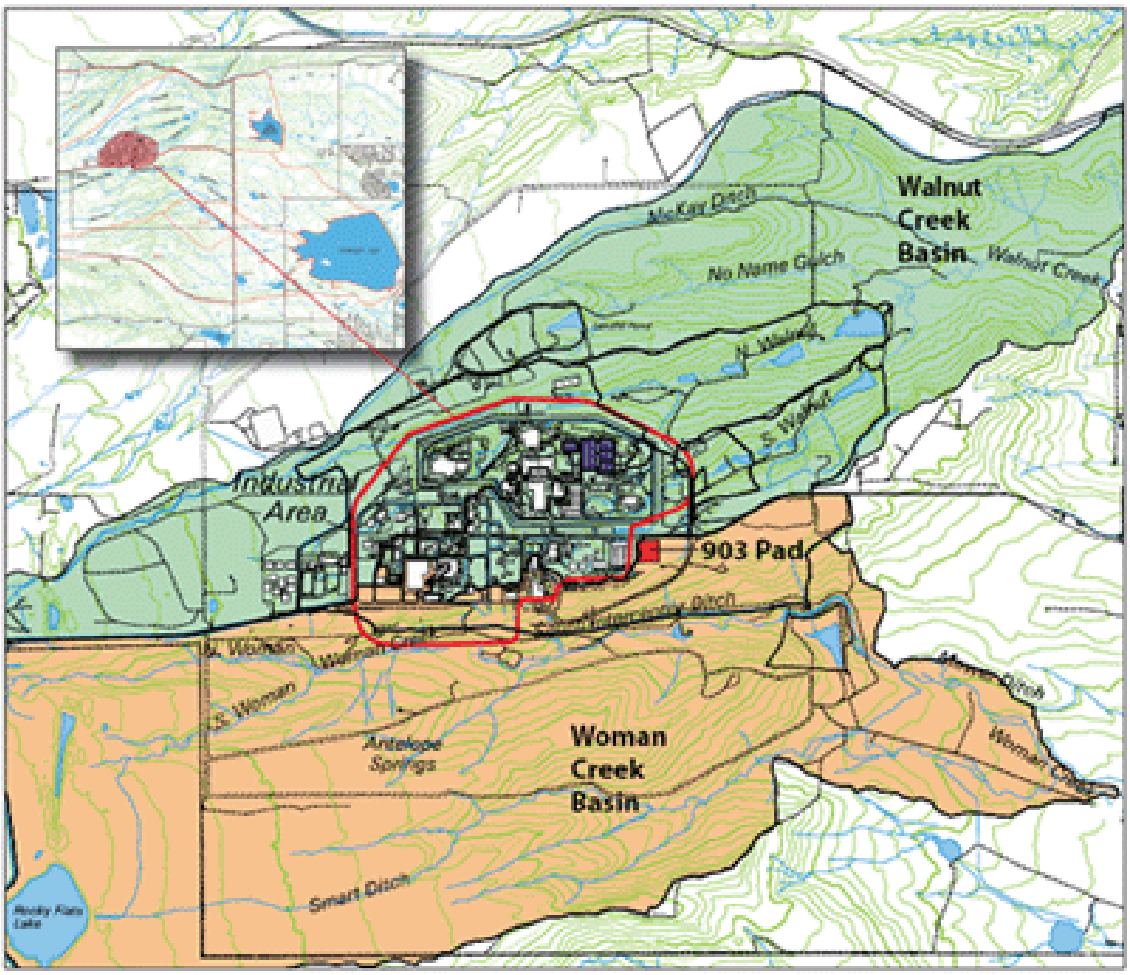

Figure 5-3. Map of Rocky Flats Facility drainage basins (from: http://lanl.gov/source/orgs/nmt/nmtdo/AQarchive/06springsummer/page5.shtml)

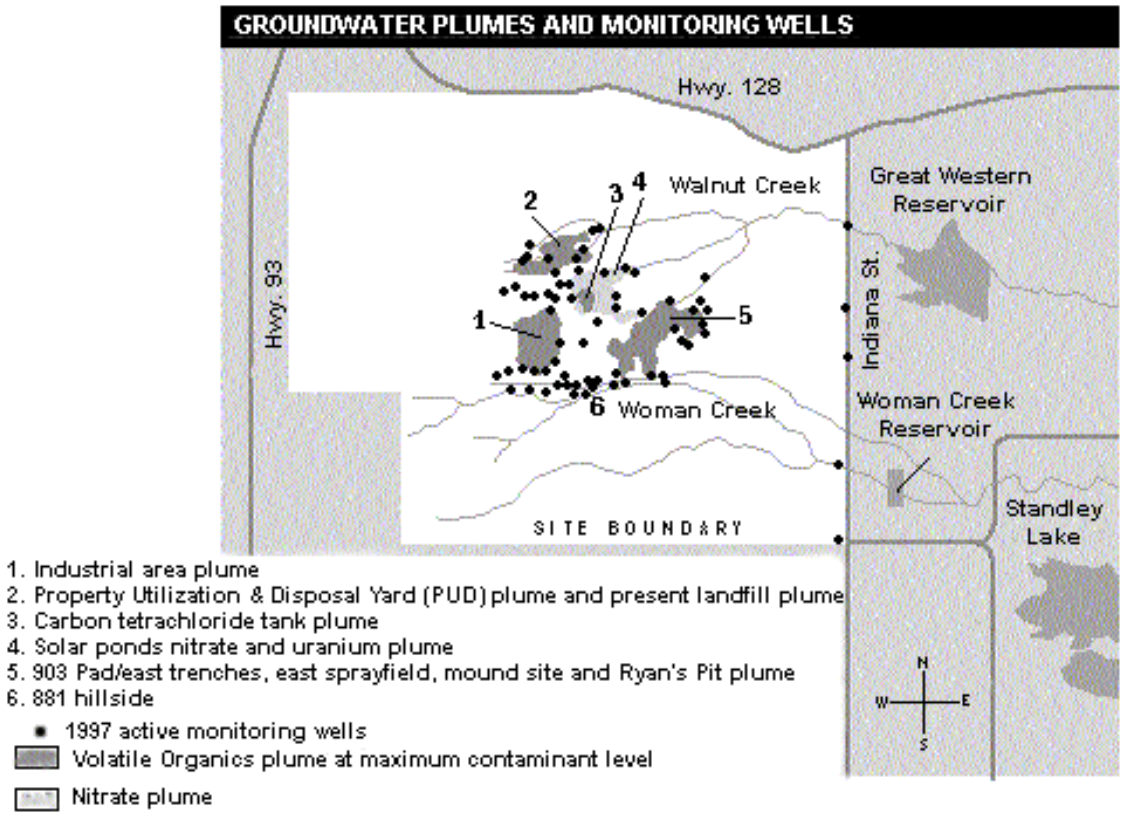

Figure 5-4. Ground-water monitoring well locations and depiction of VOC and nitrate plumes for the Rocky Flats Facility (CDPHE, (No Date))

5.4 Application of the Strategy

5.4.1 Case Study 1: Conceptual Site Model Assessment

Figure 5-5 presents a Transport Conceptual Model for the Rocky Flats Facility that was located during compilation of existing site data. This conceptual model illustrates a pathway from ground to surface water. Specifically, it shows the majority of contaminant movement within the upper alluvial aquifer. According to this model, surface water VOC concentrations are typically higher during the winter months when volatilization is reduced by low temperatures and ice covering the surface water. Risk to wildlife or wildlife workers through a surface water pathway has been a driving concern in Rocky Flats remediation efforts.

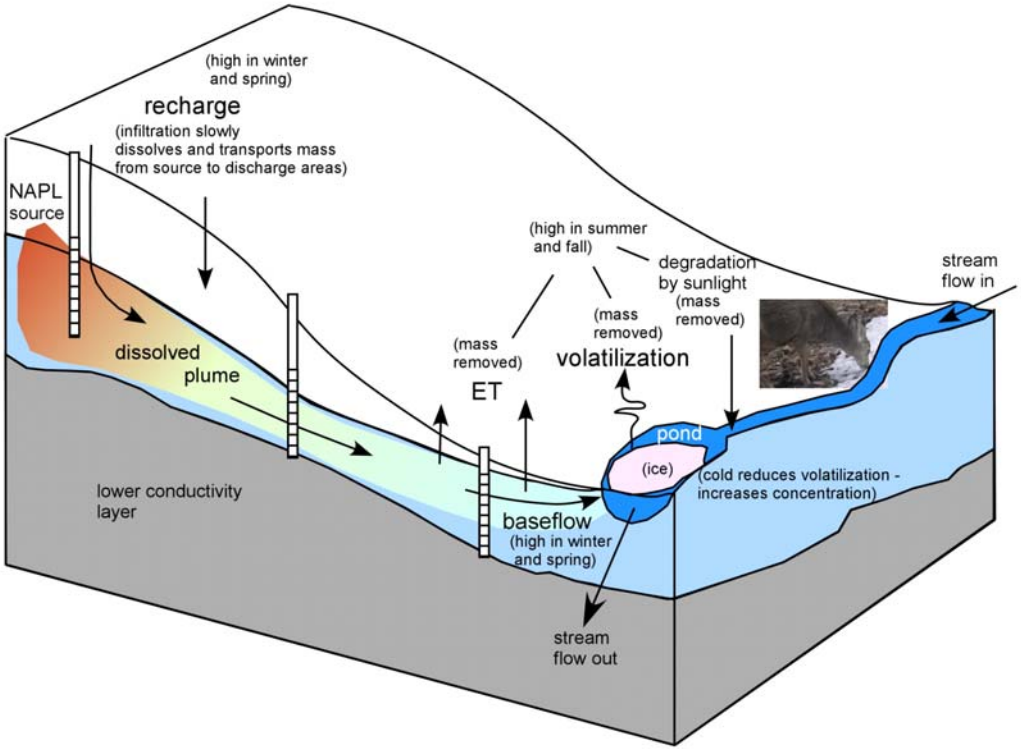

Figure 5-5. Conceptual cross-section for the Rocky Flats Facility (Modified from K-H, 2004)

5.4.2 Case 1: Existing Site Monitoring Data

Figure 5-6, below shows carbon tetrachloride concentrations in Well 3991 between 1992 and 2003. Water levels are shown as depth to ground water in feet. Between 1992 and 1995, carbon tetrachloride concentration declines in this well by a factor of 10, to below 0.005 mg/l (<5ppb). However, the fourth quarter 1995 sampling result indicates the concentration increases to over 50 ppb. Subsequently, concentrations decline, only to peak again in 1999, then steadily decline for 5 years to the end of our data set.

5.4.3 Case 1: Application of the Strategy

One possible hypothesis to explain the carbon tetrachloride concentration spikes observed in the existing monitoring data would include periodic releases or spills at the site; however, inclusion of Well 3991 water level data in a conceptual site model (Figure 5-6 and Figure 5-7) suggests that the concentration spikes are correlated to high water levels. Specifically, concentration spikes were seen immediately following well water levels between 6 to 10 feet above normal for the well.

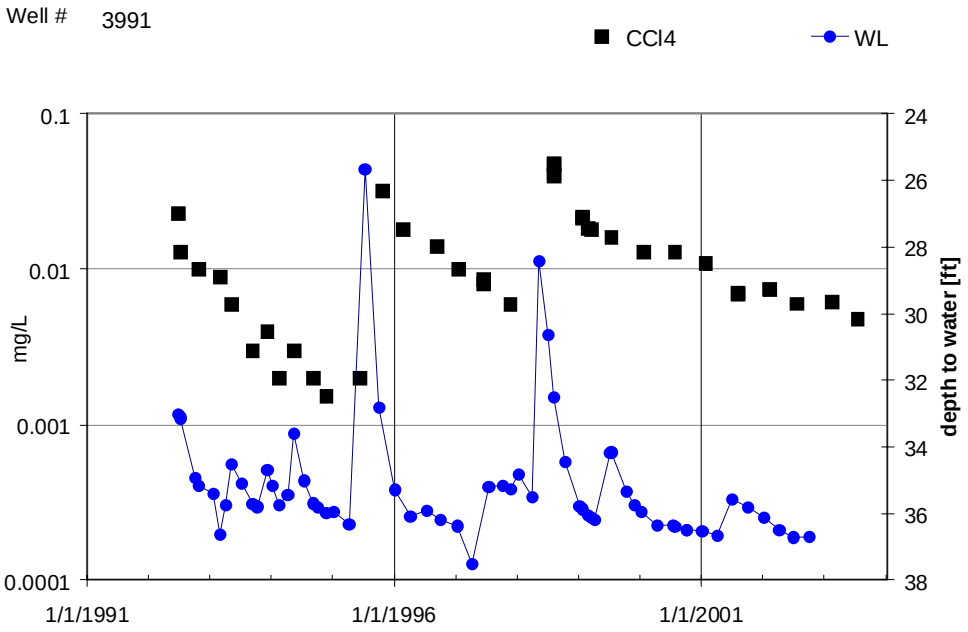

Figure 5-6. Diagram of multiyear variability in ground-water contaminant concentrations due to water table changes (K-H, 2004)

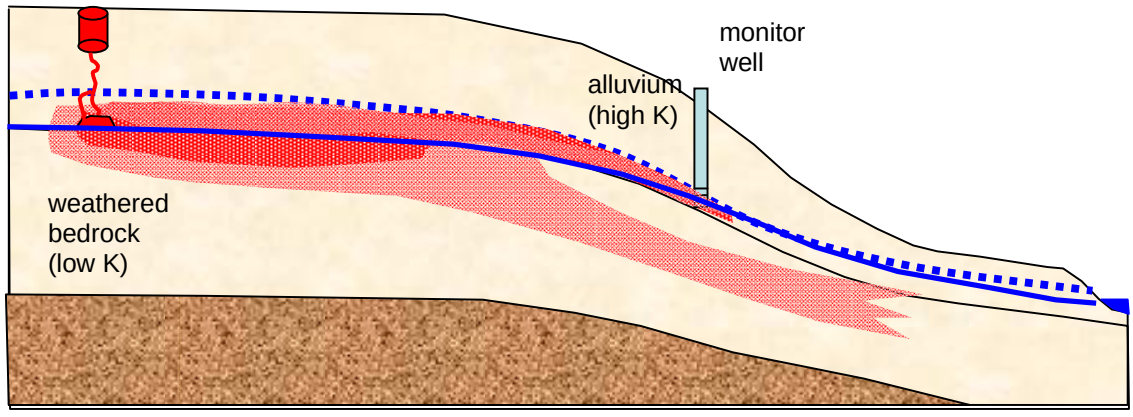

Figure 5-7. Conceptual cross section showing affects of water table changes on contaminant movement (modified from K-H, 2004)

Figure 5-7 shows the revised conceptual model which explains the observed spikes in carbon tetrachloride concentrations. This model illustrates how contamination from disposal trenches migrates through the vadose zone and collects at the interface between the higher permeability alluvium and the lower permeability weathered bedrock. The water table is typically in the weathered bedrock, but during periods of very high recharge it can rise into the high permeability alluvium and mobilize contamination

pooled at the bedrock interface, and subsequently mobilize into the weathered bedrock aquifer. The normal water table is indicated by a solid blue line. In a period of heavy rain fall or snow melt, water levels rise into the alluvium (dashed blue line) and mobilize vadose zone contamination. This results in a concentration spike followed by a slow decline as the displaced solvent dissipates.

It is most important to note that the declining concentrations at the monitoring well provide no information on the possible decline of the source pool. It is also important to note that a 3-year steep decline ending with four quarters of low concentrations might be used to argue that this well could be removed from a contaminant monitoring program. Look again at the first 12 concentrations in Figure 5-5 then look at the first 15 concentrations. Now look at the last several years - when can we stop sampling this well?

This well provides important information on the performance of the hydrologic system at this site: these spikes infer that a relatively higher concentration up gradient source is present and that water table information is a strong performance indicator.

It is important to recognize that this well is placed in a critical point to monitor system performance. We now have a model to relate observations at a well to the source and an indication that the system performance suggests that a high-concentration zone exists in the ground – but this model is not sufficient to model the extent of the plume. Management (DOE, state agencies, EPA, and other stakeholders) can decide whether long-term risk justifies an attempt to characterize and remove most of the source.

In addition to the natural variations in the water table, long term recharge changes due to facility closure need to be considered. Elimination of features such as drains, leaking water lines, and covered areas such as asphalt parking lots can affect the water table recharge (Figure 5-8). By eliminating these features the shape of the water table surface may be altered dramatically. In a 40-plus-year old facility of this size water system leaks on the order of tens of gallons per minute could be expected. This would be a major fraction of the local infiltration.

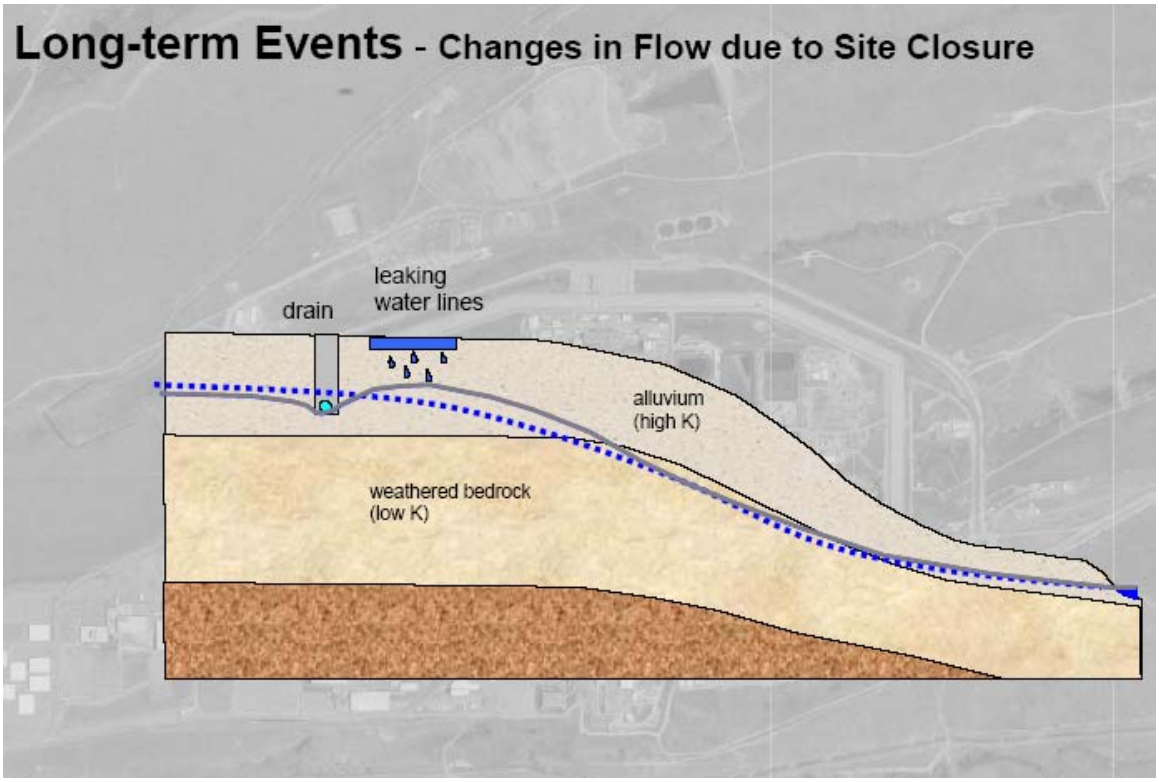

Figure 5-8. Potential changes in ground-water movement due to closure

Figure 5-9 shows predicted water level changes after site closure. Comparison of this Figure with VOC plume and source maps presented below shows the possibility of gradient changes in the vicinity of the VOC sources. This prediction was made with MIKE SHE, a modeling code that can incorporate both subsurface and subsurface flow (K-H, 2004).

Infiltration changes upon site closure require that any flow and transport models that are relied upon to justify environmental management decisions should be re-evaluated. Once again, it is a management decision to do this re-evaluation, but very simple models can be constructed to enlighten discussions surrounding the decision. These models would also include changes in surface water runoff.

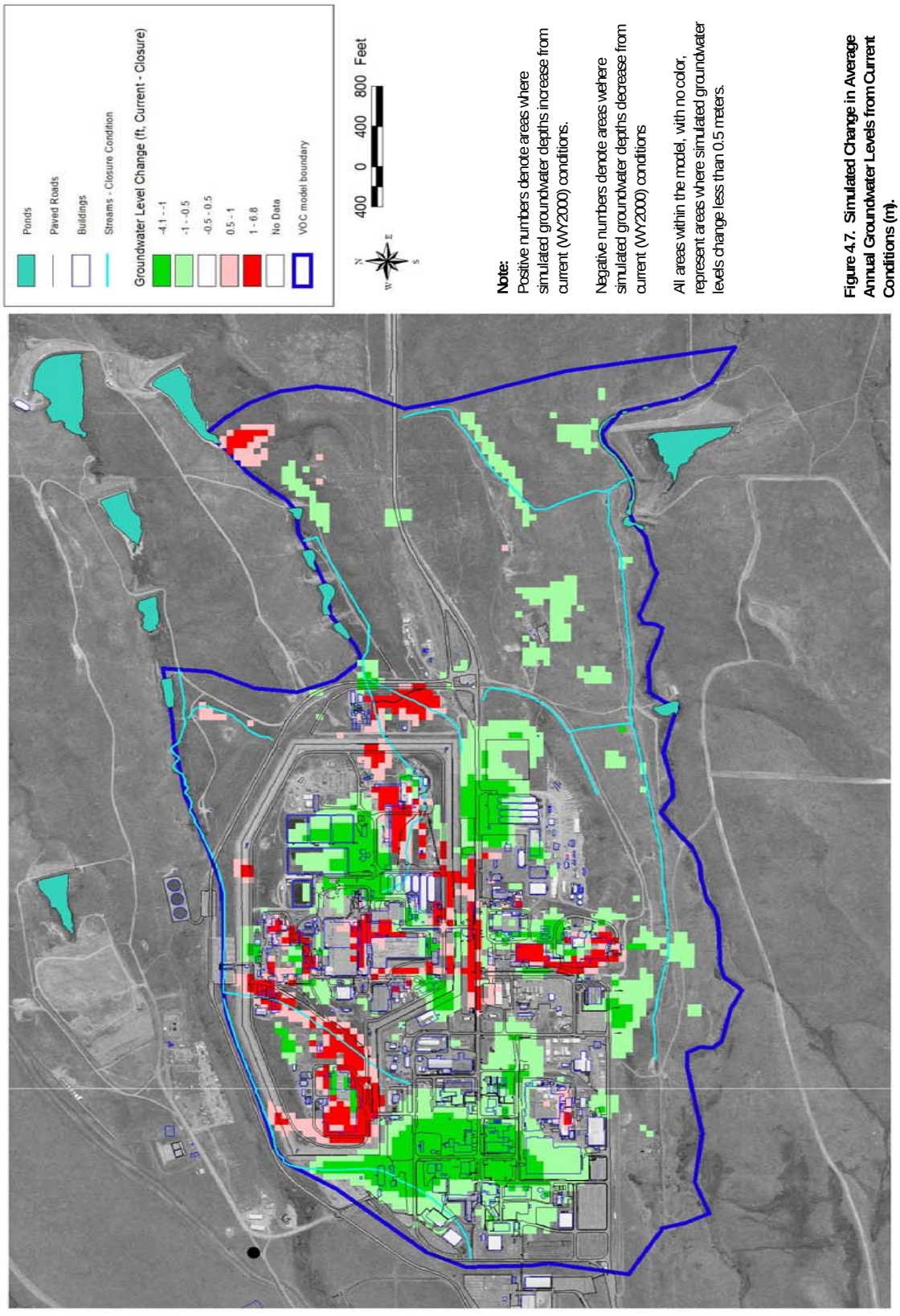

Figure 5-9. Predicted water level changes after closure (K-H, 2004)

5.4.4 Case 2: VOC Plume Analysis

The majority of VOC ground-water contamination at the Rock Flats Facility consists of chlorinated solvents including tetrachloroethylene (PCE) and trichloroethylene (TCE), with minor amounts of dichloroethylene (DCE). Identification of the original contamination can often be difficult as the chlorinated solvents break down readily to a less chlorinated state (e.g., PCE to TCE to DCE to Vinyl Chloride).

Results of ground-water monitoring at the Rocky Flats Facility show a significant TCE plume emanating from the eastern portion of the site. The initial conceptual model has historically been interpreted to be one plume with complex movement of ground water creating a radial dispersion pattern. Figure 5-10 shows the general extent of the TCE plume assuming a single plume. This figure is taken directly from a talk and not edited.

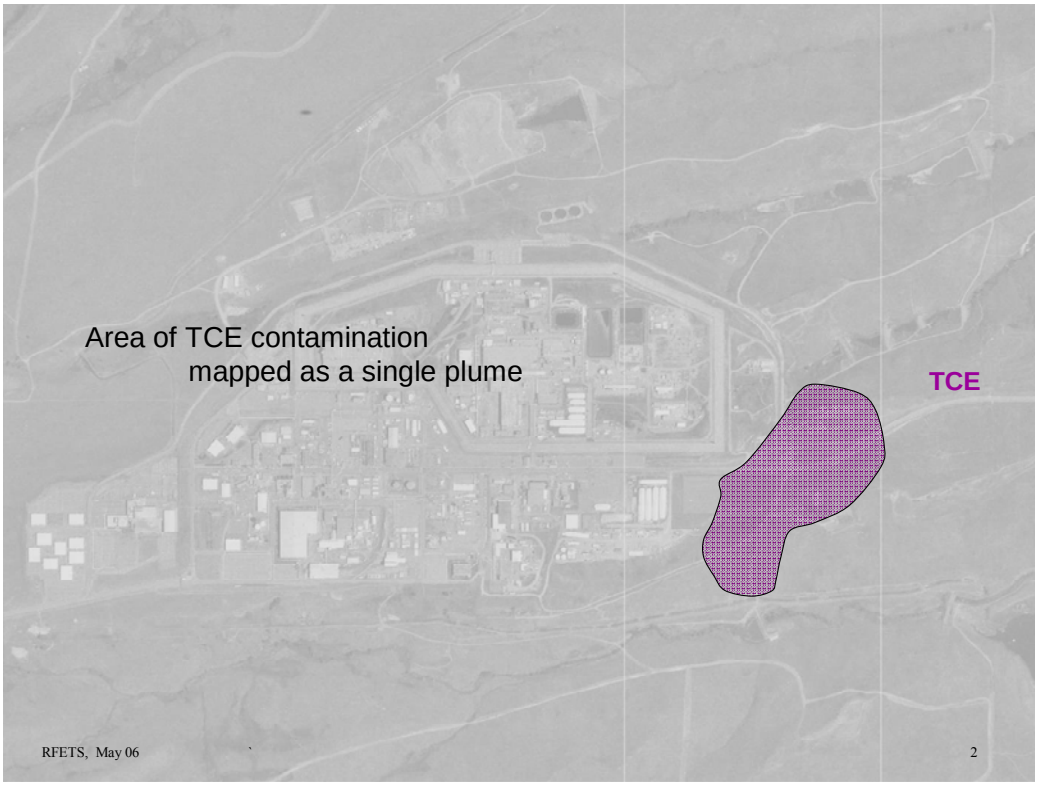

Figure 5-10. Generalized depiction of the Rocky Flats Facility TCE plume

5.4.5 Case 2: Application of the Strategy

By understanding the nature of the original spills and by evaluating the presence of daughter products from the degradation of chlorinated solvents, a revised conceptual model can be prepared.

Also, by associating sources and plumes with ground-water flow fields, it may be possible to differentiate multiple overlapping plumes. Discriminators such as probable source locations, variable ground-water flow paths, and potential daughter product

distributions can be used to prepare a refined conceptual model for contaminant movement.

Multiple sources will likely result in multiple plumes with unique fingerprints. Figure 5-11 presents an alternative conceptual model of contaminant plume source and migration based on additional information provide below. Further evaluation of ground-water monitoring data indicates that an east-west ground-water divide is present, effectively splitting the southern one-third of the plume from the northern two-thirds of the plume. By dividing the plumes based on the ground-water flow information above, it appears two plumes may be present, straddling the ground-water divide. In addition, an evaluation of the concentrations of all chlorinated solvents is undertaken as part of this Strategy application. Near the source the two plumes commingle, making differentiation difficult. Under reducing conditions, aquifer microorganisms can reductively dechlorinate PCE into less chlorinated daughter products such as TCE, DCE and vinyl chloride. By evaluating the relative concentrations of these contaminants, the separate plumes may be identified.

In Figure 5-11, the northern plume contains higher concentrations of PCE than TCE, suggesting that the TCE is derived from PCE degradation. In the southern plume TCE is present in much higher concentrations than PCE, suggesting that the original spill consisted mostly of TCE with minor amounts of PCE, or as an alternative conceptual model, that a much higher degree of anaerobic degradation is occurring in the southern plume, effectively eliminating the presence of the original PCE spill. However, in Figure 5-10, the southern plume moves down the hill side towards Woman Creek and likely represents more of an aerobic environment, thus minimizing the potential for degradation of chlorinated solvents. Based on the information provided in Figure 5-10, TCE is pervasive in both overlapping plumes; however, the use of PCE as a discriminator or performance indicator has resulted in a refined conceptual model of contaminant movement showing two separate plumes with two separate sources (Figure 5-11). If two sources were not originally identified in this area, this conceptual model would prompt the need to evaluate the potential presence of a previously unidentified spill.

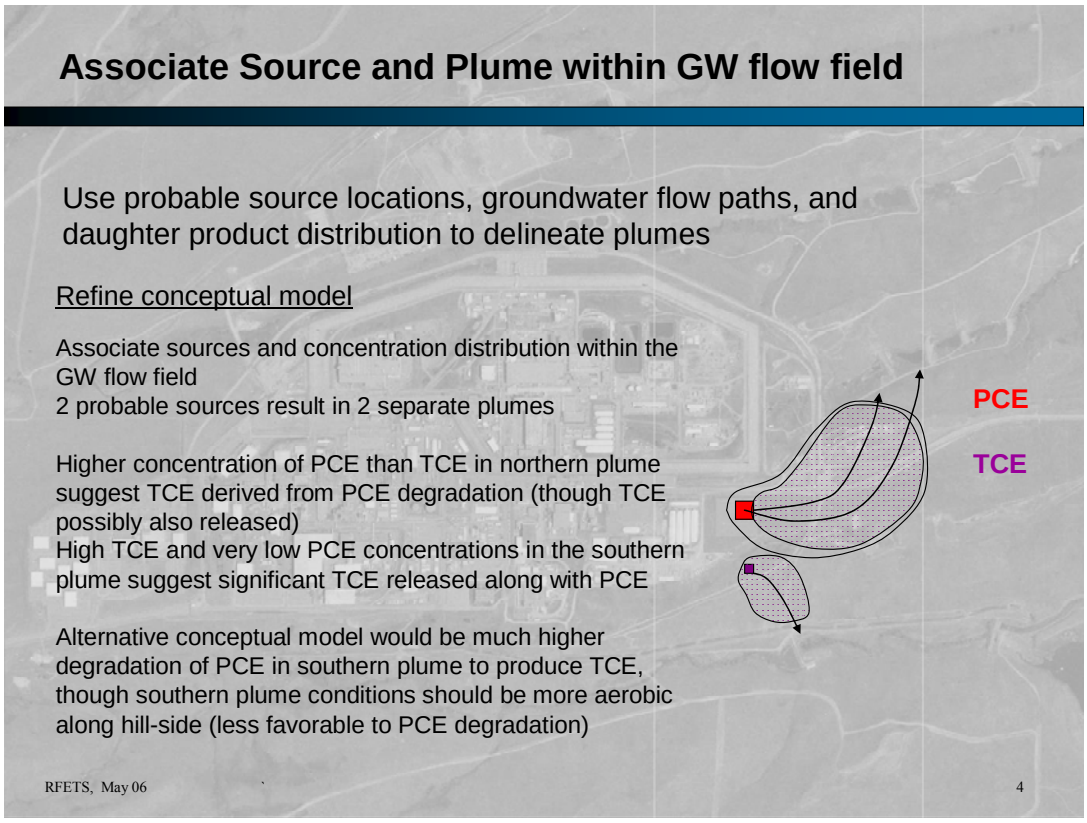

Figure 5-11. Conceptual model of complex flow of contaminants

5.4.6 Performance Indicators and FEPs

Performance indicators and features, events, or processes (FEPs) for the Rocky Flats Facility include, but are not limited to:

1) **monitor water levels**- changes in the water table surface or orientation will affect the direction of ground-water flow and the potential for remobilization of contaminants from the vadose Zone into the aquifer.

2) **time trends for ground-water contamination** – by looking at the relative concentration of contaminants over time, especially in comparison to water level readings, informed decisions can be made on when monitoring efforts can be terminated.

3) **monitor all VOC daughter products for the VOC plumes**- because the fingerprints of various VOC plumes may define multiple sources, determining the relative proportions of VOCs that make up a given plume is critical

5.5 Monitoring Strategy Application Conclusions

Based on the results of the application of the Strategy, the following conclusions can be drawn:

Case 1: Episodic changes in the water table result in the periodic remobilization of contaminants from the vadose zone, most likely at the alluvium/bedrock interface, into the ground water. By evaluating all of the available ground-water monitoring data through time trend analysis, it becomes apparent that the duration of Post-Closure ground-water monitoring may need to be extended or further characterization of the contamination within the vadose zone may need to be undertaken due to the cyclic recontamination of the water table.

Case 2: A VOC plume is emanating from the southeast corner of the Rocky Flats Facility. By evaluating the analytical results for chlorinated solvent daughter products together with likely flow directions, it becomes apparent that a revised Conceptual Site Model can be proposed with multiple sources contributing to the ground-water contamination. By examining the relative concentrations of all of the chlorinated solvents, individual plume fingerprints can be identified for the differentiating multiple sources.

Based on the results of the application of the Strategy, the following recommendations to management can be made:

1. Perform detailed time trend analysis for monitoring wells in relation to changes in the water table. In addition to the natural variations in the water table, long term recharge changes due to facility closure need to be considered due to the potential for remobilization of contaminants and changes in the water table surface. In addition, changes in the water table may result in the remobilization of contaminants from the vadose zone.
2. Evaluate the relative concentrations of contaminants to daughter products for revising plume delineation and sources.

5.6 Rocky Flats References

Colorado Department of Public Health and Environment (CDPHE). *Rocky Flats Public Exposure Studies, Movement of Contaminated Groundwater at the Rocky Flats Environmental Technology Site.* (Available online at www.cdphe.state.co.us/rf/movement.htm)

Department of Energy (DOE). Interim Measures/Interim Remedial Action and Decision Document, 881 Hillside Area Operable Unit No. 1, Rocky Flats Plant. January 1990.

DOE/EM-0319. *Linking Legacies, Connecting the Cold War Nuclear Weapons Production Processes to Their Environmental Consequences*. 1997.

ERO Resources Corporation. *Rocky Flats National Wildlife Refuge Resource Inventory*. April 2003.

K-H. *Fate and Transport Modeling of Volatile Organic Compounds*. Kaiser-Hill Company L.L.C., Rocky Flats Environmental Technology Site: Golden, Colorado. April 2004.

6 Savannah River Site, C Area

6.1 Introduction

The Savannah River Site (SRS) has a fifty-plus year history of defense nuclear research, fuel fabrication, chemical separations and waste disposal. The site covers about 300 square miles in South Carolina, along the Savannah River, about 100 miles upstream of the Atlantic Ocean (Figure 6-1). SRS includes 5 production reactors (Reactors C, K, L, P, R), a research lab, fuel fabrication, two chemical separation plants, and supporting and waste management facilities. Further description of this site and its history of operation are available in Linking Legacies, DOE publication EM-0319 (DOE 1997).

DOE has been generous in allowing access to documents and data from the Site's extensive environmental characterization and monitoring work.

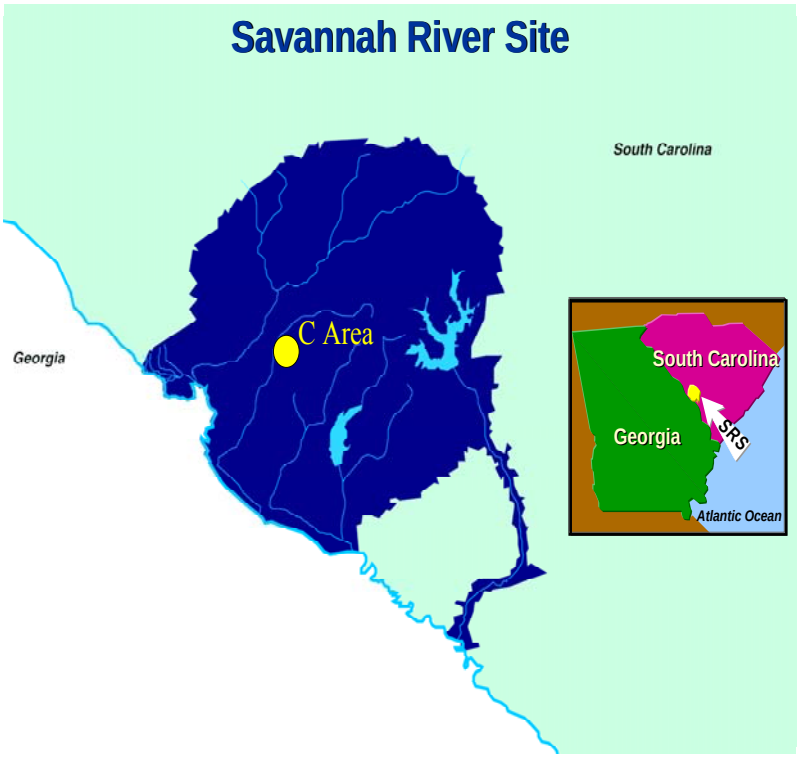

Figure 6-1. Savannah River Site location map. Courtesy of Bill Jones, SRNL.

This Chapter will use the C-Area of SRS to illustrate some results of contaminant plume characterization and monitoring. C-Reactor operated from 1955 through 1986, with construction beginning in about 1951. Within the reactor building is the disassembly basin, similar to a spent fuel pool in a power reactor. External to the reactor building are several waste facilities including reactor seepage basins (CRSB) to receive acids and caustics, low level radioactive solutions resulting primarily from maintenance, and a pit (CBRP) for burning waste and disposing of rubble that could include scrap wood, pasteboard, paint, and solvents. A photograph of the A-Area burning and rubble pit (ABRP) is shown in Figure 6-2 as an example.

Figure 6-2. Photograph of the A Area Burning/Rubble Pit during operation

In this Chapter we will look at a TCE plume from the CBRP and, to a lesser extent, a tritium plume from the CRSB. Even though the site is intensely characterized and monitored, we will show the value of computer simulation and 3-D visualization to evaluate the existing site data and present support for management decisions concerning the value of further monitoring or characterization. Further, we will show the importance of considering all sources of characterization data before using a computer simulation to support conclusions about the long-term disposition of a site.

Figure 6-3 is a map of C-Area. The reactor building (105-C), including the disassembly basin, CBRP, and three small seepage basins are shown. Wells from which monitoring data are obtained are also shown (e.g., P-18, CCB-1, and CSB-3A). This figure is from WSRC, 1998, an inventory of SRS environmental protection wells; similar documents are available online at www.osti.gov with authors Janssen or Rogers.

The wells LWR-1 through -9 were installed in 1992 as part of site characterization for a planned landfill (WSRC, 1992). They are not part of the Environmental Protection Department's waste site monitoring program, and we have found no monitoring data for them.

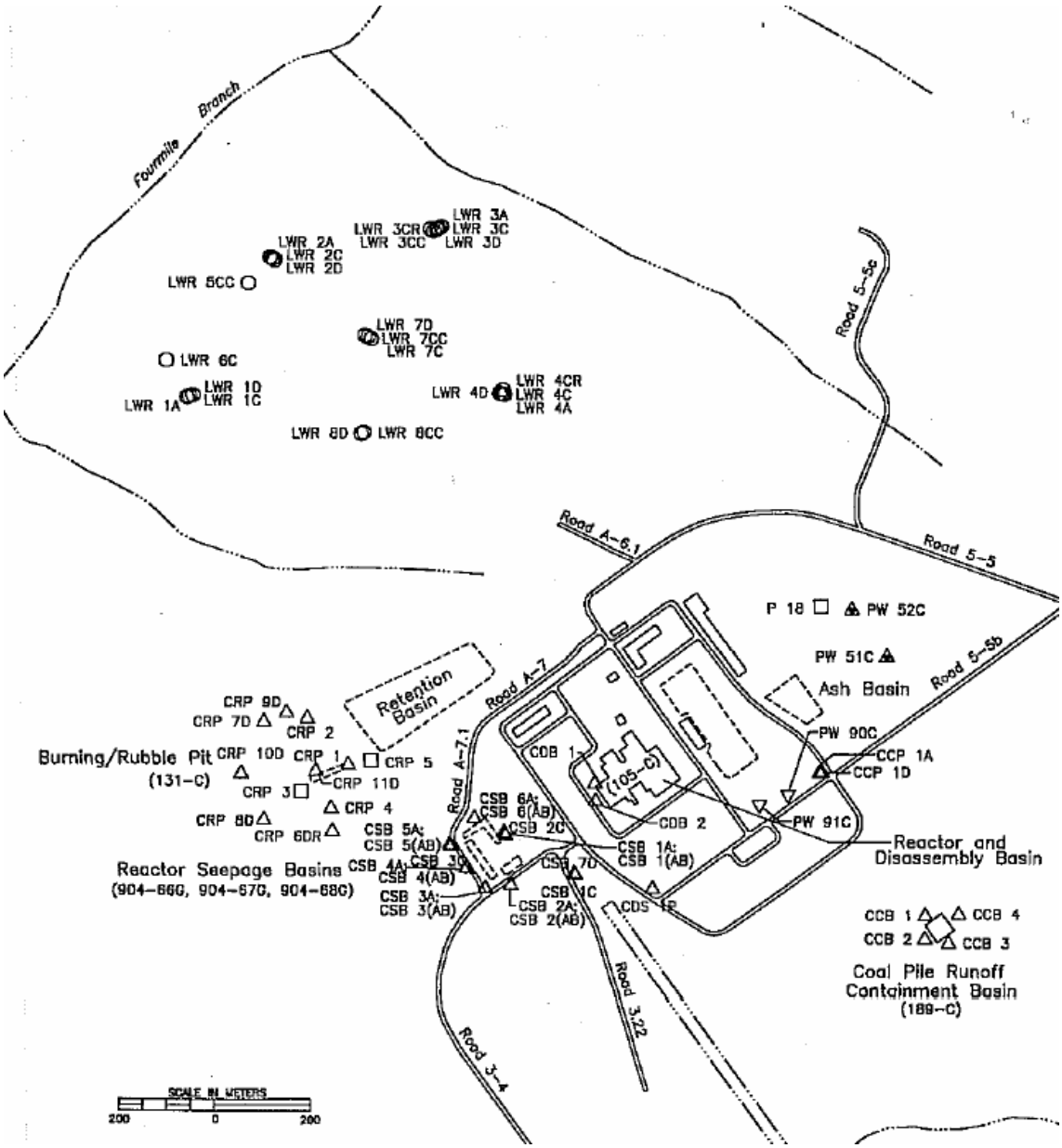

Figure 6-3. Map of C Area with facilities and wells (WSRC, 1998)

6.2 Compilation of Available Data

6.3 C-Area Background

DOE/EM-0319 (DOE, 1997), traces the history of the U.S. nuclear program from the early 1940s through 1997. Many details of reactor operations are provided in this document. While the discussions are not specific to C-reactor, the background provides information on chemicals used, processes, accidents, and environmental restoration activities. It is available at www.em.doe.gov/publications. At this time it is not available through OSTI.

WSRC-TR-99-00310 (Flach et al., 1999), published in 1999, is a modeling report covering the C-Area. Overall this is an excellent report that details data gathering, data visualization, and flow and transport modeling. It is available in pdf format online at www.osti.gov and contains more detailed information on C-Area and C-reactor history and operations than are included here. We have relied on it for data and figures in this chapter. We do, however, point to some opportunities for alternative conceptual models that might change some the model results.

6.3.1 Geology and Hydrogeology

The Savannah River Site is situated on multi-layer, interbedded, discontinuous Coastal Plain sediments that regionally dip to the SSE at about 20 ft/mile. The sediments are predominantly sands and clays deposited in fluvial to near-shore marine environments. The hydrology at C-Area is a classic unconfined, semi-confined, and confined aquifer sequence with the semi-confined aquifer becoming unconfined as it nears Four Mile Creek. High permeability pathways that affect transport can be present due to channels, gravel layers, and fractures.

Figure 6-4 shows a cross-section developed near C-Area at the MWD well field, an extensively characterized area. This area served as a field hydrogeology teaching and research site. Results of a number of aquifer performance tests, and other measurements of hydrologic properties are available from this site (e.g., Kegley et al., 1994). Site stratigraphy has been described by Fallaw et al., 1993.

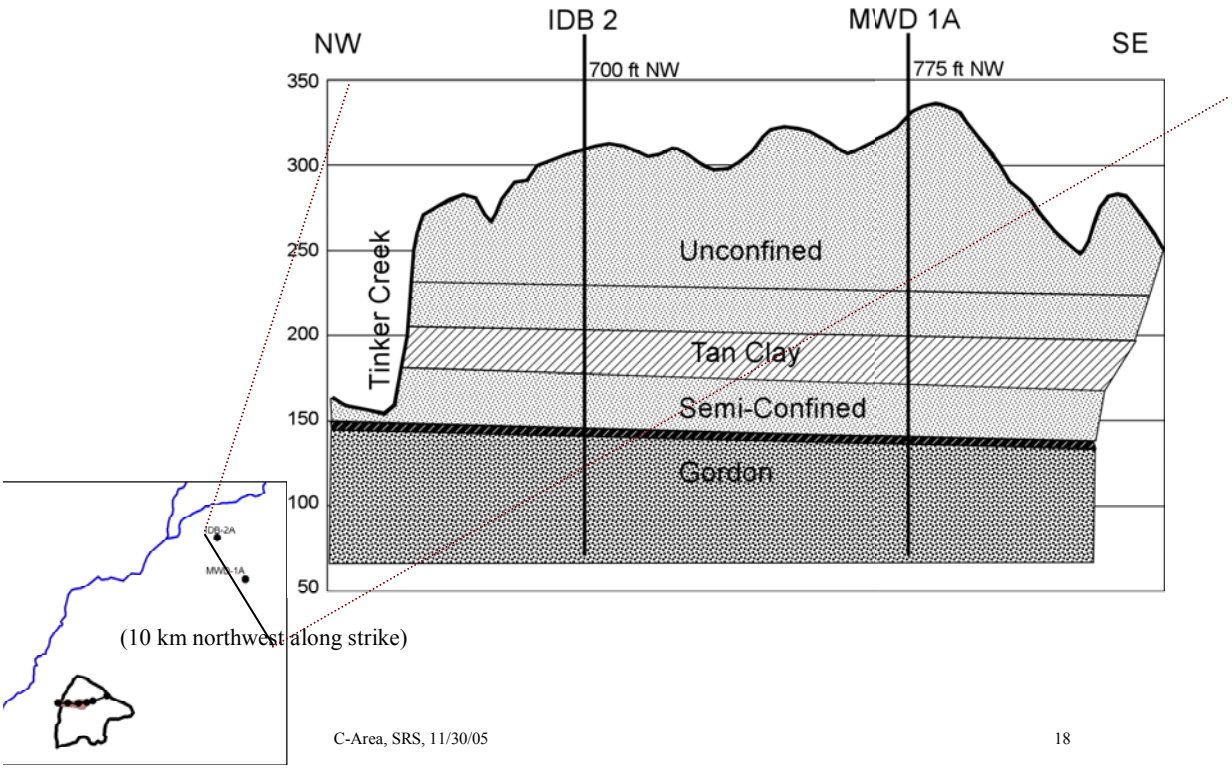

Figure 6-4. Simplified hydrogeologic cross section near C Area (Kegley et al., 1994). Courtesy of W.P. Kegley.

6.3.2 Site Characterization and Monitoring

In the late 1960s through about 1985, SRS planned and installed a site-wide network of hydrologic characterization wells, called the P-wells. The deepest well in each cluster was cored and logged, and piezometer wells were screened in permeable zones. Water level measurements, cores, and logs were produced in various programs dating back to pre-construction characterization in the late 1940s and 1950s (Siple, 1967).

Beginning in about 1981, extensive characterization was done in response to new environmental regulations. In about 1983 a core logging program was set up, and policies were instituted to core and log wells at most waste disposal sites. Data from the coring and logging programs were captured digitally. There were several plume characterization and mitigation programs, resulting in a wealth of subsurface data for the SRS.

C-Area in this report includes about 200 wells and is outlined on the map present in Figure 6-5. The left (western) boundary of this map is Four Mile Creek. A number of wells northwest of the reactor area were installed to characterize a proposed landfill site. The landfill would have been in the area north of the TCE plume. (WSRC, 1992)

More recently, a large number of direct push or cone penetrometer samples were taken to characterize both the TCE and tritium plumes.

6.3.3 Contaminant Distribution

As noted, two contaminant plumes have been described at C Area. A trichloroethene (TCE) plume migrates to the west from the C-Area burning rubble pit to Four Mile Creek. The plume is delineated by an extensive monitor network of over 150 wells or CPT samples, though no wells reach the confined aquifer beneath the plume extent (to avoid downward transport during and after well installation).

A tritium plume migrates southwest from the C-Area seepage basin to Four Mile Creek and Caster Creek. The tritium distribution (originally identified in the monitor wells) was delineated by over 200 cone penetrometer (CPT) pushes (1998-2001). Transport modeling by DOE's operating contractor, WSRC, (Flach, et al., 1999) was used to predict future plume migration and to suggest additional CPT locations. We have chosen not to discuss the tritium plume further for this report draft. Our initial reaction to the published modeling is that more characterization is needed to understand why the tritium enters two surface streams.

Modeling was also done to evaluate remediation options for the TCE plume (Geotrans, 2001). This modeling was very limited in scope.

The CBRP sits at the head of the TCE plume as shown in Figure 6-5. The tritium plume has some associated TCE, and emanates from the cluster of TCE "hits" just SW of the reactor building (105-C), which is the irregular shaped dark spot on this Figure.

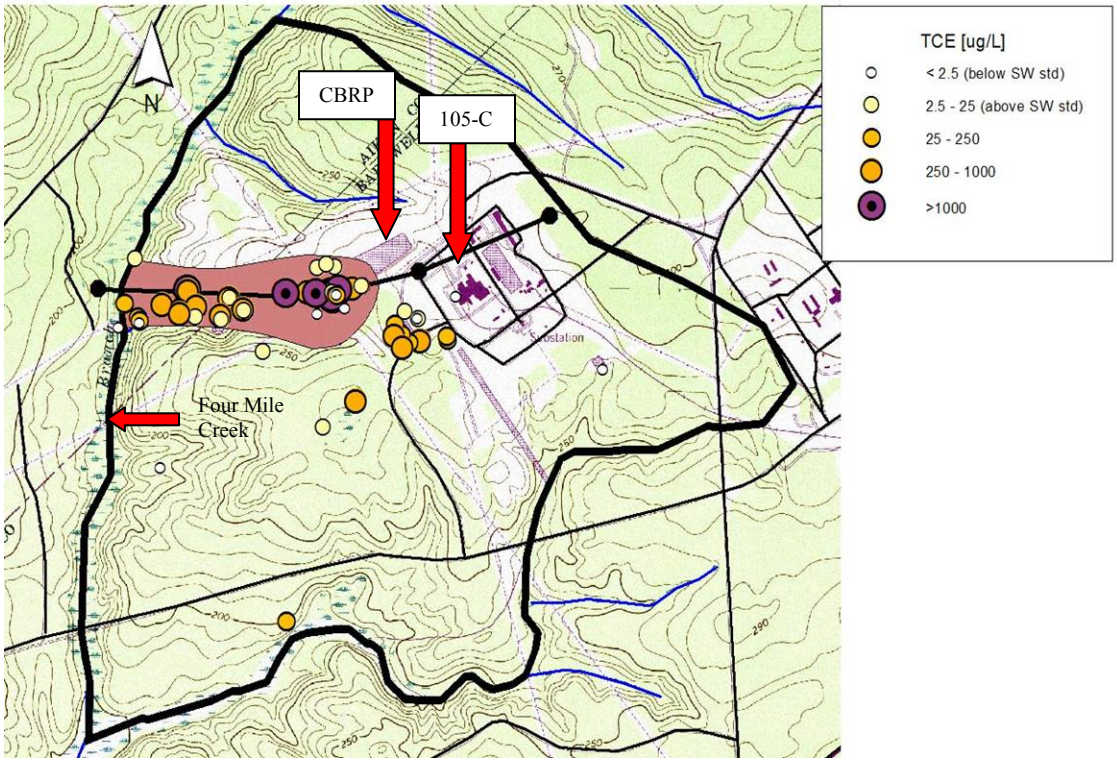

Figure 6-5. Topographic map of C-Area facility boundary with TCE plume and detected TCE concentrations

Figure 6-6 shows locations of wells sampled for tritium and Figure 6-7 shows locations of wells and CPTs sampled for TCE. CPT locations and analytical data are from Flach et al., 1999. Note that there are a very few sampling locations outside the model boundaries. These are single-event sampling sites, and not monitoring wells. At the time of sampling, no TCE was detected west of Four Mile Creek.

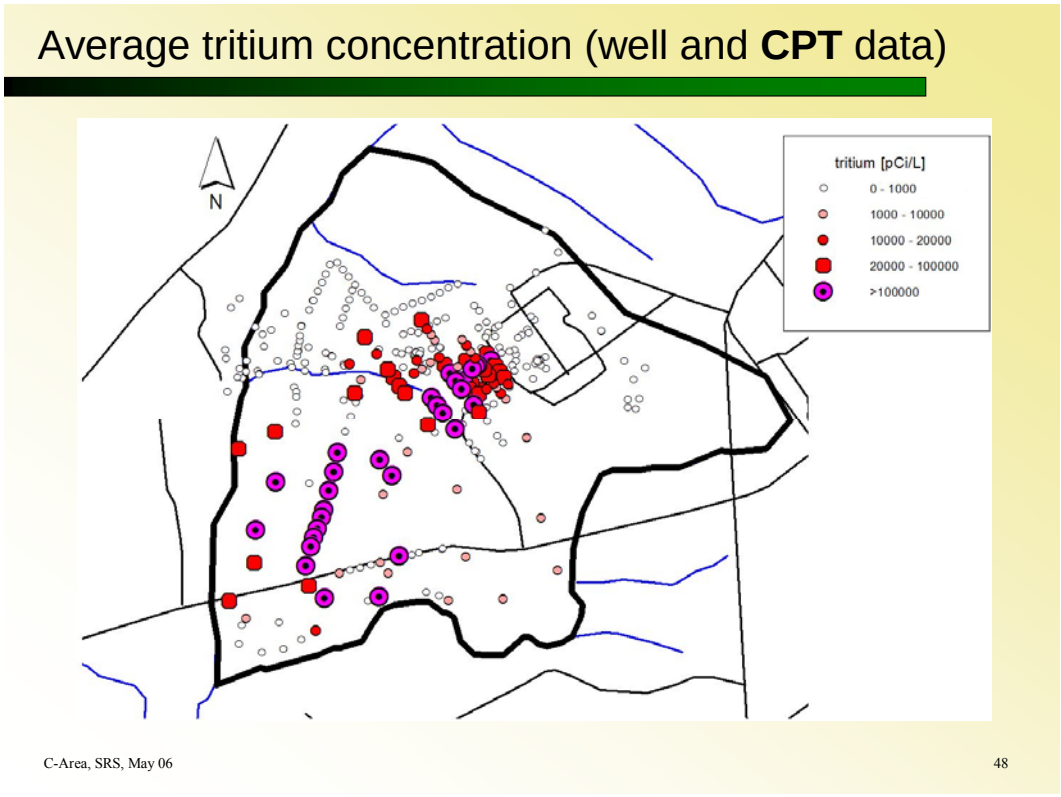

Figure 6-6. C Area tritium CPT data

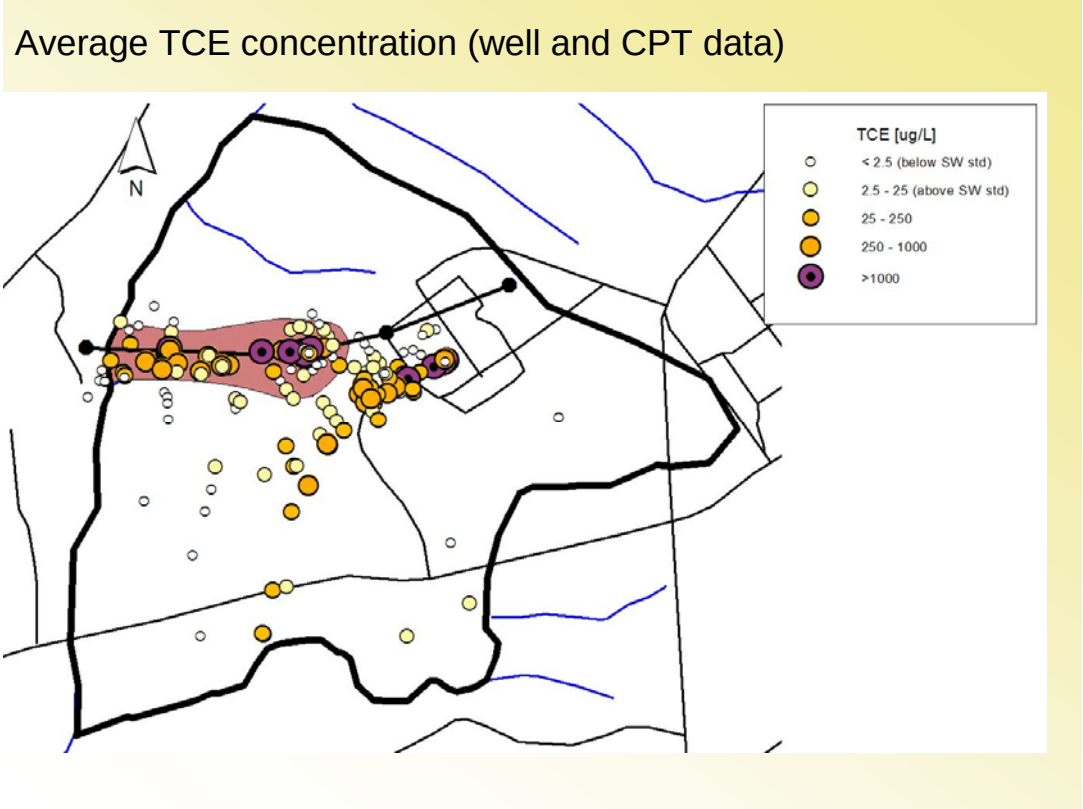

Figure 6-7. C Area TCE CPT data

6.4 Synthesis of a Conceptual Site Model and Flow and Transport Simulations

By combining the geologic cross-section in Figure 6-4 with log and core data gathered through past characterization efforts in the C-Area wells, we developed a 7-layer site hydrologic conceptual model for flow and transport simulation. This conceptualization is shown in Figure 6-8. In the paragraphs below, we present simulations performed using the conceptual model in Figure 6-8 and discuss potential Performance Indicators and monitoring strategies which were identified through analysis of this modeling exercise.

Simulation layer parameters were adapted from Flach et al. (1999) and Geotrans (2001) and are shown in Table 6-1 below.

C Area Model Mesh

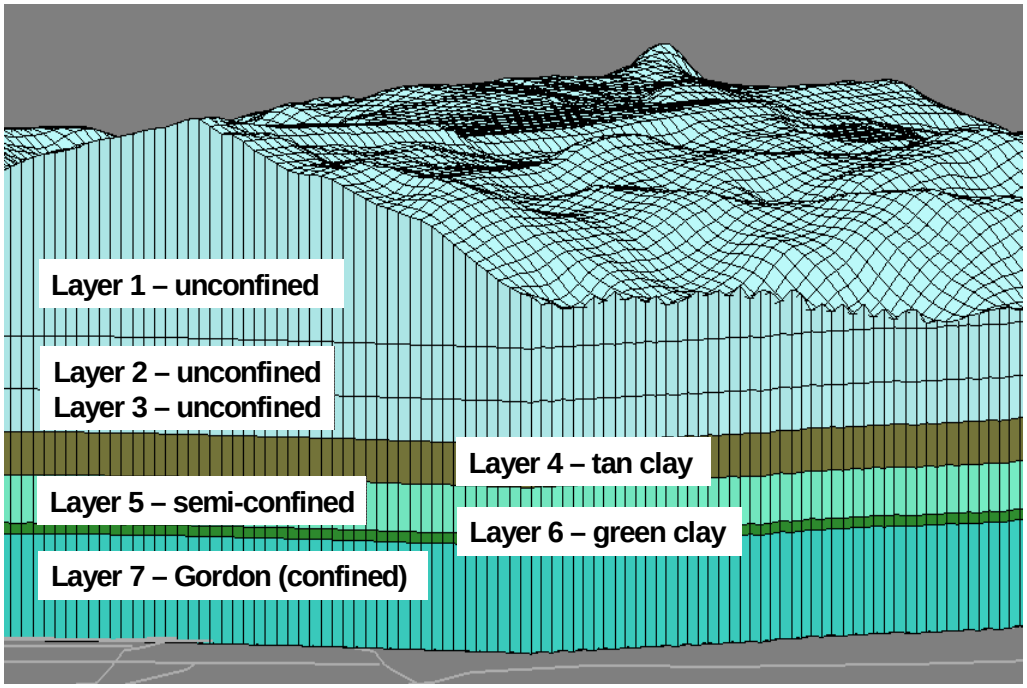

Figure 6-8. C Area hydrologic Conceptual Site Model

Table 6-1. Hydrologic layer parameters (adapted from Flach et al. (1999) and Geotrans (2001))

Layer	Name	K-horiz (m/d)	Kh/Kv	Porosity
1	Sand	10	3	0.25
2	Clay	0.01	50	0.35
3	Unconfined aquifer	3	3	0.25
4	Tan Clay	0.02	50	0.35
5	Semi-confined aquifer	2	3	0.25
6	Gordon confining unit (Green clay)	0.002	100	0.35
7	Gordon aquifer	8	3	0.25

Both the Conceptual Site Model (Figure 6-8) and the flow and transport modeling discussed below (Figure 6-9 - Figure 6-12) were prepared with GMS, a modeling package developed with NRC, EPA, DOE, and DoD support that incorporates several modeling codes such as ModFlow, MT3D, and RT3D. We have found that GMS has limited ability to incorporate well logs, so we developed conceptual geologic and hydrogeologic models with Petra, or Rockworks.

Transport modeling (with RT3D) was performed to simulate the TCE distribution and to determine if TCE could affect the confined Gordon aquifer.

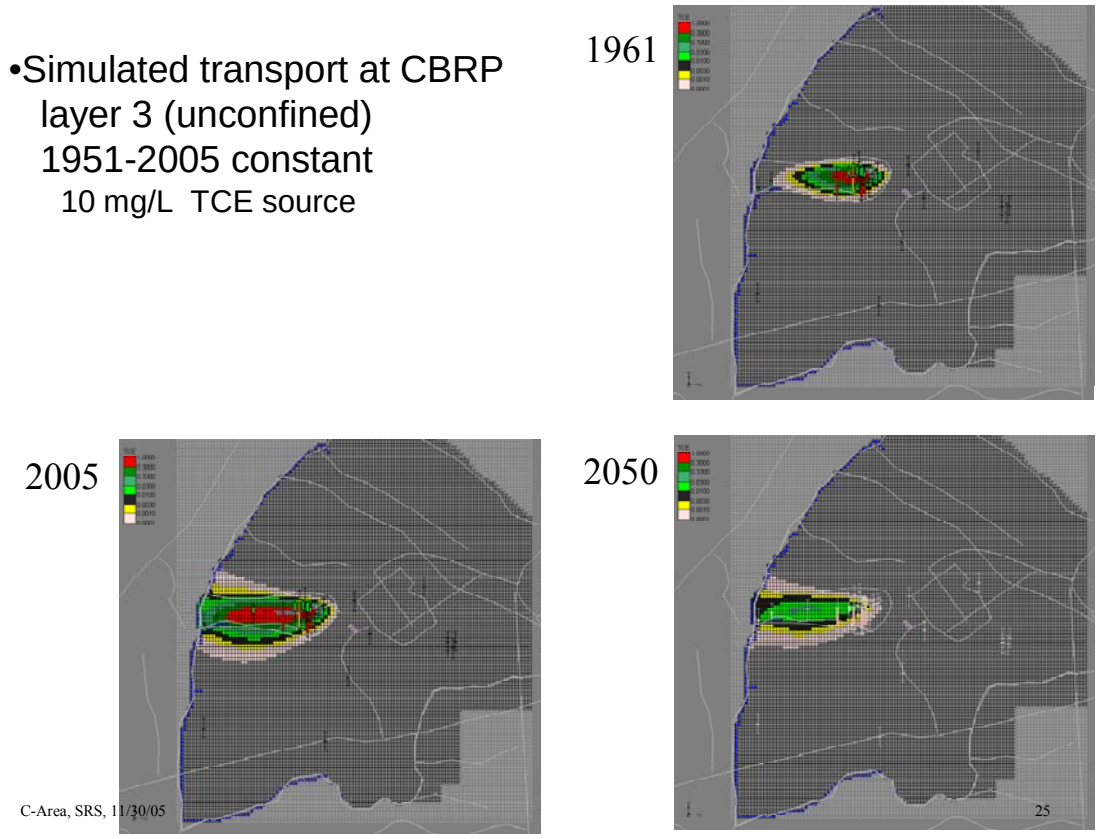

Figure 6-9. C Area simulated transport model for Layer 3 from the CBRP

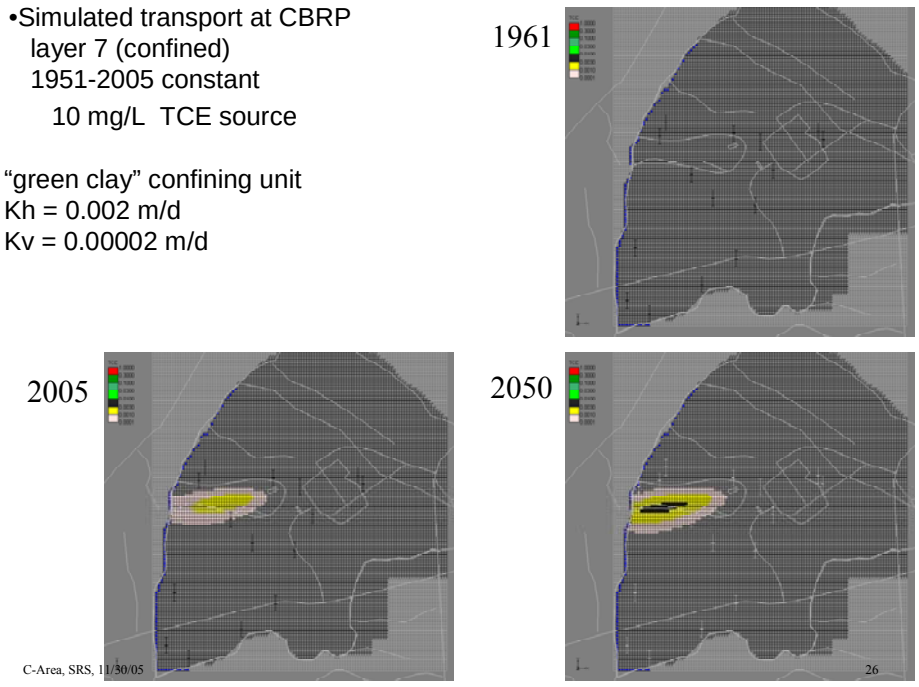

Figure 6-10. C Area simulated transport model for Layer 7 from the CBRP

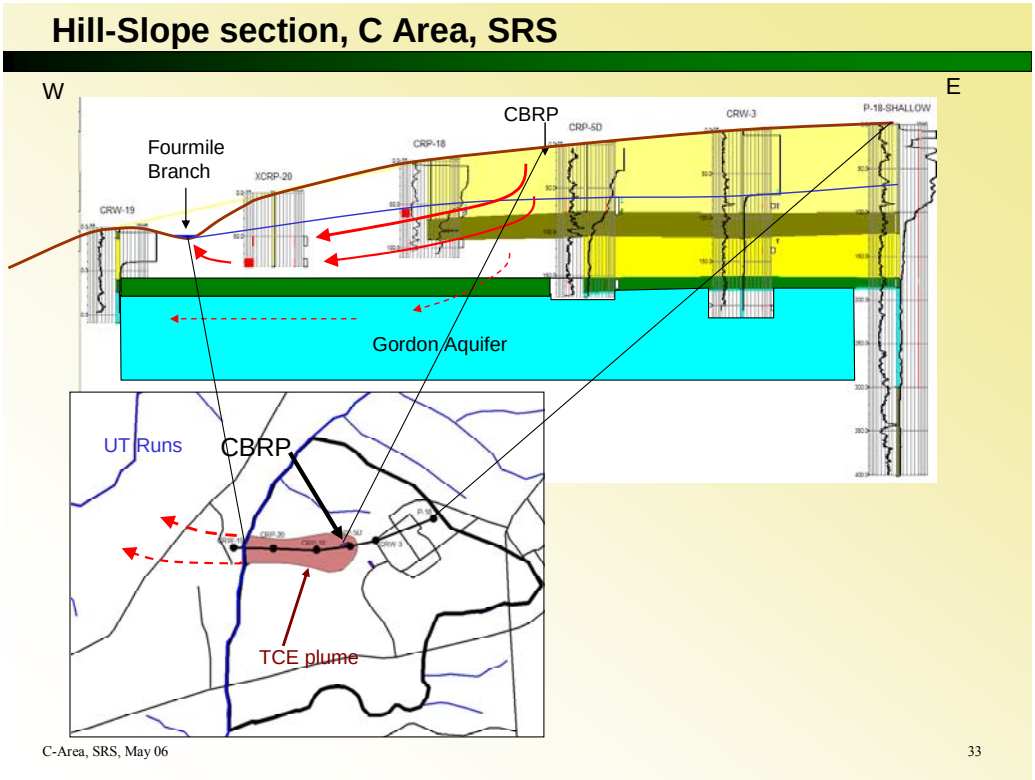

Figure 6-11. Cross section of C Area hydrogeologic conceptual model. The Gordon confining unit (green clay) is shown as a green band above the Gordon aquifer. Fourmile Branch is correctly called Four Mile Creek elsewhere in this document.

6.5 Data Visualization

Three-dimensional visualization provides a powerful tool to present data. For example, in our 7-layer conceptual model of C-Area hydrogeology, we have used a program called 3-D Analyst, part of ArcGIS, to display all the TCE analyses available for layer 7, also called The Gordon aquifer.

As shown in the cross-section of Figure 6-11, contamination in the shallower layers, those above the "green clay," (also referred to as Layer 6 in Figure 6-8 and the Gordon confining unit in Figure 6-13) should discharge to the surface at Four Mile Creek, but any contamination reaching layer 7 will leave the area of our model heading west.

Figure 6-12 presents a three-dimensional perspective of C Area, looking to the northeast and upward from below Layer 6 – the Gordon confining unit (Green Clay). CPT ground water sampling intervals above the layer 6- Gordon confining unit are represented by dim points. The three CPTs within the plume were pushed in 1999 and indicate TCE levels below detection limits (blue dots indicate non-detect). The plume outline as defined by data from the unconfined and semi-confined layers (layers 1-5), is shown as a black curtain hanging down from the surface. The four CPT samples taken north of the plume were pushed in 2000-2001 and indicate extremely low levels of TCE (white dots indicate low detection levels).

The three CPT samples (non-detect, blue) left of Four Mile Creek (shown as a blue "curtain" extruded down from the surface) were pushed in 2001. These 10-12 CPTs are all that sampled the Gordon aquifer near the TCE plume and none of the CPTs go very deep into the Gordon aquifer. The Gordon aquifer was sampled but is not being routinely monitored.

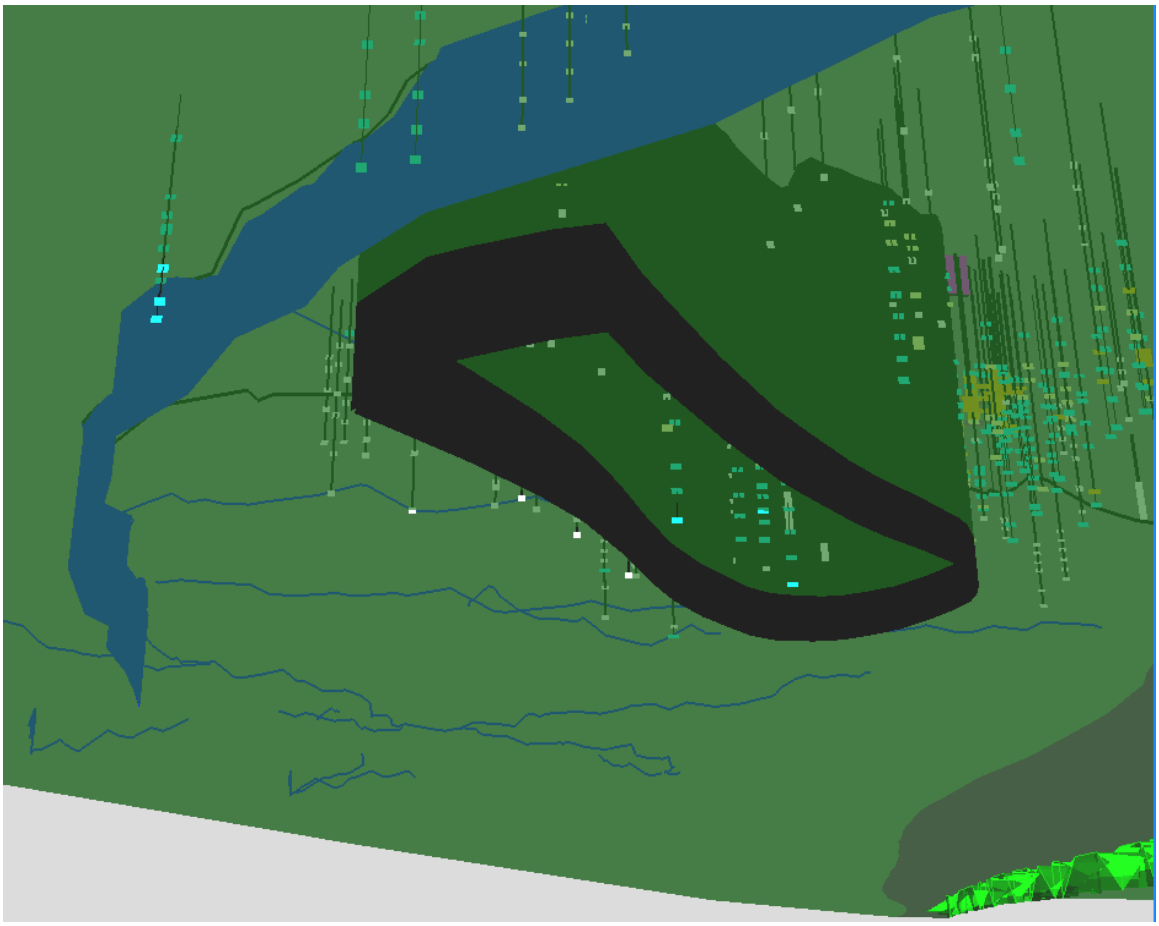

Figure 6-12. Looking from beneath the Gordon confining unit to the NE towards the plume (All dim points are above the Gordon confining unit).

Transport modeling discussed above suggested low levels of dissolved TCE could seep through the Layer 6 (Gordon confining unit) into the Gordon aquifer and travel beyond Four Mile Creek at some time in the future, perhaps by 2010-2020.

6.6 Alternative Conceptual Models

Both the flow and transport models referenced in previous characterization exercises and the flow and transport model produced by AES for this exercise show Layer 6 (also called the "green clay" or "Gordon confining unit) to be laterally continuous and uniform. However, limited information from a group of wells installed in 1992 to characterize a

possible new landfill site near C-Area suggests an alternative conceptual model for the green clay unit (Layer 6) may exist.

These wells (designated as LWR-1 through LWR-9) are not part of the environmental monitoring program for SRS. No analytical data for these wells exist in the SRS monitoring database – it appears that they have never been sampled.

The well installation report is available as WSRC-RP-92-1316, hereinafter "LWR report." This report was not referenced in existing modeling reports prepared previous to our investigation.

Figure 6-13 is from the LWR report. Its authors interpret data from these wells to indicate faulting of the green clay (Gordon confining unit). This shallow faulting was confirmed with a seismic reflection survey. The fault trend is northwesterly, similar to that of several tributaries to Four Mile Creek (see topographic map of Figure 6-5). This suggests the possibility of structural control of the streams, and hence additional faulting.

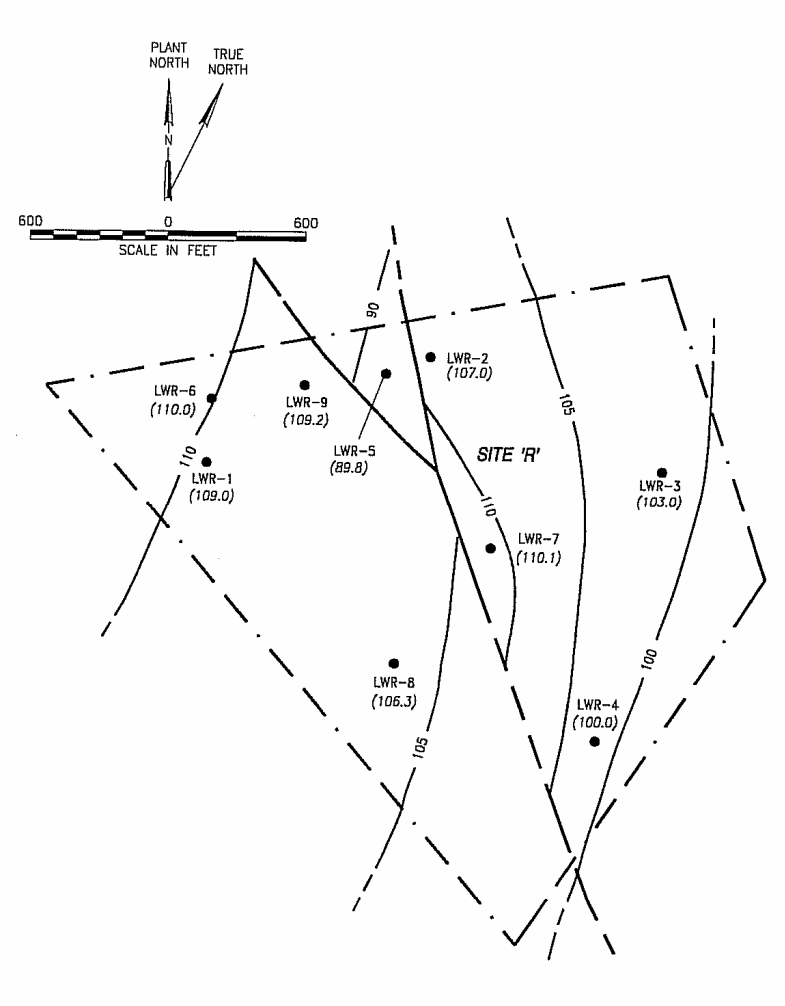

Figure 6-13. Structural contour map of the top of the Gordon confining unit (WSRC, 1992)

The maps of CPT locations suggest that those penetrating Gordon confining unit may not have been adequate in number or distribution to test any hypothesis relating to whether or not the Gordon confining unit was continuous or breached.

The maps in Flach et al. (1999) do not include scales or north arrows, so it is difficult to compare them to the LWR report, but the outline of Site R is shown on both drawings in Figure 6-14 as a reference. Gordon aquifer flow in the LWR report is about 60 degrees west of SRS plant north (left side of Figure 6-14). The modeling report Fig 4-32 (right side of Figure 6-14,) indicates a flow direction of about 38 degrees west of plant north. This modeling work was used to guide placement of sampling points in the Gordon aquifer (model Layer 7). If the flow direction is off by as much as 20 degrees, point sampling by direct push methods might have missed existing contamination altogether (see flow direction on left side of Figure 6-14).

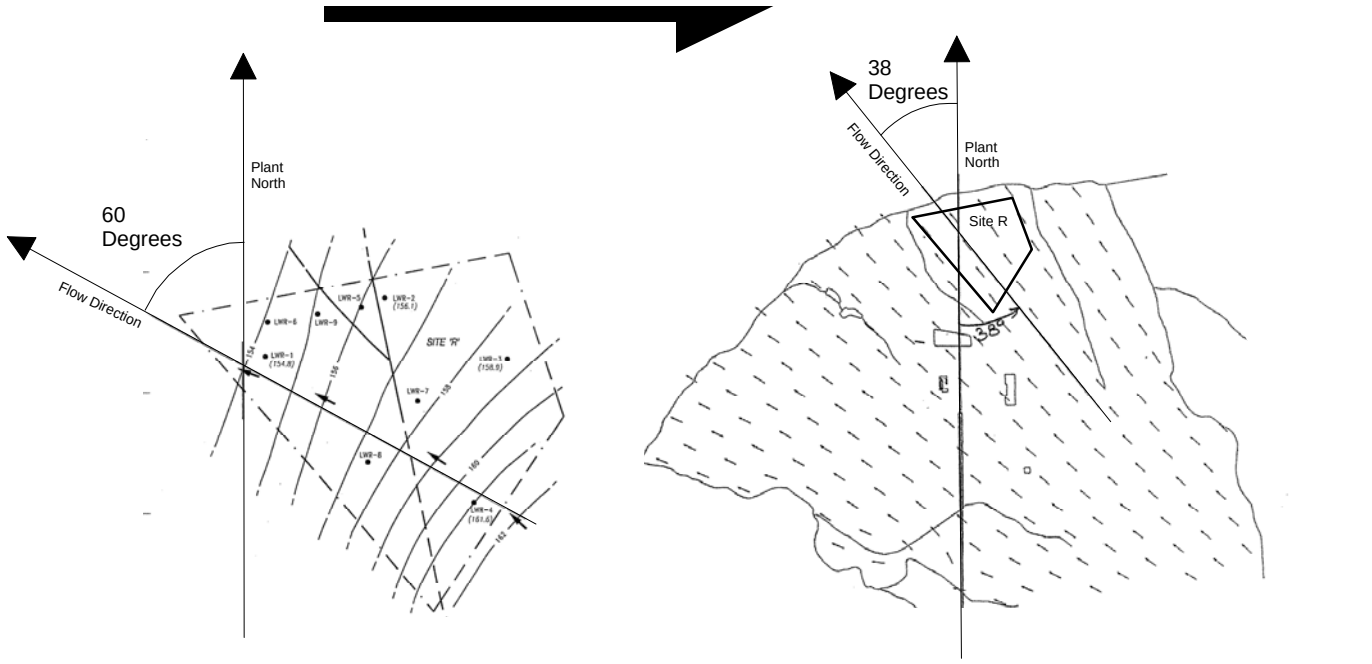

Gordon Aquifer in 1992 LWR Report

Gordon Aquifer in 1999 report WSRC-TR-99-00310

Figure 6-14. Maps of ground water flow directions within the Gordon aquifer

6.7 Performance Indicators and FEPs

The Performance Indicators for this system are primarily tritium and VOC concentrations in ground water. There is very limited testing for these PIs in the Gordon aquifer. Discrepancy between the flow directions in Figure 6-14 is noted as adding to uncertainty in the C-Area flow modeling. Faulting in the nearby LWR area is an indicator that the CSM should consider a breached confining unit.

Because C-Reactor was used largely for tritium production, lithium might be a good tracer, but has not been reported.

Integrity of the green clay / Gordon confining unit is a key assumption in flow and transport calculations. This assumption is not adequately tested. As noted, the nearby Site R report indicates faulting of this feature.

6.8 Monitoring Strategy Application Conclusions

The initial management decision was to characterize the extent of the TCE and tritium from the CBRP and the seepage basins. A subsequent decision was to simulate flow and transport of these contaminants to evaluate risk and remediation options. These decisions were made in the context of the SRS Federal Facilities Agreement and with the advice and consent of the South Carolina Department of Health and Environmental Control (DHEC).

Plume sampling and geohydrologic characterization were accomplished with CPT methods. In addition, data were compiled from existing sources comprising monitoring wells, water production wells, and so forth.

How important is the problem? Although the Gordon is a regionally important aquifer, it discharges into the Savannah River or the adjacent swamp before leaving DOE property. Shallower water-bearing zones discharge into smaller streams that lead to the Savannah River. Thus, the only reasonable pathway to an offsite receptor is through the Savannah River, which has a discharge normally in excess of 5,000 cfs to dilute any SRS contribution.

Computer modeling with 50-year projections suggest that the TCE and tritium ground-water plumes will both be greatly reduced, although not to drinking water standards.

Is any further action needed? Probably not. Sampling and modeling suggest that the contamination will decline naturally over time and that there are no offsite receptors for the ground-water pathway. Active ground-water remediation is possible, but impractical. The C-Area is totally within a government-owned site and C-reactor is shut down permanently.

Decommissioning of C-Area facilities might initiate a future review of the no further action decision. If there were a legal issue with the accuracy of the modeling, the exclusion of the LWR report could be used against the SRS.

How is C-Area different from a facility applying for an NRC license? SRS was constructed in the early 1950s to provide materials for defense. There was no private funding – cost was not an issue. There was no issue of license approval. There was no public review. There was no opportunity for antinuclear activists to intervene. There was no profit motive.

None of these statements are true for a new NRC-licensed facility. Any oversight in data collection, or failure to consider alternative Conceptual Site Models could result in costly challenges to a proposed facility.

What other hydrogeologic factors would be considered for a new facility? In the above discussion we mention three technical weaknesses that could be used against a new facility. These are all related to the LWR well installation report.

Modeling to predict the TCE plume behavior did not reference the LWR well installation report. The flow directions for the only aquifer leaving the model boundaries (Layer 7 or Gordon aquifer) was at variance as much as 20 degrees with flow shown in the LWR report.

The LWR report suggests discontinuities in the Gordon confining unit above the Gordon aquifer. These could provide fast paths for contamination to reach the Gordon aquifer with much less attenuation than currently predicted in the model.

In the context of current SRS operations and future long-term stewardship, these comments may not be important. The large buffer around the C-Area and the lack of a credible pathway to a ground-water receptor largely negate any issues related to the failure to incorporate and discuss all available data.

In the context of a commercial site with a smaller buffer and credible ground water pathways to off-site receptors, the failure to account for all available data and to thoroughly investigate the continuity of the confining unit could be used by interveners and could lead to public distrust of the licensee's motives or competence.

6.8.1 Possible Future Actions

Based on the results of the application of the Strategy, some recommendations are made for future investigations. These are made in the context of the discussion above – that is, irrespective of the results, there is very little impact to offsite risk. Additional characterization and modeling would be strongly recommended if this were a site under stakeholder scrutiny.

Modeling suggests the confined Gordon aquifer could be monitored with wells placed west of Four Mile Creek across from the plume. A new round of CPT sampling in about 2020 would also be sufficient to confirm or deny the hypotheses the TCE is leaving the C-Area facility boundary.

At least one round of ground-water samples should be collected from the LWR-series well clusters for a full suite of potential contaminants of concern for C Area. This data would help ensure that no contamination has reached this more northern portion of C Area. This additional data will also help to provide plume closure for modeling on the north side of the facility.

Lithium should be evaluated as a tracer for this Area.

Integrity of the Gordon confining unit is a key assumption in the CSM used for flow and transport modeling. Uncertainty in this assumption taints all current modeling results. A shallow seismic survey coupled with a few wells or CPT tests could test this source of uncertainty.

6.9 References

DOE/EM-0319. *Linking Legacies, Connecting the Cold War Nuclear Weapons Production Processes to Their Environmental Consequences*. 1997.

Flach, G.P., et al. WSRC-TR-99-00310. "Hydrogeological Analysis and Groundwater Flow for C-Reactor Area with Contaminant Transport for C-Reactor Seepage Basins (CRSB) and C-Area Burning/Rubble Pit (CBRP)(U)." 1999.

Fallaw, W.C. "Stratigraphic Relationships in Eocene Outcrops Along Upper Three Runs at the Savannah River Site" *Carolina Geological Society Field Trip Guidebook.* p XII1-XII2. 1992.

GeoTrans. WSRC-TR-2001-00298. "Groundwater Modeling for the C-Area Burning/Rubble Pit (U)." 2001.

Kegley, W.P.,et al. "Textural Factors Affecting Permeability at the MWD Well Field, Savannah River Site, Aiken, South Carolina." *Southeastern Geology.* Vol. 34, p 139-161. 1994.

Siple, G.E. "Geology and Ground Water of the Savannah River Site and Vicinity." South Carolina U.S. Geological Survey Water Supply Paper 1841. U.S. Government Printing Office: Washington, D.C. OpenLit. 1967.

Westinghouse Savannah River Company (WSRC). WSRC-RP-92-1316. "Summary of Drilling Program for Site R, New Sanitary Landfill Project." Westinghouse Savannah River Company: Aiken, South Carolina. November 19, 1992

WSRC. ESH-EMS-980590. "Environmental Protection Department's Well Inventory." Westinghouse Savannah River Company: Aiken, South Carolina,. July 1998.

7 Hanford 300 Area

7.1 Introduction

This report is an exercise demonstrating the application of the Advanced Environmental Solutions, LLC (AES) Strategy to a highly transmissive, near surface aquifer in the Northwestern United States. This exercise is for testing the functionality for the Strategy only. Data utilized in this evaluation are based on readily available information. Most of this chapter is a recapitulation of Hanford data. An alternative to the current Conceptual Site Model of ground water flow is offered in section 7.3.

The Hanford Site borders the Columbia River and covers 1,517 square kilometers (586 square miles) just north of the city of Richland, Washington. In this case study, the AES Strategy provides a structured approach for studying the relationship between groundwater flow in the Hanford 300 Area, which is located in the southeast portion of the Hanford site, and the Columbia River. An accurate understanding of the 300 Area groundwater flow pattern will, in turn, aid in understanding the distribution and migration of contaminants, particularly hexavalent uranium, in the 300 Area. A map depicting the Hanford Site, including the 300 Area, is presented in Figure 7-1.

The ground water beneath the 300 Area has been contaminated by liquid effluent discharges from 3 main waste sites: the 300 area, 618-11 burial ground, and the 316-4 cribs/618-10 burial ground. These releases occurred from the late 1940s through the mid-1980s. Since the end of fuel fabrication activities, contaminated discharges have largely ceased, although discharges of uncontaminated effluent continued until 1994. Remedial actions have been completed that removed the structures and contaminated soil associated with most of these disposal sites. However, residual amounts of some contaminants remain in the underlying vadose zone, and their presence is indicated in ground water monitoring results.

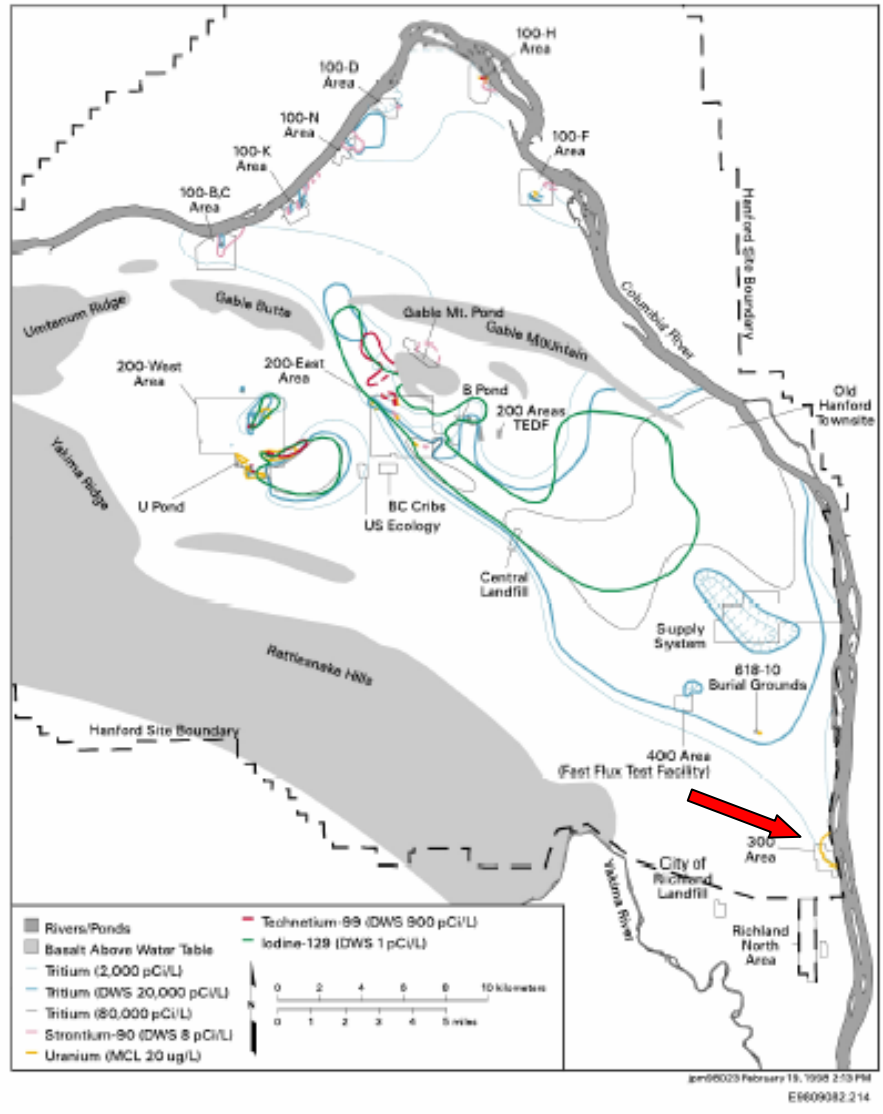

Figure 7-1. Hanford Site map including the 300 Area (DOE, 1999)

7.2 Compilation of Available Data

7.2.1 Geologic Setting

The Hanford Site lies within the Pasco Basin, a structural depression that has accumulated a relatively thick sequence of fluvial, lacustrine, and glaciofluvial sediments. Local geology as well as the regional geology play a strong role in contaminant transport.

7.2.2 Regional Geologic Information

Figure 7-2 and Figure 7-3 show the surface geology and major structural features of the area, respectively. The Pasco Basin initially developed on the underlying Columbia River Basalt Group, a sequence of continental flood basalts covering more than 160,000 km^2 (Vermeul et al., 2003).

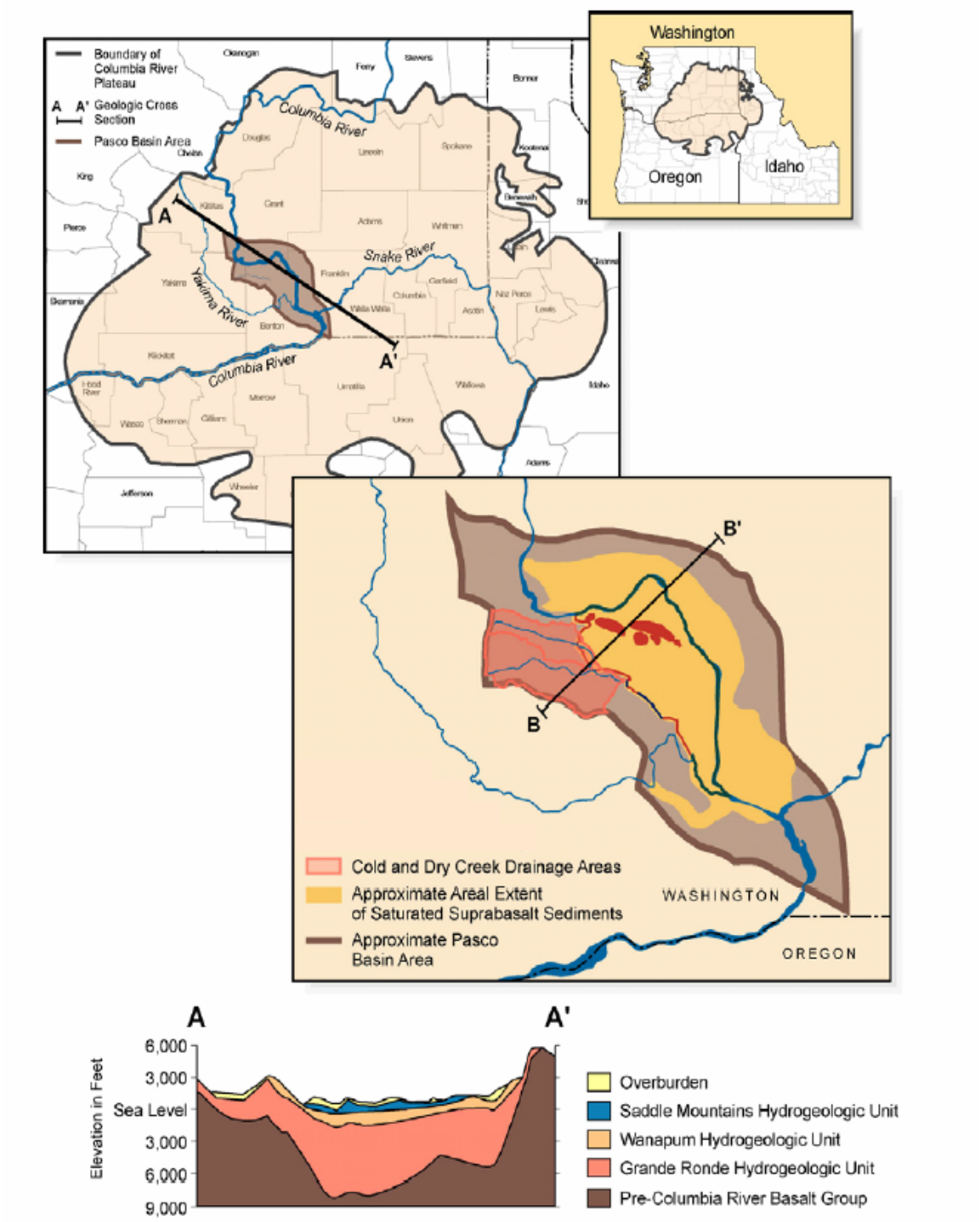

Figure 7-2. Hanford Site regional geologic setting (Vermeul et al., 2003)

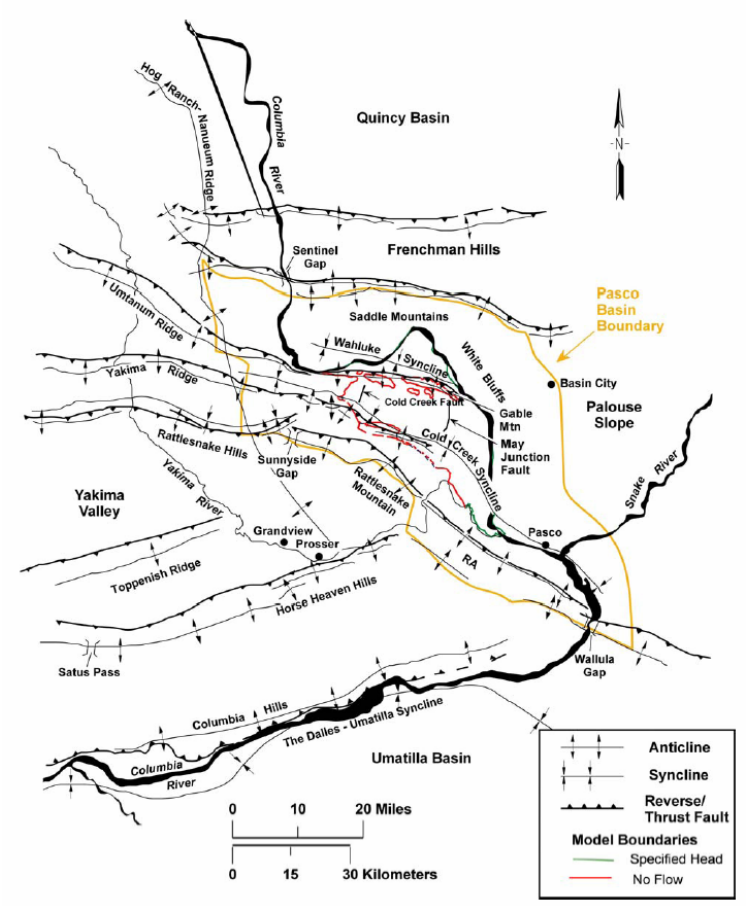

Figure 7-3. Structural geologic features of the Hanford Site within the Pasco Basin (Vermeul et al., 2003)

Overlying the basalt within the Pasco Basin are fluvial and lacustrine sediments of the Ringold Formation (Figure 7-4) (Lindsey et al., 1992). The ancestral Columbia River and its tributaries flowed into the Pasco Basin, depositing coarse-grained sediments in the migrating river channels and fine-grained sediments (silt and clay) primarily as overbank flood deposits. On at least two occasions, these river channels were blocked, forming lakes in the Pasco Basin and depositing extensive layers of fine-grained lacustrine sediments within the Ringold Formation.

7.2.3 Site-specific Geologic Information

The major geologic units in the Hanford Site area are the Miocene Columbia River Basalt Group (CRBG) and intercalated sedimentary rocks of the Ellensburg Formation. These are overlain by younger (Mio-Pliocene) sedimentary rocks of the Ringold Formation, the early "Palouse" soil/Plio- Pleistocene Unit, and the Pleistocene cataclysmic flood deposits of the Hanford Formation (Figure 7-4).

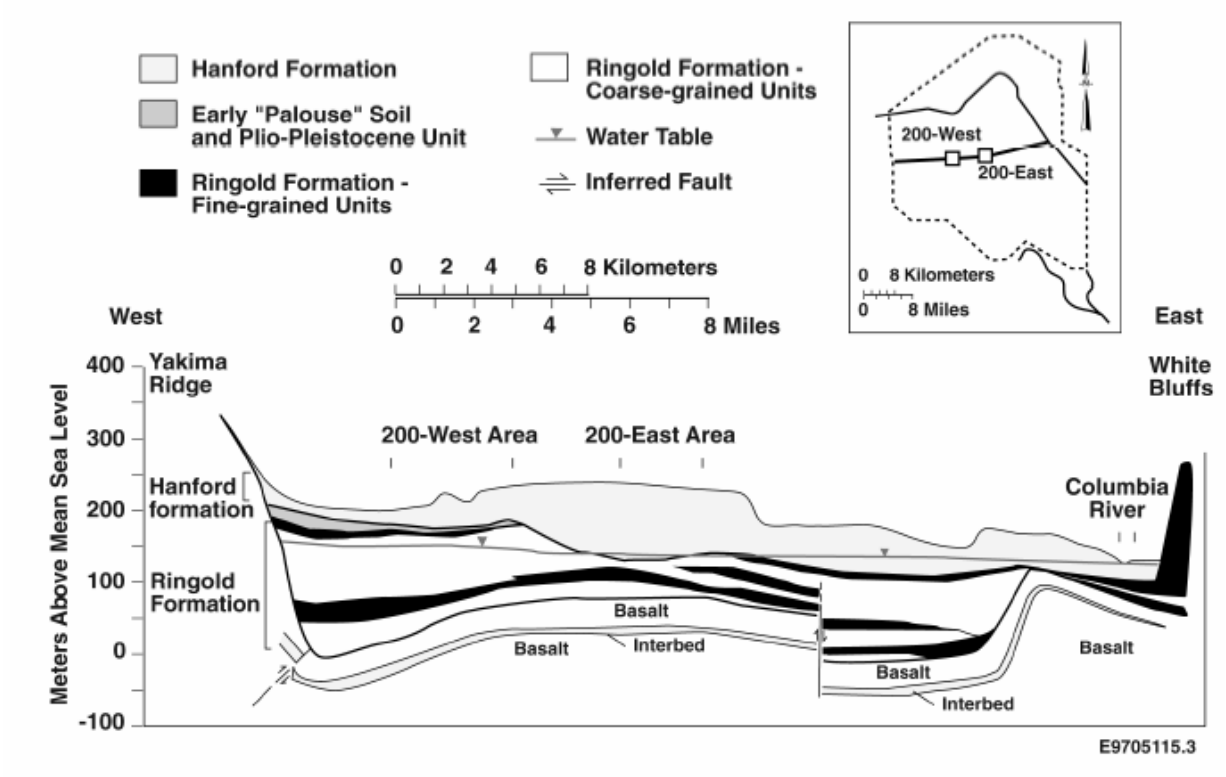

Figure 7-4. Major geological units at the Hanford Site (DOE, 1999)

The Plio-Pleistocene Unit is made up of sandy gravels that separate the Hanford Formation and the Ringold Formation in the east-central Cold Creek syncline and at the east end of the Gable Mountain anticline (east and south of the 200 East Area). These gravels are up to 25m (75 feet) thick. Along the western margin of the site, the "Palouse" soil separates the two formations. The Hanford Formation consists of pebble to boulder sized gravel, fine to coarse-grained sand, and silts of unconsolidated deposits from ice age flooding. The Hanford Formation generally lies above the water table throughout most of the Hanford Site, except in the 100 and 300 Areas (DOE, 1998).

7.2.4 Site-specific Hydrogeologic Information

Geologic descriptions are available from 67 boreholes in the 300 Area. All of these boreholes are deep enough to penetrate the contact between the Hanford and Ringold stratigraphic formations. EarthVision geologic modeling and visualization software was used to interpolate unit contacts between borehole locations and to create a three-dimensional model of the hydrogeologic framework. Figure 7-5 provides an index to the three cross sections shown in Figure 7-6, Figure 7-7, and Figure 7-8, which are drawn through the model to illustrate the framework (Peterson, 2005).

Highly transmissive Hanford formation gravels are found below the water table across portions of the 300 Area. The extent and thickness of saturated Hanford formation gravels vary as a consequence of changes in water-table elevation, which are caused by changes in the Columbia River stage. The saturated thickness of the Hanford formation in the 300 Area varies from 0 to 15 meters (0 to 49 feet). Aquifer pumping tests at five boreholes within the 300 Area reveal an average hydraulic conductivity of approximately

14,000 meters (45,932 feet) per day for saturated Hanford formation gravels. This indicates a highly transmissive hydrologic unit. The value is significantly higher than the average hydraulic conductivity for Hanford formation gravels elsewhere on the Hanford Site (i.e., approximately 2,000 meters (6,562 feet) per day (Peterson, 2005). Extrapolating from the known geology indicates that there is a high likelihood that zones of high permeability are present and are highly variable in their spatial distribution.

Ringold Formation gravels below the water-table range in thickness from 15 to 50 meters (49 to 164 feet). Aquifer pumping tests at seven boreholes in the 300 Area suggest an average hydraulic conductivity of approximately 125 meters (410 feet) per day, which is again higher than the average values for Ringold gravels elsewhere on the Hanford Site but considerably less transmissive than the overlying Hanford unit. Relatively higher conductivities may exist in the upper part of the Ringold Formation (i.e., Unit E gravel), where most pumping tests have been performed (Peterson, 2005).

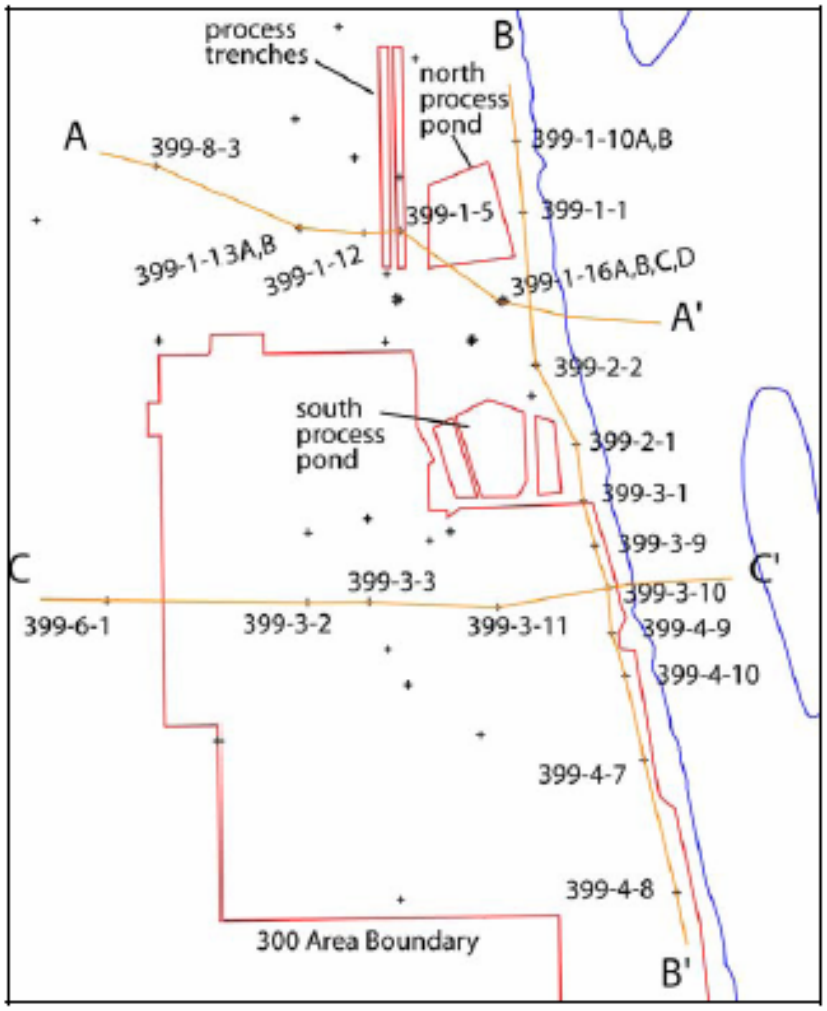

Figure 7-5. Index map to cross sections shown in Figures 6, 7, and 8 (Peterson, 2005)

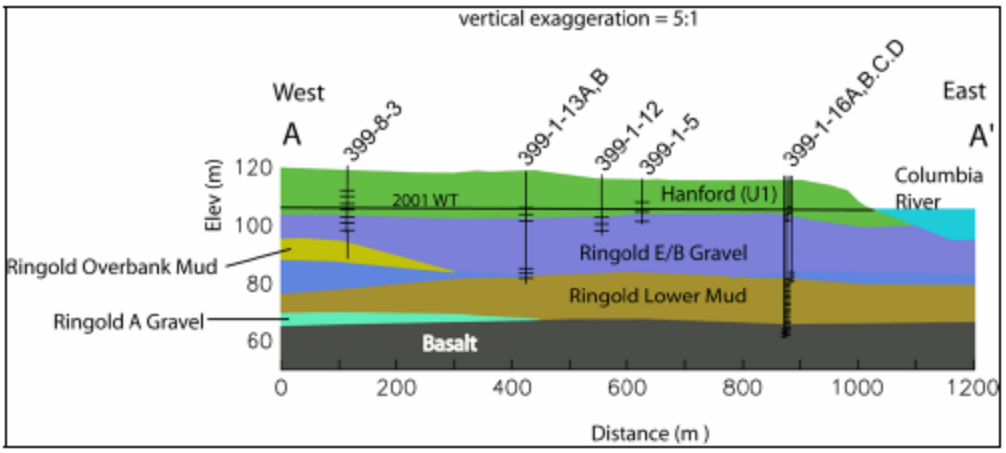

Figure 7-6. West to east cross section along flow path from 300 Area process trenches to the Columbia River (Peterson, 2005)

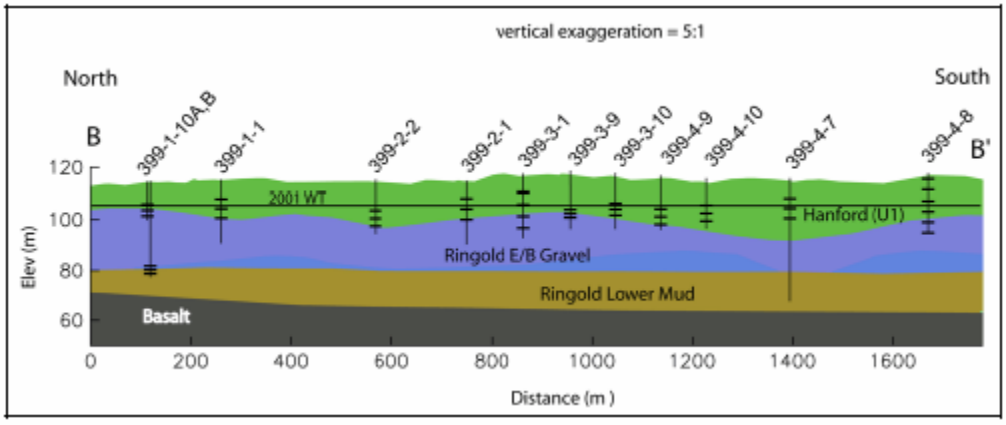

Figure 7-7. North to south cross section along shoreline wells (Peterson, 2005)

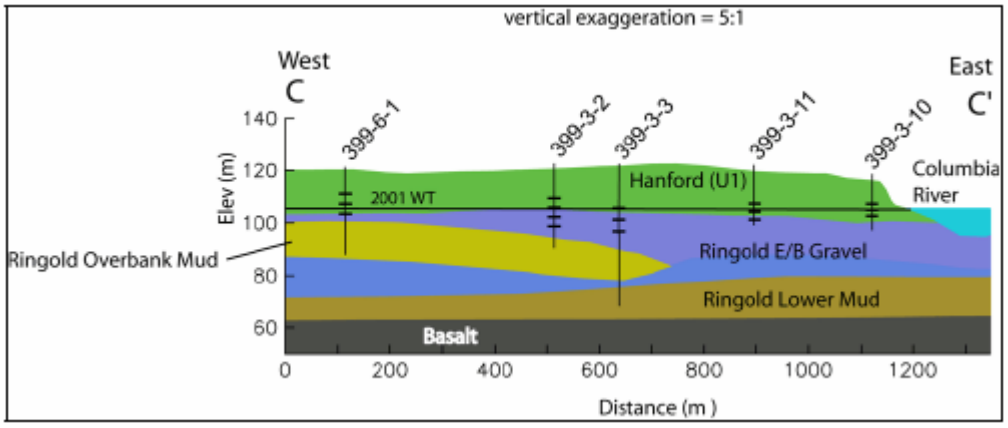

Figure 7-8. West to east cross section through central portion of 300 Area (Peterson, 2005)

7.2.5 Vadose Zone Data

The sediments beneath waste sites at Hanford are highly heterogeneous (for example, sediments include interbedded sand, silts, gravels, and boulders). Temporal and spatial variations in net water infiltration through current and past liquid discharges, water line leaks, and variable chemical interactions complicate description and understanding of contaminant transport, and lead to uncertainty in the evaluation of transport at contaminated sites. A number of knowledge gaps—including an insufficient understanding of source terms, geological and hydrologic properties, preferential flow, and chemical interactions–make current modeling of contaminant transport in the Hanford vadose zone unreliable.

Figure 7-9 presents three potential types of preferential flow models in the Hanford vadose zone: (1) fingering, (2) funnel flow, and (3) flow associated with clastic dikes or poorly sealed borehole annular space. Funnel flow can enhance lateral migration, and horizontal layering will tend to stabilize fingered flow, whereas cross-bedding concentrates and coalesces fingers. Flow through clastic dikes and poorly sealed well-annular spaces could exhibit a hysteretic Effect, which may appear during infiltration events (such as large rainfall events), and there may be flow impediments during drying (Faybishenko, 2000).

In the 300 Area, the vadose zone is relatively thin, ranging from about 1 to 30 m in thickness. It is generally composed of recent surficial deposits and portions of the Hanford formation and/or Ringold Unit E. Sediments from the upper strata of the Ringold Formation within the 300 Area is characterized by complex interstratified beds and lenses of sand and gravel. Ringold Formation deposits are generally more cemented and better sorted than those from the Hanford formation. Ringold strata typically contain a lower percentage of angular basaltic detritus than Hanford formation deposits. The Hanford formation is characterized by dark grayish-brown to dark olive-gray sandy gravel, typical of the gravel-dominated facies, with some silt and local sand stringers. The upper portion of the unit generally exhibits a pebble to boulder gravel, which becomes finer with depth, to a very fine-to-medium pebble gravel (DOE, 1998).

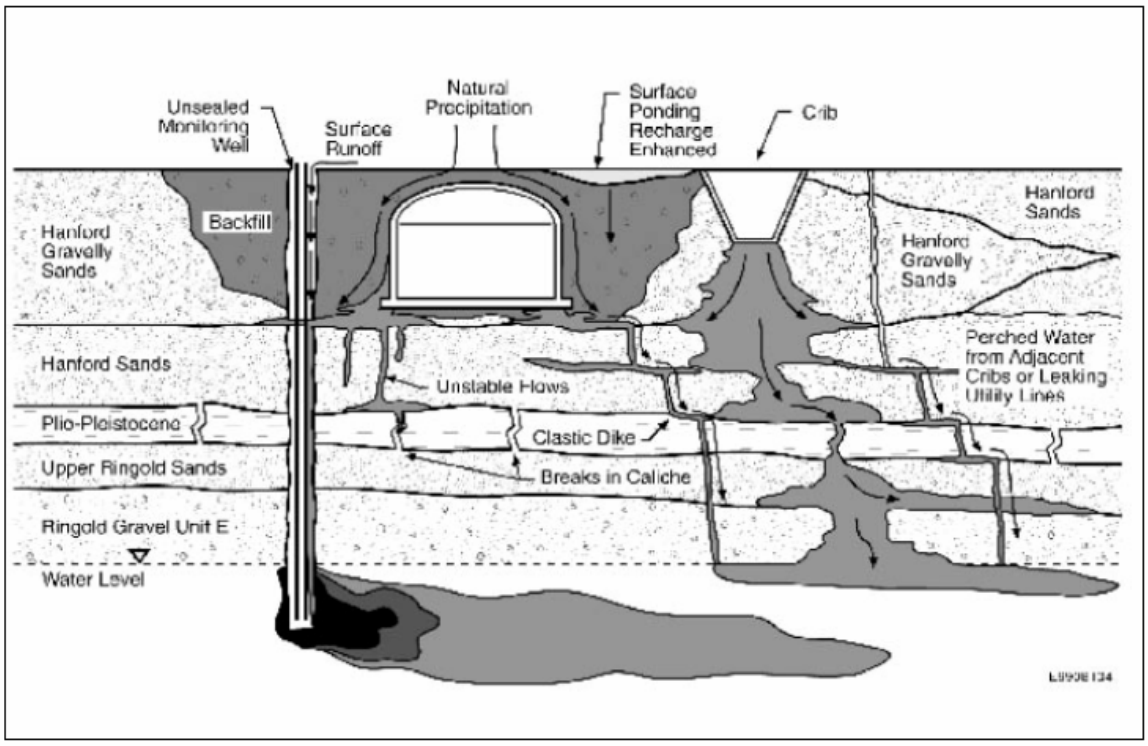

Figure 7-9. Conceptual model of fluid flow beneath single shell tanks at Hanford Site showing fingering, funnel flow, and flow associated with clastic dikes or poorly sealed borehole annular space (Faybishenko, 2000)

7.2.6 Hydrologic Data

Ground water flow beneath the 300 Area is generally directed toward the southeast. Ground water appears to converge beneath the 300 Area, with flow coming into the 300 Area from the northwest, west, and southwest. The uppermost aquifer (Hanford formation) is highly transmissive because of open framework gravelly sediment, thus leading to high flow velocities (i.e., meters per day). However, because the hydraulic gradient that drives the flow varies with Columbia River stage, actual movement paths of water can be variable when viewed on short time scales, such as days or weeks. When viewed over seasons and years, however, the net flow and movement of contaminant plumes follows the generally southeasterly course (Peterson, 2005).

It is not clear exactly what influence the Columbia River has on the overall ground water flow direction. Data indicates that the aquifer is in communication with the river and that the stage of the river does impact the lateral movement of water into and out of the aquifer. What is less clear is what influence the river has on the flow of ground water within the aquifer locally at the aquifer/ river interface. Improving our understanding of the relationship between the river and Area 300 groundwater through the implementation of the AES Strategy is the primary focus of this exercise.

7.2.7 Seasonal Variability in Water-Table Conditions

To better understand how the dynamic hydrologic system in the 300 Area influences the dispersal pattern of contaminant plumes, hourly hydraulic head data were analyzed to (a) determine the predominant ground water flow directions, and (b) assess variability in flow directions during the various seasons. The analysis used hourly measurements of hydraulic head made at 30 wells in the 300 Area during the period of March 1992 through February 1993, using pressure transducers. Water-table elevation contour maps were prepared for March, May, June, September, and December 1992 (Figure 7-10, Figure 7-11, Figure 7-12, Figure 7-13, and Figure 7-14, respectively). The contours were based on 22 wells deemed most representative of unconfined aquifer (i.e., water table) conditions. The values contoured were averages of all hourly measurements made during a particular month. The water-table maps for the various months reveal that the shape of the water table and, therefore, the inferred long-term ground water flow pattern, appears to show little variation from season to season. The overall elevation of the water table is higher during the seasonal high river discharge that occurs in May and June. The aquifer apparently equilibrates rapidly to changes in river stage, which is expected given the high transmissibility of the stratigraphic units (Peterson, 2005).

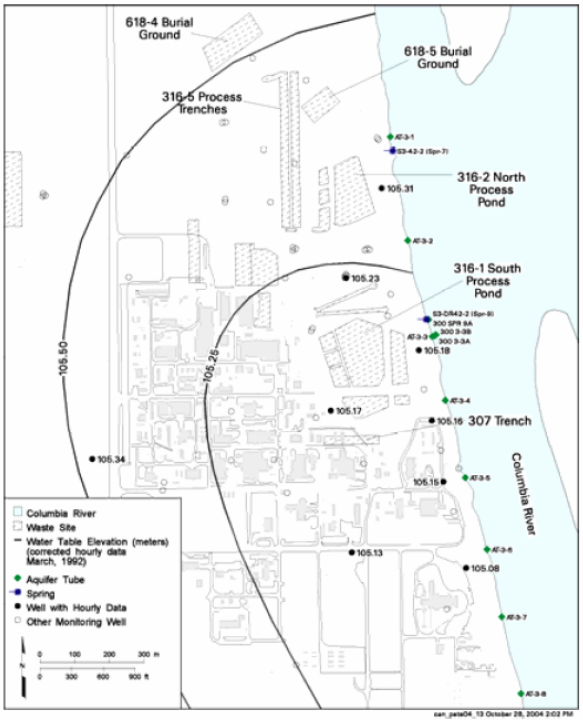

Figure 7-10. 300 Area water-table elevation, March 1992 (averaged hourly) (Peterson, 2005)

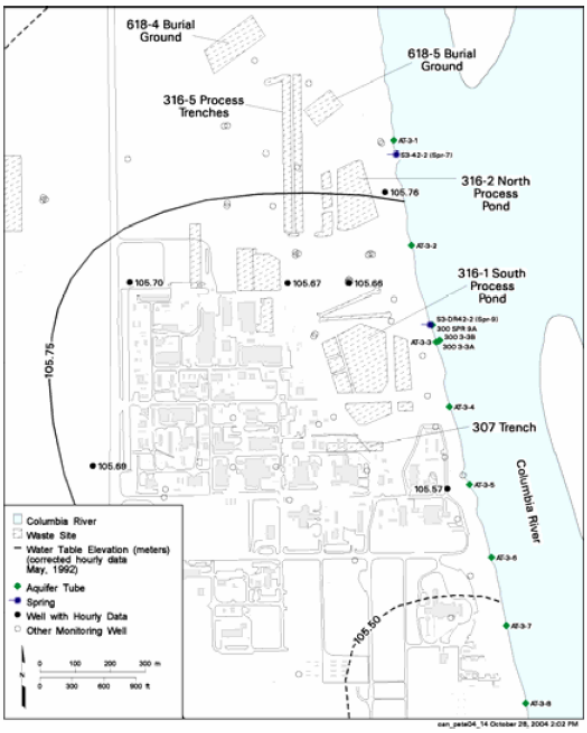

Figure 7-11. 300 Area water-table elevation, May 1992 (averaged hourly) (Peterson, 2005)

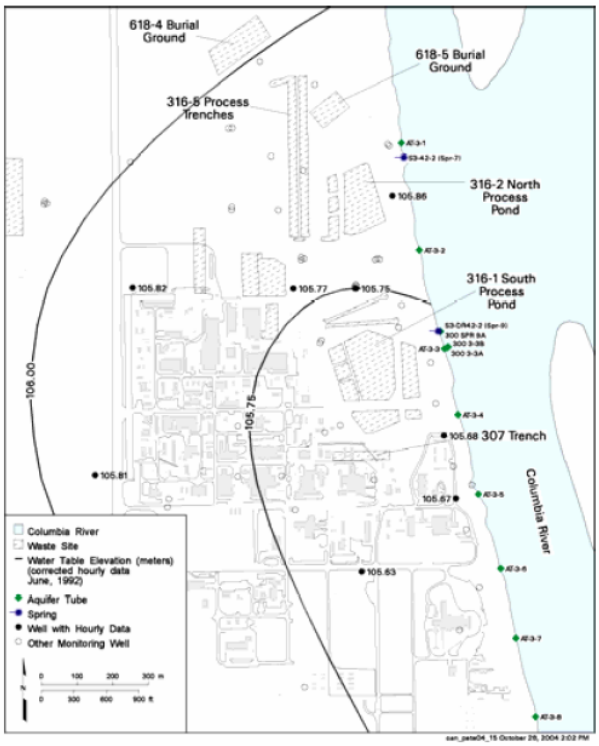

Figure 7-12. 300 Area water-table elevation, June 1992 (averaged hourly) (Peterson, 2005)

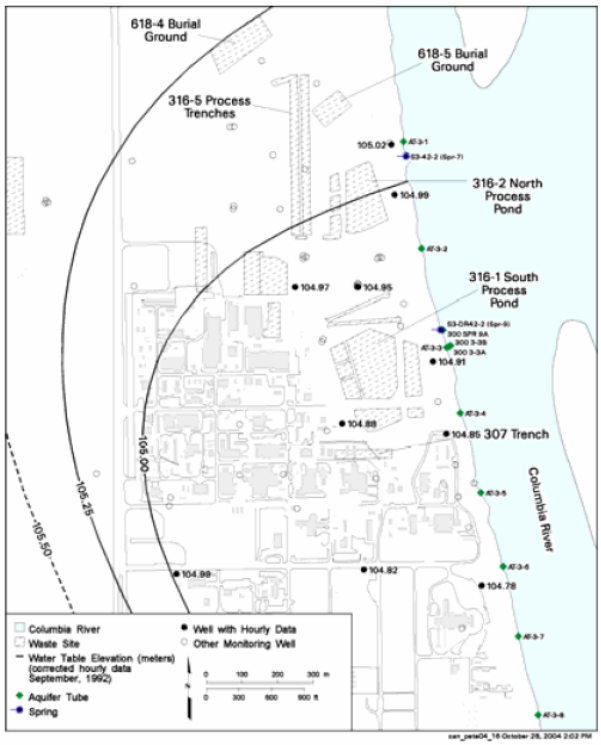

Figure 7-13. 300 Area water-table elevation, September 1992 (averaged hourly) (Peterson, 2005)

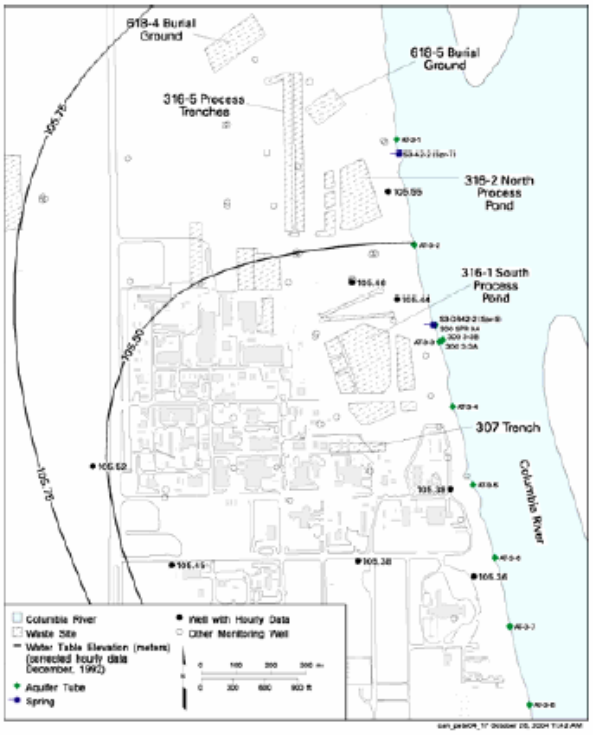

Figure 7-14. 300 Area water-table elevation, December 1992 (averaged hourly) (Peterson, 2005)

The fluctuating river stage causes corresponding fluctuations in water-table elevations. Typically, lines of equal topographic elevation result in flow in a parallel fashion from an unconfined aquifer into the adjacent stream. Water table contour shapes in the preceding Figure 7-10 through Figure 7-14 cannot be adequately explained by either topography or river infiltration into the aquifer. Contours at all seasons indicate that there could be an influence on the direction of ground water flow by the impinging river on the bank of the river. Consequently, dispersal of contaminants from a particular source may have a deflected path over the course of several years.

The water-table maps indicate that the ground water flow direction in the vicinity of the 300 Area process trenches, the last liquid waste disposal facility to receive uranium-bearing effluent, is generally to the south-southeast for all seasons (Peterson, 2005).

Periodic reversal of the hydraulic gradient (i.e., directed inland from the river) occurs near the river when the stage is high, but this change is not readily apparent in the monthly averaged data. Based on hydraulic gradients, Figure 7-10 through Figure 7-14 suggest that along the shoreline to the south of the process trenches, river water may be continually entering the aquifer, flowing south along the shore, and then discharging back to the river. The highly transmissive Hanford unit is thicker along this section of shoreline, which would possibly enhance this exchange (see cross section in Figure 7-7). The implication of having a fairly consistent long-term orientation of flow direction is that plume boundaries can be more accurately anticipated, especially when the source of the contaminant is also accurately known (Peterson, 2005). If however the flow direction is changing, then any conceptual site model and any monitoring program must take this into account.

Because of the highly transmissive character of much of the uppermost hydrologic unit beneath the 300 Area (Hanford formation), the water table elevation responds quickly to fluctuations in stage of the adjacent Columbia River. Consequently, the hydraulic gradient steepness and orientation may vary dramatically over the short time periods associated with daily river fluctuations. (Peterson, 2005).

7.2.8 300 Area Uranium Plume

The ground water beneath the 300 Area has been contaminated by liquid effluent discharges to a variety of disposal sites during a period of operations that extends from the late 1940s through the mid- 1980s. Since the end of fuel fabrication activities, contaminated discharges have largely ceased, although discharges of uncontaminated effluent continued until 1994. Remedial actions are underway and the structures and contaminated soil associated with most of these disposal sites have been removed. However, residual amounts of some contaminants remain in the underlying vadose zone, and their presence is indicated in ground water monitoring results (Peterson, 2005). Various ground water monitoring locations are provided in Figure 7-15.

The longevity of the 300 Area ground water uranium plume, despite attempted source term removal and copious water flow through the aquifer to the Columbia River, prompted an investigation into the processes controlling the release and transport of uranium at this site. The mildly alkaline pH and relatively high carbonate concentrations of the 300 Area porewaters are conditions that normally suppress hexavalent uranium

(U(VI)) adsorption on iron oxide-poor sediments as exist below the 300 Area; however, significant sorbed U(VI) concentrations (up to 250 mg kg^{-1} of uranium) are observed in the vadose zone. This sorbed U(VI) is believed to sustain the ground water plume through desorption as meteoric water infiltrates the vadose zone from above and as seasonal river stage fluctuations cycle ground water into the lower vadose zone from below. The lack of understanding of the distribution coefficient (Kd) for U(VI) makes modeling of the movement and mobility of uranium difficult.

The desorption or dissolution of uranium from capillary fringe sediments due to fluctuations in the water table controlled by changes in the adjacent river levels results in periodic pulsing of uranium into the ground water. This makes detailed characterization of the nature and extent of the contaminant plume within both the Vadose Zone and aquifer, along with compiling the detailed associated hydrogeologic and geologic conditions, paramount.

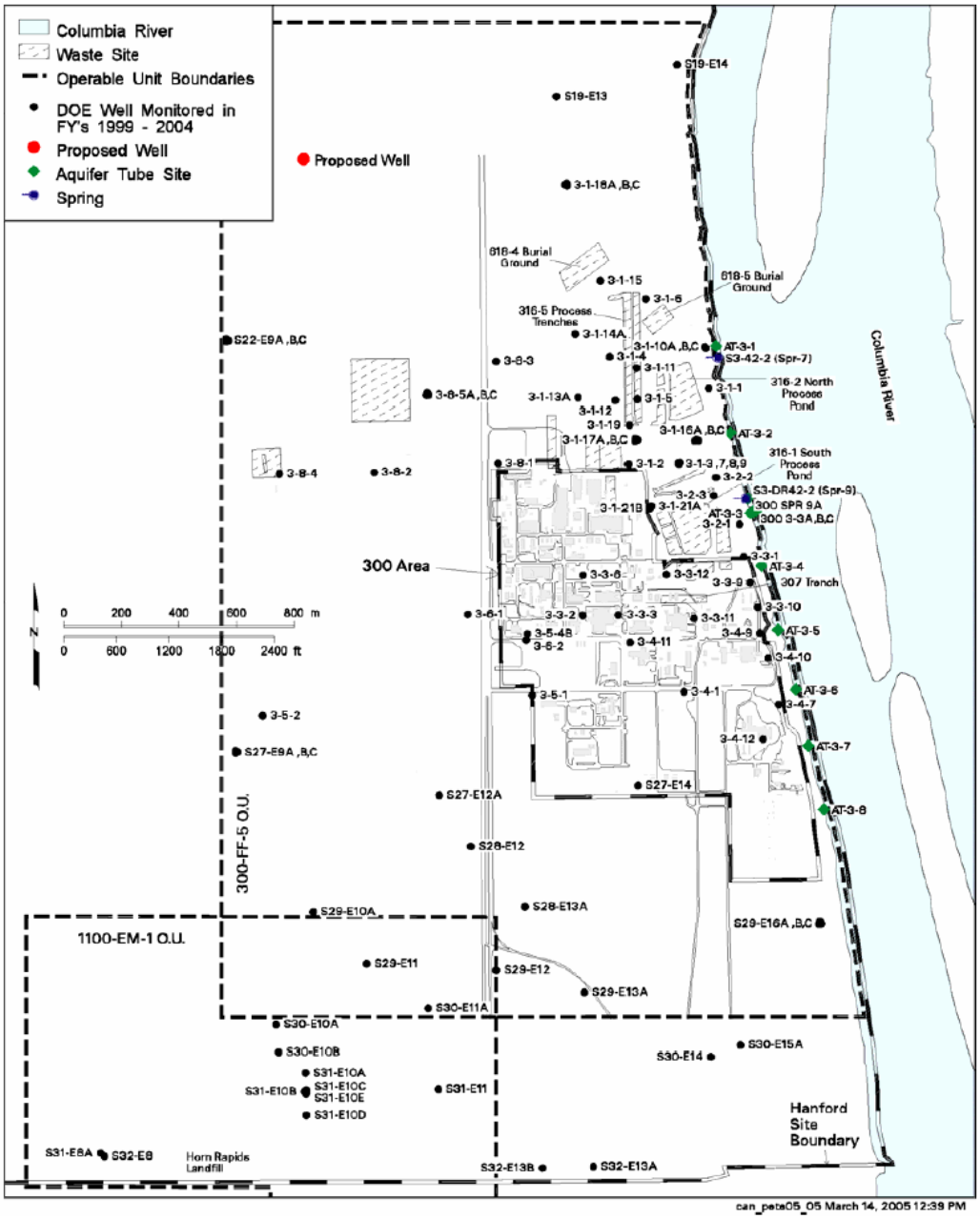

Figure 7-15. 300 Area ground water monitoring locations (Peterson, 2005)

7.2.9 Monitoring Considerations

Critical monitoring parameters to be considered in this type of environment include the collection frequency of water levels and ground-water samples. Annual monitoring of water-table levels would not likely show the short-term pulsing of the water table due to the changes in river levels. Fluctuations in the river stage not only occur seasonally, but hourly.

In addition, uranium concentrations in ground water from seeps collected at the edge of the Columbia River, near the point where ground water with the highest concentrations of uranium should discharge, were considerably lower than uranium concentrations collected from the river. This implies that there is a discharge of ground water through preferential pathways, potentially upwelling below the seep lines of the river or the uranium concentrations are coming from another source, possibly upstream. The concept of preferential pathways or the influence of river stage and pressure impact on the aquifer has not come into consideration in past ground-water models for the 300 Area. The geology consists of mostly river gravels of the Hanford Formation a highly variable formation with a likely potential for preferential pathways.

Development of semi-confined hydraulic heads due to infiltration of river water into the water table due to fluctuations in the river level could result in localized hydraulic pumping of ground water into the river. This condition may only exist for short periods of time during river level changes (Catalano et al., 2006).

Figure 7-16 provides a hydrogeologic conceptual model for movement of contaminants within the vadose zone and ground water below the 300 area in relation to changes in river stage (DOE, 2002).

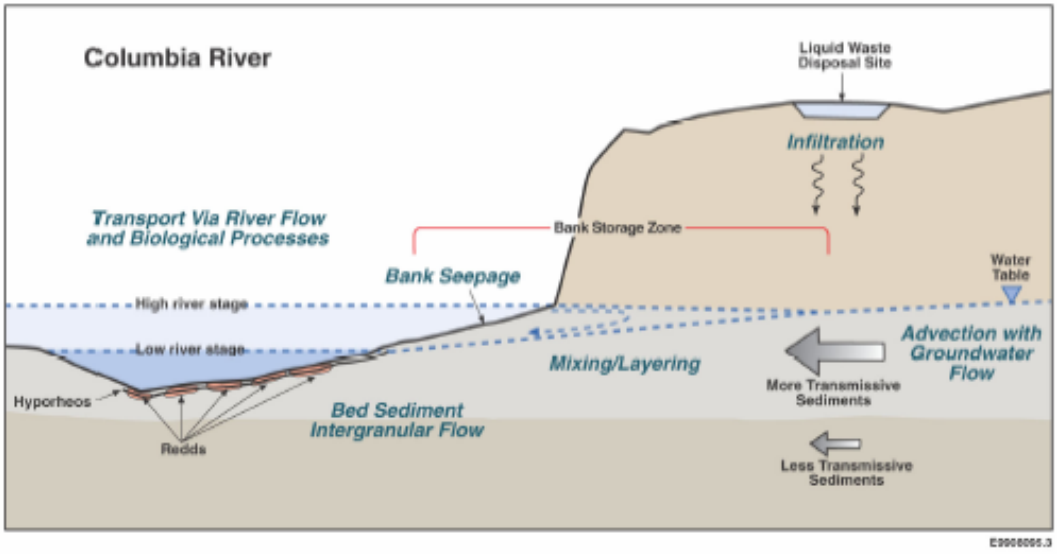

Figure 7-16. Hydrogeologic conceptual model of contaminant movement below the Hanford 300 Area (DOE, 2002)

7.3 Application of Ground Water Monitoring Performance Strategy

It is well documented that the 300-Area water table elevation changes in relation to the river stage. It is also well documented that a portion of a stream's flow may move through permeable materials adjacent to the stream. The USGS offers a stream transport simulator (OTIS) that includes inflow and storage in bank and bed materials. (Figure 7-17).

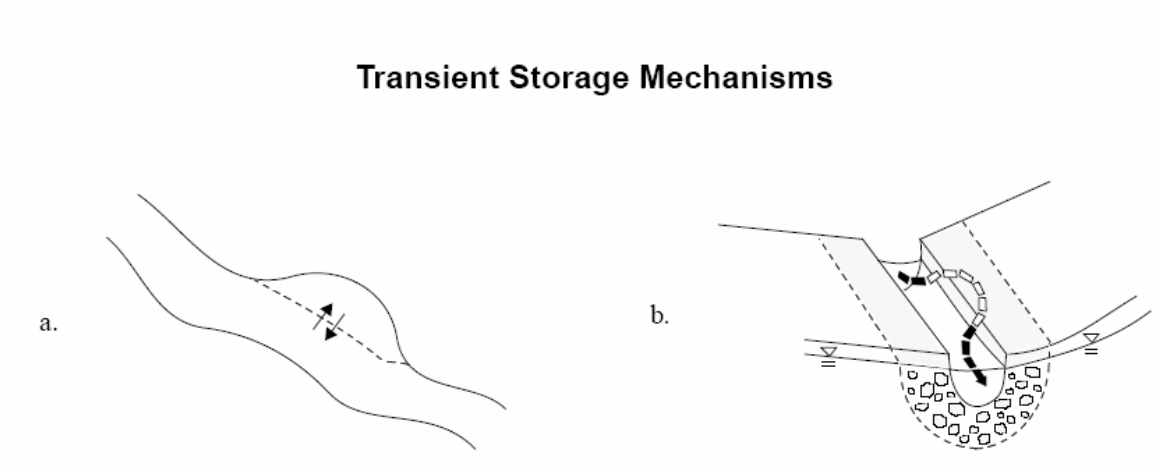

Figure 7-17. Transient storage mechanisms (Runkel, 1998)

Significant portions of the river flow may move through the coarse gravel of the streambed and, more importantly, the porous areas within the stream bank (Figure 7-17, Diagram B).

Modeling of river-ground-water interaction including surface water momentum is not generally done and requires computational hydrodynamic codes.

In the case of the Hanford 300 Area, transient migration of water into the bank of the outside bend of the adjacent Columbia River may have resulted in the downstream migration of contamination within Water Table Aquifer. As proposed in Figure 7-18, flow in the Columbia River adjacent to the 300 Area impacts the western bank (cutbank) just north of the 300 Area (north of the 618-5 Burial Ground Facility).

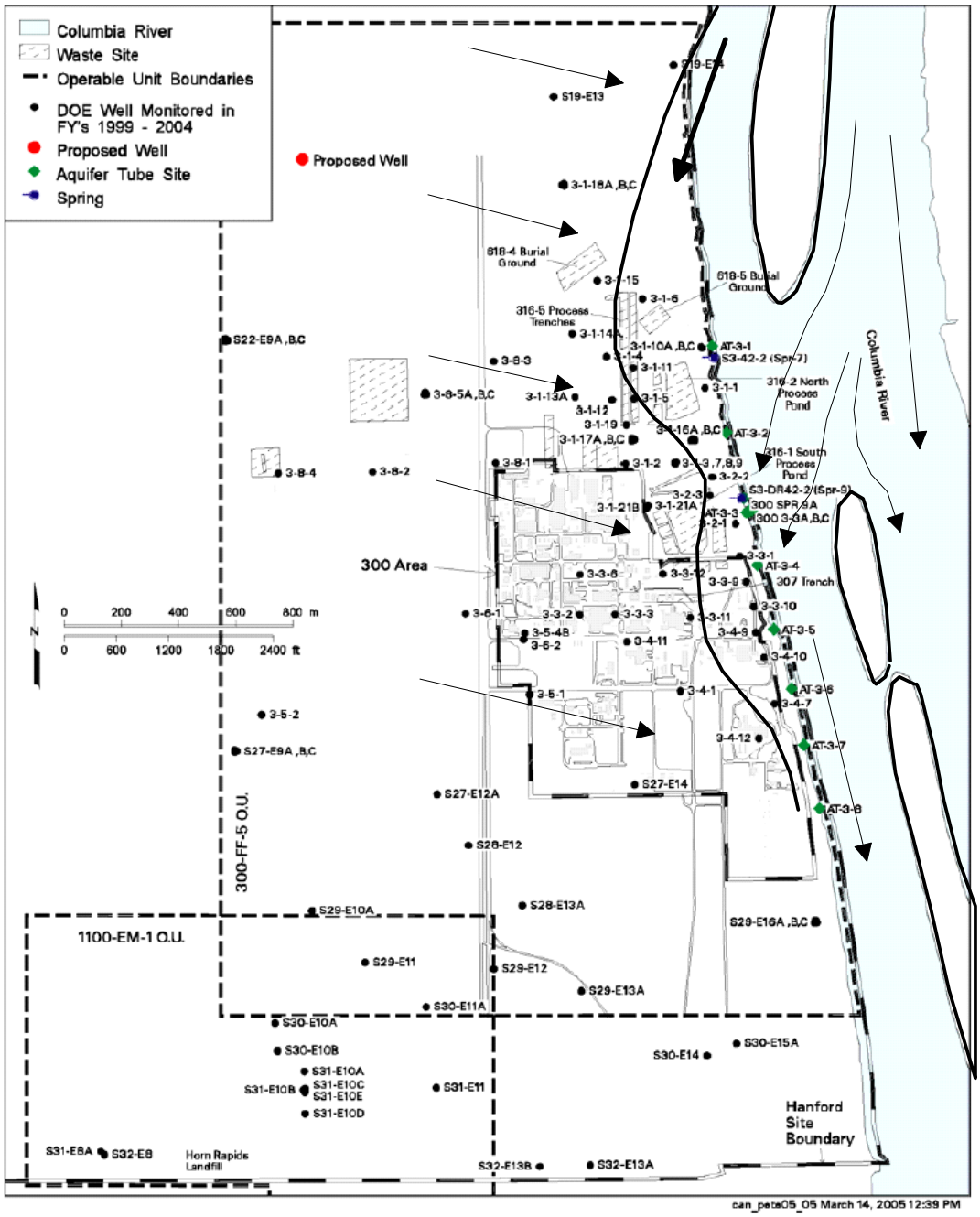

Figure 7-18. Alternative conceptual model of Hanford 300 Area showing potential infiltration and downstream flushing of formation

The arrows pointing from left to right across Figure 7-18 represent the movement of ground water towards the Columbia River. The bold arrow at the top of Figure 7-18 suggests the dominant intrusion and lateral movement of surface water from the Columbia River into the water table aquifer. The other arrows in the Columbia River follow general surface water flow. The curved line presents the conceptualized extent of surface water intrusion into the water table aquifer.

It is well documented that the water table in the 300 Area rises and falls with the changes in the river stage. The outside of bends in the river may also be impacted as well by water forced into the formation. The impact of the river on the water table may not be limited just to a simple lateral moving in and out of the formation. The water being forced into the formation can produce a "flushing effect" resulting in a downstream component of flow within the formation. Based on the geometry of the river, this flushing effect would be expected in the 300 Area in two locations: one at the upstream point where the river turns southeasterly and impacts the west river bank and adjacent to the 307 Trench, where river flow around the island adjacent to the 618-5 Burial Ground would impact the west river bank.

Figure 7-19 shows the actual extent of forced water intrusion and its effect on nitrate concentrations in ground water from 2002 (represented by the curved colored (teal) line). The shape of the contact between higher and lower nitrate concentrations mimics the shape of the water forced into the formation by the river, as proposed in Figure 7-18.

Downstream movement of water within the formation would also result in the downstream migration of contaminants as indicated for uranium in Figure 7-20 below.

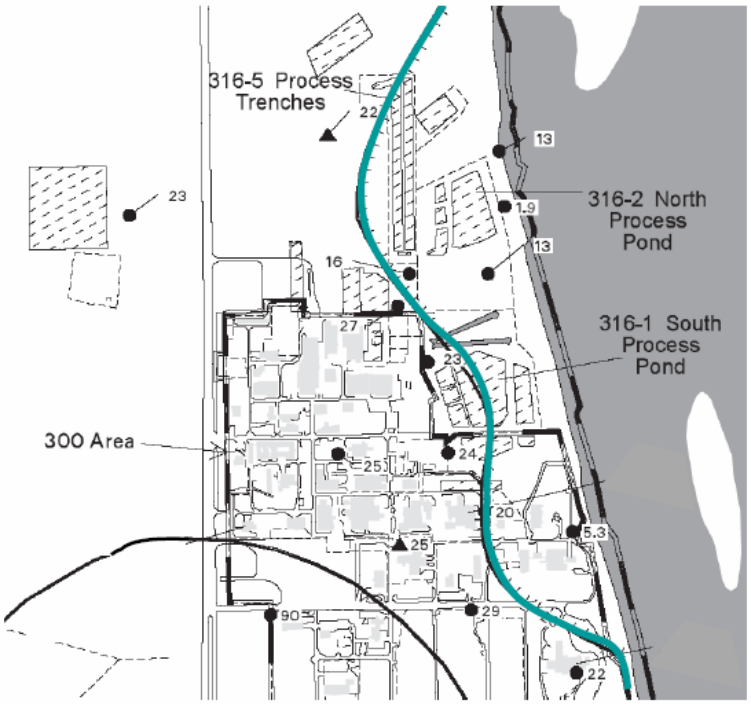

Figure 7-19. Extent of river water intrusion as estimated from nitrate concentrations in 2002(Yabusaki et al, 2004)

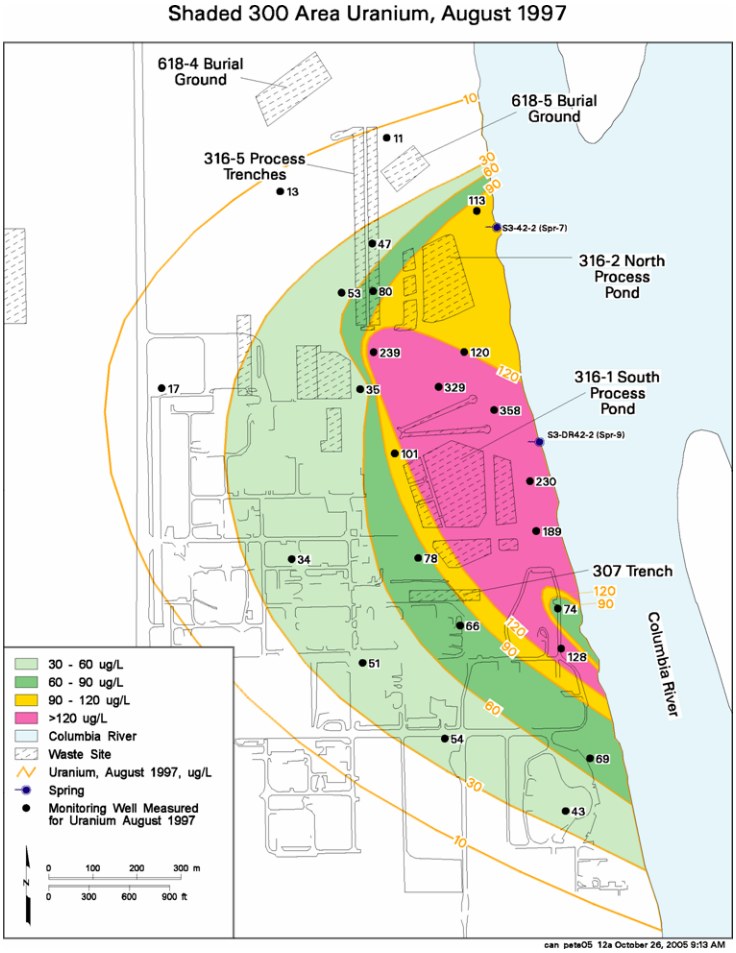

Figure 7-20. 300 Area Ground-Water Uranium Concentrations, August 1997

7.3.1 Performance Indicators and FEPs

Performance indicators and features, events, or processes (FEPs) for the Hanford 300 Area uranium plume include, but are not limited to:

The primary system performance indicators in our analysis of the Hanford 300 area are the shapes of the published uranium and nitrate contaminant plumes.

River stage is incorporated in all recent Hanford flow and transport modeling, but so far as we can determine, hydrodynamic effects of flow impinging on the cutbank of the Columbia River have not been incorporated in the CSM.

Re-analysis of existing monitoring data from wells in and near the 300 Area may provide insight into the distribution of river water components that could be related to hydrodynamic effects.

Additionally pressure measurements along the river bank might be possible.

7.4 Monitoring Strategy Application Conclusions

By applying the Strategy, we were able to perform a thorough compilation of the available geologic and hydrogeologic data for the Hanford 300 Area and gain a better understanding of the interaction of the Columbia River System with ground water.

Transient migration of water into the bank of the adjacent Columbia River at the 300 Area may produce a component of movement that can produce a "flushing effect" resulting in the downstream migration of contamination within the formation containing the Water Table Aquifer.

Thus, we have proposed an alternative to the 300 Area conceptual model that may improve the explanation of contaminant flow and transport at the Hanford 300 Area. Performance Indicators suggesting this revision to the conceptual model included the shape of the uranium plume and the position of the 300 Area on the cut bank of the Columbia River.

Hydrodynamic modeling should be evaluated as a means of evaluating the potential for a bidirectional component of contaminant movement in the water table.

Water-table monitoring collection frequencies could be adjusted to show the short-term pulsing of the water table due to the changes in river levels. Fluctuations in the river stage not only occur seasonally, but hourly. In addition, detailed changes in the river stage need to be documented. By evaluating these fluctuations in the water table in relation to the changes in river stage, conclusions can be drawn on the effects of transient migration of river water within the formation and subsequent movement of uranium.

In addition, the concept of preferential pathways could be further explored.

7.5 Hanford References

Catalano, J. G., et al. "Changes in Uranium Speciation through a Depth Sequence of Contaminate Hanford Sediments." *Environmental Science and Technology Magazine*. 2006.

Department of Energy (DOE). DOE/RL-98-48, Rev. 0, Volume II. "Ground water/Vadose Zone Integration Project Background Information and State of Knowledge." U.S. Department of Energy: Richland, Washington. 1998.

DOE. DOE/EIS-0222-F. "Hanford Comprehensive Land-Use Plan Environmental Impact Statements." U.S. Department of Energy: Richland, Washington.1999.

DOE. DOE/RL-2002-11, Rev. 0. "300-FF-5 Operable Unit Sampling and Analysis Plan." Prepared by CH2M HILL Hanford, Inc. for the U.S. Department of Energy: Richland, Washington. 2002.

DOE. Site Transition Plan for the Rocky Flats Environmental Technology Site, Office of Legacy Management and Office of Environmental Management, DOE-LM&EM/GJ-662-2005, March 2005.

Faybishenko, B. "Vadose Zone Characterization and Monitoring" in: Looney, B and Falta, R, *Vadose Zone Science and Technology Solutions*, Vol. 1.pp. 133-509. 2000.

Lindsey, K. A., et al. WHC-SD-EN-TI-012, Rev. 0 "Geology Setting of the 200 East Area: An Update." Westinghouse Hanford Company: Richland, Washington.1992.

Peterson RE (ed.). PNNL-15127. "Contaminants of Potential Concern in the 300-FF-5 Operable Unit:" Expanded Annual Ground water Report for Fiscal Year 2004. Pacific Northwest National Laboratory: Richland, Washington. 2005.

Runkel, R.L. "One-Dimensional Transport with Inflow and Storage (OTIS): A Solute Transoprt Model for Streams and Rivers." U.S Geological Survey, Water-Resources Investigations Report 98-4018. 1998.

Vermeul, V.R., et al. PNNL-14398. "Transient Inverse Calibration of the Site-Wide Groundwater Flow Model (ACM-2)." FY 2003 Progress Report. September 2003.

Yabusaki, S., et al. Powerpoint Presentation: "Objectives and Tentative Scientific Approach for Uranium Reactive transport Modeling in the 300 Area." PNNL. May 10-11, 2004.

8 Analysis of Characterization and Monitoring Data

8.1 Introduction

Accurate analysis of site characterization and monitoring data is a crucial, and often challenging, part of development of a sound ground-water monitoring strategy. This Chapter overviews data analysis methods that may aid development and implementation of the Integrated Ground-Water Monitoring Strategy, and offers suggestions for avoiding common pitfalls related to review of environmental data. While this is not a comprehensive discussion of all the issues, it focuses on lessons learned through review of site data from around the DOD, DOE, and NRC complex.

Development of an optimized ground-water monitoring strategy requires an adequate understanding of flow, transport, and risk. In some cases, careful review of existing data yields sufficient information to understand flow and transport, and thereby to choose a confirmation monitoring scheme. In other cases, additional characterization may be necessary to reduce model uncertainty in order to optimize the monitoring approach. In either case, the concepts in this chapter are intended to help you maximize the value of the data available to you. Topics covered include:

- Data types
- Basic statistical analysis
- Methods for identifying data errors and outliers
- Quality control charts and the T-Test
- Mann-Kendall Test – lessons learned
- Rainfall data – methods of analysis and sources of uncertainty
- Finding correlation between monitoring well data
- Water level measurements
- Unmixing of multimodal data
- Cluster Analysis
- Factor Analysis
- Methods for analyzing mapped data, and
- Quality assurance

In addition to these topics, we would like to emphasize the value of 3D conceptual modeling of spatial data in understanding flow and transport. In Chapters 1-7 numerous modeling examples are provided, along with modeling software recommendations. In our experience, this sort of visualization can tremendously aid in understanding a subsurface system.

8.1.1 Data Types – Characterization versus Monitoring

Generally speaking, characterization and monitoring entail different sorts of measurement activities. Specifically, characterization includes measurement of intrinsic properties of a site. Also, characterization measurements at a given point may be made only once, although some site characteristics like rainfall, response of wells to rainfall, response of

wells to tides, or establishing a water quality baseline could require extensive periods of observation. Characterization and monitoring data will have geographic and time coordinates (x, y, z, t) and may vary across the site in 4-dimensional space.

Monitoring is often measurement of something that is expected to change, with the change meaning something in terms of risk-related processes such as plume movement. Monitoring data are acquired to evaluate progress of some ongoing process, or to alert the site operator to an off-normal situation. Monitoring data are generally acquired at a fixed point in space, so vary only in time. These would include results from sampling from a device such as a lysimeter or a well that has been placed in one point. Results may derive from field measurements (e.g., pH, alkalinity, conductivity, turbidity radon …) or may derive from measurements on a sample sent to a laboratory (e.g., anion content, organic content, cation content, radionuclide content…). Establishing baseline values for measurements to be made at a monitoring point, (x, y, z, t) is part of characterization, and detecting changes in the baseline are part of monitoring effort.

Much of the uncertainty in estimating risk from subsurface contamination can be traced to uncertainty in site characterization and monitoring design. For example, it does not matter if a ground-water sample is analyzed to femto-Curie levels of Sr-90 if the sampling point is not chosen appropriately. Similarly, it does not matter if a flow and transport model is built and forced to calibrate if features in the site geology that control flow are not characterized adequately.

In addition, selection of appropriate chemical methods is important. It does no good to monitor for a given constituent of concern if the method detection limit is not below regulatory requirements or other action levels (Example: method detection limit is 10 mg/L and the MCL is 1 mg/L). Ideally methods should be chosen to provide quantitative data for all analytes at their ambient levels, with very few “below detection” results. Missing values, or truncated data sets, limit one’s ability to glean understanding of the system being tested.

An Integrated Ground-Water Monitoring Strategy does not include site characterization and pre-operational monitoring, but must include review and evaluation of characterization data and existing monitoring data in order to select critical monitoring points within the system. If characterization is adequate, and if the characterization has been used correctly in flow, transport, and risk models, then the task of confirmation monitoring design is simplified.

If characterization is not adequate, then selection of monitoring points is more difficult. The site manager must decide whether the risk associated with the remaining uncertainties is acceptable or not, and take appropriate action. This action could mean re-running a Performance Assessment (PA) model, and could also include filling gaps in characterization if the PA indicates unacceptable risk. Reducing model uncertainty by installing monitoring systems could be called characterization.

8.1.2 Data Evaluation versus Statistical Analysis

The distinction between data analysis and statistical hypothesis testing is important. Many of the data analysis techniques violate assumptions made in formal statistics, but

produce useful results; likewise, many formal statistical tests may provide useful insight even when the data tested (e.g., log-normal data) violate the test assumptions.

Data evaluation is the process of looking for associations, trends, patterns, or outliers in the data. The purpose is to alert an investigator to something in the data structure that may have implications about a process or anything that might have meaning to the investigator. Multivariate data analysis has recently been popularized as "data mining."

Statistical analysis of data is the process of testing a data point against some hypothesis about the data. Classically this comes from quality control in a production operation or manufacturing setting. Section 8.1.3, below contains a more detailed discussion on quality control analysis using the T-Test.

Below are several recommended sources for additional reading about data evaluation and statistical analysis:

Velleman, Paul F., article in The American Statistician (1993) 47:1, 65-72 (and its discussion in various internet sources) presents an enlightening discussion of this topic.

EPA (2003, 2004), in their *Guidance for Monitoring at Hazardous Waste Sites*, discusses some of the objectives of data analysis and statistical testing. Their discussion is from a different viewpoint than that presented here, but the common feature is that the purpose of the data analysis is to provide a person or team with a basis for making a decision either about the monitoring system or about what the data are telling in terms of risk so that a decision can be made.

NIST (2004) has an online statistical handbook that goes into depth on data analysis. They list the objectives of data analysis:

1. Maximize insight into a data set;
2. Uncover underlying structure;
3. Extract important variables;
4. Detect outliers and anomalies; and
5. Test underlying assumptions.

They also point out that there is no prescription for data analysis. The operator must understand the philosophy of data analysis and apply this to the problem at hand.

8.2 Univariate data

Univariate means basically that we consider one variable at a time. In nature we often find that the population from which we draw samples is formed from the mixing of several sources. For example, copper in soil samples may be ascribed to underlying bedrock, or two types of bedrock and to atmospheric deposition from a smelter. Even contaminants, such as TCE, in a given water sample may be present from leaking tanks at multiple upgradient areas.

Sometimes it is obvious that there are multiple sources for a given analyte, and we can estimate how to partition the data so as to better understand the sources. Sometimes the underlying chemical or geochemical processes leading to the observed values produce a

time-varying distribution – for example, a spill or burial may dissipate with time. This might result in monitoring observations that fit an exponential function.

Univariate populations may fit the familiar so-called normal or Gaussian distribution. Sometimes taking the logs of the data may produce an apparent fit to the normal curve. A number of distribution types have been recognized by statisticians, and statistical tests have been developed for each. Most familiar statistical terms such as the Pearson product-moment correlation coefficient assume a Gaussian distribution and lose meaning for strongly skewed data sets.

Statistical tests that do not depend on the population or sample distribution have been developed. Generally these are based on ranking the numbers and using ranks rather than values. (c.f. Kendall, 1975; Siegel, 1956) This chapter only provides a glimpse at some practical issues so that the data problem holder will seek expert help for data analysis.

8.2.1 Basic Statistical Analysis

Basic univariate analysis includes the computation of the mean (Equation 1), standard deviation (Equation 2), variance (square of the standard deviation), coefficient of variation (standard deviation divided by the mean), and identification and possible rejection of extreme observations (discussed in Section 8.2.2 below).

Equation 1. Mean

$$m = \frac{1}{N}\sum_{i=1}^{N} H_i$$

Equation 2. Standard deviation

$$\sigma = \sqrt{\frac{\sum_{i=1}^{N}(H_i - m)^2}{N-1}}$$

In the above equations, m is the sample mean of the observations, N is the number of observations, H is the observed values, σ is the standard deviation of the observations.

For time-series data sets, trend analysis with the Mann-Kendall test provides us more information about the temporal variation of the water heads and concentrations. The Mann-Kendall test is discussed in detail in Section 8.2.4 below.

8.2.2 Identification of Outlier Points

An important part of data analysis is identification and assessment of potentially erroneous data points. A measurement may be read, recorded, or transcribed wrongly, or a mistake may be made in the way in which a treatment was applied for this measurement. A major error greatly distorts the mean, the standard deviation, the variance, and the coefficient of variation, and affects conclusions about the trends and correlations. The principal safeguards are vigilance in carrying out the operating instructions in the measuring and recording process, and eye inspection of the observation data.

If a figure in the data to be analyzed looks suspicious, an inquiry about this observation sometimes shows that there was a gross error. If no explanation of an extreme observation is discovered, we may consider rejecting it. The discussion of rules for the rejection of observations began well over a century ago in astronomy and geodesy. Most rules have been based on something like a test of significance (Snedecor and Cochran, 1976). The investigator computes the probability that a residual as large as the suspect would occur by chance if there is no gross error. If this probability is sufficiently small, the suspect is rejected. Anscombe and Tukey (1963) present a rule that rejects an observation whose residual has the value of d if $|d| > Cs$, where C is a constant to be determined with the following equation which is obtained from Snedecor and Cochran (1976), and s is the standard deviation of the observations calculated from Equation 2.

Equation 3. Anscombe and Tukey significance test

$$C = K\left(1 - \frac{K^2 - 2}{4(N-1)}\right)\sqrt{\frac{N-1}{N}}$$

$$K = 1.4 + 0.85z$$

In Equation 3, N is the number of the observations, z is corresponding to the one-tailed probability value of $\frac{N-1}{N}P$ in the normal distribution, where P is the small premium which is involved in a rejection rule, say 2.5% or 5%.

After rejecting the outlier points, we carry out the statistical analysis with the treated data sets. The results are compared with those obtained with the original observation data sets.

8.2.3 Quality Control Charts: the T-Test

A classic example of statistical analysis is 'Student's T-Test'. This test is often used to analyze monitoring well results and other types of univariate analysis. Originally, William Sealy Gossett developed this test to detect off-normal conditions in the production of Guinness beer. In this case, a new measurement (e.g., sugar content, specific gravity…) can be compared with historical data representing "normal" conditions. The result is a confirmation or rejection of a hypothesis that the new measurement is drawn from the normal population. Because any introductory statistics text will include the T-test, we will not discuss it further here.

The results of a T-test can be expressed graphically in the form of a "control chart" for process monitoring on which the target value is plotted as a horizontal line against time with parallel lines at the uppermost and lowermost "normal" bounds (at some confidence level for acceptance of the "is normal" hypothesis) (Figure 8-1).

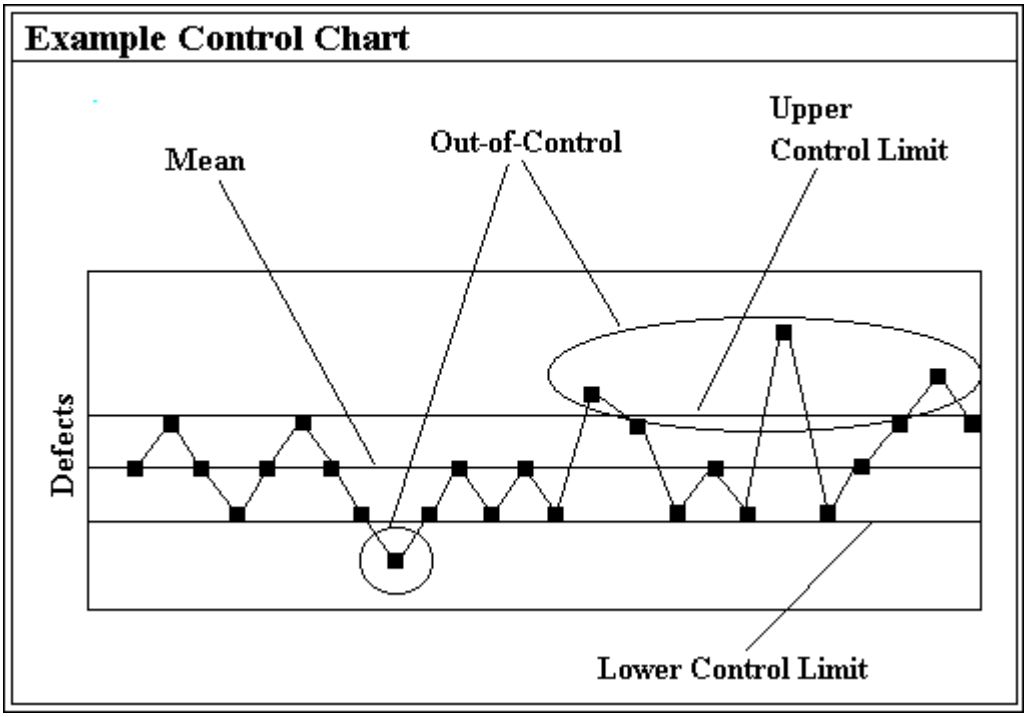

Figure 8-1. Example control chart

A version of this method is typically used in ground-water monitoring programs to spot anomalous results as they are returned from the lab. Characterization, or pre-operation monitoring is used to establish an expected range for some variable – say pH, or water level. This expected range is used to bound 'normal' values for the variable – and periodic measurements are compared to the normal value, commonly by displaying them on a chart. Visual inspection of the chart or a computerized notice alerts the operator to an off-normal condition. The operator then decides on an action. In the case of a plant producing thousands of items per hour, this may mean an immediate adjustment of operating conditions. In the case of a ground-water monitoring result, the action might include a recheck of the analysis, and following that, possible re-sampling of the field site. All off-normal results should be referred to technical experts for evaluations – the job of inspecting control charts is often assigned to technicians who may not have the perspective to fully evaluate the potential meaning of an off-normal observation..

If the off-normal condition is confirmed, then its meaning must be determined so that any possible risk implications can be judged. This may mean re-running a computer simulation, it may mean revising a conceptual model. It could indicate a release of contamination, or the impending approach of an unknown plume. It could point to an analytical or sampling problem. It may trigger a regulatory reporting requirement. Interpretation is the responsibility of the individual investigator in the context of extensive site-specific knowledge.

Time-trends are also revealed with the control chart method. Changes in variance or upward or downward trends in the mean will be revealed in such a chart. This is especially important in judging behavior of a contaminant plume, or for tracking progress of a remediation process.

The methods of univariate data analysis and statistics have been developed mainly since the 18th century: Gauss, Bayes onward. The reader is referred to basic statistics texts for information. My favorite is: Peatman, John G., (1936, '41, '47) "Descriptive and Sampling Statistics."

Guidance

When preparing a control chart:

- Plot all measurements against time.
- Watch for changes in variance.
- Watch for data outside the expected range.

8.2.4 Applying the Mann-Kendall Test

To evaluate the presence of trends in the time-series observations at individual monitoring wells in this report, we applied the Mann-Kendall test, which is commonly reliable in the interpretation of environmental data (Helsel and Hirsch, 2002; Soderberg et al., 2005). This test is often applied on data sets from monitoring wells to assess the stability of a contaminant plume and it is an important tool in the decision making process that relates to ground-water monitoring network design.

The Mann-Kendall test is non-parametric and therefore does not assume an underlying distribution in the data sets. It can address missing data values and be modified to account for seasonality or predictable fluctuations (Soderberg et al., 2005). In the Mann-Kendall test, a statistical parameter *S* is valuated with Equation 4 by comparing each data point to the data points that occur after it in the time series (Gilbert, 1987).

Equation 4. Mann-Kendall test

$$S = \sum_{i=1}^{N-1} \sum_{j=i+1}^{N} \operatorname{sgn}(H_j - H_i), \qquad \operatorname{sgn}(H_j - H_i) = \begin{cases} 1, & \text{If } H_j - H_i > 0 \\ 0, & \text{If } H_j - H_i = 0 \\ -1, & \text{If } H_j - H_i < 0 \end{cases}$$

In Equation 4 above, *H* indicates observed values, and the sign of *S* indicates the direction of the trend (i.e. positive *S* indicates an upward trend, negative indicates a down trend and 0 value indicates flat or no trend). *S* and *N* are then used to read a p-value from a statistic table (Gilbert, 1987), and the p-value is a measure of the significance of the trend. When $N < 10$, a two-tailed test is used to test for both upward and downward trends in a single alternative hypothesis.

For large data set ($N > 10$), *S* can be modified to be approximated by a normal distribution. Another statistical parameter, *Z,* is calculated by Equation 5:

Equation 5. Z calculation

$$Z = \begin{cases} (S-1)/\sigma_s & \text{If S} > 0 \\ 0 & \text{If S} = 0 \\ (S+1)/\sigma_s & \text{If S} < 0 \end{cases}$$

$$\sigma_s = \sqrt{\frac{N(N-1)(2N+5) - \sum_{i=1}^{N} T_i i(i-1)(2i+5)}{18}}$$

In the above equation, T is the number of tied values. With a calculated Z value we can compute a p-value from the normal distribution to evaluate the significance of the trend found from S value.

The example in Figure 8-2 below illustrates how simple the Mann-Kendall test really is. The next few figures illustrate that use of this simple test may, in some cases, actually obscure information that should be gleaned from the data. We provide this as an example to make the reader more aware of possible sources for misinterpretation when applying this test.

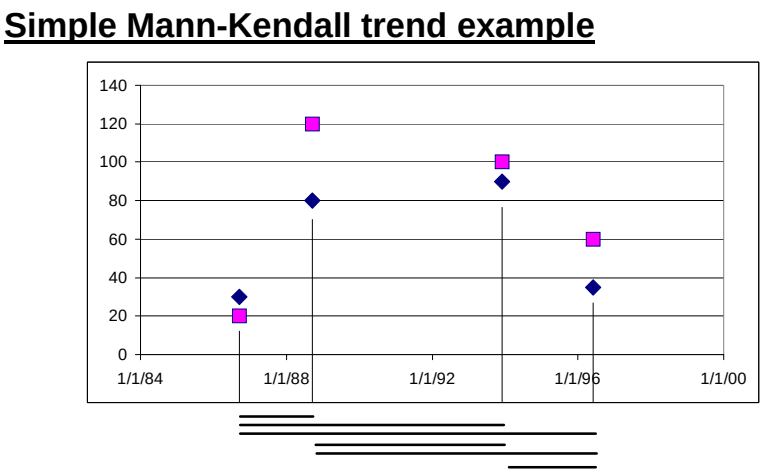

N (number of data points) = 4 (6 comparisons)

	◆	■
from initial data point --	+3	+3
from second data point --	0	-2
from third data point --	-1	-1
S (sum of sgns) =	+2	0

Data Analysis and Visualization, 11/30/05 19

Figure 8-2. Mann-Kendall Example

Figure 8-3, labeled "Seasonal Kendall Slope Estimator," shows PCE concentrations over several years at a monitoring well. For each sampling point a determination is made as to whether the subsequent sampling events result in a higher of lower concentration. The plotted data in Figure 8-3 yield a -18 value – or a strong downward trend.

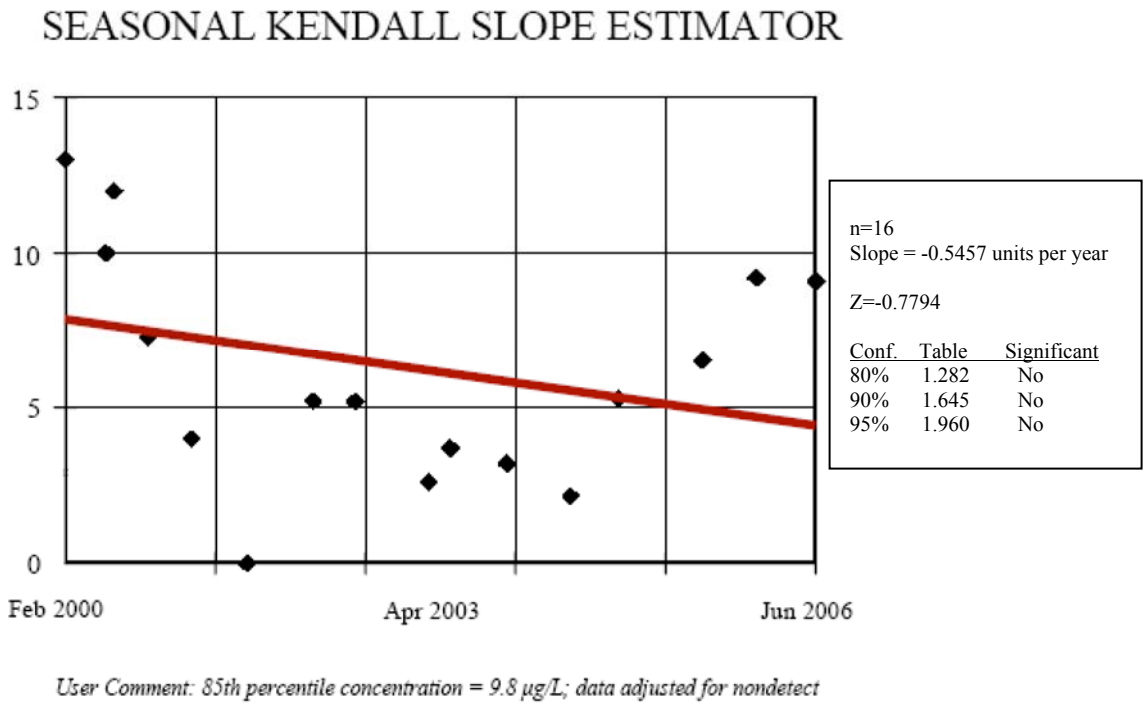

Figure 8-3. Published figure indicating declining PCE concentrations in ug/L (DOE, 2006)

A simple linear regression evaluation of the data provided in Figure 8-3 is represented in Figure 8-4. This simple regression evaluation also shows an overall reduction in PCE concentrations over time. However, a closer examination of the data reveals a steep downward trend over six sampling events, followed by an upsurge and gradual decline over the next six sampling events, and finally an increasing concentration trend for five sampling events.

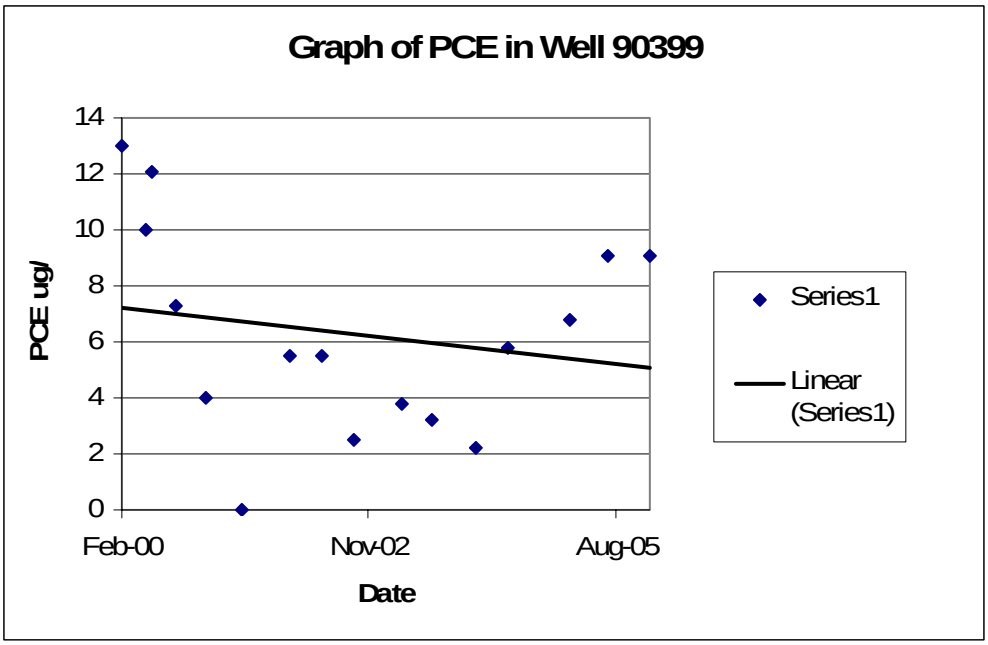

Figure 8-4. Linear regression fit to PCE data from MS-EXCEL

Figure 8-5 shows the data broken into three groups with trend lines for each. It is possible that the three slopes represent some hydrogeological phenomenon such as contaminant release from a pool or from the vadose zone as a function of infiltration or water level. We discuss a similar example at Rocky Flats elsewhere in this document. The line equations are of the form y=mx+b, where m is the slope and b the intercept. Excel uses Julian dates which are around 30,000, but displays dates as days, months, and years, thus the slope is a very small number even though the line plots as a steep line.

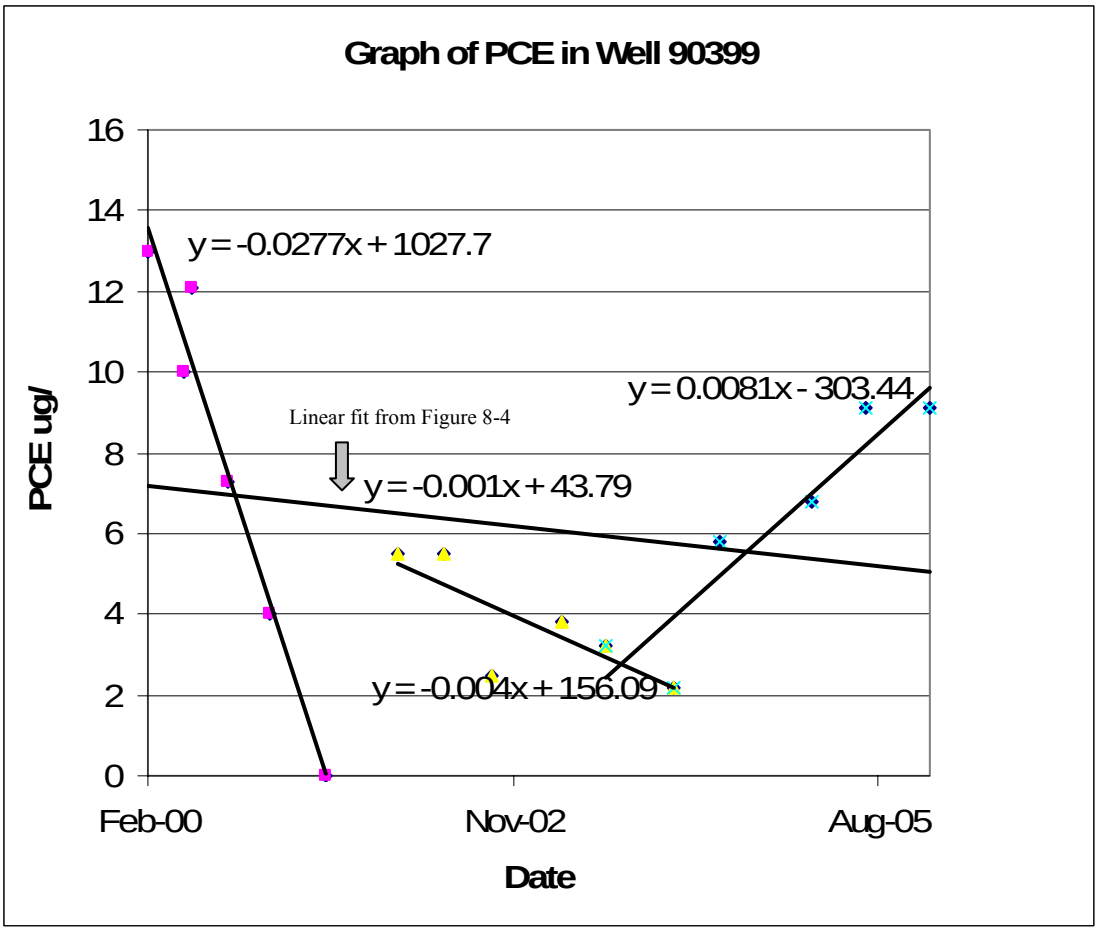

Figure 8-5. Parsing time series data into three groups.

The simple determination that there is an overall downward concentration with time at this observation point is correct. Unfortunately, presenting only this conclusion may obscure the fact that the ground water / contaminant system is displaying complex behavior that might indicate future non-compliant excursions of contaminant concentrations.

An example based on monitoring of VOCs at the DOE Rocky Flats Site is discussed in Chapter 5 above. In the example monitored results decline and remain low for long periods of time until an unusual weather event seems to flush contaminant from a bedrock pool into the water table flow system. This example provides insight into the issue of when to stop monitoring. Weather, including decade-long precipitation cycles may control apparent trends in contaminant amounts.

8.3 Rainfall Data – Sources of Uncertainty for Infiltration

Infiltration rates and permeability are two key variables controlling the accuracy of ground-water flow and transport models. Infiltration comes from rainfall and from engineered features such as leaking water systems and disposal or retention ponds. This section provides background for understanding uncertainty in infiltration. It specifically

illustrates the importance of exploring all possible water sources when developing a conceptual model, and the importance of verifying that rain station data matches observed site conditions.

8.3.1 Consider All Water Infiltration Sources

Often the amount of leakage from water supply systems is poorly known. It can be estimated by shutting off the water supply to and from storage tanks and measuring loss over a period of time. A forty year old water system at the Savannah River Site in a non-industrial area – i.e. where drinking, sanitary supply, and fire suppression were the only water lines in about a five-acre area – was shown to leak almost 100 gpm, which would have gone undetected had the supply well not been turned off in support of aquifer performance testing (ref. personal knowledge). That was about one gallon per square foot per day. Because the leakage was underground in a grassy or paved area, most of this water moves downward as infiltration. By way of contrast, infiltration from rainfall was on the order 15" of rain per year or one cubic foot per square foot per year. That was 7.5/365 gallons per square foot per year or 0.02 gallons per square foot per day. Thus infiltration from leaking water lines was much greater than natural infiltration in this area. This case illustrates the importance of identifying all known water sources, natural and man-made, that could influence a system, and assessing the impact that these sources could have on the water table and infiltration.

8.3.2 Ensure Rain Station Data Match Facility-Specific Gauging

Infiltration is often estimated from rain gauging stations and estimates of the balance between evaporation, runoff, and infiltration. In the next few paragraphs, tables and figures will illustrate that facility-specific gauging should be done if local rainfall is to be known with any precision.

The Savannah River Site has a number of weather and rain gauging stations. We are grateful to the DOE Savannah River Operations Office for access to daily rainfall data.

The raw data from the five rain gauging stations presented in Figure 8-6 include 8000 records taken over 22 years. Visual presentation of data points in scatter plots by month reveals that while winter rainfall patterns are relatively uniform over a large area, summer rainfall varies significantly even at short distances. Figure 8-7 compares rainfall data from the mid-1980's through 2002 at Stations F and H, which are located just two miles apart. In this graph, Station F data is on the Y axis and Station H is on the X axis. Perfectly correlated data would group along a single line. As we can see from the data in July, rainfall measurements are quite scattered indicating that rainfall at one station is not indicative of the same intensity of rainfall at the other due in part to frequent isolated thundershowers. January data is more tightly grouped and is representative of data seen in the winter months due in part to the passage of large weather systems.

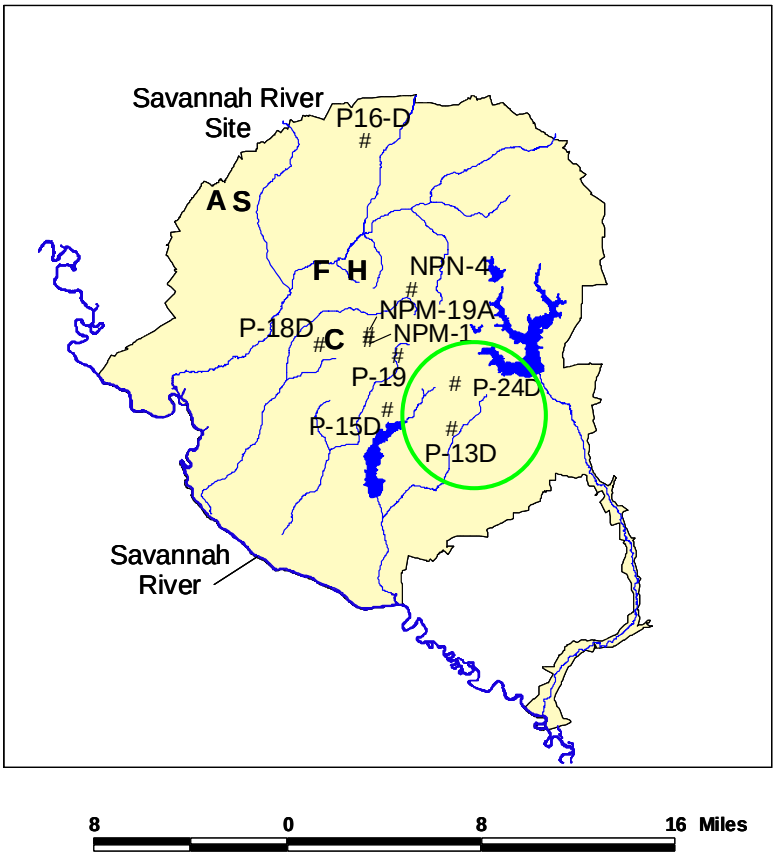

Figure 8-6. SRS rain gauging station and well locations. Rain stations are located under respective station identifier A, C, F, H, and S. Well locations are denoted by black dots. Adapted from Jones, 1990.

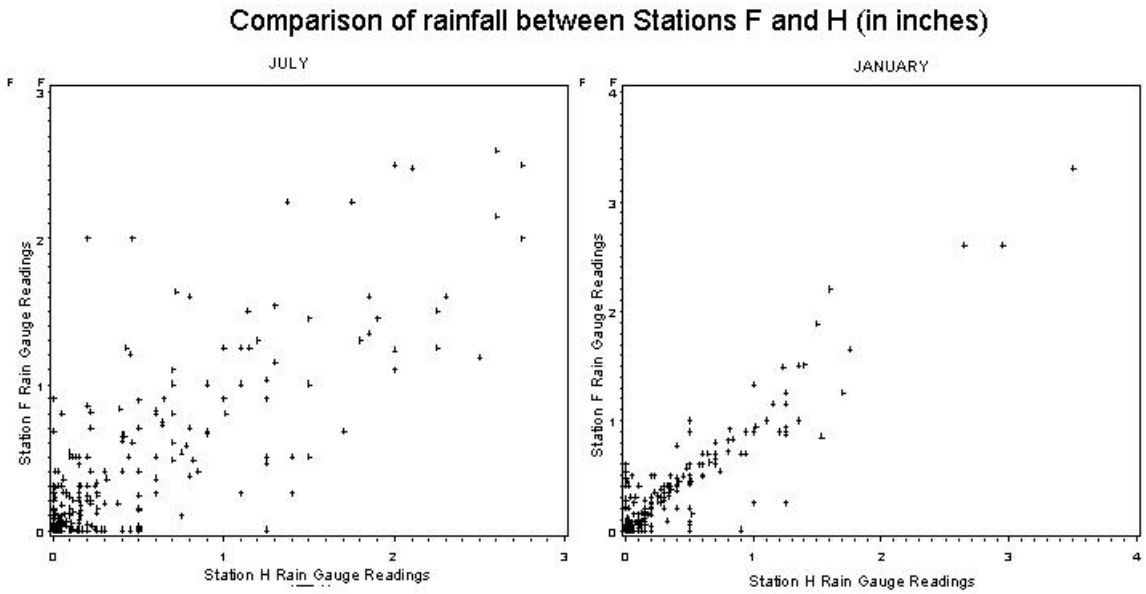

Figure 8-7. Rain data for Stations F and H, which are only two miles apart, show that particularly in summer, rainfall patterns are highly variable, even over short distances.

Figure 8-8 compares 17 years of rainfall data at Stations C and S. The Figure illustrates that at a distance of seven miles, rainfall readings vary significantly. In July, for example, it is not uncommon to see a variation of more than an inch between stations.

In Figure 8-9, data from all five stations was used to show the correlation as a function of distance. As shown in the Figure, summertime rainfall patterns are significant, and vary much more than winter rainfall. Another possible factor is the azimuthal relation between gauging stations. Winter or summer, most weather systems move from west to east in this area. Station H is almost due east of station F, whereas station S is almost due north of station C.

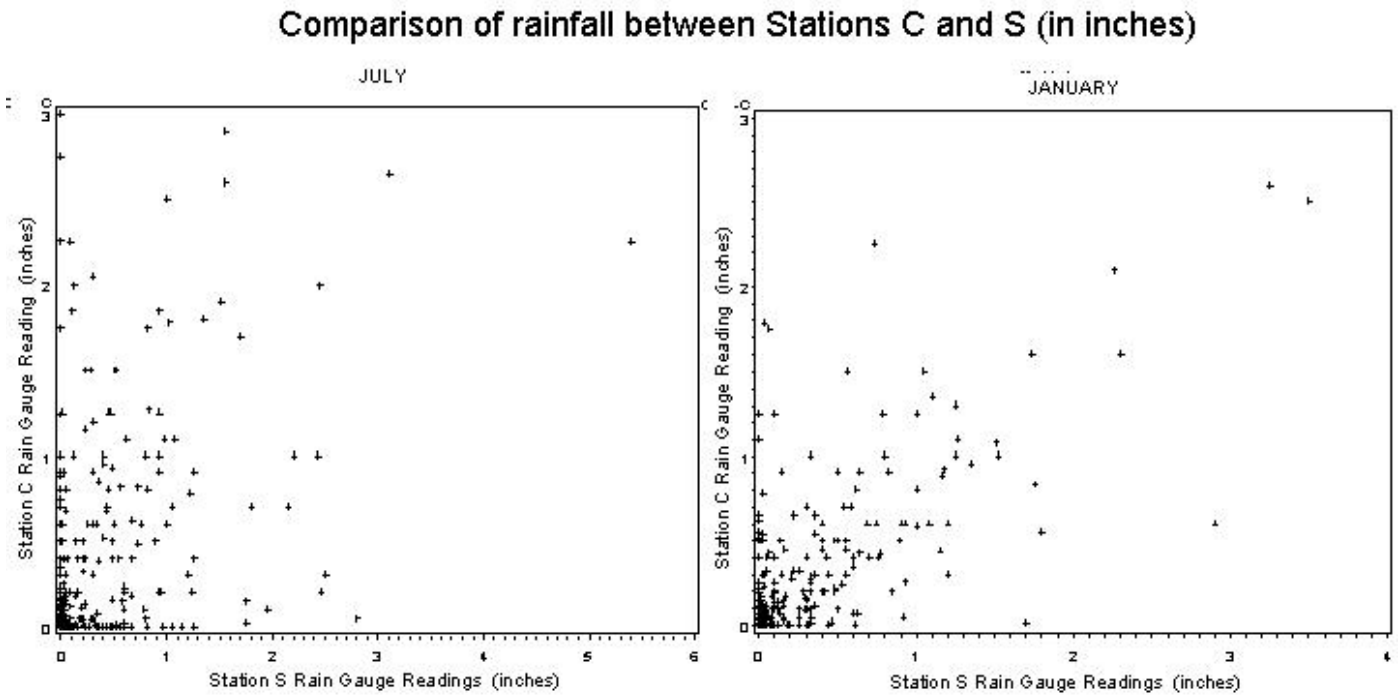

Figure 8-8. Rain Gauges C and S are about 7 miles apart and show significant variation in observed rainfall.

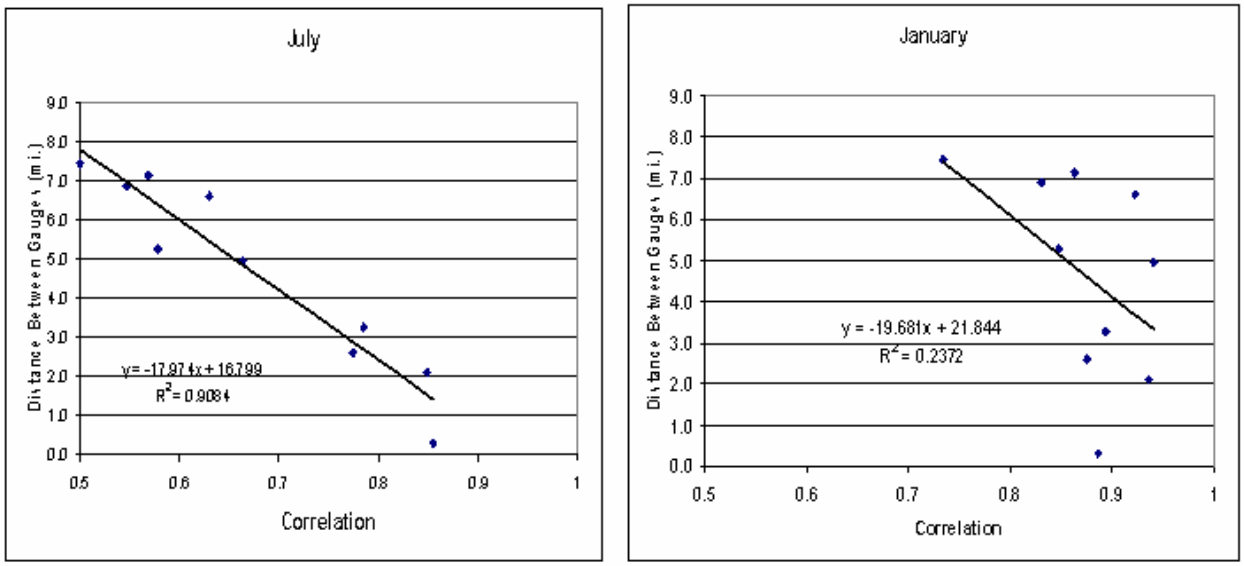

Figure 8-9. Correlation of rainfall as a function of distance in July and January.

This case illustrates the need to ensure that rain measurements used in conceptual modeling match actual observations. A surprisingly short distance can make a large difference in the amount of rainfall received. Further, the correlation between rainfall and distance to the station can vary significantly by season. Site managers should be aware of this phenomenon if observed data do not closely match modeled contaminant movement.

8.4 Correlations between different wells

To interpret the relationship between data in different monitoring wells, we can compute the correlation coefficients among them. Understanding the correlation between wells can help us to analyze the hydrogeologic conditions and build the conceptual site models. For example, the correlations between two wells which are located in two aquifers separated by a confining layer, may give us information about the continuation of the confining layer and the hydraulic connections of the two aquifers. The correlation coefficient (ρ_{ij}) is computed by Equation 6 below.

Equation 6. Correlation coefficient

$$\rho_{ij} = \frac{C_{ij}}{\sigma_i \sigma_j} = \frac{E(H_i H_j) - m_i m_j}{\sigma_i \sigma_j}$$

where C_{ij} is the covariance. H indicates the observed value, E is the expected frequency, and m is the mean. Considering the significance of the correlation, we define:

If $\rho_{ij} > 0.9$, H_i and H_j are positively correlated;
If $\rho_{ij} < -0.9$, H_i and H_j are negatively correlated;
If $-0.1 < \rho_{ij} < 0.1$, H_i and H_j are not correlated, or independent.

A real data set from Savannah River Site, South Carolina, is used to test the statistical methodology introduced above. In this data set, there are water head observations from

137 monitoring wells, in which each well includes about 16 time-series water head observations. The computer code developed here is used to compute the mean, variance, standard deviation, coefficient of variation, and the Mann-Kendall trend parameter for each well. To evaluate the significance of the trends, we also compute the p-value for each trend analysis. Finally, the correlation coefficients between different monitoring wells are calculated to help us to evaluate the conceptual site models for ground-water flow and transport modeling. The results of the first 10 wells of this data set are listed in Table 8-1. Fortran 90 code for the computations is included as Appendix B to this chapter.

Figure 8-10 presents selected water head curves to demonstrate the results from statistic analysis. Wells P-15D and P-18D, P-15D and P-19TD, P-15D and P-25TA, and P-19TD and P-25TA are positively correlated, P-15D and P-22D are negatively correlated, and P-22D has a downward trend but all others have an upward trend. An outlier point was removed from P-18D, P-19TD and P-25TA.

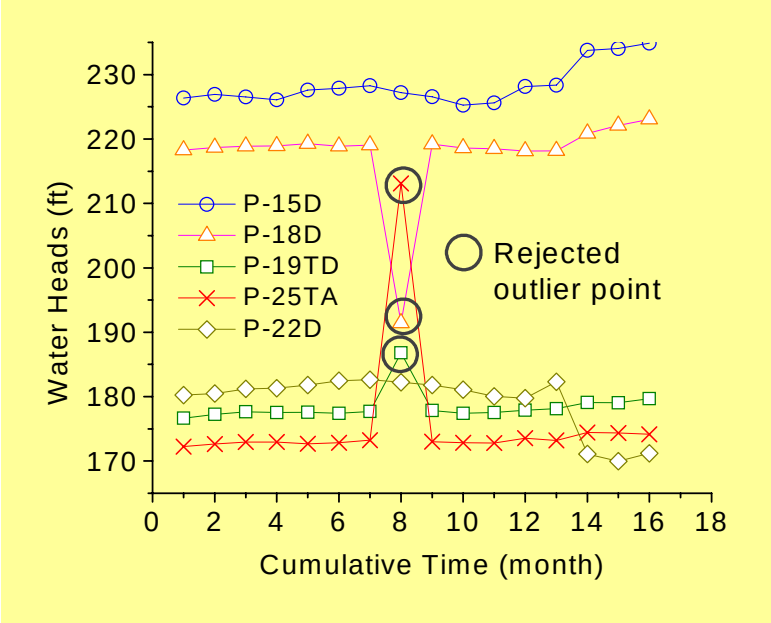

Figure 8-10. Rejection of outliers

The three outlier points shown in Figure 8-10 are on the same date at widely-spaced wells. On this same date, other wells do not show unusual water levels. It is very likely that a sampling error was made, and that no-one checked the data before they became part of the permanent database.

Laboratory analytical data for this database are always compared to trends from the previous three results, and a deviation calculated. When the deviation is greater than a certain portion of the average deviation of previous measurements or exceeds a regulatory limit, the new point is flagged for human review. This simple QA check can and should be implemented as data from field measurements are entered into any database.

QA is discussed further below.

Table 8-1 . Statistical analysis of water head observations from Savannah River Site

Original Statistic Analysis of the Observations

WellNam	AqNam	ObNm	MinVal	MaxVal	MeanV	Varian	Stand	CoefV	Mann	ModM	Trend	p-val
P-15D	WT	16	225.27	234.90	228.34	8.83	2.97	0.013	58.	2.57	Uptrend	0.005
P-16D	WT	16	210.41	216.96	214.20	3.41	1.85	0.009	-39.	-1.72	Downtren	0.044
P-16TC	uprK	16	220.15	221.50	220.74	0.11	0.33	0.002	11.	0.45	Uptrend	0.320
P-17D	WT	16	275.47	285.06	276.98	5.30	2.30	0.008	-24.	-1.04	Downtren	0.153
P-18D	WT	16	191.44	223.06	217.63	47.61	6.90	0.032	27.	1.17	Uptrend	0.122
P-19TD	TD	16	176.65	186.80	178.46	5.20	2.28	0.013	73.	3.27	Uptrend	0.001
P-19TC	uprK	16	176.72	179.59	177.99	0.45	0.67	0.004	80.	3.56	Uptrend	0.000
P-22D	WT	16	169.98	182.62	179.35	17.77	4.22	0.024	-31.	-1.37	Downtren	0.085
P-24TA	TA	16	180.85	184.34	183.11	0.69	0.83	0.005	0.	0.00	Flat	0.500
P-25TA	TA	16	172.25	213.12	175.69	93.77	9.68	0.055	63.	2.80	Uptrend	0.003

Modified Statistic Analysis of the Observations (After rejecting the outlier points)

WellNam	AqNam	ObNm	MinVal	MaxVal	MeanV	Varian	Stand	CoefV	Mann	ModM	Trend	p-val
P-15D	WT	16	225.27	234.90	228.34	8.83	2.97	0.013	58.	2.57	Uptrend	0.005
P-16D	WT	16	210.41	216.96	214.20	3.41	1.85	0.009	-39.	-1.72	Downtren	0.044
P-16TC	uprK	16	220.15	221.50	220.74	0.11	0.33	0.002	11.	0.45	Uptrend	0.320
P-17D	WT	15	275.47	279.31	276.44	1.01	1.00	0.004	-19.	-0.89	Downtren	0.189
P-18D	WT	15	218.12	223.06	219.37	2.02	1.42	0.006	26.	1.24	Uptrend	0.108
P-19TD	TD	15	176.65	179.69	177.90	0.59	0.77	0.004	74.	3.65	Uptrend	0.000
P-19TC	uprK	16	176.72	179.59	177.99	0.45	0.67	0.004	80.	3.56	Uptrend	0.000
P-22D	WT	16	169.98	182.62	179.35	17.77	4.22	0.024	-31.	-1.37	Downtren	0.085
P-24TA	TA	16	180.85	184.34	183.11	0.69	0.83	0.005	0.	0.00	Flat	0.500
P-25TA	TA	15	172.25	174.45	173.19	0.40	0.63	0.004	64.	3.13	Uptrend	0.001

Following Wells are Highly Positively Correlated: R > 0.95

P-17D	WT	and	P-18D	WT	0.95
P-19TD	TD	and	P-19TC	uprK	1.00

Following Wells are Positively Correlated: 0.9 < R < 0.95

P-15D	WT	and	P-18D	WT	0.90
P-15D	WT	and	P-19TD	TD	0.92
P-15D	WT	and	P-25TA	TA	0.91
P-19TD	TD	and	P-25TA	TA	0.94
P-19TC	uprK	and	P-25TA	TA	0.93

Following Wells are not Correlated: -0.1 < R < 0.1

P-16D	WT	and	P-16TC	uprK	0.02
P-16D	WT	and	P-17D	WT	0.07

Following Wells are Negatively Correlated: R < -0.9

P-15D	WT	and	P-22D	WT	-0.90

All Correlation Coefficients of Water Head Between Wells

		P-15D WT	P-16D WT	P-16TC uprK	P-17D WT	P-18D WT	P-19TD TD	P-19TC uprK	P-22D WT	P-24TA TA	P-25TA TA
P-15D	WT	1.000	-0.106	0.747	0.858	0.901	0.918	0.892	-0.902	-0.498	0.907
P-16D	WT	-0.106	1.000	0.017	0.073	-0.157	-0.200	-0.122	0.125	0.103	-0.324
P-16TC	uprK	0.747	0.017	1.000	0.833	0.839	0.713	0.710	-0.601	-0.357	0.590
P-17D	WT	0.858	0.073	0.833	1.000	0.953	0.781	0.751	-0.868	-0.697	0.671
P-18D	WT	0.901	-0.157	0.839	0.953	1.000	0.874	0.850	-0.887	-0.656	0.788
P-19TD	TD	0.918	-0.200	0.713	0.781	0.874	1.000	0.997	-0.842	-0.432	0.941
P-19TC	uprK	0.892	-0.122	0.710	0.751	0.850	0.997	1.000	-0.805	-0.396	0.932
P-22D	WT	-0.902	0.125	-0.601	-0.868	-0.887	-0.842	-0.805	1.000	0.574	-0.857
P-24TA	TA	-0.498	0.103	-0.357	-0.697	-0.656	-0.432	-0.396	0.574	1.000	-0.320
P-25TA	TA	0.907	-0.324	0.590	0.671	0.788	0.941	0.932	-0.857	-0.320	1.000

8.5 Water Level Measurements

Water level measurements are relied upon to estimate flow direction in aquifers. There is extensive literature on water level diurnal changes and response to rainfall. Typically, water levels are measured during quarterly sampling events. For special studies, an attempt may be made to measure all wells in a study area (e.g., model area) in a very short time span. In the Charleston Naval Weapons Station case described in Chapter 2, water levels change enough to suggest very different flow directions at different times.

Figure 8-11 illustrates the variation of water level between sampling events as captured by a continuous recorder (see line starting at March 31, 2003). Note that a change of over ten feet was missed by the periodic sampling.

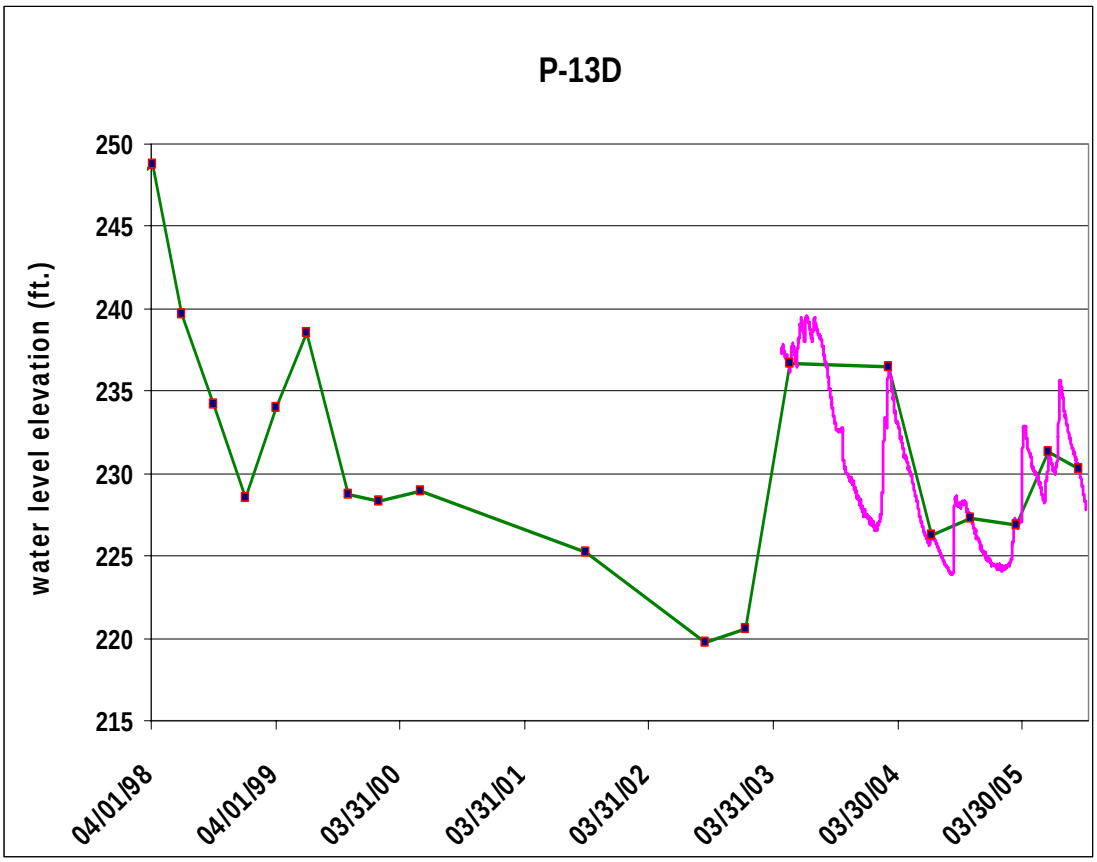

Figure 8-11 Periodic and continuous water level measurements compared for SRS well P-13D. Courtesy Bill Jones, SRNL.

8.6 Unmixing of Multimodal Data

Concentration data from different contaminant sources (or permeability measurements from different types of sediment facies) may present bi-modal or multimodal distribution. This section will introduce an inverse method to identify the individual modes or sources with statistical approaches.

Previous studies assume that if the measurements from an individual source have a log-normal distribution (Sinclair, 1981; Gilbert, 1987), then, the density function of the whole data set can be represented by the linear combination of a number of separate log-normal probability density functions (Heslop et al., 2002); that is, a distribution curve is composed of a finite number of log-normal populations. Under this assumption, a mixture of *N* separate populations can be represented at a given field by the frequency function *f*(*x*),

Equation 7

$$f(x) = \sum_{i=1}^{N} p_i \eta_i(m_i, \sigma_i)$$

$$\eta_i(m_i, \sigma_i) = \frac{1}{\sigma_i \sqrt{2\pi}} \exp^{-\frac{(x-m_i)^2}{2\sigma_i^2}}$$

$$\sum_{i=1}^{N} p_i = 1$$

where $\eta_i(m_i, \sigma_i)$ corresponds to a log-normal probability density function with mean m_i, standard deviation σ_i and non-negative mixing proportion p_i.

Sampled frequency values are therefore a discrete realization of the continuous frequency function and as such should be considered as an incomplete data set. Fitting is normally performed on the mixture frequency distribution to identify the number of modes or sources and to estimate the unknown parameters including mean, standard deviation, and proportion of each mode. For two or three mode problems, an Excel macro can be used to estimate these parameters by trial and error method. Figure 8-12 presents an example for identifying the distributions of two contaminant sources.

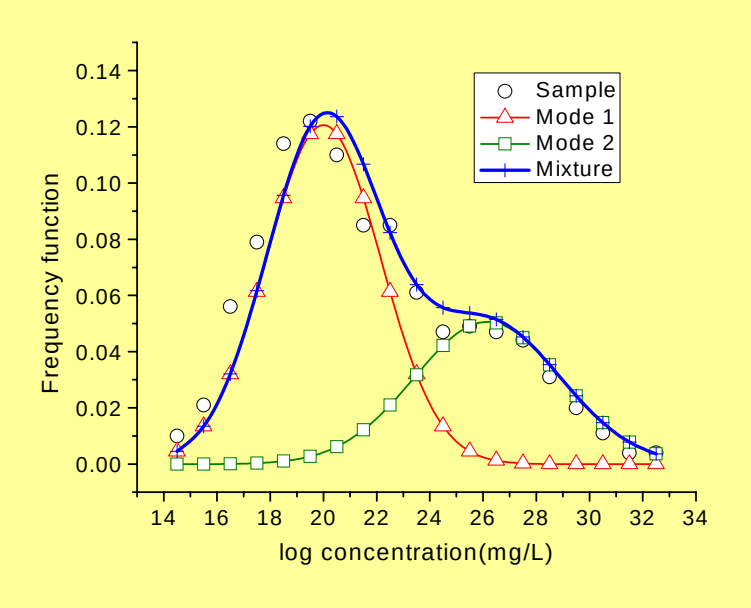

Figure 8-12. Unmixing bimodal data

The two identified modes in Figure 8-12 represent the distribution of two contaminant sources. The first has a mean log concentration of 19.96 mg/L, standard deviation of 2.15, proportion of 0.65, and the second has a mean log concentration of 26.16 mg/L, standard deviation of 2.76 and proportion of 0.35.

For the more complex problem with more than three modes or sources, the expectation-maximization (EM) algorithm (Dempster et al., 1977, and Heslop et al., 2002) can be used for the inverse analysis. This algorithm uses the maximum likelihood estimation (MLE) to maximize the probability that the sample data fit well to the computed frequency function. A brief explanation of this equation is below, but the reader is referred to the sourced text for a more detailed description on the EM algorithm.

Using a two-step procedure (expectation and maximization), the EM algorithm iteratively determines the MLE of the parameters that describe the mixture distribution of a given incomplete data set. Before EM iteration can begin, it is necessary to provide an initial estimation of the parameters. Expectation (E-step) is performed first, and involves the determination of the complete data log-likelihood constrained by the observed (incomplete) data and the previously made estimation of the parameters. MLE (the M-step) is then performed for the estimated complete data log-likelihood (obtained during the E-step). From this maximization procedure, new estimates of parameters are determined. The E- and M-steps are repeated, with the new parameter-values produced during each M-step being utilized in the complete data likelihood determination in the subsequent E-step. By the stepwise improvement of the parameter vector the log-likelihood of the observed data is increased until a predefined convergence criterion is reached. More information on the algorithm and its application to finite mixture models can be found in Dempster et al. (1977); Jones & McLachlan (1990); McLachlan & Peel (2000) and Heslop et al. (2002).

Determining the number of modes (or components) contributing to the mixture distribution is not trivial, because the goodness of fit of a finite mixture model will always improve as the number of components in the mixture is increased. To assess the number of individual components that should be included in a model, we adopted the technique of Kruiver et al. (2001), which is based on a comparison of the residuals (calculated between the measured and modeled curves) for fits involving different numbers of components. The technique compares the variances and means of the residual arrays for two competing models. If the inclusion of an additional component does not significantly reduce the variance and mean of the residual array (assessed using an F-test and Student's t-test, respectively) then the more complex (higher-component) model is unnecessary on a statistical basis. The use of the fitting procedure based on the EM algorithm provides an effective method for determining the contributions and characteristics of individual source populations.

The statistics of a concentration data set from a synthetic site with three possible contaminant sources are shown in Figure 8-13 and Figure 8-14. The identified distributions of three sources and the estimated parameters are listed in Table 8-2.

Table 8-2. The identified distributions of three sources and the estimated parameters

Source	Mean log concentration (mg/L)	Standard deviation	Proportion
Mode 1	1.58	0.126	0.54
Mode 2	2.08	0.122	0.32
Mode 3	2.55	0.100	0.14

Figure 8-13 presents the statistics of contaminant concentration data and the corresponding cumulative probability distribution whereas, Figure 8-14, presents this distribution for each of the three contaminant sources.

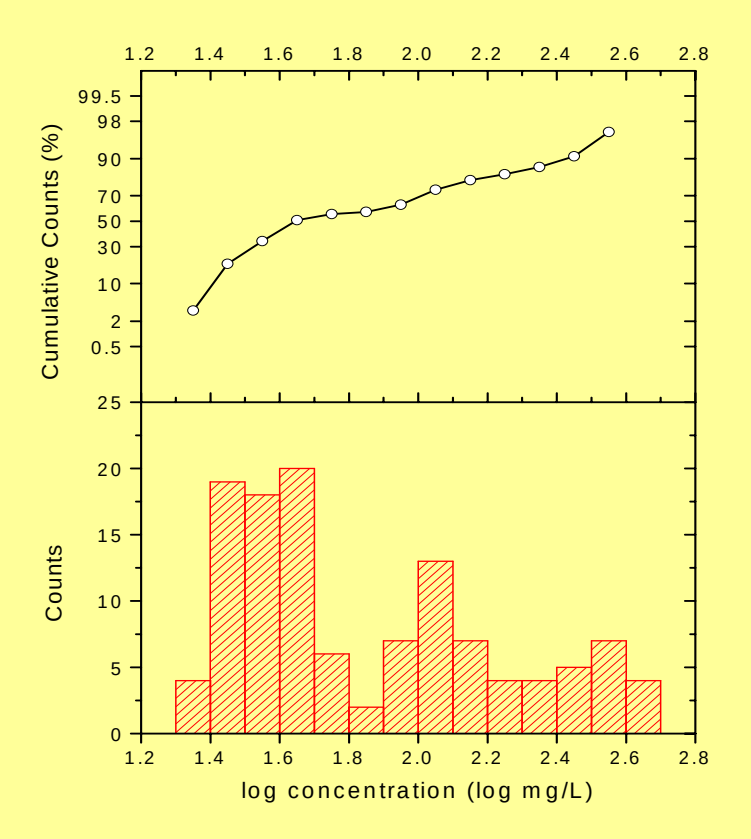

Figure 8-13. Probability plot

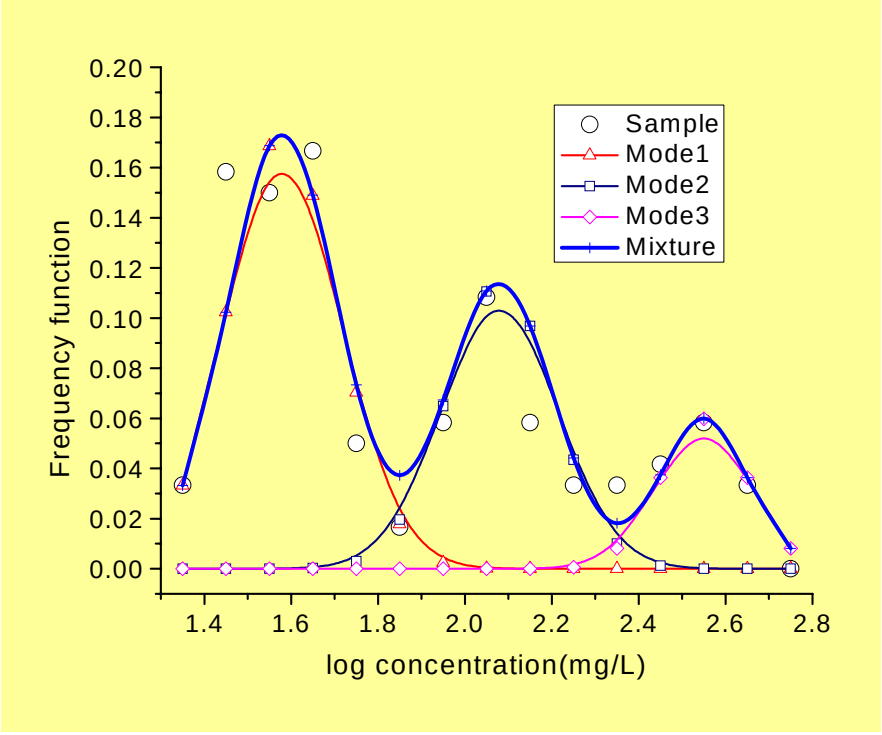

Figure 8-14. Tri-modal distribution

Dissecting plots of mixed population data has been used in exploration geochemistry for many years to distinguish mineralized from barren areas. The reader is referred to online sources starting with authors Sinclair, Miesch, and McCammon and the program Probplot, An Interactive Computer Program to Fix Mixtures of Normal (or Log Normal) Distributions with Maximum Likelihood Optimization Procedures**,** distributed by the Association of Applied Geochemists (www.appliedgeochemists.org).

8.7 Multivariate Analysis Methods: Cluster and Factor Analysis

Multivariate data analysis includes studies of cluster analysis, a method to show the closeness of relationships between samples or variables in n-space (where n is the number of variables), and correlations and structure of correlation matrices (factor analysis). (Samples in n-variable space (R-mode) or variables in n-sample space (Q-mode).)

Cluster analysis is a powerful method to examine data in part because its results can be presented in a simple graph. Analytical results containing a dozen variables can be flattened for quick review onto a plane.

Results are often displayed as a tree that reduces n-dimensional data to a 2-dimensional display. These methods were developed largely in the 20th century – the term factor analysis first appearing in 1931 and cluster analysis in 1939. Their use requires many computations – for example cluster analysis requires the computation of n! distances between samples in n-space several times. Advent of the high-speed digital computer has made the methods commonplace.

These methods are not really statistical tests – they are data analysis and presentation procedures, and they may be applied without concern for many of the assumptions underlying many statistical tests. (See NIST, 2004 and Tukey, 1977 for discussions of exploratory data analysis.) Readily available statistical packages such as SPSS and SAS are capable of performing all of these analyses. More recently, there are some shareware programs or add-ons for programs such as MS-EXCEL that will perform most of the needed multivariate data analyses. Some of these add-ons can be currently found at: http://statpages.org/javasta2.html#Excel.

8.7.1 Case Study: Multivariate Data Analysis at Mill Tailing Site

Let us go through a test case using ground-water monitoring data from a uranium mill tailings disposal site. The data were obtained from reports available in the NRC electronic reading room system. We will use factor analysis to look for structure in the data, and cluster analysis to examine a hypothesis about the possibility that the sampled wells draw from two different bodies of subsurface water.

Figure 8-15 is a cross-section of the mill tailings site looking northeast. A steep change in the elevation of a clay layer dividing an upper from a lower water-bearing zone led us to propose an alternative conceptual model in which a fault cuts the layer, as shown in Figure 8-15.

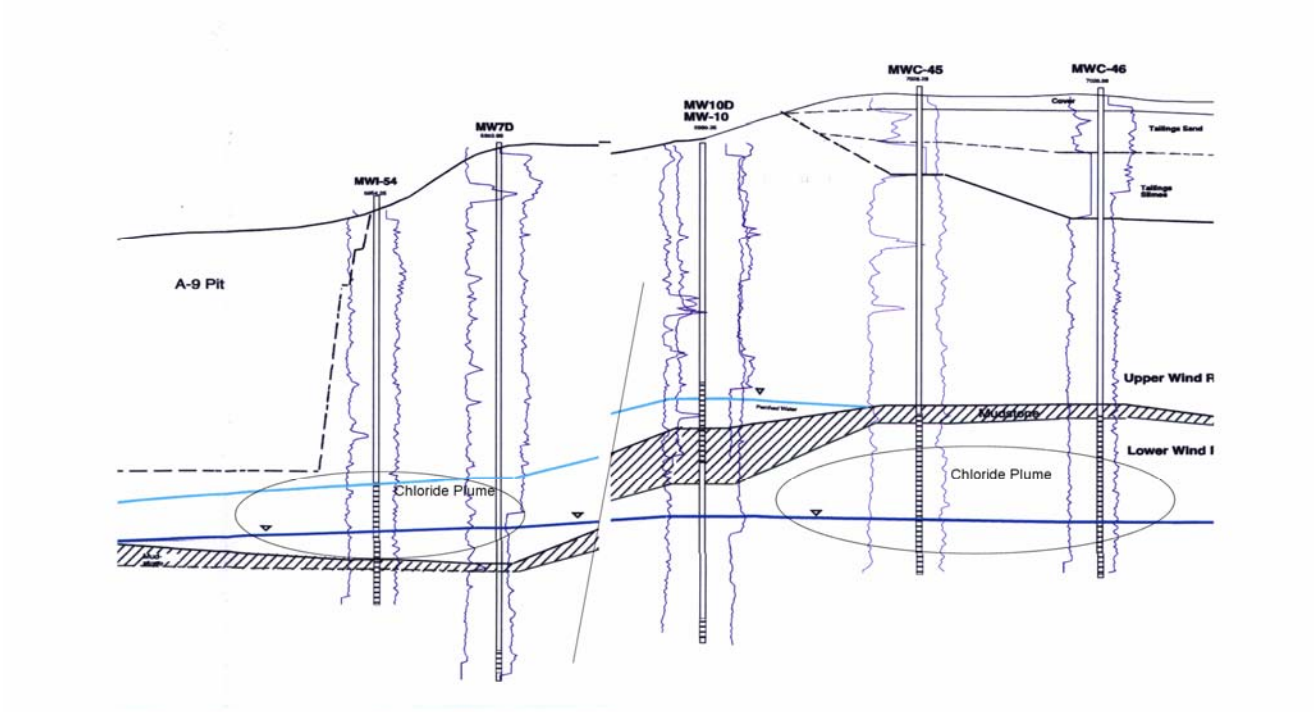

Figure 8-15. Cross section showing concept of merged water bodies. Our study examines whether this water is separated into two isolated chambers.

Chloride plumes exist at the site above the clay on the left of this figure, and below the clay on the right of the figure. This supported the conceptual site model in which there was no permeability barrier, and that the mapped plumes were really one. The water samples are designated as belonging to a West or Southwest "flow regime" in the site data report, which treats these regimes as separate water bodies.

Cluster analysis using SPSS on the data shown in Appendix 8-A support the hypothesis that the West and Southwest regime samples have different chemistry, and so the water can be presumed to represent two zones. This supports the site data report's position that the permeability barrier (clay layer) may be continuous, rather than faulted. Thus the proposed alternative CSM hypothesis is rejected. The Sections below explain in detail the methodology used to perform this multivariate analysis, and the rest of the results from this particular case study.

8.7.1.1 Multivariate Analysis – Step by Step Guidance

Step 1. Obtain the data electronically.

In this case we downloaded pdf copies of tables and re-typed them into an EXCEL spreadsheet.

Step 2. Data conditioning.

This could include standardizing data to z-scores or ranks, or converting data to logs or roots in order to limit the range of magnitudes. It also includes deciding what to do with

truncated or censored data sets. It our case we eliminated about 15 of the samples because they were not analyzed for a number of constituents. We eliminated one analyte (Beryllium) because it was not detected in any samples, and we converted a lot of the non-detects for Arsenic into half the value reported as the detection limit. We also simplified the variable names to save space.

We will not write step-by-step instructions for data conditioning because it should only be conducted by someone familiar with the process.

Step 3. Develop hypotheses to be evaluated, or questions to be answered.

In this case, questions to address included:

- Do the data readily reveal any underlying controlling processes; and
- Can we use water chemistry to substantiate or refute the hypothesis that that the wells represented two "flow regimes" – perhaps different aquifers?
- Are there any outlier samples? (The operator must decide what these mean once they are identified.)

Step 4. Decide what analysis to apply.

- Factor analysis looks at correlations among all the variables. This method is typically ideal for discovering close associations or lack of associations between variables.
- Cluster analysis can quickly reveal outliers and can show whether samples fall into natural groupings in variable space.

Step 5. Use available software for the analysis.

We used SAS and SPSS. Results are discussed below.

8.7.1.2 Cluster Analysis Results

SPSS was used to divide the 137 observations (from Appendix 8-A) into ten groups based on their proximity in variable space. The data were then examined using cluster analysis to help identify outlying data points and look for data trends, and factor analysis to identify correlations in the data. (Similar results were obtained with SAS, but are not presented here.)

Figure 8-16 presents some of the cluster results discussed above in a "family tree" format called a dendrogram. It is clear that Observations 5 from well LA2, 64 from A8, 69 from DOMW1, and 115 from MW30 are outliers because these observations fell into clusters unique for their wells (see data table in Appendix 8-A). They are marked by decreased water quality that does not follow a trend across time, as the subsequent observations at the wells contain normal data for the wells.

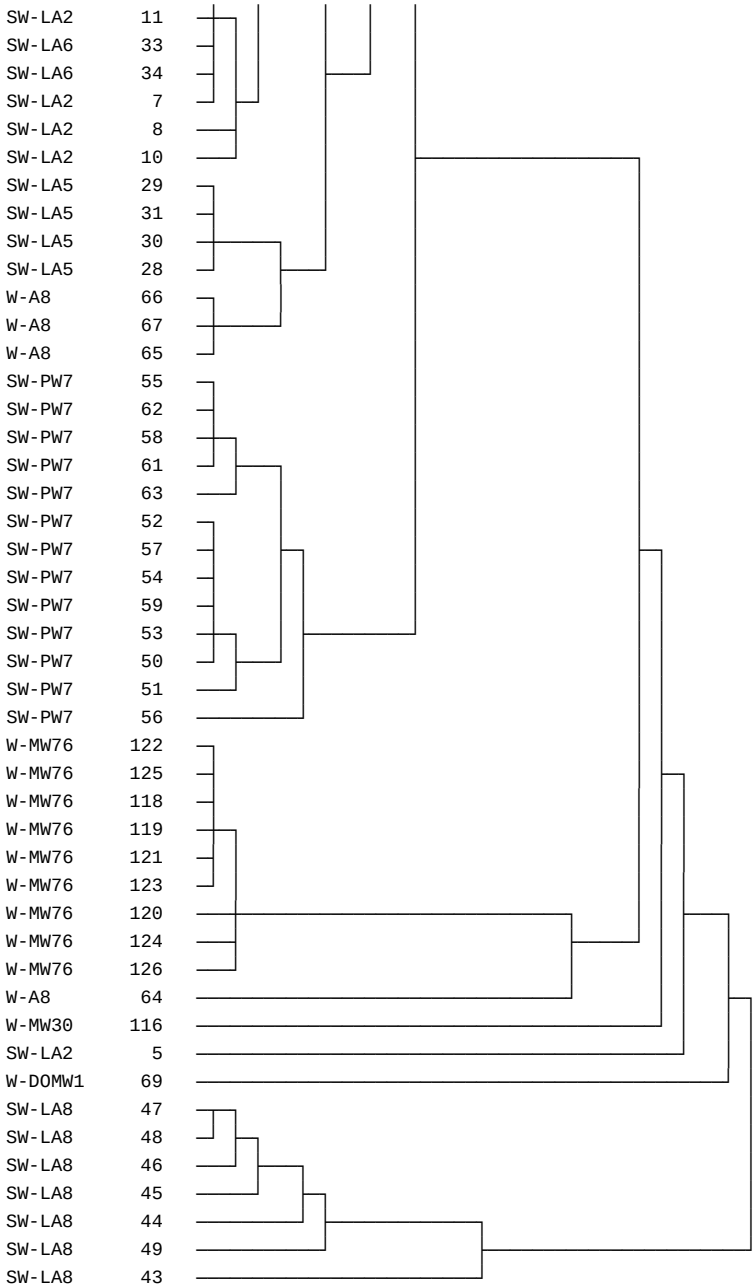

Figure 8-16. Dendrogram (partial) of the clusters for the water analyses presented in Appendix 8-A. The left-most column is the well name and the right column indicates the observation number.

Once the outliers have been identified through cluster analysis, the data can be evaluated to determine what causes these samples to stand out. Before rejecting or removing these outliers, it is critical to evaluate results of other constituents from the same well during the same sampling period or from other wells in the same sampling period to determine if the results represent potential sampling errors or real pulses of contaminants.

Examination of Figure 8-16 reveals the following:

- Out of 4 observations from well A8, 3 fell in Cluster 1. Observation 64 stands out as an outlier (single-member cluster 7). Examination of the data table reveals this sample has higher gross-alpha and radium than other samples from that well.
- Out of 15 observations from well MW30 all fell in Cluster 1, with the exception of observation 115, which fell in Cluster 9. A very high sulfate analysis was reported for this sample. This could represent a bad analysis, or the passage of a plume not otherwise observed in the semi-annual sampling.
- 14 of 15 Samples (observations) from well LA2 fell in cluster 3. Observation 5 again represents a single-member cluster (number 2) and reference to the data table reveals a Th230 analysis that is out of line with the entire data table, suggesting a typographical error in recording data.
- 6 of 7 observations from well DOMW1 clustered together. Observation 69 is identified as an outlier, and is high in sulfate, chloride and total dissolved solids relative to other samples from this well.
- Not all wells sampled have odd observations, for example all 9 observations from well MW76 fell in Cluster 10,

Water chemistry data further supports dividing the wells into two major groups. The majority of the wells screened in the Southwest flow regime falling into Clusters 1 and 3 and the majority of wells screened in the West flow regime falling only into Cluster 1 thus, supporting the hypothesis that the West and Southwest flow regimes are separated into two isolated water bodies.

Please note that there is abundant material on cluster analysis and cluster dendrograms on the Internet. These materials should be consulted for further general information.

8.7.1.3 Factor Analysis Results

Next, a factor analysis was performed on the data in Appendix 8-A to determine relationships between samples or variables in n-space. Factors are not presented here, but results of correlation coefficients are presented in Table 8-3**.**

Table 8-3. Correlations between monitoring data variables

	as	Cl	galpha	pb210	ra	Ra226	ra228	so4	tds	u	th230
as	1.00000	-0.24668	0.22502	0.03648	0.06288	0.07260	-0.00517	0.12385	0.10167	0.11758	0.01139
cl	-0.24668	1.00000	0.27811	-0.07228	0.14136	0.05518	0.42869	0.41603	0.41539	0.29323	0.16194
galpha	0.22502	0.27811	1.00000	0.18202	0.06628	0.05021	0.10118	0.49497	0.60718	0.96203	0.24884
pb210	0.03648	-0.07228	0.18202	1.00000	0.49116	0.53849	0.04436	0.15358	0.09250	0.16585	0.07580
ra	0.06288	0.14136	0.06628	0.49116	1.00000	0.98053	0.57561	0.57808	0.54190	0.00793	-0.01624
ra226	0.07260	0.05518	0.05021	0.53849	0.98053	1.00000	0.40389	0.49020	0.44462	-0.00777	-0.05480
ra228	-0.00517	0.42869	0.10118	0.04436	0.57561	0.40389	1.00000	0.65338	0.67449	0.07046	0.15290
so4	0.12385	0.41603	0.49497	0.15358	0.57808	0.49020	0.65338	1.00000	0.92958	0.45045	0.12761
tds	0.10167	0.41539	0.60718	0.09250	0.54190	0.44462	0.67449	0.92958	1.00000	0.57897	0.17896
u	0.11758	0.29323	0.96203	0.16585	0.00793	-0.00777	0.07046	0.45045	0.57897	1.00000	0.29619
th230	0.01139	0.16194	0.24884	0.07580	-0.01624	-0.05480	0.15290	0.12761	0.17896	0.29619	1.00000

Correlations obtained in the factor analysis indicate:

- Gross alpha correlates with uranium (R=.96)
- Radium is highly correlated with Radium 226 (R=.98), but only moderately correlated with Radium 228 (R=.57) and lead 210 (R=.49)
- Radium correlates with Sulfate (R=.58) and total dissolved solids (R=.54).
- Radium does not correlate with Uranium (R=.008)
- Uranium correlates with sulfate (R=.45) and total dissolved solids (R=.58).

A possible interpretation is that Ra comes from the mill tailings in which it has been separated from U and that much of the observed U is natural.

8.8 Analysis of Mapped (Spatial) Data

This Section discusses data analysis of spatial data. Specifically, if focuses on a discussion of the following three topic areas:

- Testing for outliers in mapped data;
- Determining the distribution of uncertainty – the completeness transform;
- Incongruity;

Information learned in these three areas often provides useful insight about site performance, or rather, help locate areas of uncertainty at the site. The areas of uncertainty then become candidate areas for validation monitoring points.

For characterization data, spatial statistical analysis methods developed within the mining industry for mine planning are often useful for determining whether a site has been adequately characterized. We did not include geostatistics in this analysis.

Parameters being measured may fall into a number of classes that may vary across the site in different patterns. If we were developing a gold mine, we might only test core samples for gold. More generalized site characterization will include measurements for many things, but the general approach is similar for each.

8.8.1 Outliers in Mapped Data

Generally, mapped data are presented in the form of contoured maps. Such maps may be produced with computers, but for data analysis it is best to hand contour the data. In the process of hand contouring, any points that cause problems in the drawing of smooth contours will become apparent. With computer contouring the operator has less opportunity to interact with the data, and thus less opportunity to spot outliers, but these may still produce contoured "bulls eyes." Any bulls-eyes in contoured data, or deviations from smooth contours in a variable, such as water levels (piezometric surfaces) should be visited to determine whether the data point is valid and whether it represents an opportunity to re-evaluate the conceptual model.

Characterization and monitoring data should be evaluated for outliers and trends that might suggest alternative conceptual models. Examples might include water levels that deviate from smoothed contour piezometric maps or trend surfaces.

Guidance includes:

- Hand contour spatial data to gain insight
- Computer contouring is highly dependent on data point spacing and is accurate only for regularly spaced data
- Question any closed contours (bulls eyes) in a piezometric or concentration map in the context of the site model.

8.8.2 Uncertainty in Mapped Data

Geostatistical methods were developed to quantify uncertainty in geologic measurements so that decisions about whether to proceed with mining in an area, or to determine whether additional drilling was needed to fill in data gaps before a risk-informed decision could be made. This is a very active field of research today, especially as applied to petroleum reservoirs. (Yarus and Chambers, 1994).

This section presents case studies drawn from real data that illustrate site-specific conceptual model revisions required by anomalous data. In two cases the non-fitting data were first discarded, and only after subsequent analysis, were identified as clues leading to revision of the conceptual site model.

For the purpose of preparing a map, a geologic variable such as a stratigraphic top, water level, or other parameters, can only be known with certainty at the control points. While there may be errors in measuring variables at control points, these are distinct from errors in estimating values between control points.

The interrelationships between spatial autocorrelation of the surface, the spacing between control points, and the likely error of interpolated points are formalized in regionalized variable theory, a branch of statistics devised initially for the analysis of mining problems (Matheron, 1965). Under this statistical theory, geologic variables are considered to be composed of two components:

1) a gentle regional trend or *drift*; and
2) autocorrelated residuals or deviations from the drift.

Once the drift has been removed (by subtracting a series of trend surfaces or moving averages) the degree of similarity between points is given by the semivariance. This is the variance of the differences between all possible pairs of points on the map that are the same distance apart, and is closely related to the autocorrelation. A plot of semivariance vs distance is called a semivariogram, and rises from zero at zero distance to a maximum value equal to the total variance around the drift. The distance at which the semivariance becomes a maximum is called the "range," and is also the distance at which the autocorrelation of the mapped surface will drop to zero. The value at which the autocorrelation reaches maximum on the semivariogram is called the "sill". The autocorrelation (y axis) of a semivariogram plot may not always start at zero. This is due to the "nugget effect", which represents inherent variability plus sampling variability at zero distance for the database.

Once the form of the semivariogram has been determined, it may be used in a surface estimation procedure called universal kriging (Matheron, 1965). Provided the drift has been properly removed, this procedure provides a contoured surface with the smallest errors possible with any estimation procedure. Kriging also yields an estimate, in the form of a map, of the possible errors at all estimated points. This is a map of the +or– bounds on the mapped surface at every point within the map area. Areas of high estimation error then become the subject of additional characterization input. Estimation error could refer to a contoured map of pressure heads, to a contoured map of contaminant concentrations, or to patterns on a geologic map.

A recent paper by Cumbest and others (Personal communication, 2004 – it remains unpublished in 2007) gives a refined technique to apply geostatistical methodology to evaluate the thoroughness of a geotechnical investigation relative to investigation design goals. The technique basically uses the spatial distribution of the model error to map the probabilities that the model estimation values are in exceedance of specified design values. This is accomplished by calculating the probability of exceedance using the probability density function ($\eta_i(m_i,\sigma_i)$ (Equation 7) for the standard normal variable. The standard normal variable in this case is defined as the difference between the estimated value and the specified design value. The resulting probabilities are then converted to thoroughness by using the complement to the binominal entropy function. In essence, in locations where the estimated model values are known to be in exceedance of the specified design value (i.e. probabilities very near 1 or very near 0) result in thoroughness of very near 100 percent. At locations where the model error is large relative to the difference between the estimated and design values the probabilities of exceedance are not well known (i.e. very near 0.5) are associated with a thoroughness very near zero. Other locations exhibit a continuum of thoroughness values depending on their assigned probabilities.

Guidance

- Areas of poor characterization coverage are areas where monitoring points are needed.
- Kriged estimates of errors (see discussion in Section 8.8.2), or the geotechnical thoroughness transform may be useful.

8.8.3 Incongruity between Mapped Variables

The investigator should visually compare all sets of mapped variables for a site. One obvious test of a computer flow model, for example, is to see if model flow directions are consistent with apparent plume movement from monitoring data. In Figure 8-17, below, water table gradients from a site flow model indicate a dominantly westward flow direction, but plumes suggest a northwestward flow direction, which is more consistent with regional geology.

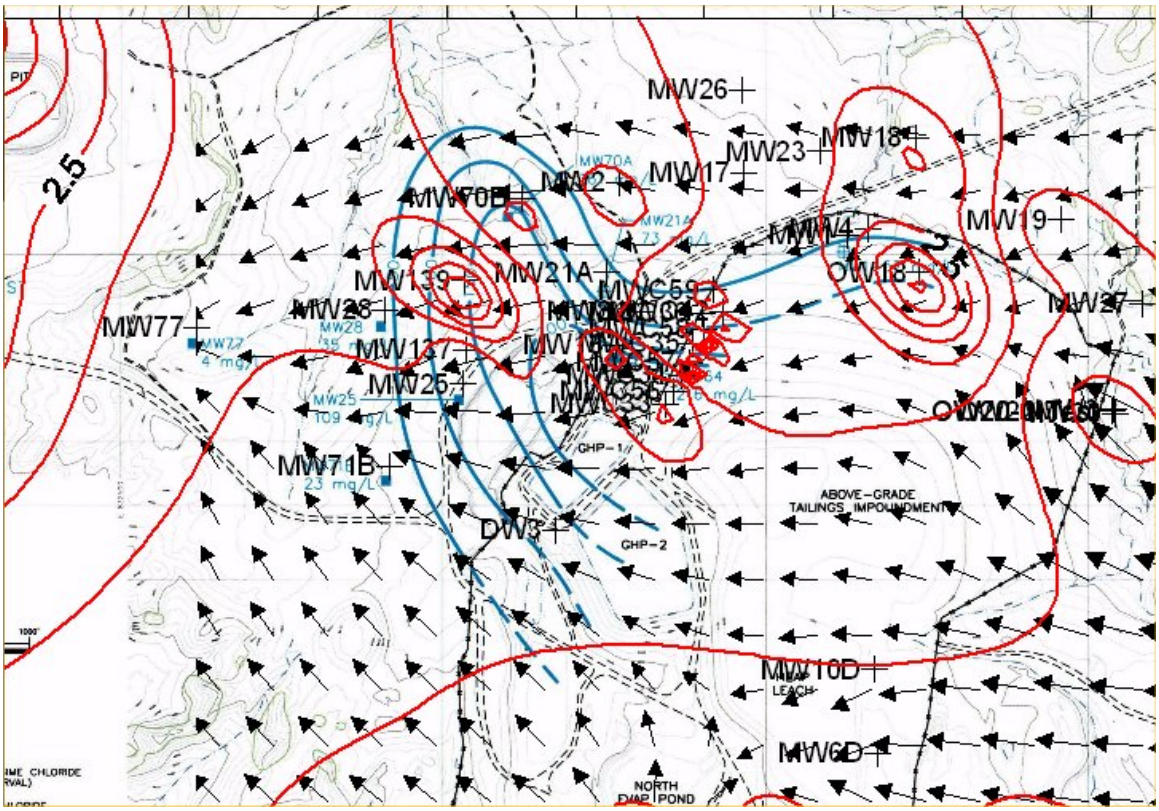

Figure 8-17. Map of chloride plume (blue) superimposed on a vector potentiometric data (arrows), and contoured hydraulic conductivity data (red).

Figure 8-17 shows that the direction of plume flow is in good agreement with the zone of high hydraulic conductivity. This indicates that the hydraulic conductivity has a greater influence on plume migration direction than does the potentiometric surface.

Figure 8-18. Typical alluvial fan

Published reports for the site in Figure 8-17 suggest that the environment of deposition was a series of alluvial fans. As shown in the photograph in Figure 8-18, alluvial fans are deposited by radial streams exiting from mountains onto a plain or valley. With the abrupt drop in stream gradient, sediments are deposited, the channel is choked and flow escapes to form another channel, resulting over time in a fan-shaped deposit. Before this channel switching occurs flooding may transport fine-grained sediment outside the channels, while coarser sediment remains in the channel bottom. From time to time lakes and swamps may fill the valley, resulting in deposition of fine grained and organic-rich sediments. The channel deposits will tend to be more permeable than the overbank sediments, and thus offer preferential flow directions to underground water.

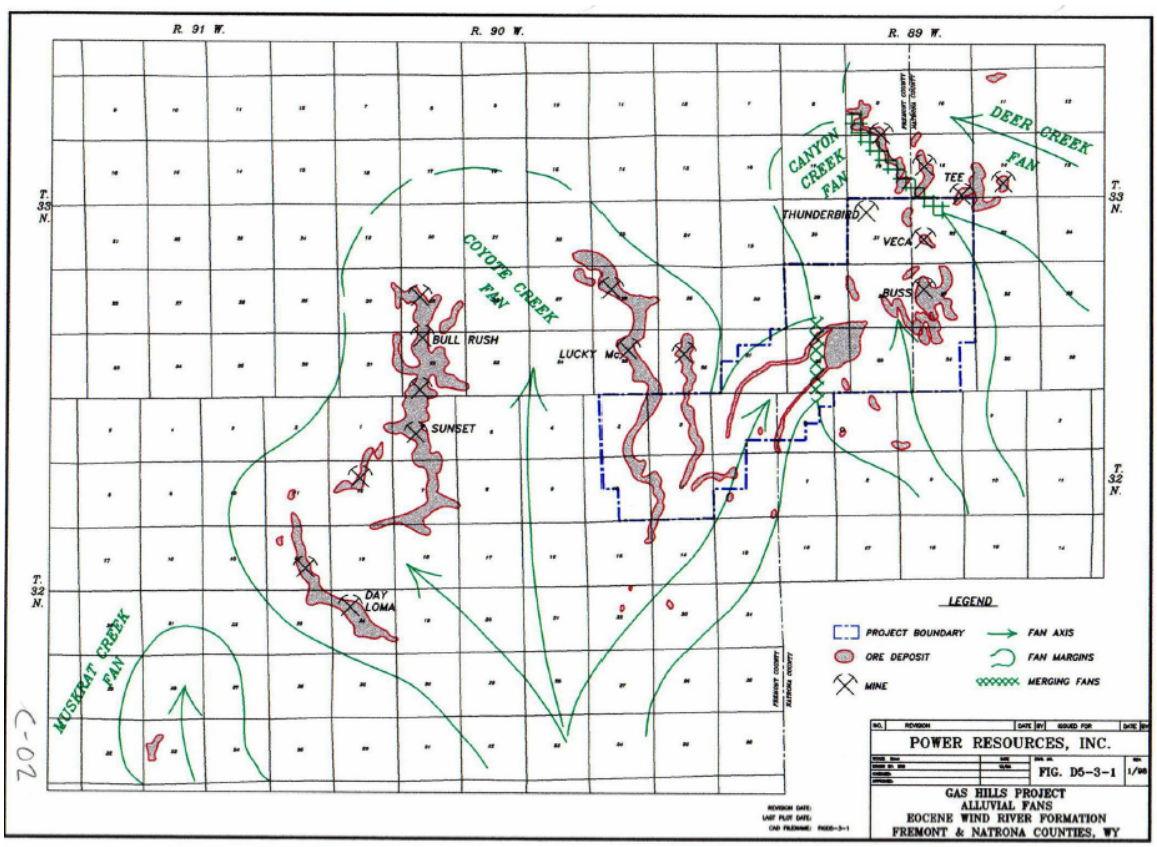

Figure 8-19. Diagram of alluvial fans in Wyoming

The site presented in Figure 8-17 is near the area of Figure 8-19 and has a similar geologic setting. Any high permeability zones at the site should follow trends suggested by the arrows on this figure. Permeability data for the site are presented in Table 8-4. Two companies performed aquifer testing on six wells, but used different aquifer thicknesses in computing hydraulic conductivity, K, from transmissivity results. We suspect that one company (referred to in this report as Company A) may have used screen lengths, while the other company (referred to in this report as Company B) used an estimate of total aquifer thickness of 240. We have used the screen length from Company B's results to compute a column of K adjusted for screen length.

It appears that there are two groups of hydraulic conductivity results– one set between about 0.1 and 1.0 ft/d and another ranging up to 6 ft/d. If we accept the alluvial fan conceptual model for deposition, then we should infer that the higher numbers represent in-channel measurements, and the lower numbers out-of-channel measurements. A revised flow and transport model incorporating high permeability zones might better represent the site.

Table 8-4. Hydraulic conductivity data

Well ID	Company	Method	Perm (ft/day)	Perm (ft/min.)	Trans	Thickness	Adjusted K
MWC33	A	Jacob	0.22	1.53E-04	53	240	0.53
MWC33	B	Theis	0.23	1.60E-04	22.7	100	0.227
MWC33	B	Jacob	0.45	3.13E-04	45.1	100	0.451
MWC34	A	Jacob	0.28	1.94E-04	67	240	0.279167
MWC35	A	Jacob	0.78	5.42E-04	187	240	1.87
MWC35	B	Theis	0.12	8.33E-05	12	100	0.12
MWC36	A	Jacob	1.23	8.54E-04	341	240	6.82
MWC36	B	Theis	2.1	1.46E-03	105	50	2.1
MWC36	B	Jacob	3.3	2.29E-03	163	50	3.26
MWC37	B	Jacob	2	1.39E-03	40.8	20	2.04
MWC37	B	Theis	2.7	1.88E-03	53.5	20	2.675
MWC42	A	Jacob	0.6	4.17E-04	165	240	1.833333
MWC42	B	Theis	1	6.94E-04	90	90	1
MWC42	B	Jacob	3.34	2.32E-03	301	90	3.344444

8.9 Quality Assurance

Most sources of error in ground-water data can be controlled through a good quality assurance (QA) program. This is easy to say, but the hard part comes from the fact that a good QA program can only be designed and implemented if the physical principles and processes leading to some numerical result are well understood.

Error control in general can be approached using the principles of systems engineering. Each entity –feature or process – must be thought of as an assembly of components. Each component plays a role in meeting the requirements set forth for the whole system or process. Each is a link in a chain, and failure of any one leads to failure of the chain. Quality assurance requires a comprehensive plan that ensures data integrity through each step of the process. It is important to be aware of possible sources of error in every step. **A ground-water monitoring system, for example, has a number of subsystems:**

- Sampling
- Analysis
- Data storage
- Reporting

Drilling down, each subsystem has a number of components which introduce possible sources of error as well. Sampling, for example includes:

- Choice of monitoring point

- Access to monitoring point – usually a well
- Sampling method – pump, bailer…
- Sampling protocol – length of pumping, duplicates, transport of samples, documentation..
- Field measurements of pH, alkalinity, conductivity, temperature.

8.9.1 Quality Assurance Case Studies

Let us examine a case study to illustrate QA analysis for just one component in a system: the well. Figure 8-20 is a diagram of a typical well along with some notes on well construction. The well is the one component in this system that is usually trusted to reliably yield water samples whose chemistry is representative of the water-bearing zone being sampled. Yet well construction often includes several reactive parts:

- Bentonite, a clay with very high ion exchange capacity;
- Portland cement – essentially calcium hydroxide, a strong base, and
- (Usually) electrical wiring which may allow currents to flow between the ground surface and the zone being sampled.

Voltages between about plus 1 and minus 1 have been measured between galvanized or copper clad ground rods at the well head, and the grounding wire to the submerged pump at wells at the DOE-SRS. To the best of my knowledge, no systematic study has ever been made of electrochemical or electrophoretic effects of monitoring wells. (Electrical methods are used to reduce fouling of screens in production wells.)

The filter sand, bentonite seal, and the cement grout are poured from the surface through a 2" pipe called a tremie. The bentonite is a slurry of dried clay pellets which absorb water and swell to make a tight seal between the well casing and the earth. Either the tremie pipe or a separate tag line is used to verify that the various layers are at the correct depth – but it is almost impossible to assure that the casing to earth annulus is uniformly filled. Another issue is pouring cement weighing about half again as much as water through a 2" pipe without creating a jet that eats through or around the bentonite seal. The tremie can be very long, depending on the depth of the well. Once the cement is poured, it is not possible to view details of the "as built" configuration. Only care in the installation can assure proper construction. One approach is to pour a small amount of cement (perhaps mixed in a bucket) and wait for it to cure before pouring the rest.

Ideal Monitoring Well

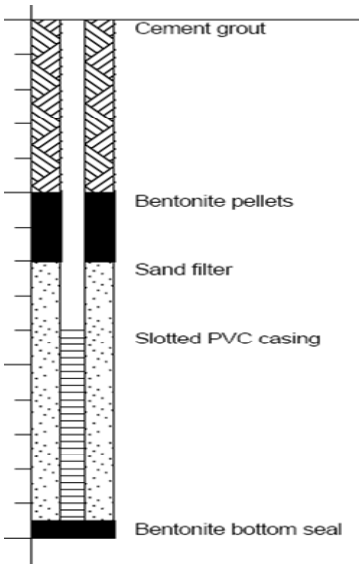

Drill Hole – walls are caked with mud

Insert casing with screen (slotted section)

Pour filter sand - get it right, like in the picture

Pour swelling clay seal pellets – wait until they swell – like in the picture

Pour cement in through a pipe. Do not jet a hole through the seal.

Develop well – pump until all drilling mud is removed from screen zone

Figure 8-20. Schematic of monitoring well with steps in installation.

The next few figures show pH measurements for several wells at the DOE SRS. In well ASB8B, field pH results are relatively stable, varying in the range of about 4 to 6 pH units (see Figure 8-21). The actual range in the aquifer may be a little less. Sample aeration and possible calibration errors for field pH meters may account for the observed range of measurements.

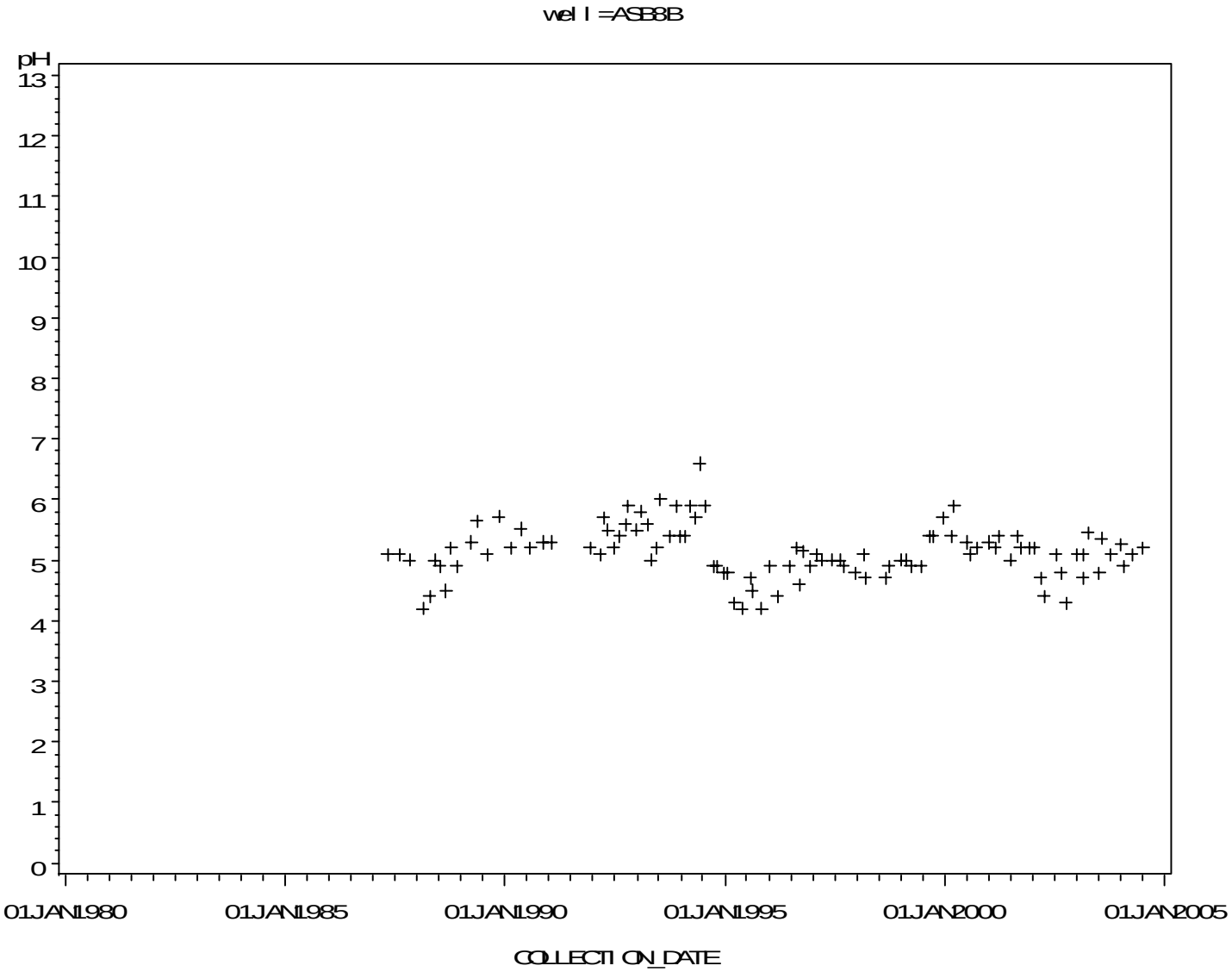

Figure 8-21. pH with time for well ASB8B

By contrast well ABP3 yields pHs between 12 and 3 (see Figure 8-22). Calcium hydroxide (cement) in water produces a pH of about 12.5. At this pH aluminum and zinc form soluble anions, and many transition metals are precipitated as hydroxides. Thus the disturbance in aquifer chemistry likely caused by poor well construction can render any effort to interpret metal chemistry useless.

As shown in Figure 8-22, with time, the pH lowers. The steepest decline is in about 1988, when sampling protocols were changed from pumping a fixed volume of water, to pumping until indicator parameters, including pH stabilized. The variation in pH is then about the same as observed in well ASB8 for a few years. Variance again increases at about the time that a change in sampling contractors went into effect.

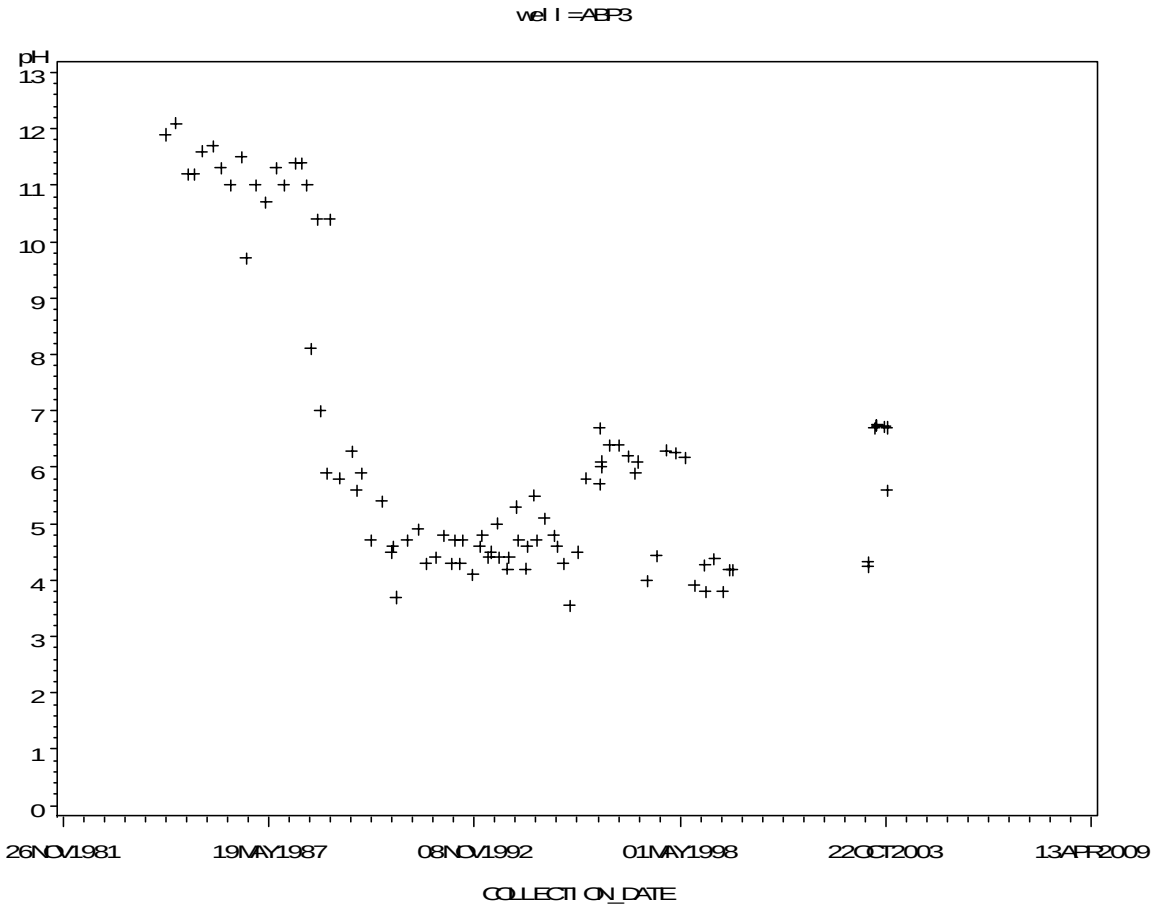

Figure 8-22. pH with time for well ABP3

Although wells are installed according to design specifications, it is almost impossible to inspect the as-built well. Acceptance criteria that include testing for well efficiency and for chemical parameters related to construction defects should be included in installation contracts. Training of samplers is important, but beyond this discussion.

This leads our discussion back to QA issues. Several sources of error can be found throughout the sample/data handling process. When analyzing data or assessing data anomalies, it is important to carefully consider factors that could be introduced throughout the sample process. This case illustrates how factors such as well construction, can significantly impact sample quality, and result in misconceptions about site conditions.

Obviously any geochemical understanding relying on accurate pH measurements from pumped wells could be clouded to the extent that the sampled values do not reflect aquifer conditions. Not only could pH be wrong, but concentrations of grout components, such as calcium, and concentrations of pH-sensitive chemicals – Zn, Al, to mention two - could be affected by highly alkaline conditions near the well.

Another issue with pH is the related to the chemicals that control ground-water pH. Commonly pH is controlled by calcium bicarbonate. When ground water is brought to the surface and exposed to the atmosphere, carbon dioxide can be gained or lost by exchange with the atmosphere. Figure 8-23 is taken from an unpublished report and shows results of pH and conductivity measured in the field and later in the laboratory. The samples are from an area underlain by limestone. Note that in every case pH decreases and conductivity increases between the field and the lab. There was no indication that the samples were acidified between collection and laboratory analysis, leading to the hypothesis that the observed changes are related to carbon dioxide exchange with the atmosphere.

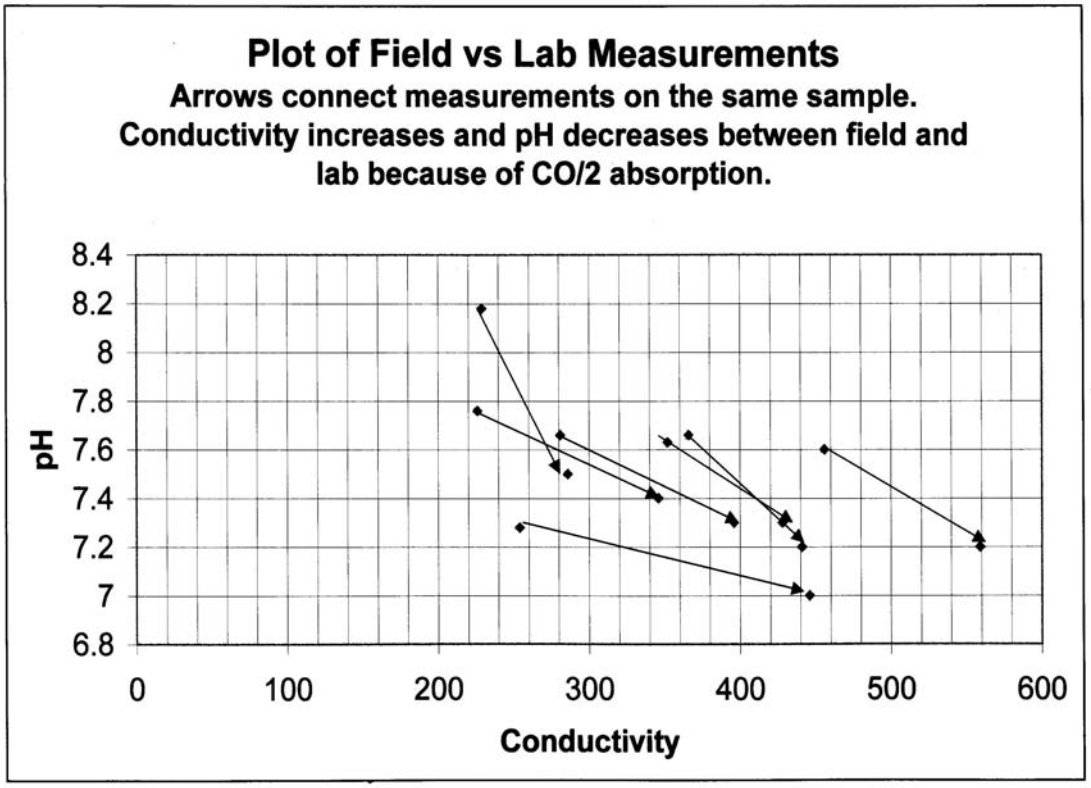

Figure 8-23 Field and laboratory measurements compared.

8.10 References

Anscombe, F.J. and J.W. Tukey. "Analysis of Residuals." *Technometrics*. pp.141. 1963.

Cumbest and others (Personal communication, 2004)

Dempster, A.P., N.M Laird, and D.B Rubin. "Maximum Likelihood from Incomplete Data via the EM Algorithm." *J. R. statist. Soc. B*. Vol. 39: 1–38.1977.

Environmental Protection Agency (EPA). "Guidance for Monitoring at Hazardous Waste Sites: Framework for Monitoring Plan Development and Implementation." OSWER

Directive No. 9355.4- 28, EPA. 2003. (access to this publication through www.clu-in.org)

Gilbert, R.O. *Statistical Methods for Environmental Pollution Monitoring*. New York:Van Nostrand Reinhold Company.1987.

Helsel, D. R. and R. M. Hirsch. "Statistical Methods in Water Resources." Chapter A3, in Water-Resources Investigations Report of U. S. Geological Survey, Book 4, Hydrologic Analysis and Interpretation. U. S. Geological Survey. 2002.

Heslop, D., et al. "Analysis of Isothermal Remnant Magnetization Acquisition Curves Using the Expectation-Maximization Algorithm." *Geophys. J. Int*. Vol.148: 58-64. 2002.

Jones, P.N. & G.J. McLachlan. "Algorithm AS 254: "Maximum Likelihood Estimation from Grouped and Truncated Data with Finite Normal Mixture Models." *Applied. Statistics.* Vol. 39: 273–282. 1990.

Kendall. M.G. *Rank Correlation Methods*. 4th ed. London: Charles Griffin & Company. pp. 202. 1975.

Kruiver, P.P., M.J Dekkers,& D. Heslop. "Quantification of Magnetic Coercivity Components by the Analysis of Acquisition Curves of Isothermal Remnant Magnetization." *Earth Planet. Sci. Lett.* VOl.189: 269–276. 2001.

Matheron, G. *Les Variables Regionalisees et Leur Estimation: Une Application de la Theorie des Fonctions Aleatoires Aux Sciences de la Nature*. Paris: Masson et Cie, Editeurs. pp. 305. 1965.

McLachlan, G. & D. Peel. *Finite Mixture Models*. New York: Wiley-Interscience. 2000.

National Institute of Standards and Technology (NIST)/SEMATECH e-Handbook of Statistical Methods, http://www.itl.nist.gov/div898/handbook/, date. Date created: 6/01/2003, Last updated: 7/18/2006

Peatman, John G. *Descriptive and Sampling Statistics*. New York: Harper & Brothers. 1936, '41, '47.

Siegel, S. *Nonparametric Statistics for the Behavioral Sciences.* New York: McGraw-Hill. 312 p.1956.

Sinclair, J. A. "Application of Probability Graphs in Mineral Exploration." *The Association of Exploration Geochemists, Special*. Vol. 4: 95. 1981.

Snedecor, G.W. and W.G. Cochran. *Statistical Methods*. Ames, Iowa: The Iowa State University Press. Sixth Ed. 593pp.1976.

Soderberg K., R. Hennet and C. Muffels. "Uncertainty and Trend Analysis for Radium in Groundwater and Drinking Water." Proceeding of 2005 NGWR Naturally Occurring Contaminants Conference: Arsenic, Radium, Radon, and Uranium, Charleston, South Carolina. p30-43. February 24-25. 2005.

Tukey, J. W. *Exploratory Data Analysis*. Massachusetts: Addison-Wesley, Reading. 688p. 1977.

Vanderbilt website control chart diagram (http://www.vanderbilt.edu/Engineering/CIS/Sloan/web/es130/quality/oldtool.htm#control)

Velleman, P.F. and L. Wilkinson. "Nominal, Ordinal, Interval, and Ratio Typologies are Misleading." *The American Statistician*. Vol.47, No1: pp65-72. 1993.

Yarus, J.M. and R.L Chambers. "Stochastic Modeling and Geostatistics, Principles, Methods, and Case Studies." *AAPG Computer Applications in Geology*. No. 3: 379p. 1994.

Appendix 8-A

Monitoring Well Analyses from Mill Tailings Site with Results of Cluster Analysis

Rads in pCi/l; non-rads and U in ppm. Galpha is gross alpha, which is a surrogate for radium plus uranium and other alpha-emitters. FL is West or Southwest flow direction – implied separate water bodies for wells. C is cluster number as assigned in SPSS

Obs#	Fl.	C	well	Date	ra226	ra228	ra	th230	u	pb210	G alpha	so4	tds	cl	as
1	SW	1	LA1	12/12/1996	7.2	6.0	13.2	0.050	0.029	0.60	49	851	1350	17.0	0.0005
2	SW	1	LA1	9/2/1997	4.7	5.3	10.0	0.005	0.013	0.05	30	893	1380	19.0	0.0020
3	SW	1	LA1	4/28/1998	4.1	4.6	8.7	0.010	0.006	0.20	36	875	1380	18.0	0.0005
4	SW	1	LA1	6/24/1998	2.1	1.6	3.7	0.090	0.002	0.40	28	862	1380	17.0	0.0060
5	SW	2	LA2	3/13/1996	11.0	11.0	22.0	20.000	0.074	1.80	51	770	1400	19.0	0.0005
6	SW	3	LA2	6/12/1996	13.0	9.9	22.9	0.050	0.042	0.05	67	768	1480	21.0	0.0015
7	SW	3	LA2	8/28/1996	14.0	7.0	21.0	0.200	0.059	0.40	55	760	1480	22.0	0.0010
8	SW	3	LA2	10/28/1996	11.0	11.0	22.0	0.050	0.051	1.70	57	710	1370	22.0	0.0005
9	SW	3	LA2	2/11/1997	10.0	9.6	19.6	0.100	0.051	0.80	62	704	1460	21.0	0.0030
10	SW	3	LA2	6/6/1997	11.0	6.0	17.0	0.005	0.110	1.90	98	788	1420	24.0	0.0020
11	SW	3	LA2	8/7/1997	21.0	9.2	30.2	0.150	0.008	0.50	81	812	1510	24.0	0.0030
12	SW	3	LA2	11/3/1997	13.0	10.0	23.0	0.050	0.096	0.60	72	780	1400	24.0	0.0020
13	SW	3	LA2	4/28/1998	13.7	9.7	23.4	0.100	0.078	0.10	84	818	1470	24.0	0.0015
14	SW	3	LA2	6/23/1998	15.1	9.1	24.2	0.400	0.150	0.90	155	786	1500	23.0	0.0050
15	SW	3	LA2	9/1/1998	14.9	9.7	24.6	0.020	0.075	0.30	84	792	1470	24.0	0.0040
16	SW	3	LA2	11/17/1998	16.0	9.4	25.4	0.020	0.063	0.60	67	814	1490	22.0	0.0020
17	SW	3	LA2	1/6/1999	12.7	9.6	22.3	0.050	0.073	0.40	48	834	1440	22.0	0.0060
18	SW	3	LA2	8/25/1999	16.8	9.8	26.6	0.030	0.066	0.80	54	763	1440	21.0	0.0015
19	SW	3	LA2	2/15/2000	14.0	8.8	22.8	0.500	0.063	0.67	74	780	1500	22.0	0.0015
20	SW	1	LA3	12/12/1996	5.1	5.4	10.5	0.050	0.017	1.80	42	790	1290	6.0	0.0010
21	SW	1	LA3	6/10/1997	3.8	6.8	10.6	0.100	0.420	0.40	356	831	1340	5.0	0.0020
22	SW	1	LA3	9/2/1997	5.3	6.8	12.1	0.100	0.012	0.50	30	877	1220	6.0	0.0020
23	SW	1	LA3	11/23/1997	5.0	5.8	10.8	0.050	0.020	0.30	29	890	1560	6.0	0.0005
24	SW	1	LA3	4/21/1998	6.2	6.6	12.8	0.100	0.016	0.10	41	914	1380	6.0	0.0020
25	SW	1	LA3	6/23/1998	7.8	7.6	15.4	0.200	0.032	0.20	46	836	1390	5.0	0.0050
26	SW	1	LA5	6/10/1997	6.0	2.4	8.4	0.100	0.130	0.10	123	632	1120	4.0	0.0005
27	SW	1	LA5	8/28/1997	14.0	3.5	17.5	0.100	0.040	0.10	58	677	1220	5.0	0.0030
28	SW	3	LA5	11/22/1997	33.0	7.2	40.2	0.400	0.066	2.50	126	937	1670	5.0	0.0050
29		3	LA5	4/21/1998	29.1	7.1	36.2	0.005	0.120	1.40	148	889	1610	5.0	0.0060

	SW														
30	SW	3	LA5	6/23/1998	24.3	6.9	31.2	0.100	0.091	0.90	122	905	1700	5.0	0.0120
31	SW	3	LA5	3/2/2000	26.0	7.8	33.8	0.240	0.073	1.40	150	890	1600	4.4	0.0040
32	SW	3	LA6	12/12/1996	17.0	8.7	25.7	0.050	0.470	2.10	551	990	1570	21.0	0.0160
33	SW	3	LA6	6/10/1997	15.0	7.7	22.7	0.100	0.053	0.90	74	962	1480	23.0	0.0160
34	SW	3	LA6	9/2/1997	12.0	7.8	19.8	0.005	0.044	1.00	97	968	1560	24.0	0.0170
35	SW	3	LA6	11/22/1997	18.0	8.4	26.4	0.500	1.200	1.70	906	1100	1830	20.0	0.0130
36	SW	3	LA6	4/21/1998	18.8	8.9	27.7	0.530	0.800	1.30	791	1130	1700	20.0	0.0150
37	SW	3	LA6	6/23/1998	18.3	9.8	28.1	0.800	0.830	0.80	865	1090	1760	20.0	0.0240
38	SW	1	LA7	6/10/1997	1.7	3.3	5.0	0.050	0.010	0.10	15	302	616	6.0	0.0010
39	SW	1	LA7	9/3/1997	2.0	3.1	5.1	0.005	0.005	0.20	10	497	910	11.0	0.0020
40	SW	1	LA7	12/1/1997	1.1	1.6	2.7	0.050	0.003	0.20	8.6	308	562	7.0	0.0040
41	SW	1	LA7	4/29/1998	2.7	2.3	5.0	0.050	0.006	0.10	14	323	604	7.0	0.0005
42	SW	1	LA7	6/25/1998	0.6	1.1	1.7	0.100	0.001	0.25	13	361	674	7.0	0.0040
43	SW	4	LA8	12/13/1996	12.0	7.3	19.3	0.400	4.400	6.40	2670	1480	2690	18.0	0.0150
44	SW	5	LA8	6/9/1997	9.5	4.6	14.1	0.200	2.000	0.20	1380	1400	2480	19.0	0.0040
45	SW	5	LA8	9/2/1997	6.1	3.8	9.9	6.900	4.100	1.10	2660	1180	2120	18.0	0.0030
46	SW	5	LA8	11/21/1997	16.0	6.5	22.5	1.800	4.900	1.10	2080	1500	2770	20.0	0.0080
47	SW	5	LA8	4/21/1998	11.6	4.4	16.0	1.180	3.300	1.20	2190	1580	2730	19.0	0.0060
48	SW	5	LA8	6/23/1998	11.2	4.8	16.0	2.300	3.500	0.70	2220	1500	2760	20.0	0.0150
49	SW	5	LA8	3/6/2000	10.0	6.4	16.4	8.200	3.600	3.30	1300	1400	2500	18.0	0.0015
50	SW	6	PW7	3/11/1996	15.0	6.8	21.8	0.200	0.660	1.60	553	830	1290	3.0	1.0800
51	SW	6	PW7	5/22/1996	19.0	5.0	24.0	0.800	0.730	0.90	757	850	1340	3.0	1.2600
52	SW	6	PW7	9/4/1996	17.0	5.7	22.7	1.500	0.660	1.40	558	819	1350	3.0	0.8890
53	SW	6	PW7	11/17/1996	14.0	5.4	19.4	2.700	0.700	2.30	509	860	1300	3.0	0.9460
54	SW	6	PW7	3/12/1997	15.0	5.0	20.0	0.005	0.710	1.90	762	860	1360	3.0	0.8500
55	SW	6	PW7	6/9/1997	12.0	5.1	17.1	0.200	0.640	1.80	621	814	1260	4.0	0.5130
56	SW	6	PW7	8/5/1997	16.0	0.0	15.6	0.200	0.700	0.50	579	840	1330	3.0	0.8620
57	SW	6	PW7	11/3/1997	15.0	5.4	20.4	0.300	0.600	0.80	638	859	1220	3.0	0.8120
58	SW	6	PW7	3/10/1998	17.0	5.6	22.6	0.005	0.510	2.00	597	787	1310	3.0	0.4400
59	SW	6	PW7	6/15/1998	15.0	6.5	21.5	0.300	0.560	1.70	480	692	1360	3.0	0.8100
60	SW	1	PW7	9/22/1998	12.6	4.3	16.9	0.070	0.500	0.60	433	484	796	21.0	0.3380
61	SW	6	PW7	12/8/1998	10.6	3.9	14.5	0.100	0.460	1.00	446	879	1200	3.0	0.3120
62	SW	6	PW7	3/2/1999	13.2	5.2	18.4	0.050	0.490	1.30	460	764	1300	3.0	0.4550
63	SW	6	PW7	2/15/2000	15.0	5.3	20.3	0.240	0.500	3.50	540	820	1400	2.5	0.4700

64	W	7	A8	7/8/1996	72.0	7.3	79.3	0.050	0.018	6.10	161	647	1160	8.0	0.0060
65	W	3	A8	9/19/1996	40.0	2.6	42.6	0.005	0.023	0.10	96	796	1210	11.0	0.0010
66	W	3	A8	9/8/1997	29.0	2.7	31.7	0.200	0.047	0.10	101	865	1370	13.0	0.0050
67	W	3	A8	10/14/1998	26.0	3.8	29.9	0.200	0.067	0.60	94	900	1420	14.0	0.0020
68	W	1	DOMW1	3/20/1995	0.5	0.5	1.5	0.100	0.006	1.30	0.5	133	441	4.6	0.0050
69	W	8	DOMW1	6/29/1995	1.0	2.2	3.2	0.500	0.620	0.50	1.6	388	8571	33.0	0.0050
70	W	1	DOMW1	8/23/1995	0.2	0.9	1.1	0.200	0.032	0.10	33	152	366	5.0	0.0010
71	W	1	DOMW1	12/14/1995	7.1	0.6	7.7	0.005	0.006	1.40	11	145	452	4.0	0.0020
72	W	1	DOMW1	3/22/1996	0.4	1.5	1.9	0.005	0.004	0.15	6.6	130	414	4.0	0.0010
73	W	1	DOMW1	7/1/1996	0.3	0.4	0.7	0.005	0.004	0.30	5.7	128	398	4.0	0.0005
74	W	1	DOMW1	11/11/1996	0.4	2.0	2.4	0.005	0.003	1.20	6.9	137	418	4.0	0.0005
75	W	1	MW27	3/13/1996	8.1	6.2	14.3	0.005	0.004	2.90	20	450	738	6.0	0.0070
76	W	1	MW27	6/11/1996	8.5	4.0	12.5	0.050	0.005	1.00	23	438	780	6.0	0.0050
77	W	1	MW27	8/22/1996	8.5	3.1	11.6	0.900	0.005	0.50	18	433	702	6.0	0.0080
78	W	1	MW27	10/11/1996	7.6	1.9	9.5	0.050	0.001	1.60	26	431	758	6.0	0.0080
79	W	1	MW27	5/7/1997	7.4	4.0	11.4	0.005	0.003	1.00	24	398	726	5.0	0.0100
80	W	1	MW27	7/28/1997	8.3	2.5	10.8	0.050	0.005	1.60	26	424	806	6.0	0.0120
81	W	1	MW27	10/13/1997	6.3	4.2	10.5	0.050	0.004	1.10	22	408	746	5.0	0.0080
82	W	1	MW27	2/4/1998	7.1	3.6	10.7	0.050	0.002	1.60	21	411	720	5.0	0.0060
83	W	1	MW27	5/6/1998	8.7	3.9	12.6	0.020	0.004	1.40	19	407	746	9.0	0.0080
84	W	1	MW27	7/29/1998	8.3	4.2	12.5	0.010	0.003	1.40	22	415	762	5.0	0.0110
85	W	1	MW27	10/21/1998	7.0	3.8	10.8	0.050	0.004	2.60	9.6	390	728	5.0	0.0090
86	W	1	MW27	1/6/1999	6.4	4.7	11.1	0.005	0.001	1.30	22	428	746	5.0	0.0120
87	W	1	MW27	8/9/1999	5.1	3.3	8.4	0.030	0.001	1.50	17	378	760	5.0	0.0080
88	W	1	MW27	1/20/2000	6.3	3.1	9.4	0.160	0.001	2.70	37	390	710	3.8	0.0065
89	W	1	MW28	3/29/1996	9.2	5.8	15.0	0.005	0.003	1.20	26	380	688	5.0	0.0100
90	W	1	MW28	6/5/1996	8.7	5.0	13.7	0.050	0.003	2.40	24	358	656	5.0	0.0080
91	W	1	MW28	8/14/1996	7.5	3.8	11.3	0.005	0.001	0.50	29	386	670	5.0	0.0070
92	W	1	MW28	10/28/1996	11.0	6.4	17.4	0.050	0.001	0.90	19	381	636	5.0	0.0060
93	W	1	MW28	2/3/1997	11.0	3.8	14.8	0.100	0.004	1.40	51	359	678	4.0	0.0090
94	W	1	MW28	4/30/1997	11.0	4.6	15.6	0.100	0.002	1.40	33	388	692	6.0	0.0090
95	W	1	MW28	7/25/1997	6.6	4.4	11.0	0.050	0.003	1.10	20	374	688	5.0	0.0060
96	W	1	MW28	10/8/1997	9.6	4.2	13.8	0.050	0.002	1.40	33	407	678	6.0	0.0090
97	W	1	MW28	1/28/1998	10.0	4.5	14.5	0.200	0.002	1.00	30	435	748	6.0	0.0070
98	W	1	MW28	4/28/1998	10.4	5.4	15.8	0.070	0.001	1.10	41	432	732	6.0	0.0040
99	W	1	MW28	7/29/1998	12.3	7.1	19.4	0.010	0.002	0.20	32	445	798	6.0	0.0090
100	W	1	MW28	10/20/1998	10.7	5.0	15.7	0.050	0.003	1.00	23	435	782	5.0	0.0100
101	W	1	MW28	1/19/1999	10.3	4.0	14.3	0.100	0.004	1.20	27	479	818	6.0	0.0080
102	W	1	MW28	1/20/2000	12.0	4.9	16.9	1.000	0.001	3.70	46	500	810	5.8	0.0078
103	W	1	MW30	3/20/1996	15.0	1.7	16.7	0.005	0.056	2.00	60	250	540	3.0	0.0005
104	W	1	MW30	6/17/1996	14.0	2.6	16.6	0.050	0.090	2.00	40	252	538	4.0	0.0050
105	W	1	MW30	8/26/1996	18.0	2.3	20.3	0.200	0.053	1.80	73	264	478	4.0	0.0040
106	W	1	MW30	10/29/1996	22.0	1.6	23.6	0.005	0.060	3.30	105	260	533	4.0	0.0040
107	W	1	MW30	2/13/1997	31.0	3.0	34.0	0.005	0.062	3.90	69	256	590	6.0	0.0020
108	W	1	MW30	5/7/1997	24.0	2.5	26.5	0.050	0.059	3.80	94	272	540	5.0	0.0060
109	W	1	MW30	7/29/1997	12.0	4.0	16.0	0.005	0.019	1.50	58	284	606	2.0	0.0090
110	W	1	MW30	10/22/1997	30.0	1.7	31.7	0.005	0.066	4.20	91	278	584	6.0	0.0050
111	W	1	MW30	2/3/1998	14.0	4.0	18.0	0.100	0.061	1.90	50	283	610	5.0	0.0040
112	W	1	MW30	6/16/1998	32.3	3.4	35.7	0.040	0.067	3.80	95	271	612	6.0	0.0070
113	W	1	MW30	8/13/1998	25.6	2.8	28.4	0.010	0.063	2.10	94	288	614	6.0	0.0050

114	W	1	MW30	11/11/1998	35.1	2.3	37.4	0.050	0.075	3.40	114	259	618	8.0	0.0090
115	W	1	MW30	1/7/1999	20.4	2.6	23.0	0.100	0.056	2.80	63	306	574	6.0	0.0080
116	W	9	MW30	8/17/1999	20.3	3.5	23.8	0.030	0.070	4.10	142	1840	602	39.0	0.0015
117	W	1	MW30	1/24/2000	28.0	3.5	31.5	1.000	0.065	4.60	180	310	620	6.5	0.0073
118	W	10	MW76	6/6/1997	42.0	12.0	54.0	0.100	0.240	2.20	276	1710	2480	7.0	0.0680
119	W	10	MW76	8/4/1997	35.0	9.8	44.8	0.005	0.200	2.20	380	1860	2570	8.0	0.0780
120	W	10	MW76	11/4/1997	42.0	11.0	53.0	0.100	0.250	3.10	161	1830	2510	16.0	0.0830
121	W	10	MW76	2/4/1998	36.0	11.0	47.0	0.100	0.260	3.00	355	1830	2610	7.0	0.0820
122	W	10	MW76	5/5/1998	36.0	12.0	48.0	0.080	0.250	2.00	255	1880	2360	8.0	0.0890
123	W	10	MW76	8/10/1998	42.8	9.8	52.6	0.100	0.230	1.70	220	1870	2710	7.0	0.0890
124	W	10	MW76	10/14/1998	54.2	11.0	65.2	0.100	0.220	2.00	209	1780	2640	7.0	0.0920
125	W	10	MW76	1/6/1999	39.0	11.0	50.0	0.100	0.220	2.30	249	1920	2600	6.0	0.0990
126	W	10	MW76	1/24/2000	35.0	8.9	43.9	0.800	0.240	3.80	210	1900	2600	6.1	0.0740
127	W	1	MW77	3/20/1997	4.2	5.4	9.6	0.050	0.003	0.90	16	444	730	0.5	0.0030
128	W	1	MW77	6/6/1997	5.5	5.0	10.5	0.005	0.018	0.40	21	437	740	4.0	0.0050
129	W	1	MW77	8/4/1997	5.7	4.9	10.6	0.005	0.001	0.80	24	442	714	4.0	0.0070
130	W	1	MW77	11/4/1997	5.3	4.8	10.1	0.100	0.004	0.80	22	507	780	4.0	0.0080
131	W	1	MW77	1/28/1998	6.3	5.4	11.7	0.005	0.001	0.60	11	511	798	4.0	0.0060
132	W	1	MW77	4/29/1998	5.6	5.7	11.3	0.050	0.001	1.00	28	558	812	4.0	0.0050
133	W	1	MW77	8/11/1998	6.8	5.6	12.4	0.020	0.005	0.30	26	573	876	4.0	0.0080
134	W	1	MW77	11/3/1998	6.3	5.7	12.0	0.050	0.001	0.05	41	531	866	4.0	0.0070
135	W	1	MW77	1/26/1999	5.2	6.4	11.6	0.040	0.001	0.70	30	560	878	4.0	0.0100
136	W	1	MW77	8/9/1999	7.5	5.6	13.1	0.050	0.001	0.80	17	520	868	4.0	0.0070
137	W	1	MW77	1/19/2000	6.7	5.4	12.1	6.200	0.001	1.20	43	590	900	3.2	0.0059

Appendix 8-B Fortran 90 code for well-well correlations and for the Mann-Kendall test

```
!   program trend.for
!   Developed on March 8, 2005 by Zhenxue Dai
! ************************************************************
!   This code carries out the basic statistic analysis of the observed data
!   including the water heads and the concentrations, as well as the other types of data.
!   It uses the Mann-Kendall test to evaluate the trends of the time series observations.
!   This code also calculate the water head correlations between different wells
!   from the observation data to identify the connections of the groundwater at
!   different aquifers or geological structures.
!   The input data format is: first well name, then water heads in this well
!   W123456 120, 122, 123,....
!   W123457 120, 122, 123,....
!   nw== number of observation wells
!   nt== number of observation points in each well
!   Wnam== wall name; WHH== water heads; ave== mean; Var==Variance
!   Stan== standard deviation; Cv== Coefficients of variation; Cov==Covariance
!   Trend== Uptrend, Downtrend, or Flat
!   Pval== p-value, p<0.1 trend test significant, p>0.1, test result uncertain
```

```
!  Sman==Mann-Kendall statistic parameter in each well
!  Sz==modified Mann-Kendall statistic parameter in each well
!  Ssd==modified coefficient for each well.
!  Rela(k,i)== Correlation Coefficients between well k and well i.
!    alfa=1.68 for water head, and 1000 for concentrations
!  ***************************************************************

       parameter (nw=150,nt=20)
       IMPLICIT DOUBLE PRECISION(A-H,O-Z),INTEGER(I-N)
       dimension WHH(nw,nt),Var(nw),ave(nw), Stan(nw),Cv(nw)
       dimension Rela(nw,nw),Cov(nw,nw),Hmin(nw),Hmax(nw),Pval(nw),
     +           Numt(nw),Sman(nw),Sz(nw),Ntie(nw),Ssd(nw)
       character*8 Wnam(nw),trend(nw)
       character*5 Waqu(nw)
       character*80 str1
       character*4 str2
       character*8 out
       alfa=1.0
          write(*,*) "ENTER INPUT FILENAME (NO HEADER): "
       read(*,'(a)')str1
          write(*,*) "ENTER 4 CHARACTERS FOR OUTPUT FILENAME "
       read(*,'(a)')str2
       open(99,file=str1,status='old')
       OUT=str2//'.out'

       open(91,file=out,status='unknown')

           write(*,*)  " "
           write(*,*)  "THINKING... "
           write(*,*)  " "
           num1 = 0
           tranN0=0

!  BRING IN FIRST LINE OF INPUT FROM DATA FILE
       read(99,*)Nww      !=137, number of observation wells
       read(99,*)Ntt      !=16, max number of data at one well


           do i=1,Nww
        read(99,*) Wnam(i),Waqu(i),(WHH(i,j), j=1,Ntt)
!        if(id(i).eq.0) go to 50 (commented out by ZDai)
        write(*,*) Wnam(i),Waqu(i)
      end do


 50    continue
```

```
          Iout=0
499       continue
      If(Iout.eq.0) Write(91,500)
500   format(/,'Statistic Analysis of the Original Observations'
     +  ,/,'WellNam AqNam ObNm MinVal MaxVal ',
     +     'MeanV  Varian Stand CoefV ',
     +     'Mann  ModM   Trend  p-val')
      If(Iout.eq.1) Write(91,801)
801   format(/,'Statistic Analysis of the Observations',
     +  ' After Rejecting the Outlier Points',
     +   /,'WellNam AqNam ObNm MinVal MaxVal ',
     +     'MeanV  Varian Stand CoefV ',
     +     'Mann  ModM   Trend  p-val')

!   calculate mean, variance of water head in each well(Var(nw),ave(nw), Stan(nw))
      do 60 i=1,Nww
            nwt=0
            hhh=0
            st=0
            Hm=0
            Hn=1.0e25
            Sm=0

       do j=1,Ntt
            Ntie(j)=0
                  if(WHH(i,j).eq.-100) go to 62
            nwt=nwt+1
        hhh=hhh+WHH(i,j)
            if(WHH(i,j).gt.Hm)Hm=WHH(i,j)    !Max value
            if(WHH(i,j).lt.Hn)Hn=WHH(i,j)    !Min Value

            do k=1,Ntt
              if(k.gt.j.and.WHH(i,k).ne.-100)then
                aa=WHH(i,k)-WHH(i,j)
                if(aa.gt.0.0) Ms=1
                if(aa.eq.0.0) then
                  Ms=0
                  Ntie(j)=Ntie(j)+1
                end if
                if(aa.lt.0.0) Ms=-1
                Sm=Sm+Ms
           end if
              end do

 62       continue
```

```
      end do

          Numt(i)=nwt
          Hmax(i)=Hm
          Hmin(i)=Hn
          Sman(i)=Sm
         if(nwt.ne.0)ave(i)=hhh/nwt
         Stie=0
         do k2=1,ntt
          Stie=Stie+Ntie(k2)*k2*(k2-1)*(2*k2+5)
         end do
         Ssd(i)=((Numt(i)*(Numt(i)-1)*(2*Numt(i)+5)-Stie)/18.0)
         If(Ssd(i).gt.0.0) Ssd(i)=Ssd(i)**0.5
         if(Sman(i).gt.0.0) then
         if(ssd(i).ne.0.0) Sz(i)=(Sman(i)-1.0)/Ssd(i)
                   trend(i)=' Uptrend'
          end if
         if(Sman(i).eq.0.0) then
             Sz(i)=0
                   trend(i)=' Flat'
          end if
         if(Sman(i).lt.0.0) then
          if(ssd(i).ne.0.0)Sz(i)=(Sman(i)+1.0)/Ssd(i)
                   trend(i)='Downtren'
          end if
          Szz=abs(Sz(i))
          if(Szz.gt.5) Pval(i)=0.00000
          if(Szz.gt.3.09.and.Szz.lt.5)
     +  Pval(i)=66.21327*exp(-szz/0.27834)-9.9998E-7
          if(Szz.gt.1.96.and.Szz.lt.3.09)
     +  Pval(i)=2.59485*exp(-szz/0.42511)-0.00081
          if(Szz.lt.1.96.and.Szz.gt.1.28)
     +  Pval(i)=0.8051*exp(-szz/0.66358)-0.01698
          if(Szz.lt.1.28) Pval(i)=0.71701*exp(-szz/1.56831)-0.21701
       do j=1,ntt
                    if(WHH(i,j).eq.-100) go to 63
        st=st+(WHH(i,j)-ave(i))**2.0
63     continue
      end do
          if(nwt.ne.0.0)then
          Var(i)=st/nwt
      Stan(i)=(st/nwt)**0.5
      end if
          if(ave(i).ne.0.0)Cv(i)= stan(i)/ave(i)
          if(nwt.eq.0)then
       Write(91,901)Wnam(i),Waqu(i),Numt(i)
```

```
901     format(A8,1x,A5,I3,1x,'This well is deleted!')
        go to 60
                end if
!     Write(*,501) Wnam(i),Ave(i),Var(i),Stan(i),Cv(i)
      Write(91,501)Wnam(i),Waqu(i),Numt(i),Hmin(i),Hmax(i),Ave(i),
   +     Var(i),Stan(i),Cv(i),Sman(i),Sz(i),Trend(i),Pval(i)
 60   continue
501    format(A8,1x,A5,I3,1x,3f7.2,F7.2,f6.2,f6.3,1x,f4.0,f6.2,
   +       1x,A8,f6.3)
         If(Iout.eq.1) go to 808
!
!        Reject the extremal observation points
!
         aSd=0.0
         do i=1,nww
                asd=asd+Stan(i)
         end do
                asd=asd/nww
        do iw=1,nww
         Sp=0.025
     pp=(Numt(iw)-1)*Sp/Numt(iw)
        if(pp.le.0.00003) zz=4
        if(pp.gt.0.00003.and.pp.le.0.0062)
   +     zz=1.54688*exp(-pp/0.00117)+2.49239
        if(pp.le.0.0688.and.pp.gt.0.0062)
   +     zz=1.41193*exp(-pp/0.02866)+1.36272
        if(pp.gt.0.0688)
   +     zz=2.50842*exp(-pp/0.328)-0.54623
         if(zz.le.0.0) zz=0.0
!        write(*,*)pp, zz
        vk=1.4+0.85*zz
        vc=vk*(1.0-(vk**2.0-2.0)/(4.0*(Numt(iw)-1.0)))
   +       *((Numt(iw)-1.0)/Numt(iw))**0.5
         vCs=alfa*(vc*stan(iw))**2.0
!        write(*,*)Wnam(iw), vCs
        do j=1,ntt
        If(whh(iw,j).le.-100.0) go to 3721
        vd=(whh(iw,j)-ave(iw))**2.0
!        vd=abs(whh(iw,j)-ave(iw))*(1.0-2*Sp)
        if(vd.gt.vCs.or.vd.gt.100*alfa*asd)then
          orig=whh(iw,j)
     whh(iw,j)=-100
!        Numt(iw)=Numt(iw)-1
        write(*,*)Wnam(iw),orig,'vd=',vd,'st=',vCs

        end if
```

```
3721   continue
         end do
         end do
         Iout=1
         go to 499


!  LOOP calculate correlation coefficients between wells
!
808    continue
     do 80 k=1,Nww
     do 80 i=1,Nww
          nwt=0
          hhk=0
          hhi=0
          st=0
          vari=0
          vark=0
     do j=1,Ntt
                    if(WHH(k,j).eq.-100.or.WHH(i,j).eq.-100) go to 82
           nwt=nwt+1
      hhk=hhk+WHH(k,j)
      hhi=hhi+WHH(i,j)
 82     continue
      end do
          if(nwt.ge.1)then
      avek=hhk/nwt
      avei=hhi/nwt
           end if
      do j=1,ntt
                    if(WHH(k,j).eq.-100.or.WHH(i,j).eq.-100) go to 83
        st=st+(WHH(k,j)-avek)*(WHH(i,j)-avei)
        vari=vari+(WHH(i,j)-avei)**2.0
        vark=vark+(WHH(k,j)-avek)**2.0
 83     continue
      end do
          if(nwt.ge.1)then
            Cov(k,i)=st/nwt
            Varii=(vari/nwt)**0.5
            Varkk=(vark/nwt)**0.5
      Rela(k,i)=Cov(k,i)/(Varkk*Varii)
          end if
 80    continue

     Write(91,502)
502     format(/,'Following Wells are Highly Positively Correlated:',
```

```
     +         ' R > 0.95')

          do k=1,Nww
          do i=1,Nww
             If(i.le.k) go to 21
             If (Rela(k,i).ge.0.95) then
         Write(91,503) Wnam(k),Waqu(k),Wnam(i),Waqu(i),Rela(k,i)
503        format(A8,A5,'and  ',A8,A5,f5.2)
          end if
21         continue
          end do
          end do

          Write(91,602)
602        format(/,'Following Wells are Positively Correlated:',
     +         ' 0.9 < R < 0.95')

          do k=1,Nww
          do i=1,Nww
             If(i.le.k) go to 23
             If (Rela(k,i).ge.0.9.and.Rela(k,i).lt.0.95) then
         Write(91,603)Wnam(k),Waqu(k),Wnam(i),Waqu(i),Rela(k,i)
603        format(A8,A5,'and  ',A8,A5,f5.2)
          end if
23         continue
          end do
          end do


          Write(91,604)
604        format(/,'Following Wells are not Correlated:',
     +         ' -0.1 < R < 0.1')

          do k=1,Nww
          do i=1,Nww
             If(i.le.k) go to 84
             If (Rela(k,i).le.0.1.and.Rela(k,i).ge.-0.1) then
         Write(91,605)Wnam(k),Waqu(k),Wnam(i),Waqu(i),Rela(k,i)
605        format(A8,A5,'and  ',A8,A5,f5.2)
          end if
84         continue
          end do
          end do


          Write(91,504)
```

```
504   format(/,'Following Wells are Negatively Correlated:',
   +         ' R < -0.9')

      do k=1,Nww
      do i=1,Nww
         If(i.le.k) go to 88
         If (Rela(k,i).le.-0.9) then
     Write(91,505)Wnam(k),Waqu(k),Wnam(i),Waqu(i),Rela(k,i)
505     format(A8,A5,'and  ',A8,A5,f5.2)
       end if
88     continue
      end do
      end do


      Write(91,506) (Wnam(i), i=1,Nww)
506    format(/,'All Correlation Coeff of Water Head Between Wells',
   +     /,15x,137(A7))
      Write(91,406) (Waqu(i), i=1,Nww)
406    Format(15x,137(A5,2x))
       do k=1,Nww
     Write(91,508) Wnam(k), Waqu(k),(Rela(k,i),i=1,Nww)
508     format(A8,A5,137(f7.3))
      end do

     CALL BEEPQQ(200,400)
      CALL BEEPQQ(30,400)
     CALL BEEPQQ(200,400)
     CALL BEEPQQ(30,400)
     CALL BEEPQQ(400,1500)
          write(*,*) "  DONE! "
          stop
          End
```

GLOSSARY

Alluvium	A general term for clay, silt, sand, gravel, or similar unconsolidated detrital material, deposited during comparatively recent geologic time by a stream or other body of running water, as a sorted or semi sorted sediment in the bed of the stream or on its floodplain or delta, as a cone or fan at the base of a mountain slope.
Aquifer	A geological formation capable of storing and yielding significant quantities of water. It is usually composed of sand, gravel, or permeable rock which lies upon a layer of clay or other impermeable material.
Aquitard	Less permeable beds, also saturated with water, from which water can't be produced through wells, but where the flow is significant enough to feed adjacent aquifers through vertical leakage.
Becquerel (Bq)	The International System (SI) unit of activity equal to one nuclear transformation (disintegration) per second. 1 *Bq* = 2.7x10-11 *Curies (Ci)* = 27.03 picocuries (pCi).
Colluvium	A general term applied to any loose, mixed, and incoherent mass of soil material and/or rock fragments deposited by rainwash, sheetwash, or slow continuous downslope creep, usually collecting at the base of gentle slopes or hillsides.
Comprehensive Environmental Response, Compensation, and Liability Act (CERCLA)	Commonly referred to as "CERCLA" or "Superfund," this federal statute was enacted by Congress in 1980 and was amended several times thereafter. CERCLA was designed to respond to situations involving past disposal of hazardous substances. CERCLA provides EPA the authority to clean up hazardous substance sites under "response" or "remedial" provisions of the National Contingency Plan (NCP) and other implementing regulations. 42 U.S.C. §§ 9601 *et seq.*
Conceptual site model	A qualitative description of the processes, geometry, and boundary conditions associated with a disposal site or site sub-system component (i.e., ground-water system, flow-through covers, source term, etc.). Conceptual model development includes abstracting system, or sub-system, descriptions into more simplified forms that can be mathematically modeled.
Contaminant of Concern (COC)	A contaminant or a chemical that poses potential public health risks. Potential contaminants of concern (PCOCs) are all chemicals that have been detected at the site. Only those contaminants retained for the risk assessment are referred to as COCs.
Cuesta	A ridge with a gentle slope on one side and a steep slope on the other.
Curie (Ci)	The customary unit of radioactivity. One *curie* (Ci) is equal to 37 billion disintegrations per second (3.7 x 1010 dps = 3.7 x 1010 *Bq*), which is approximately equal to the decay rate of one gram of 226Ra.
Direct current electrical resistivity (DC-resistivity)	A geophysical technique used to measure the resistance of a rock formation to an electric current.

Effluent	Any substance, particularly a liquid, which enters the environment from a point source. Generally refers to wastewater from a sewage treatment or industrial plant.
Erratics	Boulders and other rock fragments transported by glacial ice from their place of origin to an area where the bedrock is different.
Ground-penetrating radar (gpr)	Geophysical exploration technique that utilizes pulses of electromagnetic radiation in the microwave band (UHF/VHF frequencies) of the radio spectrum, and reads the reflected signal to detect subsurface structures and objects without drilling, probing or otherwise breaking the ground surface.
Half-life (t1/2)	The time required for one-half of the radioactive isotopes in a sample to decay to radiogenic (daughter) isotopes or disintegrate.
Hazardous Waste	A category of waste regulated under RCRA. To be considered hazardous, a waste under RCRA must be a solid waste and must exhibit at least one of four characteristics described in 40 CFR 261.20 through 40 CFR 261.24 (i.e., ignitability, corrosivity, reactivity, or toxicity) or be specifically listed by EPA in 40 CFR 261.31 through 40 CFR 261.33. Hazardous waste does not include source, special nuclear, or by-product materials as defined by the AEA, nor material contained in point source discharges regulated under the Clean Water Act.
Infiltration	The net water intake into the native soils at the site or into a disposal unit(s) through the land or cover surface(s).
Kd	distribution coefficient.
Kriging	A geostatistical method of evaluating mine reserves based on a mathematical function known as a semivariogram.
Lacustrine	Of or applying to the sedimentary environment of a lake.
Low-Level Waste (LLW)	Radioactive waste that is not high level radioactive waste, spent nuclear fuel, transuranic waste, byproduct material (as defined in section 11e.(2) of the Atomic Energy Act of 1954, as amended), or naturally occurring radioactive material. [Adapted from *Nuclear Waste Policy Act* of 1982, as amended]
Maximum Contaminant Level (MCL)	Under the Safe Drinking Water Act, the maximum permissible level of a contaminant in water delivered to any user of a public water system.
Non-Aqueous Phase Liquid (NAPL)	Organic compounds or mixtures of such compounds that do not mix with water. A NAPL that is lighter than water is called light non-aqueous phase liquid (LNAPL) or a floater. A NAPL that is heavier than water is called dense non-aqueous phase liquid (DNAPL) or a sinker.
Neutron probe	A device used to measure the quantity of water present in soil.
Ohm-m	Unit of measure of electrical resistivity.
Operable Unit (OU)	A term given to large areas where remediation may be focused by grouping multiple units into a single management unit.
Performance Assessment (PA)	An analysis of a radioactive waste disposal facility conducted to demonstrate there is a reasonable expectation that performance objectives established for the long-term protection of the public and the environment will not be exceeded following closure of the facility. [DOE 435.1-1]

Petra	Software developed by the GeoPLUS Corporation. It's primary use is to store and provide tools for interpreting geologic data.
Picocurie (pCi)	A "picocurie" is one-trillionth of a curie. The same mass (one gram) of other radioactive elements may have an activity higher or lower than one curie.
pCi/L	Represents the number of picocuries in a liter of water.
Plume	A body of contaminated groundwater flowing from a specific source.
Remediate	To cleanup or decontaminate ground water or soil.
Resource Conservation and Recovery Act (RCRA)	A federal law enacted in 1976 to address solid waste and the treatment, storage, and disposal of hazardous waste. 42 U.S.C. §§ 6901-6992k.
Semivariogram	A key function in geostatistics used to fit a model of the spatial/temporal correlation of an observed phenomenon.
Sorption coefficient (Kd)	The ratio of the mass of solute on the solid phase per unit mass of solid phase to the concentration of solute in solution. The validity of this ratio requires that the reactions that cause the partitioning are fast and reversible (e.g., chemical equilibrium is achieved) and the sorption isotherm is linear.
Stratigraphy	The sequence or order of rock or soil layers in a geologic formation.
Surface-based seismic surveys	A geophysical technique to determine the detailed structure of rocks underlying a particular area by passing acoustic shock waves from the surface into the underlying strata and detecting and measuring the reflected signals.
Surficial	Of, relating to, or occurring on or near the surface of the earth.
Thermocouple psychrometers (TCPs)	Probes for determining soil water potential in situ.
Till	A mix of fine silt, sand, gravel, and large boulders, usually in a glacial setting.
Tritium units	One tritium unit is equal to one molecule of tritium per 10^{18} molecules of hydrogen and has an activity of 0.118 Bq/kg (3.19 pCi/kg or pCi/L).
Vadose zone	The horizon between the earth's surface and the water table, also know as the "unsaturated zone". Vadose zone wells installed by the USGS at the ADRS are designated with the prefix "UZB-x".

NRC FORM 335 (9-2004) NRCMD 3.7

U.S. NUCLEAR REGULATORY COMMISSION

BIBLIOGRAPHIC DATA SHEET

(See instructions on the reverse)

1. REPORT NUMBER (Assigned by NRC, Add Vol., Supp., Rev., and Addendum Numbers, if any.)

NUREG/CR-6948, Vol 2

2. TITLE AND SUBTITLE

Integrated Ground-Water Monitoring Strategy for NRC-Licensed Facilities and Sites: Case Study Applications

3. DATE REPORT PUBLISHED

MONTH	YEAR
November	2007

4. FIN OR GRANT NUMBER

Y6020

5. AUTHOR(S)

Van Price, Tom Temples, Rex Hodges, Zhenxue Dai, David Watkins and Janice Imrich

6. TYPE OF REPORT

Technical

7. PERIOD COVERED *(Inclusive Dates)*

February 2003 - September 2007

8. PERFORMING ORGANIZATION - NAME AND ADDRESS *(If NRC, provide Division, Office or Region, U.S. Nuclear Regulatory Commission, and mailing address; if contractor, provide name and mailing address.)*

Advanced Enivironmental Solutions, LLC
407 West Main Street
Lexington, SC 29072

9. SPONSORING ORGANIZATION - NAME AND ADDRESS *(If NRC, type "Same as above"; if contractor, provide NRC Division, Office or Region, U.S. Nuclear Regulatory Commission, and mailing address.)*

Division of Fuel, Engineering and Radiological Research
Office of Nuclear Regulatory Research
U.S. Nuclear Regulatory Commission
Washington, DC 20555-0001

10. SUPPLEMENTARY NOTES

T.J. Nicholson, NRC Project Manager

11. ABSTRACT *(200 words or less)*

This document discusses results of applying the Integrated Ground-Water Monitoring Strategy (the Strategy) to actual waste sites using existing field characterization and monitoring data. The Strategy is a systematic approach to dealing with complex sites. Application of such a systematic approach will reduce uncertainty associated with site analysis, and therefore uncertainty associated with management decisions about a site. The Strategy can be used to guide the development of a ground-water monitoring program or to review an existing one. The sites selected for study fall within a wide range of geologic and climatic settings, waste compositions, and site design characteristics and represent realistic cases that might be encountered by the NRC. No one case study illustrates a comprehensive application of the Strategy using all available site data. Rather, within each case study we focus on certain aspects of the Strategy, to illustrate concepts that can be applied generically to all sites. The test sites selected include:

- Charleston, South Carolina, Naval Weapons Station,
- Brookhaven National Laboratory on Long Island, New York,
- The USGS Amargosa Desert Research Site in Nevada,
- Rocky Flats in Colorado,
- C-Area at the Savannah River Site in South Carolina, and
- The Hanford 300 Area.

A Data Analysis section provides examples of detailed data analysis of monitoring data.

12. KEY WORDS/DESCRIPTORS *(List words or phrases that will assist researchers in locating the report.)*

conceptual site model
data management
geology
ground water
monitoring
outlier
Performance Indicator
tritium
vadose
wells

13. AVAILABILITY STATEMENT

unlimited

14. SECURITY CLASSIFICATION

(This Page)

unclassified

(This Report)

unclassified

15. NUMBER OF PAGES

16. PRICE

Federal Recycling Program